



Efficient Utilization of LEDs and LDs for Illumination and Visible Light Communication (VLC)

FAHAD ZAFAR

SUBMITTED IN TOTAL FULFILMENT OF THE REQUIREMENTS FOR THE DEGREE OF
DOCTOR OF PHILOSOPHY

Electrical and Computer Systems Engineering
FACULTY OF ENGINEERING
MONASH UNIVERSITY

2017

© 2017 Fahad Zafar. Except as provided in the Copyright Act 1968, this thesis may not be reproduced in any form without the written permission of the author.

I certify that I have made all reasonable efforts to secure copyright permissions for third-party content included in this thesis and have not knowingly added copyright content to my work without the owner's permission.

Efficient Utilization of LEDs and LDs for Illumination and Visible Light Communication (VLC)

FAHAD ZAFAR

Visible light communication (VLC) can simultaneously provide illumination and communication for indoor lighting systems by operating on unregulated electromagnetic spectrum in the visible region. For making a VLC system commercially competent, it is necessary to have high speed communication, which does not compromise the overall quality of illumination in terms of illuminance, correlated color temperature (CCT) and color rendering index (CRI). The growing urgency towards higher data rates has shifted focus from the widely used light emitting diodes (LEDs) towards laser diodes (LDs), which can provide gigabit class communication by utilizing simple non-return to zero on-off-keying (NRZ-OOK) modulation. This work investigates the trade-off between communication and illumination in VLC systems by considering three types of sources: phosphor converted LEDs (pc-LEDs), which are widely used nowadays, red green blue LEDs (RGB-LEDs), which are recently emerging, and LDs, which are foreseen to take over in future.

Pc-LEDs generate white light at a fixed CCT depending on the amount of phosphor. The only adjustable parameter for pc-LED-VLC is the overall illuminance that can be regulated for energy savings and ecological benefits by dimming schemes like continuous current reduction (CCR) and pulse width modulation (PWM). However, CCR decreases the signal to noise ratio (SNR) and might cause undesirable chromaticity shifts, which has not been quantified from a VLC system perspective. For PWM, data transmission is allowed only when the duty cycle is high, which decreases the achievable data rate. These problems can be resolved by using adaptive schemes such as slot utilization (SU) and rate adaptation (RA). SU transmits data bits regardless of the state of PWM dimming signals with superimposed bits; this causes dimming shift that hampers the precision over illuminance. RA cannot be fully utilized due to the limited modulation bandwidth (i.e. bandwidth available to send data) of LEDs. In this work, by simultaneous characterization of chromaticity and dimming shifts, a dimming algorithm has been proposed, which utilizes multiple adaptive techniques. It could maintain the data rate of 10 Mb/s at an acceptable bit error rate (BER) and avoided a dimming shift of 40 %. The achievable data rate is low, since only a single communication channel can be used, when pc-LEDs are used as transmitters.

RGB-LEDs can increase the aggregate data rate by parallel channels using wavelength division multiplexing (WDM). The data rate has been increased to

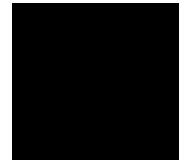
45 Mb/s in this work by introducing a RGB-LED. Each LED chip can be individually adjusted to control the CCT of the light. CCT alters the emotional effect of a space and the appearance of illuminated objects; its regulation can lead to intelligent lighting solutions. Although the effect of CCT on VLC has been analysed in certain works, the use of dimming schemes for its regulation has not been investigated. Regulation of CCT can enhance link performance of individual channels with stringent biasing requirements. The CCT of the VLC system was regulated at a practical range of 2700 K to 6500 K in this work, which demonstrated that CCR scheme deteriorated the link capacity of blue channel for warmer light. Based on experimental, analytical and simulation based investigations, adaptive schemes were characterized for each CCT. Compared to PWM scheme, which achieved an overall data rate of 26 Mb/s for 2700 K, the SU scheme sustained the target data rate of 45 Mb/s at an acceptable BER. Although RGB LEDs substantially increased the data rate, this speed is still low, when faster applications expected to operate in the emerging 5G wireless standards are considered.

For achieving gigabit class communication, a RGB LD-based VLC system was developed in this work. Most of the RGB-LD-VLC systems have high CCTs of around 8000 K. Speckle pattern is a concern in LDs, which can be characterized by the speckle contrast ratio, but has been widely overlooked. Although human perception investigation for LD-based lighting has been done, this has not been examined from VLC perspective with human participants. In this work, by implementing adaptive dimming schemes, CCT in the practical range of 2700 K to 6500 K was achieved, but the overall data rate was reduced from 2.01 Gb/s to 1.16 Gb/s. A further red LD was added to form a RRGB based system, which could operate at a data rate of 2.24 Gb/s. A vibrating diffuser module was designed to reduce speckle contrast ratio by 68 %. The proposed system generated homogeneous white light, which was preferred by 74 % of the total 40 human participants. However, a maximum CRI of 35 was achieved for cool white light, which was quite low compared to the values expected in commercial lighting infrastructures (i.e. above 90).

CRI is an illumination centric parameter, which measures the light sources capabilities in replicating colors of illuminated objects. Pc-LEDs also have lower CRI of 75-80, when compared to incandescent sources due to their inability in producing light output in the higher wavelength region. Red enhanced LEDs had been proposed in such cases to increase the overall CRI. In this work, the concept of red enhanced lighting is implemented using a LD to form a hybrid LED-LD based VLC system. For the hybrid system, the LED provides greater spectral continuity for high CRI and the LD provides gigabit class communication. The concept of combining LDs with LEDs is quite unique, the only work on such a hybrid system utilized a red LD with a pc-LED to achieve a CRI of 83 for a data rate of 400 Mb/s. Different link configurations with unique combination of LEDs and LDs were characterized and a system was proposed utilizing 3 LDs and a single pc-LED, which could achieve an overall data rate of 1.26 Gb/s and CRI of 89.

This thesis contains no material which has been accepted for the award of any other degree or diploma at any university or equivalent institution and that, to the best of my knowledge and belief, this thesis contains no material previously published or written by another person, except where due reference is made in the text of the thesis.

Signature _____



Print Name FAHAD ZAFAR

Date 10/04/2018

Acknowledgments

First and foremost, I would like to thank my father for inspiring me in every step of life and letting me chase my dreams by cushioning me from the reality. My mother, for her unconditional love, countless sacrifices and unremitting motivation. This thesis is dedicated to both of you. My late brother, who had been a loving sibling, an amazing friend and probably the best teacher of mathematics, which got me to this stage; I miss you every single day.

I would like to express my sincere gratitude towards my supervisors A/Prof. R. Parthiban and Dr. Masduzzaman Bakaul, for generously offering their time and knowledge. Dr. Vineetha Kalavally, for her insightful feedback and support. Prof. Jussi Parkkinen, for sharing his ideas regarding color science. Dr. Dilukshan Karunatilaka, for his numerous valuable advices and discussions regarding VLC. The ECSE laboratory staff - Hasnan, Suresh, Manan and Rozidah for their hardware assistance. All FYP students, who collaborated with me, specially Tharindu, Urmila, Jian and Elaine, your efforts had helped me in understanding as much as I have taught you about VLC.

To Nahiyan and Yasser, for always believing in me, at times when I had given up on myself. All my childhood buddies from SEMS. My friends from Monash, undergrad and postgrad life would have been difficult without you all. My grandparents, uncles, aunts, sister in law, nephews, nieces and cousins for their love.

Last, but not the least, I would like to thank my better half, Fariha, for her endless encouragement, relentless support and continual tolerance of me and my habits; thank you for coming to my life.

Contents

1	Introduction	1
1.1	The Recent Drive Towards VLC	1
1.2	Focus of Thesis	4
1.3	Organization of Thesis	11
1.4	Contribution of Thesis	13
1.5	Publications	17
2	LED and LD-based VLC under Illumination Constraints	19
2.1	Introduction	19
2.2	Benefits of VLC	21
2.3	Fundamental Aspects of VLC	24
2.3.1	Illumination	24
2.3.2	Communication	32
2.4	Transmitters for VLC	35
2.4.1	Types of Transmitters	36
2.4.2	Differences between LEDs and LDs	38
2.5	Modulation Schemes	40
2.6	Dimming Schemes	43
2.6.1	Types of Dimming Schemes	44
2.6.2	Adaptive Dimming Schemes for VLC	47
2.7	Wavelength Division Multiplexing (WDM)	50
2.8	Receivers for VLC	51
2.9	Performance Enhancement in VLC	52
2.10	Illumination Control for VLC Systems	54
2.10.1	Illumination Control in pc-LED Systems	55
2.10.2	Illumination Control in RGB-LED Systems	56
2.10.3	Illumination Control in LD-based Systems	57
2.10.4	Psychophysical Evaluation of LD Lighting	62
2.11	Conclusion	64
3	Dimmable pc-LED-VLC System with Concurrent Data Transmission	67
3.1	Introduction	67
3.2	Experimental Setup of LED-based VLC	69

3.3	Characterization of pc-LED	73
3.4	Analytical Model of pc-LED-based VLC	75
3.5	Methodology	77
3.6	Investigation of Pulse Regulated Dimming Schemes	78
3.7	Investigation of PWM and CCR Dimming for Illumination and VLC	82
3.8	Slot Utilization (SU) Scheme	87
3.9	Rate Adaptation (RA) Scheme	92
3.10	Proposed Dimming Algorithm	95
3.11	Conclusion	99
4	RGB-LED-based VLC System with Enhanced Illumination	103
4.1	Introduction	103
4.2	Characterization of RGBA LED	105
4.3	Experimental Setup of WDM-LED-VLC	107
4.4	Simulation of WDM-LED-VLC	108
4.5	Analytical Model of WDM-LED-VLC	109
4.5.1	Biasing Condition for Target Illumination Constraint	110
4.5.2	Analytical Model of Link Performance of RGB LED-based VLC	111
4.6	Methodology	112
4.7	Effect of CCT Regulation on Channel Performance	113
4.8	Dimming Schemes for CCT Regulation	116
4.8.1	Analog Dimming for CCT Control	117
4.8.2	Digital Dimming for CCT Control	117
4.8.3	Slot Utilization for CCT Control	118
4.8.4	Rate Adaptation for CCT Control	118
4.9	Comparison of Investigated Dimming Schemes for CCT Control	119
4.10	Conclusion	120
5	RGB-LD-based VLC System with Enhanced Illumination	123
5.1	Introduction	123
5.2	Characterization of LDs	125
5.3	Experimental Setup of WDM-LD-VLC	127
5.4	Simulation of WDM-LD-VLC	128
5.5	Analytical Model of WDM-LD-VLC	131
5.6	Methodology	132
5.7	Individual R, G, and B LD-based VLC System	133
5.8	CCT Tunable RGB-based VLC System	135
5.9	Adaptive Dimming Control for CCT Regulation of RGB-based LD VLC	137
5.10	RRGB LD-based VLC System	139
5.11	Simulation Results at Proposed Approaches	142
5.12	Homogeneous Illumination from LD based Lighting System	143
5.12.1	Speckle Mitigation	143
5.12.2	Diffuser Characterization	147
5.12.3	Human Perception Investigation	149

5.13	Conclusion	154
6	Hybrid LED-LD-based VLC System with Superior Color Rendering	157
6.1	Introduction	157
6.2	Methodology	159
6.3	Quantitative Comparison of LEDs and LDs	160
6.3.1	Bandwidth Characterization	160
6.3.2	Thermal Performance Characterization	163
6.4	Photometric Aspects of Hybrid LED-LD based VLC System	166
6.4.1	Case 1: Single Red LD-LED Hybrid System	167
6.4.2	Case 2: Multiple Red LDs-LED Hybrid System	169
6.4.3	Case 3: Multiple LDs-LED Hybrid System	170
6.4.4	Overall Comparison	170
6.5	Communication Aspects of Hybrid LED-LD-based VLC System	172
6.5.1	Experimental Analysis	172
6.5.2	Simulation Results	176
6.6	Conclusion	177
7	Conclusion	179
7.1	Looking Back	179
7.2	Overview of Thesis	180
7.3	Future Work	185
7.3.1	Development of High Speed Dimmable VLC Driver	185
7.3.2	Implementation of Adaptive Schemes for RGBA LED-VLC System	186
7.3.3	Incorporating other Modulation Schemes for the Dimming Algorithm	186
7.3.4	Addition of Amber LD for Higher CRI	187
7.3.5	Consideration of Color Blindness when Conducting Psychophysical Tests	187
7.3.6	Miniaturization of LD-based Transmitter System for Practical Adaptability	188
8	Bibliography	189
A	Psychophysical Evaluation Data	211
A.1	Questionnaire for Psychophysical Evaluation	211
A.2	Human Ethics Approval	217
A.3	Data Obtained from Psychophysical Evaluation	218

List of Figures

1.1	Electromagnetic spectrum	2
1.2	Timeline of evolution of wireless standards, LiFi, LEDs and LDs . .	4
1.3	Functional block diagram of a dimmable LED/LD-based VLC system	5
2.1	LED-based VLC system depicting the dual functionality of illumination and communication	23
2.2	Relation between scotopic and photopic vision based on cone and rod cells	25
2.3	CIE 1931 color space and color matching functions	26
2.4	CIE 1931 and CIE 1976 color spaces showing the location of the planckian locus alongside a CCT chart	29
2.5	Sample colors used for calculating CRI	32
2.6	Block diagram of an IM/DD VLC system	33
2.7	Current-output power behaviour, with input current swing, I_{SP} . .	35
2.8	Difference between GaN based LEDs and LDs	39
2.9	Pulse regulated schemes in terms of discrete time equations	46
2.10	NRZ-OOK data stream resulting from implementation of adaptive schemes for different dimming targets	48
2.11	Fundamental WDM VLC system using red, green and blue sources	51
2.12	Normalized SPDs and respective locations on CIE 1931 diagram for pc-LED, RGB LED and RGB LD	55
2.13	Concept of increase in saturation of red objects under red enhanced lighting	56
2.14	Illustration of three different techniques generally implemented to reduce speckle contrast for laser based lighting sources	60
3.1	VLC system utilizing pc-LED as its transmitter and a Si PD as the receiver (a) front view, (b) top view, (c) side view	70
3.2	Transmittance of filter as a function of wavelength	71
3.3	Instantaneous eye diagram obtained using the serial data analysis software and the corresponding BER values computed from the Q factor and by off-line demodulation.	72
3.4	Experimental setup of the pc-LED based VLC system	73

3.5	Experimental setup for investigation of the photometric and radiometric response of dimming schemes.	74
3.6	LVI characteristics of pc-LED	74
3.7	Normalized spectral power distribution of pc-LED and photodiode responsivity for different wavelengths in the visible range . . .	75
3.8	Methodology used for comparison and analysis of dimming schemes for pc-LED based VLC system	78
3.9	Investigated pulse regulated waveforms	79
3.10	Experimental setup for the analysis of pulse regulated dimming schemes	79
3.11	Distribution of illuminance, CCT and CRI for investigated pulse regulated dimming schemes	80
3.12	NRZ-OOK data stream after implementation of analog and digital dimming for different dimming targets	83
3.13	Variation of luminous flux with dimming targets for analog (blue) and digital (red) dimming. The MacAdam ellipse at a SDCM of 3500 K for these two schemes are provided.	85
3.14	Relative variation of CCT due to PWM and CCR dimming techniques	85
3.15	NRZ-OOK data stream after implementation of slot utilization scheme for different dimming targets	87
3.16	Eye diagrams of the received waveforms for different value of amplitude scaling factor during the off duration of the dimming signal	88
3.17	BER distribution of slot utilization scheme for increasing values of amplitude scaling factor (A).	89
3.18	Illuminance distribution of slot utilization scheme for increasing values of amplitude scaling factor (A).	90
3.19	Dimming precision obtained for increasing values of amplitude scaling factor (A)	91
3.20	NRZ-OOK data stream after implementation of rate adaptation scheme for different dimming targets	92
3.21	Required instantaneous data rate for different dimming targets . .	93
3.22	BER distribution for adaptive data rate	94
3.23	Flowchart of the proposed scheme	96
3.24	Power consumed by the investigated schemes for different levels of dimming target (d)	97
3.25	Overall comparison of the proposed scheme and standard digital dimming scheme for different values of dimming target in terms of illuminance (left), power consumption (middle) and achievable data rate (right)	98
3.26	Concept of VLC system integrated with an intelligent lighting framework	101
4.1	Experimental setup for characterization of the luminous response of the RGBA LED	105
4.2	LVI response of the RGB LED	106

4.3	Normalized spectral power distribution of the LED and photodiode responsivity for different wavelengths in the visible range.	106
4.4	Experimental Setup of WDM VLC System utilizing a single RGBA LED as its transmitter	108
4.5	Flow chart associated with optimization of biasing conditions and validation of experimental and simulation based results	113
4.6	Spectral power distribution for CCTs of 2700K, 3500 K and 6500 K for RGB LED-based VLC.	114
4.7	BER distribution as function of data rate for separate channels at each color temperatures.	115
4.8	Eye diagram of the blue channel for CCT of a) 2700 K, b) 3500 K and c) 6500 K.	116
4.9	Dimming schemes utilized to control the CCT of emitted light for the WDM-VLC system.	117
4.10	The x,y coordinates for digital dimming and slot utilization in the CIE 1931 diagram and their position in the MacAdam ellipse at SDCM of 2700 K.	120
5.1	Experimental setup for characterizing LVI response of LDs.	126
5.2	LVI characteristics of (a) HL6501MG (b)PL520 (c) PL450B LDs.	127
5.3	Normalized spectral power distribution of the LDs and photodiode responsivity for different wavelengths in the visible range.	128
5.4	Experimental setup of WDM VLC utilizing LDs to generate white white light while providing communication.	129
5.5	Simulation of BER distribution against received power for each channel at their maximum achievable data rate	130
5.6	Methodology used for CCT regulation and generation of high quality lighting for a LD-based VLC system	132
5.7	BER distribution as a function of data rate for red, green and blue laser diodes for a link distance of 2.15m for link operating at maximum biasing conditions.	134
5.8	Normalized SPD and the corresponding CIE 1931 diagram for the RGB LD-based VLC System.	135
5.9	Normalized spectral power distribution for CCTs of 2700 K, 3500 K and 6500 K for RGB LD-based VLC system.	136
5.10	Experimental setup of RRGB LD-based VLC utilizing 2 red LDs along with green and blue LD to generate white white light while providing communication.	139
5.11	Normalized spectral power distribution for CCTs of 2700 K, 3500 K and 6500 K for RRGB LD-based VLC system.	140
5.12	Experimental setup for measurement of speckle patterns	143
5.13	(a) 3D autocad drawing of vibrating mount for diffuser (b) Speckle pattern obtained from MIS and random points selected to calculate intensity fluctuations	144
5.14	(a) Speckle contrast ratio for different LDs (b) Speckle patterns for different LDs	144

5.15	(a) Speckle contrast ratio for warm, neutral and cool-white light generated from RGB LDs (b) Speckle patterns for different CCTs of light generated	145
5.16	Speckle contrast ratios of different types of diffusers	148
5.17	Experimental setup for psychophysical evaluation of human preference of LD-based and LED-based lighting	149
5.18	Bar charts of preferences for visual comfort, color rendering, saturation, contrast, naturalness, brightness and pleasantness	151
5.19	Overall preference of participants for LED/LD	153
5.20	Concept of practical implementation of CCT regulation of LD-VLC for an office space	156
6.1	Methodology implemented for development and evaluation of LED-LD hybrid VLC system	159
6.2	Step response, derivative impulse function and FFT of the derivative (frequency response of the investigated system)	161
6.3	Analytical and experimental frequency response of the pc-LED after blue filtering	162
6.4	Frequency responses of blue LD (PL450B), red LD (HL63163DG), green LD (L520P120), pc-LED (Osram LCW) and RGB-LED (LED Engin RGBA)	163
6.5	Thermal performance of pc-LED and green LD over a span 430 seconds	164
6.6	LVI responses of LD for different case temperatures	165
6.7	Experimental setup for measurement of illumination quality of hybrid LED-LD-based VLC utilizing a red LD and a neutral white LED array	167
6.8	Normalized spectral power distribution of Case 1 along with the coordinates in the CIE 1931 diagram	168
6.9	Normalized spectral power distribution of Case 2 along with the CIE 1931 diagram	168
6.10	Normalized spectral power distribution of Case 3 along with the CIE 1931 diagram	169
6.11	a) CRI of individual colors for the three cases (b) Overall CRI of the investigated cases	171
6.12	Experimental setup of hybrid LED-LD-based VLC utilizing a red LD, which is directly modulated along with a neutral white LED array used for communication exclusively	172
6.13	BER and CRI distribution for case 1	173
6.14	BER and CRI distribution for case 3	174

List of Tables

2.1	Effect, mood and applications of different color temperatures	28
2.2	Acceptable CCT and D_{uv} Range for different nominal CCTs	30
2.3	Comparison of different types of transmitters for VLC	40
2.4	Qualitative comparison of popular modulation schemes	40
2.5	Recent progress in LED-based VLC	43
2.6	Summary of work done for dimming in NRZ-OOK based VLC systems	56
2.7	Comparison of CCTs and CRIs achieved for LD-based VLC systems	58
2.8	Laser safety classes based on transmitted power	61
3.1	System description	70
3.2	System parameters for analytical model of LED-based VLC system	76
3.3	Overall Comparison of Dimming Schemes for CCT Regulation	100
4.1	System parameters for simulation of RGB WDM LED-VLC link	109
4.2	System parameters for analytical model of RGB WDM LED-VLC link	112
4.3	Biasing conditions required for target CCTs for RGB LED-based VLC	114
4.4	Analytical, simulation based and experimental BER values for different CCTs	116
4.5	Photometric results of digital dimming and slot utilization for achieving CCT of 2700 K	119
4.6	Overall Comparison of Dimming Schemes for CCT Regulation	121
5.1	Ratings of the LDs used for the WDM-LD-VLC	126
5.2	System parameters for simulation of RGB WDM LD-VLC link	130
5.3	System Parameters for Analytical Model of RGB LD-based VLC	131
5.4	Result from experimental LD-based VLC System	134
5.5	Biasing conditions required for target CCTs for RGB LD-based VLC	135
5.6	Photometric results for targeted CCTs of RGB LD-based VLC system	136
5.7	Communication performance of adaptive dimming schemes for CCT regulation of blue channel	138
5.8	Photometric results for targeted CCTs of RRGB LD-based VLC system	140

5.9	BER and maximum achievable data rate for each channel of RRGB LD-based VLC for different CCTs	141
5.10	Simulation results of LD-VLC at different CCTs	142
5.11	Summary of statistical data for psychophysical evaluation of LD and LED-based lighting	152
6.1	Comparison of photometric parameters for different investigated cases of hybrid LED-LD-based VLC system	171
6.2	Comparison of parameters concerning communication for different scenarios of hybrid LED-LD-based VLC system	175
6.3	Simulation of different configurations of hybrid LED-LD-based VLC system	176
7.1	Overall summary of key outcomes and investigated parameters . .	184

Acronyms

ANSI	American National Standards Institute
APD	Avalanche Photodiode
AWG	Arbitrary Waveform Generator
BER	Bit Error Rate
CCR	Constant Current Reduction
CCT	Correlated Color Temperature
CFL	Compact Fluorescent Lamp
CIE	International Commission on Illumination
CMOS	Complementary Metal Oxide Semiconductor
CPFM	Constant Pulse Frequency Modulation
CQS	Color Quality Scale
CRI	Color Rendering Index
CSK	Color Shift Keying
CT	Color Temperature
CZFM	Constant Zero Frequency Modulation
DC	Direct Current
DD	Direct Detection
DFE	Discreet Feedback Equalization
DWDM	Dense Wavelength Division Multiplexing
EM	Electro Magnetic
EMI	Electromagnetic Interference
FEC	Forward Error Correction
FM	Frequency Modulation
GAI	Gamut Area Index
IEEE	Institute of Electrical and Electronics Engineers
IM	Intensity Modulation
InGaN	Indium Gallium Nitride
IoT	Internet of Things
IR	Infra-Red
IrDA	Infra-Red Data Association
ISI	Inter Symbol Interference
JEITA	Japan Electronics and Information Technology Industries

	Association
LD	Laser Diode
LD-VLC	LD-based VLC
Li-Fi	Light Fidelity
LED	Light Emitting Diode
LMS	Least Mean Squares
LOS	Line of Sight
LVI	Luminous Flux - Forward Voltage - Forward Current
MATLAB	MATrix LABoratory
μ -LED	Micro Light Emitting Diode
MIS	Multispectral Imaging System
MIMO	Multiple Input Multiple Output
NLOS	Non Line of Sight
NRZ-OOK	Non-Return to Zero On-Off-Keying
OFDM	Orthogonal Frequency Division Multiplexing
OLED	Organic Light Emitting Diodes
OOK	On-Off Keying
OWC	Optical Wireless Communication
PAM	Pulse Amplitude Modulation
PAPR	Peak to Average Power Ratio
PCE	Power Conversion Efficiency
Pc-LED	Phosphor Converted Light Emitting Diode
PD	Photo Diode
POF	Plastic Optical Fiber
PPM	Pulse Position Modulation
PSD	Power Spectral Density
PSK	Phase Shift Keying
PWM	Pulse Width Modulation
QAM	Quadrature Amplitude Modulation
RAGB	Red, Amber, Green, Blue
RC-LED	Resonant Cavity Light Emitting Diode
RF	Radio Frequency
RGB	Red, Green, Blue
RPO-OFDM	Reverse Polarity Optical Orthogonal Frequency Division Multiplexing
RRGB	Red, Red, Green, Blue
SDCM	Standard Deviation of Color Matching
SDVLC	Software Defined Visible Light Communication
SLM	Spatial Light Modulator
SNR	Signal to Noise Ratio
SPD	Spectral Power Density
SSL	Solid State Lighting
SU	Slot Utilization
TEC	Thermoelectric Cooler
TIA	Trans Impedance Amplifier

TOV	Turn-On-Voltage
UV	Ultra Violet
VLC	Visible Light Communication
VLCC	Visible Light Communications Consortium
VOOK	Variable On-Off Keying
VPPM	Variable Pulse Position Modulation
Wi-Fi	Wireless Fidelity
WDM	Wavelength Division Multiplexing
YAG	Yttrium Aluminum Garnet

INTRODUCTION

Imagine a world, where ubiquitous internet connectivity can be obtained from over 14 billion light points operating all across our planet. This vision can be turned into reality by visible light communication (VLC), an emerging technology which uses light sources as transmitters by encoding information into the current driving them. With the exponential growth of wireless communication devices, the rapidly dwindling radio frequency spectrum, the futuristic aspects of internet of things (IoT) and the recent trend towards solid state lighting, the prospects and scopes of implementing VLC eventually leading to light fidelity (Li-Fi) access points catering to various applications is very promising.

1.1 The Recent Drive Towards VLC

Li-Fi was listed in *Time Magazine's* 50 best inventions of 2011, when first coined by Harold Haas at a TED Talk event in 2011 [1, 2]. In 2015, an Estonian start up group, Velmenni demonstrated speeds of upto 1 Gb/s using a Li-Fi enabled light bulb which sparked the news claiming Li-Fi to be 100 times faster than the traditional wireless fidelity (Wi-Fi) [3]. The fundamental aspects of Li-Fi technology is built around VLC by considering link level algorithms, networking protocols and security [4]. This means, VLC is a paramount part, when the implementation of Li-Fi is considered for practical applications, especially when physical layer and

front-end components are being considered.

The earliest known use of VLC comes from Alexander Graham Bell, who in 1880 developed a photophone which transmitted voice data over 200 m using beams of sunlight [5]. Several other demonstrations featuring fluorescent lights for communication were investigated, with low data rates [6]. In 2001, RONJA (reasonable optical near joint access) used visible light beams to transmit data at 10 Mb/s over 1.4 km [7]. Utilizing white LEDs for illumination and communication began to take shape in the early 2000s in Japan, pioneered by Tanaka *et al.* at Keio University [8]. In 2003, the visible light communication consortium (VLCC) was founded to promote and standardize VLC technology [9]. The IEEE 802.15 working group for wireless personal area networks (WPAN) established the IEEE 802.15.7 VLC task group and chartered it to write PHY and MAC standards for VLC in 2011 [10].

At the end of 2016, global mobile data traffic reached 7.2 exabytes per month, accounting for a 63 % increase compared to 4.4 exabytes per month at the end of 2015 [11]. Around half a billion mobile devices and connections were added in 2016 [11]. Besides getting smarter in computing capabilities, these wireless communication devices are also expanding from lower generation network connectivity (2G) to higher-generation network connectivity (3G, 3.5G and 4G/LTE)

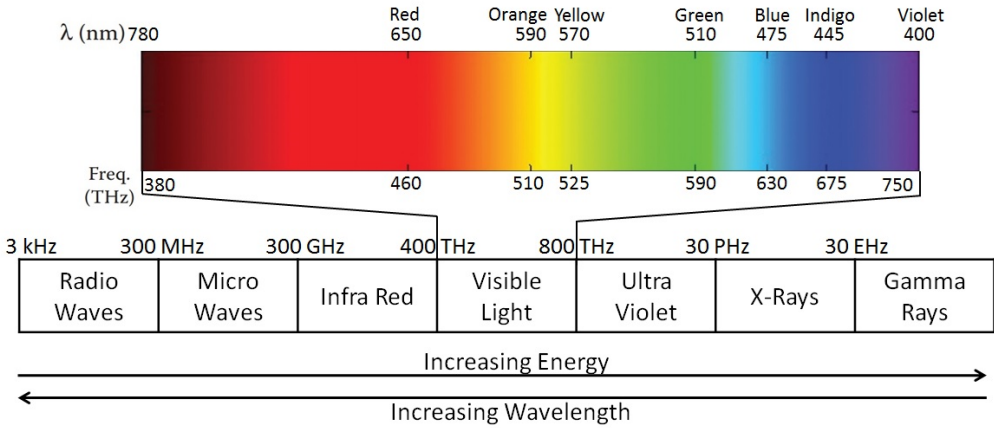


Figure 1.1: Electromagnetic spectrum

[12]. It is estimated that 5G connections will appear on the scene in 2020 and will grow by more than a thousand percent with even higher bandwidth requirements (above 1 Gb/s) [11]. This unprecedented growth of wireless communication devices and the expeditiously evolving connectivity standards are creating a huge pressure on the limited spectrum of radio frequency (RF) [13]. To enhance capacity, acquiring new spectrum is economical compared to building more base stations [14]. Although there have been developments in the Terahertz frequency range (between RF and microwave spectrum), it would require creating an entirely new class of infrastructure [15, 16]. Visible light on the other hand has 10,000 times larger unregulated spectrum (~ 400 THz) as depicted in Figure 1.1 and needs no additional acquirement cost [17].

Besides spectrum availability, the global trend of replacing incandescent and fluorescent light bulbs with energy efficient light emitting diodes (LEDs) is another vital reason for the increasing attention towards VLC, because that will allow this technology to be implemented into existing lighting infrastructures into sources which are available everywhere [18]. Unlike traditional light sources, LEDs can be switched at much higher speeds which VLC can fully capitalize on. LED installations increased from 215 million in 2014 to 874 million units in 2016 and provided energy savings equivalent to 4.7 billion dollars [19]. The value based market share of LEDs is expected to reach 60 % by 2020 [20]. Thus LiFi enabled LED bulbs can provide ubiquitous communication services opening doors to the IoT. Although LEDs are superior to traditional light bulbs, their modulation bandwidth is still limited when gigabit class communication is being considered for 5G standards. Recently, laser diodes (LDs) had been demonstrated to generate high quality lighting without compromising the user experience [21]. This brings them into the vital consideration of providing communication at even higher speeds.

Figure 1.2 summarizes the key outcomes associated with the evolution of cel-

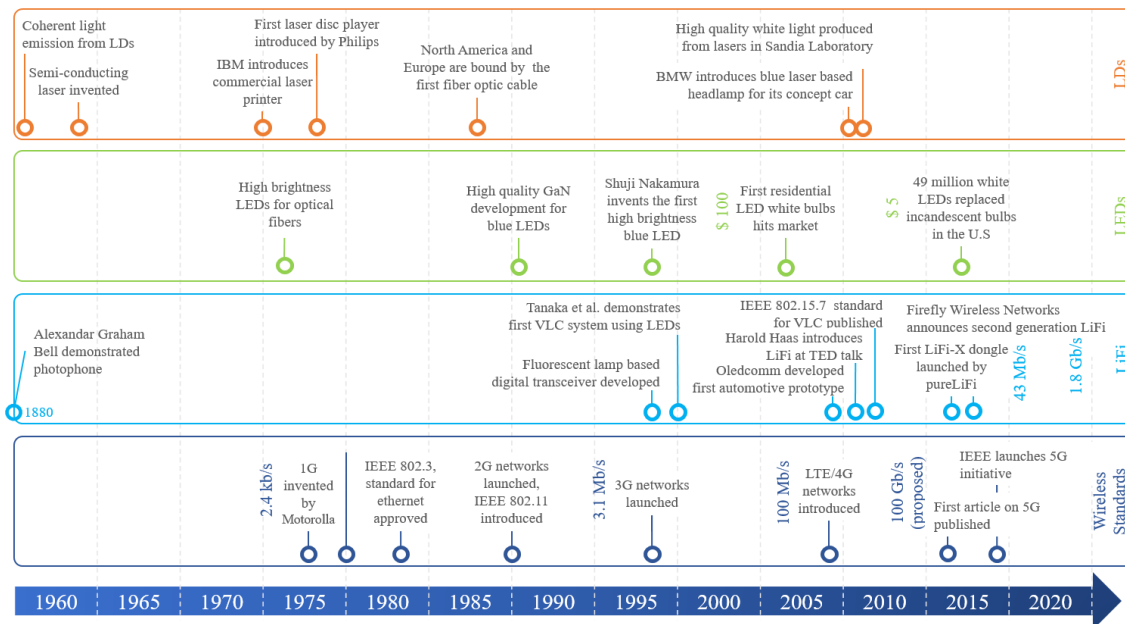


Figure 1.2: Timeline of evolution of wireless standards, LiFi, LEDs and LDs

lular technology, LiFi systems, LEDs and LDs. It is clearly evident, that each of these fields are rapidly evolving with significant improvements being made regularly. Thus the incorporation and consolidation of these unique fields of technology is an interesting aspect to consider for rapid practical adaptation of VLC.

1.2 Focus of Thesis

Optical wireless communication (OWC) is an established technology that requires the transmission of information-laden optical radiation through the free-space channel [22]. The optical domain of the electromagnetic spectrum consist of infra-red (IR), visible and ultra-violet (UV) radiation which occupies the frequency range of 300 GHz to 30 PHz as shown in Figure 1.1. VLC is an extension of OWC which generally uses a fast switching LED or LD as its source and possesses the ability to simultaneously provide illumination and communication for short range indoor links [23]. As an indoor OWC technology, VLC has several advantages. It is intrinsically safe, has no health concerns, provides better security and does not cause any electro-magnetic interference (EMI) [24, 25, 26]. All

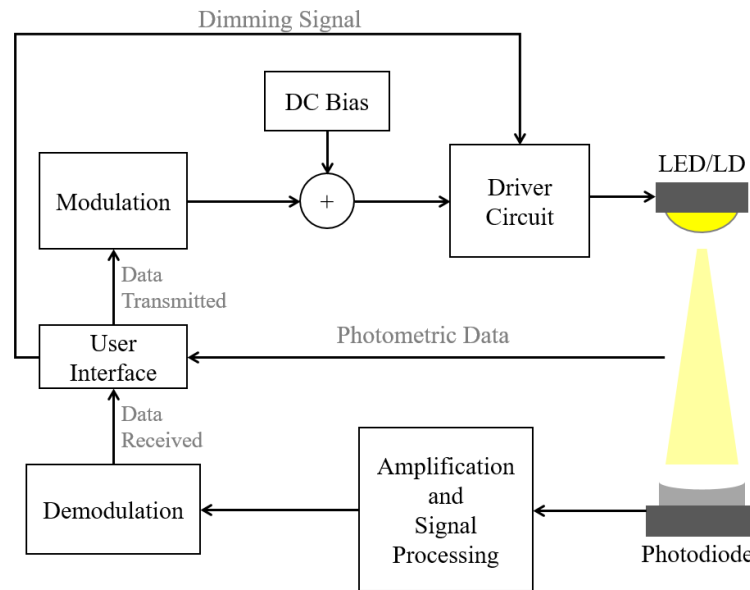


Figure 1.3: Functional block diagram of a dimmable LED/LD-based VLC system

these unique characteristics made VLC a subject of increasing interest and development [23]. A generalized block diagram depicting the functionality of VLC is presented in Figure 1.3. The data that needs to be transmitted from the user is modulated into an electrical signal, a DC offset is then added to the modulating signal to ensure it is within the linear operating region of the optical source, dimming signal that is required for control of illumination is then added by means of a driver circuitry based on the dimming requirement of the user. The transmission takes place across free space and then the received optical signal is converted back to an electrical signal by the photodiode, which is received by the user after signal processing and demodulation [27].

VLC is uncommon compared to most of the communication technologies, due to its bifold functionality of communication and illumination [28]. Thus, apart from high speed communication, high integrity color quality controlled lighting must be provided by commercially competent VLC systems [28]. Most of the work done on VLC systems had solely focused on the communication aspects, although some factors had been considered, there are other important aspects re-

garding human factor component and illumination features that need to be considered [29, 30].

For practical VLC systems, an end user would expect to have high speed wireless communication alongside full control over illumination. This makes ‘dimming functionality’ an obligation for consideration [31]. Dimming control can provide energy savings and ecological benefits which are key considerations in the recent trend towards conservation of natural resources [32]. However dimming has an adverse effect on communication since it fixes the average intensity of a light source according to user requirement thereby reducing the achievable data rate [33]. One of the main advantages of VLC is high speed indoor communication and due to dimming control this might get undermined. Dimming can be either achieved by pulse regulated schemes, which utilizes pulse trains to drive the LEDs or analog dimming (commonly referred to as continuous current reduction (CCR)) that requires the regulation of current amplitude. Pulse regulated schemes can be classified into frequency modulation (FM) and pulse width modulation (PWM). Despite investigation of driver circuitry efficiency under pulse regulated dimming schemes for white LEDs [34], these schemes had not been compared in terms of photometric parameters like correlated color temperature (CCT), color rendering index (CRI) and linearity in dimming. CCT is a measure of appearance of white light. CRI is also an important parameter, which is the most widely accepted measure of color rendering capabilities of a light source. This raises a research question:

1. How does FM perform compared to PWM when photometric parameters such as CRI, CCT and linearity of illuminance are being considered?

On the other hand, although CCR is the simplest form of dimming, there had been reports of certain chromaticity shifts in phosphor converted LEDs (pc-LEDs) due to its use [35]. Chromaticity shifts are undesirable in standard lighting appli-

cations, since occupants can observe changes in color of emitted light and illuminated objects. Compared to CCR, PWM scheme achieves dimming more linearly [36]. Thus for a pc-LED-based VLC system, an important inquiry needs to be done:

2. How much chromaticity shift is induced when CCR and PWM are implemented in a VLC system?

When dimming schemes are consolidated with communication, each technique has its own separate adverse effect on communication depending on its type [23]. For CCR scheme, the optical power at the receiver is affected due to transmission of bits with lower amplitude at higher dimming requirements. PWM scheme hampers the data rate by transmitting bits only when the duty cycle is high. Although adaptive schemes like rate adaptation (RA) and slot utilization (SU) had been proposed previously which allows concurrent data transmission and PWM dimming [37, 38, 39], these works do not aim at characterizing the impact of the modification made to the pre-existing dimming schemes on the photometric results. SU involves the transmission of superimposed bits when the duty cycle is low, which can have an impact on the average illuminance and precision of dimming (i.e. the expected level of illuminance at a dimming target and the achieved level of illuminance). The bandwidth limitation of LEDs is another factor, which limits the extent of utilizing RA. Thus, the combination of multiple dimming techniques to develop an adaptive dimming algorithm, which can fully capitalize on the limitations set by each and achieve superior dimming and seamless communication is a promising aspect for consideration. These issues raises the following research questions:

3. How does transmission of bits when the duty cycle is low in slot utilization affect the overall illuminance and does it hamper the dimming precision?
4. Can different adaptive schemes be simultaneously utilized to subdue the

stringent requirement on either of them enabling dimming with better performance in terms of communication?

Wavelength division multiplexed (WDM) VLC systems utilizing red-green-blue (RGB) sources can provide significant improvement to the transmission capacity by utilizing parallel channels. RGB sources provide possibilities of tuning individual colors which helps in controlling the color temperature of the white light being generated [40]. Color temperature changes the emotional effect of a space and has a profound impact on the appearance, productivity and environment of illuminated objects, occupants and space [41]. Thus controllability of CCT is a promising feature ideal for next generation intelligent lighting solutions where VLC system can provide high speed wireless communication and high quality controllable illumination. Although the effect of CCT on communication aspects of VLC had been analyzed theoretically in certain works [42, 40, 29], to the best of our knowledge, there has been no work on using adaptive dimming schemes predominantly used for dimmable VLC systems using white LEDs for CCT regulation. For generating warmer light, the biasing current for the blue channel needs to be limited. Regulating the blue channel using CCR can cause the bit error rate (BER) to increase, while PWM can decrease the achievable bit rate. In such a scenario, adaptive schemes like RA and SU can help in controlling the intensity of the blue channel, while maintaining the data rate at an acceptable BER raising another open issue:

5. Can adaptive dimming schemes be implemented for regulating the CCT of RGB LED-based VLC systems for maintaining the data rate and the BER of the system at acceptable limits?

Although RGB LEDs can give higher aggregate data rate compared to white LEDs, the modulation bandwidth for off-the-shelf LEDs is considered to be quite low for gigabit class communication [43]. LDs on the other hand exhibit much

higher modulation bandwidth (i.e. the available bandwidth to transmit data), which are at least an order of magnitude higher [44]. Besides this advantage, the narrow emission profile of LDs creates opportunities for utilizing dense WDM for higher data rates and greater rejection of ambient noise by using narrow optical filters [44]. Till date, most of the LD-based VLC systems had generated white light with very high correlated color temperature (CCT) (~ 8000 K) which is quite high when practical illumination systems are being considered [45, 46, 47]. Thus, it is necessary to develop LD-based VLC systems operating at realistic CCTs in the cool white to warm white region for facilitating practical adoption. The power of the blue and green channels is normally moderated to obtain high quality illumination with CCTs near the warmer region for LD-based lighting [48]. This moderation of blue LDs can be achieved by implementing adaptive techniques or utilizing higher number of red LDs. Adaptive dimming schemes can lead to a LD-based VLC system with CCT controllability which had not been demonstrated till date. Higher number of red sources can capitalize on the narrow emission profile of LDs for increasing aggregate data rate. Although this was briefly suggested in [44], a practical system employing multiple LDs in parallel apart from the conventional RGB based configuration had not been demonstrated experimentally. Laser based lighting also have speckle patterns due to high coherence of the sources, which can have adverse effects on the health [49]. Laser speckles can lead to eye irritation and headaches under prolonged observation by occupants [50]. Although different methods utilizing homogenizer, rotating diffusers and piezoelectric actuators achieved speckle reduction for projection systems, to the best of our knowledge, no work has been done in characterizing and reducing speckle in a VLC system [51, 52, 53]. Human perception towards the LD-VLC system is also required to be quantified by psychophysical evaluation, to validate that the system is competent for practical implementation. Therefore, for RGB LD-based VLC systems, the issues which need to be addressed are:

6. Can adaptive dimming schemes be implemented for regulating the blue and green channels to generate light within the usable CCT range and safety standards for RGB LD-based VLC systems?
7. Can easily incorporable vibrating diffuser mitigate speckles in the white light generated from a LD-based VLC system?
8. How is the human perception of LD-based lighting in comparison to LED-based lighting in terms of overall preference, contrast, saturation, visual comfort, naturalness of colors and pleasantness?

Another major drawback of LD-based lighting is the low CRI caused by spectrum discontinuity, arising from the narrow emission profiles of LDs. This can be effectively resolved by adding a pc-LED to the system which helps in creating a broader spectrum. RGB-LEDs cannot be considered for such a case because their spectral profile is a wider version of the profiles of RGB-LDs. Although pc-LEDs have higher CRI than RGB-LEDs and LDs, the value is still quite low in comparison to incandescent sources. This occurs due to the inability of pc-LEDs in generating light in the higher wavelength region, which under-saturates red colors. LED manufacturers like Epistar and Siemens have announced that adding a red LED to white phosphor based LED improves color temperature and energy efficiency of the light [54, 55]. A hybrid system where a LED is used for illumination and spectrum continuity and a LD is used for communication and red enhancement can be used to effectively avoid each of the source's lackings. In [55], such a system was proposed where a single red LD was used alongside white LED to obtain a CRI of 83 and a CCT of 4767 K at, a data rate of 500 Mb/s. However, general white LEDs already have CRIs of ~ 75 and this increase is not sufficient and multiple LDs can be incorporated to the system for higher achievable data rate. Thus, an experimental investigation of multiple LED-LD hybrid configuration needs to be carried out which would result in an overall hybrid LED-LD

based VLC system capable of providing gigabit class communication alongside high quality illumination. Thus an important research investigation that needs to be conducted is:

9. Is it possible to employ red enhancement to obtain a high value for CRI for LD and pc-LED based lighting system?

The focus of the thesis is on answering the key questions that were raised considering the three sources pc-LEDs, RGB LEDs and RGB LDs. All the investigation were conducted considering the parameters associated with communication and photometry by experimental analysis, simulation and analytical validation.

1.3 Organization of Thesis

The rest of the chapters in the thesis are organized as follows:

Chapter 2: LED and LD-based VLC under Illumination Constraints surveys the relevant literature associated with LED and LD-based VLC systems. The parameters associated with communication and illumination are discussed which were used in subsequent parts of this thesis. Different types of transmitters that can be used in VLC were discussed with the focus being towards pc-LED, RGB LED and LDs. Modulation schemes that had been predominantly used along with dimming techniques implemented for intensity regulation for LEDs and methods of incorporating data with dimming signal are explained. Finally, the key outcomes reported in the literature for concurrent illumination control alongside data transmission with these three sources are discussed and linked to the research questions.

Chapter 3: Dimmable pc-LED-VLC System with Concurrent Data Transmission focuses on the implementation and investigation of different dimming techniques for a pc-LED based system. Research questions 1, 2, 3 and 4 are answered

in this chapter. It lays out the fundamental analytical model used for theoretical calculation of OWC links and investigates each dimming techniques experimentally and by simulation, which leads to the proposed adaptive dimming algorithm.

Chapter 4: RGB-LED-based VLC System with Enhanced Illumination moves towards WDM based system using RGB LED for increasing the overall data rate. It focuses on the CCT regulation aspects and discusses the simulation framework that had been designed for the VLC system. The effect of CCT regulation on the performance of each channel is individually analysed and adaptive techniques are implemented to diminish the loss of capacity, which answers research question 5, discussed in the previous section.

Chapter 5: RGB-LD-based VLC System with Enhanced Illumination directs at employing the CCT regulating framework developed in the previous chapter into RGB LD-based system for achieving gigabit class communication. The impact of CCT regulation on each channel is characterized and based on that adaptive techniques and modifications of link configuration are investigated, which answers research question 6. The challenges with presence of speckles is identified and by means of subjective and objective testing of a proposed vibrating diffuser module, homogeneous illumination is ensured from the LD-based VLC system, which answers research question 7 and 8.

Chapter 6: Hybrid LED-LD-based VLC System with Superior Color Rendering focuses on the possibilities of combining LEDs and LDs for a hybrid system which can have superior capabilities compared to each system being operated individually. The fundamental differences between LEDs and LDs are experimentally characterized and a hybrid system with multiple LDs and LEDs is proposed on

the basis of experimental validation that answers the final research question.

Chapter 7: Conclusion summarizes the major outcomes from this thesis and outlines the future work that can be pursued in this area.

1.4 Contribution of Thesis

The contribution of each chapter in this thesis are outlined and explained in detail below:

1. **Chapter 2:** A comprehensive literature survey is compiled looking into the relevant areas associated with pc-LED, RGB LEDs and LDs. This chapter provides the foundation based on what the key contribution were identified for the subsequent chapters. The review highlights
 - (a) Properties and limitations of different transmitters when considered for simultaneous communication and illumination
 - (b) Classification of pulse regulated schemes and the lack of photometric quantification of their effect on LED dimming
 - (c) Properties of analog and digital dimming schemes and the importance of consideration of chromaticity shifts when dimming is investigated for lighting applications
 - (d) Impact of digital dimming on communication capacity, the utilization of adaptive schemes for maintaining transmission under digital dimming and limitation of quantification of dimming shift introduced by these schemes
 - (e) Prospects of simultaneous implementation of adaptive schemes to alleviate the limitations of exclusive utilization of these schemes

- (f) Benefits of CCT regulation and the possibilities of implementation of adaptive schemes for controlling the CCT for WDM based VLC utilizing RGB LEDs and LDs
 - (g) Lack of speckle pattern characterization in LD-VLC systems and scopes of designing an attachable diffuser mitigating module
 - (h) Inadequate investigation of human perception towards LD-based VLC lighting involving aspects like naturalness, saturation, pleasantness and overall preference
 - (i) Limitations of pc-LEDs, RGB LEDs and RGB LDs in terms of CRI in comparison to incandescent sources and prospects of combination of LEDs and LDs for hybrid systems that can capitalize on their unique features for an overall balanced performance regarding communication and illumination
2. **Chapter 3:** This chapter proposes a novel dimming algorithm for a pc-LED based VLC system. This is achieved based on:
- (a) Accurate characterization of pulse regulated schemes which justifies the utilization of PWM compared to FM based on linearity in illuminance distribution, CCT and CRI
 - (b) Quantification of chromaticity shifts induced by CCR compared to PWM for a NRZ-OOK based VLC system
 - (c) Development of an experimental framework which incorporates NRZ-OOK data with CCR, PWM, SU and RA schemes
 - (d) Photometric quantification of the dimming shift caused by SU scheme
 - (e) Limitation imposed by RA considering the slow modulation response of LEDs in a practical scenario

- (f) Characterization of the proposed dimming algorithm in terms of power consumption, dimming linearity, achievable data rate and BER distribution in comparison to the widely accepted PWM dimming
3. **Chapter 4:** This chapter provides a mapping of effective adaptive dimming schemes for CCT regulation in a RGB-LED based VLC system on the basis of:
- (a) Characterization of influence of color temperature on the transmission capacity of RGB LED-based VLC
 - (b) Development of an analytical framework which formulates the biasing condition of a RGB LED based on target CCT
 - (c) Formulation of a simulation framework that closely replicates the experimental link that is ideal for instantaneous analysis
 - (d) An RGB LED-based WDM VLC system operating at a CCT range of 2700 K - 6500 K by utilizing adaptive dimming schemes, where the target data rate was maintained at an acceptable BER
4. **Chapter 5:** This chapter looks into the challenges associated with CCT regulation and homogeneous illumination for LD based VLC system. The specific contributions are:
- (a) Characterization of influence of color temperature on the transmission capacity of RGB LD-based VLC
 - (b) Investigation of different link configurations of WDM LD-based VLC systems for realistic CCT and high quality illumination
 - (c) Enhancement of individual link performance by incorporation of adaptive schemes for CCT regulation
 - (d) Analysis of dense WDM link configurations for enabling operation of LD-VLC at lower CCTs without the utilization of adaptive schemes

- (e) Quantification and investigation of presence of speckle in LD-based illumination
 - (f) Design and implementation of a vibrating diffuser that mitigates speckle by destroying spatial coherence
 - (g) Subjective examination of LD-VLC lighting by human participants based on factors of naturalness, pleasantness, overall preference etc.
5. **Chapter 6:** This chapter combines the sources used in the previous chapters and proposes a hybrid system with superior color rendering capabilities on the basis of:
- (a) Quantitative comparison of LEDs and LDs under a single experimental framework regarding bandwidth, thermal and beam characteristics
 - (b) Experimental characterization of CRI due to different configurations of hybrid LED-LD based sources
 - (c) Investigation of BER performance of different link configurations of hybrid LED-LD VLC system
 - (d) Simulation of maximum achievable data rate for hybrid LED-LD VLC system

1.5 Publications

During the course of this project, a number of journal and conference papers were published based on the work presented in this thesis. A few more manuscripts were submitted for publication, which are currently under review.

1. D. Karunatilaka, **F. Zafar**, V. Kalavally, and R. Parthiban, "Led based indoor visible light communications: State of the art," *IEEE Communications Surveys Tutorials*, vol. 17, no. 3, pp. 1649-1678, 2015 [56].
2. **F. Zafar**, D. Karunatilaka, and R. Parthiban, "Dimming schemes for visible light communication: the state of research," *IEEE Wireless Communications*, vol. 22, no. 2, pp. 29-35, 2015 [23].
3. **F. Zafar**, M. Bakaul and R. Parthiban, "Laser-Diode-Based Visible Light Communication: Toward Gigabit Class Communication," in *IEEE Communications Magazine*, vol. 55, no. 2, pp. 144-151, 2017 [57].
4. **F. Zafar**, V. Kalavally, M. Bakaul, and R. Parthiban, "Experimental investigation of analog and digital dimming techniques on photometric performance of an indoor visible light communication (vlc) system," in *Fourteenth International Conference on Solid State Lighting and LED based Illumination Systems*, vol. Proc. SPIE 9571,, San Diego, California, USA, 2015, pp. 95710D957108 [33].
5. **F. Zafar**, V. Kalavally, and R. Parthiban, "Effect of Slot Utilization Dimming Scheme on the Photometric Performance of a High Speed Visible Light Communication (VLC) System," in *15th International Symposium on the Science and Technology of Lighting*, Kyoto, Japan, 2016 [58].
6. D. Karunatilaka, **F. Zafar**, V. Kalavally and R. Parthiban, "A viable model for SNR determination in OFDM based visible light communication systems," *IEEE Summer Topicals Meeting Series (SUM)*, Nassau, 2015, pp. 53-54 [59].

7. **F. Zafar**, M. Bakaul, and R. Parthiban, "Adaptive Dimming Scheme for Visible Light Communication under Lighting Constraint," *IEEE Wireless Communications* [Under Review].
8. **F. Zafar**, M. Bakaul, and R. Parthiban, "Adaptive Dimming Schemes for Regulating the Color Temperature in NRZ-OOK based WDM VLC Systems," *IEEE Photonics Technology Letters* [Under Review].
9. **F. Zafar**, T. Navodya, M. Bakaul, and R. Parthiban, "Enhancing the Illumination Aspects of Laser-Diode-Based Visible Light Communication (LD-VLC)," *IEEE Communications Magazine* [Under Review].
10. **F. Zafar**, M. Bakaul, and R. Parthiban, "Hybrid LED-LD Visible Light Communication System with Enhanced Color Rendering Capabilities," *Journal of Lightwave Technology* [Under Review].

LED AND LD-BASED VLC UNDER ILLUMINATION CONSTRAINTS

2.1 Introduction

The increased wireless data traffic from the rapidly growing wireless mobile devices is creating a pressure on the dwindling radio frequency (RF) spectrum, which is driving the needs of alternative technologies [23]. Mobile data will grow 6.3 times between 2013 and 2018 and the growth will be strongest outside Europe and North America [60]. The global appetite for wireless broadband data access is increasing by the day, with forecasts of a 18 fold increase in mobile traffic in 2016 compared to 2011, fueled by the smartphone, laptop and tablet popularity [56]. There have been developments to use up the Terahertz frequency range, which lies between the RF and microwave spectrum, but it would mean creating an entirely new class of infrastructure compatible with the wavelength band [15, 16]. On the other hand, visible light has 10,000 times greater spectrum than radio waves (radio waves correspond to a frequency band of ~ 3 kHz to ~ 300 GHz, while the visible light correspond to a frequency band of ~ 400 THz to ~ 780 THz) [61].

The growing trend towards replacement of traditional lighting infrastructures with energy efficient LEDs is one of the driving force behind the increasing at-

tention towards VLC. If all conventional light sources are replaced by LEDs, the global electricity consumption would reduce by as much as 50 percent [62], the CO_2 emissions will reduce by over 10 gigatons and crude oil consumption by 962 million barrels, amounting to financial savings in excess of one trillion dollars, and energy savings of 1.9×10^{20} joules over a decade [63]. According to a U.S Department of Energy report, by the year 2025, solid state lighting (SSL) technology has the possibility of providing energy savings of up to 217 terawatt-hours (TWh) [64]. Unlike the widely used compact fluorescent lamps (CFLs) and incandescent bulbs, LEDs can be switched at much higher rates. Thus, these devices can be exploited to provide a dual role as a communication device besides providing illumination [65]. Recently, LDs are even emerging as potential candidates for illumination, which can even provide higher data rates for VLC [66, 44].

The prospects of easy implementation into existing lighting systems with the addition of a few cheap front-end components operating in baseband can open the scopes of getting communication as a complimentary technology to illumination, which makes VLC an area of increasing industrial interest and research [67, 68].

2.2 Benefits of VLC

Communication by visible light had been gaining popularity in the recent years, which is driven by several factors:

- *Unregulated Spectrum:* The RF spectrum traditionally used for communication is a natural resource of the state, and its usage is regulated to remove signal interference and pollution, as well as for efficient spectral usage [69]. It is cheaper for mobile operators to acquire spectrum, rather than building more base stations to enhance capacity [14]. As the demand for wireless data transmission is constantly increasing, the radio frequency spectrum is becoming increasingly congested [70]. Thus the remaining spectrum is dwindling and spectral management is fast becoming a concern [71]. Due to explosions in data usage, there is a major concern for mobile operators to focus on public Wireless Fidelity (Wi-Fi) and other alternative technologies. Level one mobile network operators expect 22% of their capacity they add in 2013 to come from public Wi-Fi and by 2018, 75% of their small cells will have integrated Wi-Fi [72]. As a result, in contrast to limited spectra of traditional RF, VLC systems have huge available unregulated bandwidth resource to compliment short-range wireless transmission and there is no cost needed to acquire this spectrum [73, 74, 75]. With 12 billion light bulbs in operation around the world with unlicensed and reusable bandwidth, there can be 12 billion potential VLC transmitters [56].
- *Interference:* VLC is intrinsically safe and does not cause any interference with RF signals [76]. Thus this technology is perfectly suitable for communication in hospitals, industries and aerospace applications where RF communication (RFC) is strictly prohibited [65].
- *Security:* RF waves pass through walls and are susceptible to intrusion.

Since light is confined to an area surrounded by opaque boundaries, there can be well defined coverage zones with enhanced security for VLC [77].

- *Spatial reuse*: Since VLC is facilitated by emission of highly directional and confined visible light, there can be coexistence of many non-interfering links in close proximity, which allows greater data density and spatial reuse of modulation bandwidth in adjacent communication cells [78, 79, 80].
- *Safety*: In illumination conditions, there are no health hazards of visible light [81]. Unlike IR, visible light satisfies the eye-and-skin safety regulations making it safe for usage in any scenario with far larger emitted optical power giving VLC communication an edge in terms of transmission distance over IR [80, 65]. Furthermore, fluorescent lamps are known to have mercury emissions from broken lamps during their disposal that can have adverse environmental and health effects, which is not a concern for LEDs or LDs [82, 83]. However, LD-based VLC (LD-VLC) is an area where skin and eye safety regulations are far more stricter than LED-based VLC, which would be discussed in further details in Section 2.10.3.
- *Low cost*: Another advantage of VLC devices is their comparative low cost [84]. Some popular RF links operating over approximately 10 m provide data rates of up to 1 Mb/s in the 2.4 GHz band for a cost of near US \$5 per module. While, VLC links can transmit at 4 Mb/s over short distances of 1 m using optoelectronic devices, which cost approximately US \$1 per module [85]. The implementation cost of VLC is less since only a few upgrades of existing lighting infrastructure is required rather than the initial set up cost of an entire communication system. Besides, LED infrastructures had become much more affordable and LDs are also expected to decrease in pricing in the coming years [86, 46].

The inherent benefits of utilizing the visible spectrum for communication com-

pared to other parts of the EM spectrum had been discussed in this section. When sources are being considered (LEDs, LDs etc.), there are other potential advantages, which would be discussed with greater details in the coming sections. Looking back at the unique features of VLC, it is quite clear that VLC has the potential to be one of the most significant technological breakthrough in communication systems.

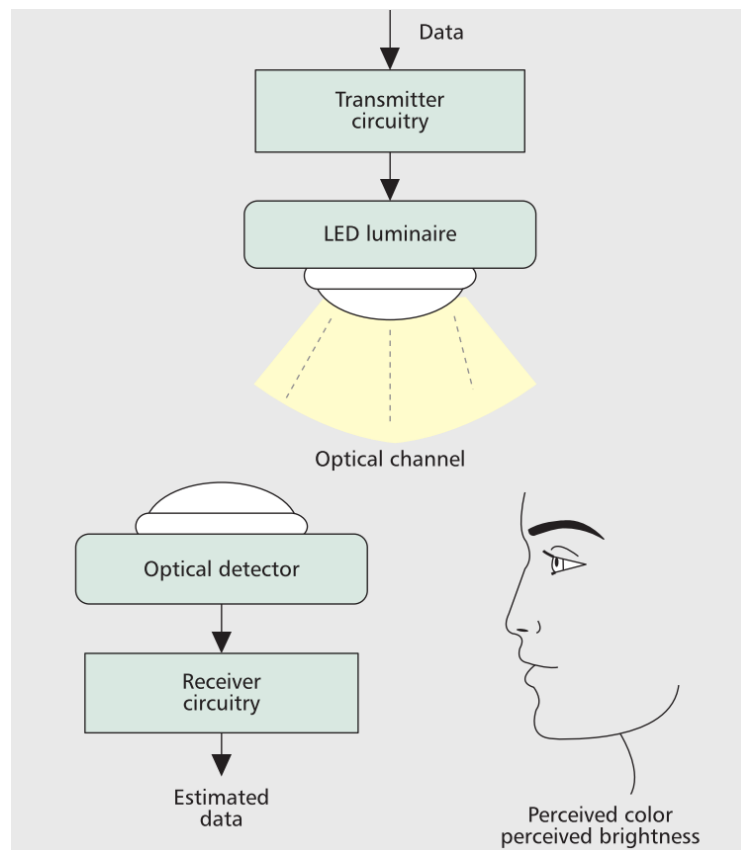


Figure 2.1: LED-based VLC system depicting the dual functionality of illumination and communication [28]

2.3 Fundamental Aspects of VLC

The two main functions of VLC are illumination and communication, therefore a competent VLC system must have a symmetry between them where neither of the functions are compromised at the cost of enhancing the other. Figure 2.1 depicts how the dual functionality of VLC makes the simultaneous consideration of illumination and communication vital. In this section, the fundamentals behind assessing them in terms of parameters outlined by industry standards would be discussed.

2.3.1 Illumination

The most important recipient of illumination from a lighting system is the human eye. As shown in Figure 2.2, the human eye is clad by the retina, which is the light-sensitive part of the eye and consists of cone and rod cells [87]. Rod cells, which are more abundant compared to cone cells, are sensitive over the entire visible spectrum and mediate vision in low lighting conditions. Cone cells are more sensitive in either of the red, green or blue spectral range and are active at higher light levels [87].

The vision regimes for the human eye are driven by the type of cells, which are stimulated. **Photopic** vision is the perception at high ambient light levels mediated by the cones, while **Scotopic** vision relates to human vision at low ambient light levels driven by rods. The human eye sensitivities in the photopic and scotopic regime are also depicted in Figure 2.2. The peak for photopic vision occurs at 555 nm whereas the peak for scotopic occurs at around 506 nm.

With the basic concept of perceived vision being summarized, this section would focus on different photometric¹ and radiometric² parameters required to characterize the illumination and emission profile of a VLC system.

¹Photometry is the measurement science of light as perceived by the human eye

²Radiometry is the science of measuring light in any portion of the electromagnetic spectrum

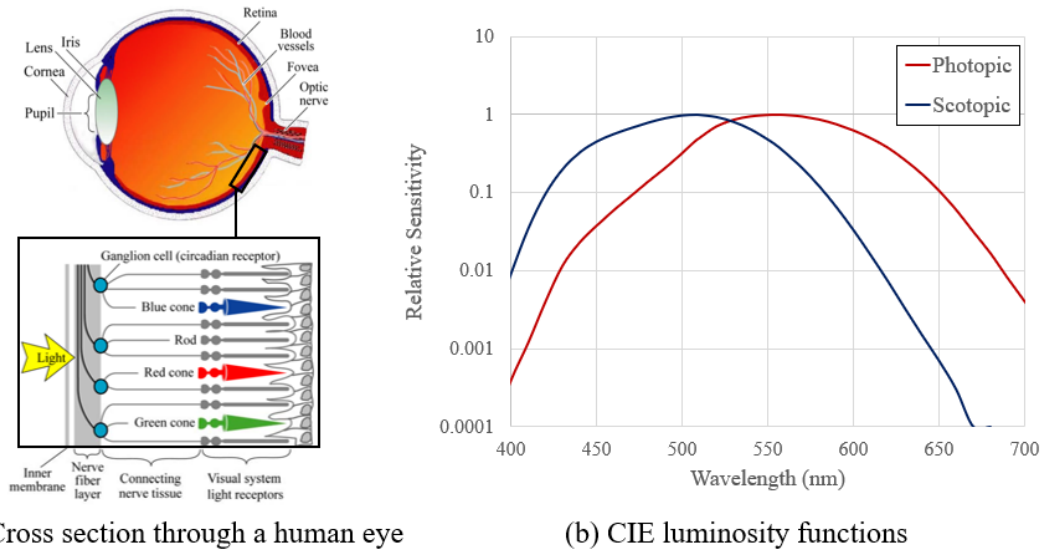


Figure 2.2: Relation between scotopic and photopic vision based on cone and rod cells

Luminous flux

The luminous flux is the total emitted flux scaled according to the fluctuating sensitivity of the human eye to different wavelengths (SI unit:lumen [lm]) [22]. The luminous flux L can be defined as [22]

$$L = 683 \int_0^{\infty} V(\lambda)P(\lambda)d\lambda \quad (2.1)$$

where $P(\lambda)$ is the radiant spectral power density and $V(\lambda)$ is the human eye sensitivity function as shown in Figure 2.2. For photopic vision, 1 W of radiant power corresponds to a luminous flux of 683 lm (at 555 nm). On the other hand, for scotopic vision, the sensitivity is higher corresponding to a luminous flux of 1745 lm (at 506 nm).

Illuminance

The illuminance (E) is the total luminous flux incident on a flat surface per unit area (SI unit: lux [lm/m^2]). A typical office environment requires an illuminance of 200-1000 lux [88].

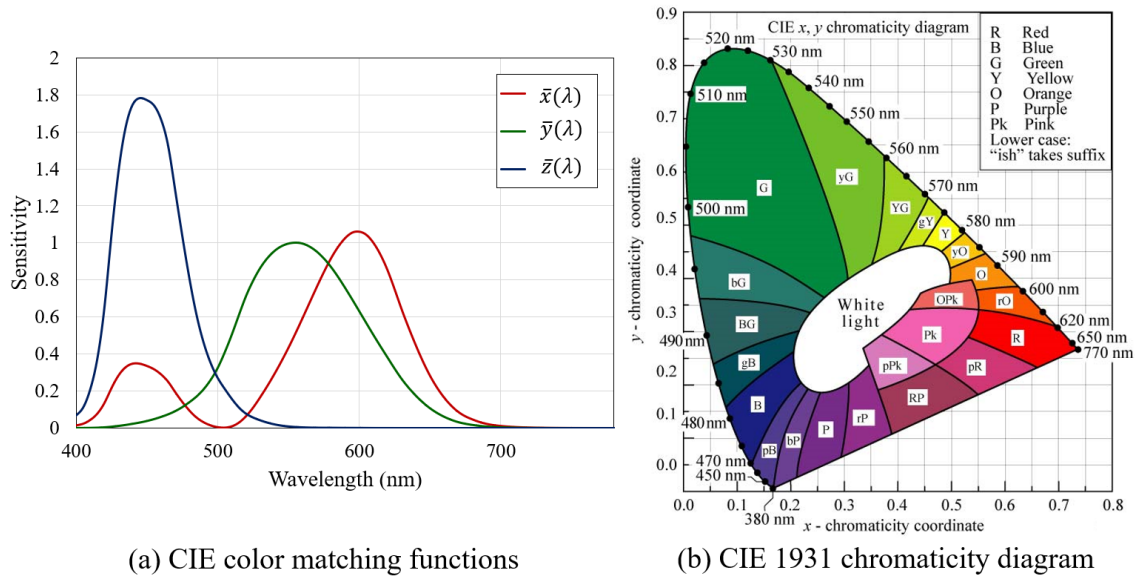


Figure 2.3: CIE 1931 color space and color matching functions

Spectral Power Distribution (SPD)

Although optical packaging and luminaire enclosure predominantly determines the emission profile of a light source, the remaining properties can be derived from the spectral power distribution (SPD) [28]. It is mathematically defined to be the derivative of the luminous flux with respect to wavelength [28]. It provides information about the output intensity of the light at different wavelengths, which helps in representing its spectral composition.

Color Metrics

As mentioned earlier, human color perception is driven by cone cells. A color is perceived based on the relative excitation of each type of cone cell. Principle of univariance states that a visual receptor cell can be excited by different combinations of wavelength and intensity, which means that the brain cannot determine the color of a certain point of the retinal image [89]. In color vision, the sensation of color is additive, which means two different monochromatic sources combined together would appear as a single color without the scopes of recognizing the original composition.

The coordinates and color matching functions defined by International Commission on Illumination (CIE) are specified with respect to the CIE 1931 color space. The color matching functions $\bar{x}(\lambda)$, $\bar{y}(\lambda)$, $\bar{z}(\lambda)$ as shown in Figure 2.3(a) generate the Tristimulus values X, Y, Z , which are used to calculate the chromaticity of a source [90]. The color matching function for green ($\bar{y}(\lambda)$) is equivalent to the human eye sensitivity function ($V(\lambda)$). The tristimulus values are generated by the color matching functions from $P(\lambda)$ as

$$X = \int_0^{\infty} \bar{x}(\lambda)P(\lambda)d\lambda \quad (2.2)$$

$$Y = \int_0^{\infty} \bar{y}(\lambda)P(\lambda)d\lambda \quad (2.3)$$

$$Z = \int_0^{\infty} \bar{z}(\lambda)P(\lambda)d\lambda \quad (2.4)$$

The coordinates (x, y) in the CIE1931 chromaticity diagram are derived from the tristimulus values by [91]

$$x = \frac{X}{X + Y + Z} \quad (2.5)$$

$$y = \frac{Y}{X + Y + Z} \quad (2.6)$$

Figure 2.3(b) shows the CIE 1931 color space. The perimeter of the chromaticity diagram corresponds to monochromatic or pure colors. White light with different hues is found at the center of the diagram. A red, green and blue (RGB) source would create three vertices of a triangle inside the color space, within which all the possible color coordinates that can be generated by the combination of the sources lie. The culminated final coordinate depends on the relative intensity of each sources.

However, the human sensitivity to color differences is not uniform when the CIE 1931 chromaticity diagram is considered, specially in the blue and green regions [92]. The regions within the human eye perceives the same color can be

Table 2.1: Effect, mood and applications of different color temperatures [41]

Color Temperature	Warm 2700K	White 3000 K	Neutral 3500 K	Cool 4100 K	Daylight 5000-6500 K
Effects and Moods	Warm Cozy Open	Friendly Intimate Personal	Friendly Inviting	Neat Clean Efficient	Bright Alert Exacting Coloration
Applications	Restaurants Hotel lobbies Homes	Libraries Office areas Retail stores	Showrooms Bookstores Office areas	Office areas Classrooms Hospitals	Galleries Museums Jewelry stores

shown in ellipses, which grow in size towards green. To move towards a more uniform color space, CIE proposed the CIE1960 (u, v) and CIE1976 (u', v') color spaces.

Color Temperature (CT)

The color temperature (CT) of a white light source (SI unit: kelvin [K]), is the temperature of a planckian black-body radiator that has the same chromaticity location as the source being considered [87]. The planckian black body radiation spectrum is characterized by the temperature of an ideal black body radiator heated to the point of incandescence [41]. The location of the black body radiation in the CIE 1931 and CIE 1976 diagrams are shown in Figure 2.4. As the temperature of the black-body increases, the chromaticity moves from red wavelength region towards the center of the diagram. CTs above 5000 K are deemed to be ‘cool white’ and appears bluish and exert bright, alert moods. While lower CTs (~ 3000 K) are considered ‘warm white’, which has a yellow-orange hue. The interquartile range of CCT for daylight demonstrated values from 5712 K to 7757 K, with a minimum value of 3600 K reported in rare conditions [93]. The effect, mood and applications that can be provided by lighting of different CTs are tabulated in Table 2.1.

However, it is not necessary that the color of the white light source will exactly fall on the planckian locus, thus another parameter known as correlated

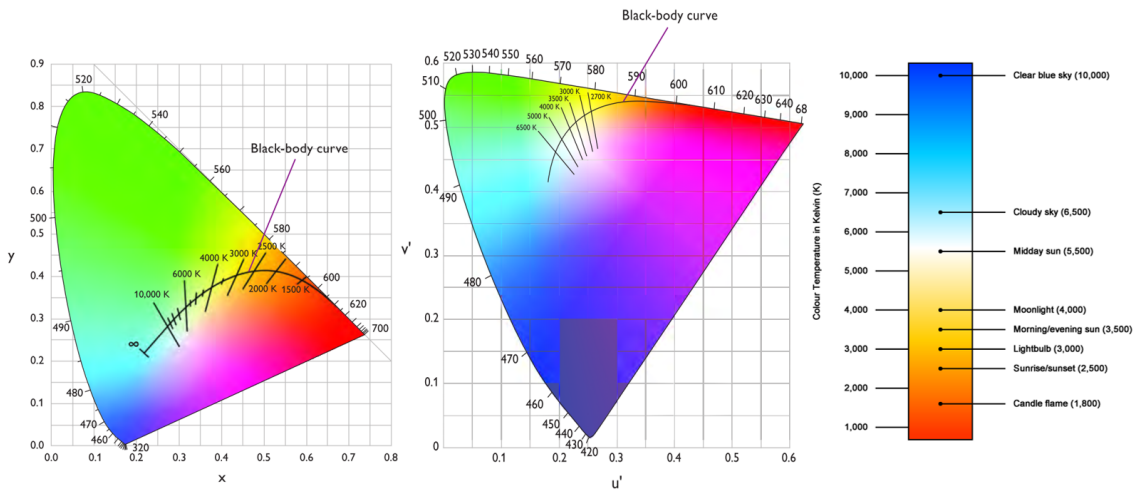


Figure 2.4: CIE 1931 and CIE 1976 color spaces showing the location of the planckian locus alongside a CCT chart [41, 94]

color temperature (CCT) is used to define the appearance of the white light. It has the same units as CT and is defined as the temperature of the black-body radiator when the color is closest to the color of the source being considered [87]. Nonetheless, it is more convenient to use the inverse of CCT that is denoted by mired (unit: MK^{-1}), which produces a uniform scale, more capable of describing human color sensitivity than CCT [95]. In this work, this parameter was not considered and CCT was mainly used since it is a more popular metric and helps in comparison with the VLC systems in [28, 40, 47, 66, 96].

Variation along the black-body curve or planckian locus is measured in K while variations perpendicular to the blackbody curve are notated as D_{uv} . D_{uv} ranges are defined in the CIE 1976 diagram rather than the CIE 1931 color space due to the suitability of the former color space for evaluating difference in color. D_{uv} measures the degree of color change. A positive D_{uv} indicates a position above the locus while a negative value indicates a position below. Based on the US Department of Energy and American National Standards Institute (ANSI), the D_{uv} must be within the acceptable range of ± 0.006 [97, 98]. The acceptable CCT and D_{uv} ranges based on the ANSI standards are tabulated in Table 2.2. Allowable variations to the black-body curve can be defined by a quadrangle for each color

temperature in the CIE color space. The size of each quadrangle varies according to the D_{uv} ranges specified by the ANSI standards, thereby giving different acceptable ranges of CCT [41].

Table 2.2: Acceptable CCT and D_{uv} Range for different nominal CCTs [98]

CCT (K)	CCT Range (K)	D_{uv} Range
2700	2725 ± 145	0.000 ± 0.006
3000	3045 ± 175	0.000 ± 0.006
3500	3465 ± 245	0.000 ± 0.006
4000	3985 ± 275	0.001 ± 0.006
4500	4503 ± 243	0.001 ± 0.006
5000	5028 ± 283	0.002 ± 0.006
5700	5665 ± 355	0.002 ± 0.006
6500	6530 ± 510	0.003 ± 0.006

The threshold at which the difference between chromaticity coordinates of a light source from the nominal CT can be perceived is defined by MacAdam ellipse. A MacAdam ellipse is drawn over the color space to establish that the color at the center point deviates by a certain amount from colors at any point along its edge. The scale of a MacAdam ellipse is determined by the standard deviation of color matching (SDCM). A difference of 1 SDCM step is not noticeable, 2 to 4 steps is slightly visible; and 5 or more steps is readily visible [41].

Color Quality Evaluation

Besides the perceived hue of lighting, which is characterized by CCT, the ability of a light source to render the colors of illuminated objects with high accuracy is essential [28, 99]. Although the number of colors that can be distinguished by the human eye varies based on observing conditions, a realistic interpretation was provided by Pointer *et al.*, where it was stated that the number of discernible colors in the CIE uniform color space was 2.28 million [100]. The colour of an object depends on viewing environment, particularly under daylight, which varies depending on time, solar elevations and different meteorologic conditions [99, 101].

The main motivation for white light sources is to match the photometric qualities of the sun. The widely accepted measure of color rendering capabilities is the color rendering index (CRI). The CRI is calculated based on color difference measurements between 14 specified color samples illuminated by a luminaire under testing and the same samples illuminated by a reference light source [28]. It is mainly influenced by the SPD of a light source and has a maximum value of 100 [102].

The samples generally used for measurement of CRI is presented in Figure 2.5. Initially 8 samples were used (R_1 to R_8) for calculating what is referred to as 'general' CRI (denoted by R_a); but later, the CIE introduced 6 more samples (R_9 to R_{14}), which can provide deeper information about how a lamp's SPD influences specific colors. Generally, the average CRI (R_a) is used to describe the color rendering capabilities of a lamp. For calculating R_a , initially the 2° standard observer is used to measure the coordinates of the reflected light from each samples in CIE 1964 color space. Then, the color difference for each sample (ΔE_i) is measured by the Euclidean distance between the pair of coordinates. The mean color difference (ΔE) is calculated from the individual color differences. Finally the average CRI is calculated using:

$$R_a = 100 - 4.6 \times \Delta E \quad (2.7)$$

However, CRI was developed keeping incandescent and daylight as reference light sources, which limited the metrics ability in quantifying the color rendering capability of a lighting system as a whole [103]. Thus, other metrics such as color quality scale (CQS), gamut area index (GAI) etc. had been designed to diminish the shortcomings of CRI [104].



Figure 2.5: Sample colors used for calculating CRI

2.3.2 Communication

Being an extension of optical wireless communication (OWC), the channel model for VLC is similar to the infrared (IR) channel, although the reflectivity of the surfaces enclosing the system differs causing changes in delay spread³ [57]. Typical VLC links use LOS configuration, due to its illumination purpose. Furthermore, lower path loss and dispersion over short distances gives way to higher bandwidth. VLC systems use intensity modulation (IM), where data is modulated into the intensity of the optical source, which is controlled by the forward current. Thus, direct detection (DD) is used for down conversion where the received optical power is converted to a proportional electrical current. An IM/DD VLC system is depicted in Figure 2.6. The data that needs to be transmitted by the user is modulated and a DC bias is added to make sure that the signal is in the operating region of the source, which can be either an LED or LD [57]. The source converts the electrical signal into intensity modulated optical signal, which then travels across a free space optical channel and is passed through an optical filter and detected by the photodiode. The photodiode generates equivalent electrical signal, which is amplified and demodulated to retrieve the original transmitted data.

³Delay spread is a measure of multipath richness of a communications channel and is a critical performance criterion for the upper bound of data transmission rate

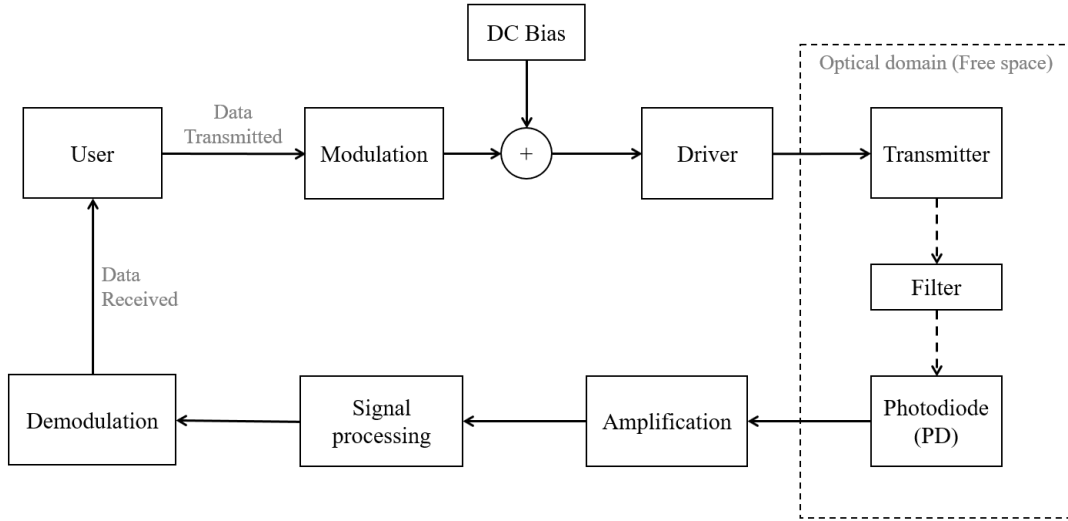


Figure 2.6: Block diagram of an IM/DD VLC system

VLC System Model

A baseband IM/DD optical wireless link can be summarized as

$$y(t) = Rx(t) * h(t) + n(t) \quad (2.8)$$

where $y(t)$ is the photocurrent that is generated, R is the responsivity of the photodiode (PD), $h(t)$ is the channel impulse response, which can be expressed as $H(f)$ in the frequency domain by taking the Fourier transform, $*$ is the convolution operator and $n(t)$ is the channel noise [22].

The channel response is composed of both line of sight (LOS) and non-LOS (NLOS) components given as [22]

$$h(t) = h_{LOS}(t) + h_{NLOS}(t) \quad (2.9)$$

Since the optical power is proportional to the generated electrical current in the IM/DD link, the transmitted signal must be non-negative. Thus, compared to RF channels where the optical **signal to noise ratio** (SNR) is proportional to the average received power, in VLC it is proportional to the square of the average

received optical signal power given as [22]

$$SNR = \frac{R^2 H^2(0) P_r^2}{R_b N_0} \quad (2.10)$$

where R_b is the bit rate, N_0 is the noise spectral density and $H(0)$ is the DC channel gain given by

$$H(0) = \int_{-\infty}^{\infty} h(t) dt \quad (2.11)$$

In case of diffuse channels where reflections are taken into consideration, although the VLC channel model is similar to the IR channel model, the reflectivity of the surfaces enclosing the FSO channel differs leading to difference in delay spread and ISI. The reflectivity of the walls depends on the wavelength of incident light and materials used in the wall. Most reflections are assumed to be diffuse in nature and modelled as Lambertian emitters [77, 88], which scatters incident light omni-directionally with the same power. Considering reflections from the wall, the received power can be calculated from channel DC gain on direct path $H_d(0)$ and reflected path $H_{ref}(0)$ by [77]

$$P_r = \sum^{N_{LEDS}} \left\{ P_t H_d(0) + \int_{reflections} P_t H_{ref}(0) \right\} \quad (2.12)$$

Based on eq. 2.12, the total received power for multipath scenario is given by [77]

$$P_{rT} = \sum_{i=1}^M P_{d,i} + \sum_{j=1}^N P_{ref,i} \quad (2.13)$$

where M and N represent the number of direct paths and reflected paths from transmitter to receiver respectively. $P_{d,i}$ is the received optical power from the i^{th} direct path and $P_{ref,i}$ is the received optical power from the j^{th} reflected path.

2.4 Transmitters for VLC

The typical current-output power behaviour for optical transmitters in an IM/DD link is presented in Figure 2.7. Ideally, an input current I_{TX} with constant DC bias current I_{DC} and current swing I_{SP} , which will produce an equivalent output power (P_t) can be expressed as [56]

$$I_{TX} = I_{DC} + I_{SP} \quad (2.14)$$

$$P_t = P_{DC} + P_{SP} \quad (2.15)$$

The non-linearity is a key issue, which needs to be considered for transmitters in VLC. LEDs and LDs generally have non-linear luminous flux-forward voltage-forward current (LVI) relationship, which results in amplitude distortion at turn-on-voltage (TOV) and saturation current at high peaks.

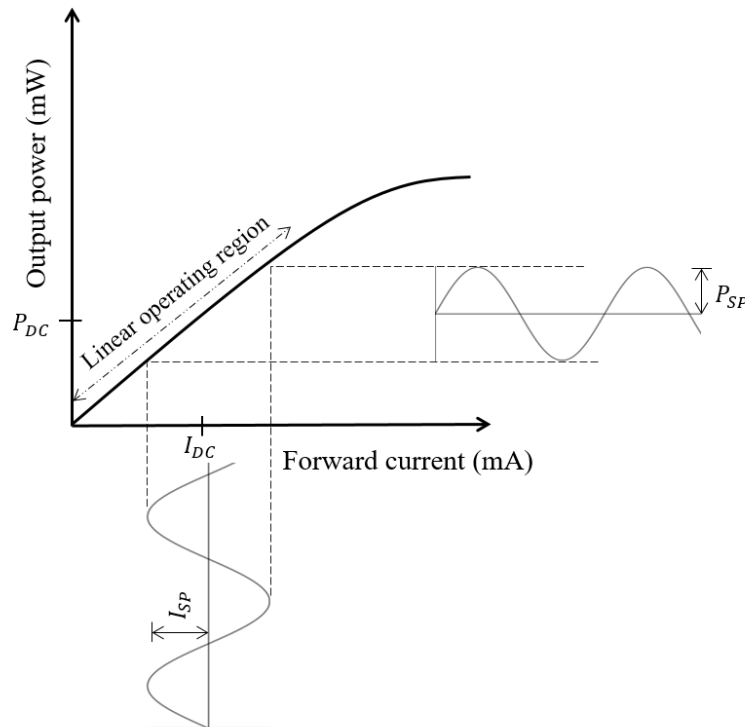


Figure 2.7: Current-output power behaviour, with input current swing, I_{SP}

2.4.1 Types of Transmitters

The different categories of transmitters that had either been traditionally used or are recently emerging in VLC are discussed below:

- ***pc-LED***: White light by LEDs is produced primarily using two methods. The first method, using a pc-LED employs a blue Indium Gallium Nitride (InGaN) LED chip to pump a Yttrium Aluminum Garnet (YAG) phosphor coating. The phosphor converts part of the blue light to green, yellow and red portion of the spectrum while the other part of the blue light is leaked out, the mixture of that produces white [105]. Different amount of phosphor determines the CCT at which the white light is being produced. Compared to RGB-LEDs, pc-LEDs are cost effective and easily implementable [106].
- ***Multi-chip LED***: The ‘multi-chip’ approach utilizes 3 or more LED chips emitting different colors, typically RGB to produce white light. Depending on the light intensities of the different chips, color control can be achieved. RGB LEDs have lower CRI compared to pc-LEDs. Although pc-LEDs are cheaper and less complex, they have lower bandwidth due to the low phosphor conversion efficiency compared to the RGB LEDs.
- ***OLED***: Organic light emitting diodes (OLEDs) generate light using an organic layer sandwiched between positive and negative carriers, and are used mainly in flat panel displays. The typical frequency response for OLEDs are in the order of 100’s of kHz, far lower than inorganic LEDs, which makes OLEDs less suitable for high speed applications. The lifetime of typical white OLEDs is ~50,000 hours, less than the typical inorganic LED lifetime. But since its a more flexible light source than inorganic LEDs, research has been ongoing to improve the frequency response by equalization [107, 108, 109, 110].

- **μ -LED:** AlGaIn based micro-light emitting diode (μ -LED) arrays have been in development for VLC and Polymer Optical Fiber (POF) recently [111]. μ -LEDs have the potential to be used as display panels incorporating high density parallel communication. Each individual pixel ranges from 14-84 μm , the 3-dB bandwidth reaches 450 MHz allowing speeds of up to 1.5 Gb/s [111, 112, 113, 114]. The high bandwidth is possible due the very low capacitance in the μ -LEDs.
- **rc-LED:** The extraction efficiency of conventional LEDs is poor due to the large difference in refractive index between the narrow gap semiconductor and the surrounding medium, which is typically air. To improve light extraction near IR wavelength range, resonant cavity enhancement was first demonstrated by Schubert *et al.* in 1992 [115]. Developing high brightness resonant cavity LEDs (rc-LEDs) would benefit VLC for color displays. rc-LEDs typically emit light at ~ 650 nm with a narrow line width, and can be modulated in excess of 100 MHz [116, 117].
- **LD:** LD is an electrically pumped semiconductor device that produces coherent radiation in the visible or IR spectrum when current passes through it [57]. In LDs, an effective laser resonance is stimulated due to the presence of coated or uncoated end facets, which behave like mirror with different reflectivities resulting in an eventual gain in stimulated emission of highly directional photons [57]. The emission profile of LD is in the order of 2-3 nm, which favors efficient utilization of the available visible spectrum by WDM and allows the use of narrow optical filter for greater rejection of ambient noise [44, 55]. The modulation speed in case of LDs is much higher because it is controlled by the photon lifetime (in the order of ps), which is much shorter than material carrier lifetime in case of LEDs [118].

2.4.2 Differences between LEDs and LDs

Compared to traditional pc-LEDs and RGB LEDs, LDs can be modulated at higher frequencies, which is attributed to their ability to be driven at higher current densities [57]. At high current densities, LEDs suffer from *efficiency droop*, which occurs due to electron overflow and hence the maximum radiant flux specified for an LED may not be at the optimal point of efficiency. Efficiency droop limits drive currents, leading to a higher initial cost per lumen of LEDs, which undermines one of the fundamental features of economical SSL [57]. The fundamental differences between GaN based LEDs and LDs are presented in Figure 2.8. LEDs typically emit light by spontaneous emission, which is generated by radiative recombination of electrons and holes in the p-n junction, which emits photons that are out of phase (incoherent). LDs on the other hand emit light by stimulated emission of photons which are in phase (coherent). The typical area of illumination of commercial LEDs and LDs are also illustrated in the figure. The relative distribution of external quantum efficiency of LEDs and LDs as a function of current density clearly demonstrates the efficiency droop, which the LEDs suffer at higher current density.

At present, LDs are more expensive than LEDs with comparable output power. However, LDs can be packed much more densely on a chip than LEDs, which will give way to brighter sources with higher energy efficiency on a dollars per-lumen basis [119]. The current state-of-the-art power conversion efficiency (PCE) is 70 % for LEDs and 30 % for LDs, which occurs at input power densities of 10 W/cm² for LEDs and 25 kW/cm² respectively [120]. Areal chip cost necessary for economical lighting depends on input power density. Achieving low enough chip cost for LEDs to be operated at input power densities at which their PCEs peak is much more challenging compared to LDs. Because of higher bandwidth, the cost per bit for LD-VLC systems will be much lower. LD manufacturing cost can also be decreased by the elimination or reconfiguration of some of the processes.

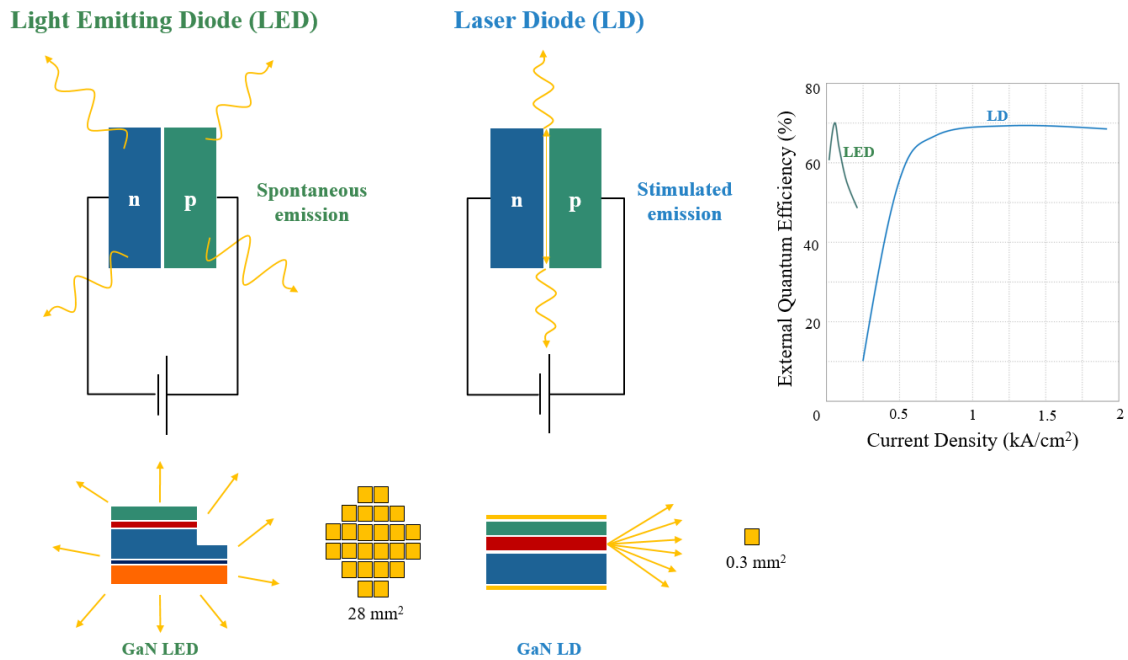


Figure 2.8: Difference between GaN based LEDs and LDs

By keeping much of the high power diode fabrication at the wafer-scale, the need for cleaving and facet coating can be eliminated. The laser based semiconductor lighting industry is a maturing industry with chip development on a steep upward curve and costs falling rapidly along with some indications that the overall system cost may be lower than LED based approaches in the future [46]. The high demand for LEDs plays an important role for their lower cost since they are produced in massive numbers. Highly stringent applications requiring LDs is foreseen to enable a rise in their demand, which would further decrease their prices.

In this work, the main focus is in using sources, which are currently widely available in indoor lighting systems or have the capabilities of becoming popular in the near future. The prospects of LDs as VLC transmitters for the future are far more promising than μ -LEDs, rc-LEDs and OLEDs. Hence, the sources that are mainly considered for this work are pc-LEDs and RGB LEDs, which are widely used in the current circumstances and LDs, which have the potential for the future. The differences between LEDs and LDs considering parameters important

Table 2.3: Comparison of different types of transmitters for VLC

Parameter	pc-LED	RGB LED	LD
Bandwidth	3-5 MHz	10-20 MHz	≥ 200 MHz
Efficacy	130 lm/W	65 lm/W	75 lm/w
Quantum Efficiency	Low	Low	High
Cost	Low	Moderate	High
Complexity	Low	Moderate	High

to VLC are summarized in Table 2.3.

2.5 Modulation Schemes

In VLC, the modulating signals can switch the transmitters at desired frequencies, which contains the information to be transmitted. The modulation frequency is generally above 300 Hz so that the occupants assume the source to be normally lit and flicker is avoided, which can have adverse health effects [121].

Single carrier modulations like on-off-keying (OOK), pulse position modulation (PPM) and pulse amplitude modulation (PAM) had been widely used in IR communications [122]. For achieving higher data rates, multiple sub-carrier modulation techniques such as orthogonal frequency division multiplexing (OFDM) had also been implemented in VLC systems. This section gives a brief overview of various features and properties of different modulation schemes that had been used in VLC. A summarized comparison of a few of the selected schemes is presented in Table 2.4.

Table 2.4: Qualitative comparison of popular modulation schemes

Modulation	Spectral Efficiency	Power Efficiency	System Complexity	Comment
OOK	High	Low	Low	Prone to flickering
PPM	Low	High	Moderate	Complex transceiver structure
PAM	Moderate	Low	Low	Non-linearity in LED's luminosity
CAP	High	High	Moderate	Lower cost than OFDM
OFDM	High	Moderate	High	Non-linearity for high PAPR
CSK	Moderate	Low	High	Requires feedback mechanism

- **On-off keying (OOK):** OOK is one of the simplest modulation techniques used to switch a LED between a high (bit 1) and low (bit 0) to modulate data. In non-return to zero-OOK (NRZ-OOK), 0s and 1s are represented by positive and negative voltages. This technique had been widely used in VLC [123, 124, 125, 126, 127] and can carry more information since there is no rest state. Despite the slow response of the phosphorescent component, which limits the bandwidth of pc-LEDs, by implementation of post equalization circuit, bandwidth could be extended to 151 MHz, which allowed data rates of upto 340 Mb/s [128]. Data rate of ~ 614 Mb/s had been demonstrated by the utilization of duo-binary technique with bandwidth enhancement (using transmitter and receiver equalization) for RGB LED-based systems [129]. In LD-based VLC systems, NRZ-OOK was utilized to achieve data rates of 2.5 Gb/s and 4 Gb/s utilizing GaN blue LD [45, 130].
- **Pulse position modulation (PPM):** In L-PPM, a pulse corresponding to a certain bit is transmitted in one of L time slots within a symbol period. The average power requirement for PPM is lower than OOK [131] since it avoids the DC and lower frequency component of the spectrum [132], but it is less efficient in terms of bandwidth [122, 133]. System complexity is increased on PPM compared with OOK, as it requires stricter bit and symbol synchronization at the receiver [134, 135].
- **Pulse amplitude modulation (PAM):** PAM is a very basic modulation scheme, which is bandwidth efficient. Data is modulated into the amplitude of the signal pulse. Modulation schemes employing multiple intensity levels such as PAM may undergo nonlinearity in LEDs luminous efficacy. Due to the dependence of the color of LED emission on input current and temperature, multiple symbol levels of PAM are subject to shifts in color temperature due to variation in drive current [136].

- **Color Shift Keying (CSK):** Using multi-chip LEDs for VLC has been introduced in the IEEE 802.15.7 standards published in 2011 [31]. The CSK scheme does not modulate the colored chips independently for WDM. The transmitted bit corresponds to a specific color in the CIE 1931 coordinates. However, a feedback loop from the receiver is sometimes used for color calibration and interference mitigation from other light sources [10].
- **Orthogonal Frequency Division Multiplexing (OFDM):** High data rates are realized by utilizing multiple orthogonal sub-carriers to transmit parallel data streams simultaneously, reducing inter symbol interference (ISI) and the need for complex equalizers [137]. OFDM is spectrally efficient, and is robust against channel dispersion. Since VLC uses IM, a real and unipolar valued signal needs to be produced. VLC system utilizing OFDM had reached values in the gigabit range [138, 139, 140]. For LD-VLC, by utilizing DC offset OFDM, data rates of 6.52 Gb/s and 8.8 Gb/s was achieved [46, 47].

However, the use of OFDM is not generally ideal for VLC. Due to the limitation in transmitted power for concern towards eye safety, the dynamic range is limited [141]. It is also susceptible to non-linear distortion and clipping noise [142]. It has a high peak to average power ratio (PAPR), making OFDM signals sensitive to non-linear devices [143]. Compared to RF outdoor channels, the indoor environment is generally static with no deep fading. Hence, the main reason behind using OFDM can only be for getting higher data rate but at the cost of higher PAPR. Thus, NRZ-OOK scheme is chosen for this work. It reduces system complexity and cost compared to other modulation schemes with higher spectral efficiency [144]. The recent progress in terms of data rates achieved by LED and LD-based systems is summarized in Table 2.5. Only the three categories of transmitters previously chosen were considered for comparison. It is clearly evi-

Table 2.5: Recent progress in LED-based VLC

Year	Data rate	Distance (m)	Transmitter	Receiver	Modulation	Comment	Ref
2014	340 Mb/s	0.43	pc-LED	PIN	NRZ-OOK	Post equalization	[128]
2013	1.1 Gb/s	1	pc-LED	N/A	OFDM (WDM)	4 X 9 MIMO system	[139]
2013	477 Mb/s	0.40	RGB	PIN	NRZ-OOK		[145]
2013	150 Mb/s	0.5	pc-LED	PIN	NRZ-OOK	Neural network based receiver	[146]
2013	300 Mb/s	11	rc-LED	PIN	NRZ-OOK	Current shaping circuit	[147]
2013	2 Mb/s	0.4	white-LED	PIN	NRZ-OOK	Duplex communication between android mobiles	[148]
2012	3.4 Gb/s	0.3	RGB	APD	OFDM (WDM)		[140]
2012	614 Mb/s	0.40	RGB	PIN	OOK	Duobinary technique was used	[129]
2012	80 Mb/s	0.1	pc-LED	PIN	OOK	Pre-equalization	[124]
2010	230 Mb/s	0.27	pc-LED	APD	OOK		[149]
2009	125 Mb/s	5	pc-LED	PIN	OOK		[125]
2008	40 Mb/s	2	pc-LED	PIN	OOK	Multiple resonant equalization	[150]
2017	8.8 Gb/s	0.5	RGB LD	APD	OFDM		[47]
2015	6.52 Gb/s	1	Blue LD	PIN	OFDM	Fixed-rate and adaptive loading	[46]
2015	5.2 Gb/s	0.6	Blue LD	APD	OFDM	Relative intensity noise suppression	[96]
2015	4.4 Gb/s	0.2	RGB LD	APD	OFDM	Throughput optimization	[48]
2015	3.43 Gb/s	0.3	RGB LD	PIN	DCO-OFDM	Adaptive bit and energy loading algorithm	[44]
2015	4 Gb/s	0.15	Blue LD	PIN	NRZ-OOK	Bandwidth extended PD	[130]

dent that LDs outperform LEDs when data rate is considered, however there are issues regarding illumination quality and safety, which need to be addressed as discussed in Section 2.10.3.

2.6 Dimming Schemes

In a commercially competent VLC system, an end user would expect to have high speed wireless communication alongside full control over illumination. This makes ‘dimming functionality’ an obligation for consideration in VLC systems [151]. Dimming control can provide energy savings and ecological benefits, which are key considerations in the recent trend towards conservation of natural resources. However, dimming has an adverse effect on communication, since it fixes the average intensity of a light source according to user requirement, thereby reducing the achievable data rate [33]. This section summarizes the basic funda-

mentals associated with concurrent dimming and data transmission in VLC.

2.6.1 Types of Dimming Schemes

The brightness of an LED is adjusted by varying the forward current, which can be decreased to provide dimming control. This adjustment can be generally implemented by two techniques:

- Analog Dimming

- Pulse regulated schemes

The first technique known as analog dimming also popular as continuous current reduction (CCR) is the simplest approach in dimming control. The radiated optical flux is directly decreased by adjusting the current amplitude [23]. It is relatively easy to implement and the luminous intensity is reduced proportionally to the current. Experiments performed in [152, 35] show that luminous efficacy is always higher for CCR dimming scheme. However, for monochromatic LEDs, the dominant wavelength of photons emitted changes with direct current causing chromaticity shifts, thereby causing a slight change in the CCT [35, 153, 154]. However, a proper quantification of chromaticity shifts in a VLC system due to CCR scheme had not been demonstrated till date.

The second technique utilizes pulse trains to drive the LEDs. Pulse regulation schemes can be classified as:

- Pulse width modulation (PWM)

- Frequency modulation (FM)
 - Constant Pulse Frequency Modulation (CPF_M)
 - Constant Pause Frequency Modulation (CZFM)

PWM also known as digital dimming uses digitally modulated pulse train to drive the LED at a constant current level. The average duty cycle⁴ represents the equivalent analog dimming level and is varied proportionally to acquire the desired dimming percentage [33]. The duty cycle can be expressed as

$$D = \frac{t_{ON}}{T} \quad (2.16)$$

where t_{ON} is the amount of time the pulse is on and T is the PWM symbol duration [155].

In FM, the instantaneous frequency is varied according to the user input. FM schemes are believed to increase driver efficiency and duty cycle accuracy [34]. Unlike PWM technique, the time period of the signals does not remain constant, which can increase complexity for VLC systems when data needs to be incorporated with the dimming signal. For ease of comparison of PWM with CPFM and CZFM, the analysis of discrete time equation can be done. If the time period and the 'ON' and 'OFF' duration of pulses are being considered, it can be said that the modulation period of PWM (T) is constant, which is proportional to minimal countable time step Δt ($T = N.\Delta t$). At the same time, pulse width is variable ($t_P = n.\Delta t$), where n is an integer defined by the control system depending on the dimming requirement and N is a constant. Thus the duty cycle in discrete time becomes

$$D(n) = \frac{t_P}{T} = \frac{n}{N} \quad (2.17)$$

The difference between PWM, CPFM and CZFM in terms of discrete time equation is depicted in Figure 2.9. For CPFM, pulse duration is proportional to the elementary step Δt . The pulse width defined by number of such periods (P), is constant ($t_P = P.\Delta t$) but the time period, T is varying ($T = n.\Delta t$). For CZFM, the pause between two neighbouring high pulses remains constant and

⁴Proportion of the time during which the signal is on compared to the total time the signal is transmitted

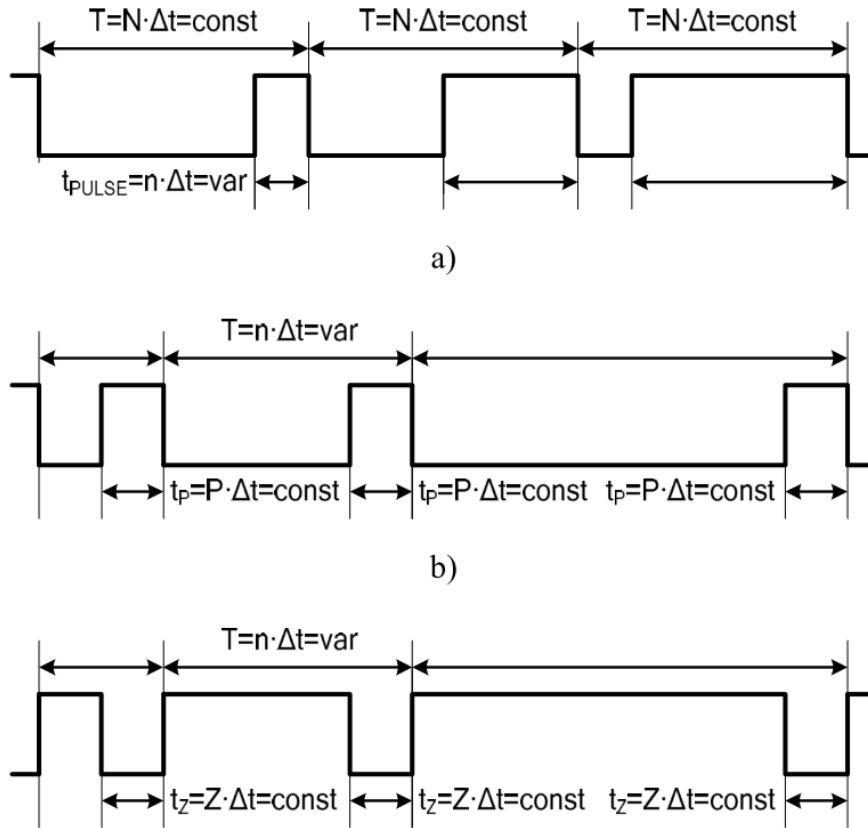


Figure 2.9: Pulse regulated schemes in terms of discrete time equations [34]

can be generated by a short series of elementary steps with constant 'OFF' time ($t_{\text{PAUSE}} = Z \cdot \Delta t$) where Z is the number of steps. At the same time the pulse width for 'ON' pulse is increasing at each step since the overall time period is increasing ($T = n \cdot \Delta t$).

Although the comparison of these pulse regulated techniques had been done in terms of driver circuit efficiency and control performance in [34], it is necessary to investigate the performance of pulse regulated dimming schemes based on photometric parameters. It is also necessary to identify the optimum scheme in terms of chromaticity shifts. This links to two vital research questions defined in Section 1.2:

- How does FM perform compared to PWM when photometric parameters such as CRI, CCT and linearity of illuminance are being considered?

- How much chromaticity shift is induced when CCR and PWM are implemented in a VLC system?

2.6.2 Adaptive Dimming Schemes for VLC

The incorporation of high speed NRZ-OOK data with low speed dimming signal using different dimming techniques is summarized in Figure 2.10. When simultaneous dimming and data transmission is considered for VLC, there are several challenges that need to be addressed. CCR dimming fixes the average intensity according to user requirements, which decreases achievable SNR of a VLC link. Although PWM dimming transmits at the original signal amplitude, it hampers the achievable data rate since it only allows transmission of data when duty cycle is high. A uniform parameter called the 'dimming target'⁵ denoted by d can be used to create an analogy between digital and analog dimming. d is the desired illumination output from the system and is inversely related to the duty cycle (D) given as

$$d = 1 - \frac{D}{100}, \quad 0 \leq d \leq 1 \quad (2.18)$$

As reported in [33], for digital dimming, the instantaneous bit rate (R_{ad}) is related to the original data rate (R) and the dimming target (d) by the following equation:

$$R = R_{ad} \times (1 - d) \quad 0 \leq d \leq 1 \quad (2.19)$$

One of the main advantages of VLC is high speed communication and due to dimming control this might get undermined. As a result an adaptive dimming technique is necessary, which will ensure the communication performance of a VLC link remains consistent when an end user arbitrarily dims the light. Adaptive communication schemes had been demonstrated in several wireless RFC systems, VLC can also improve from an adaptive framework [28]. Because

⁵ $d = 0$ at full brightness, $d=0.5$ at half brightness and $d=1$ at no brightness

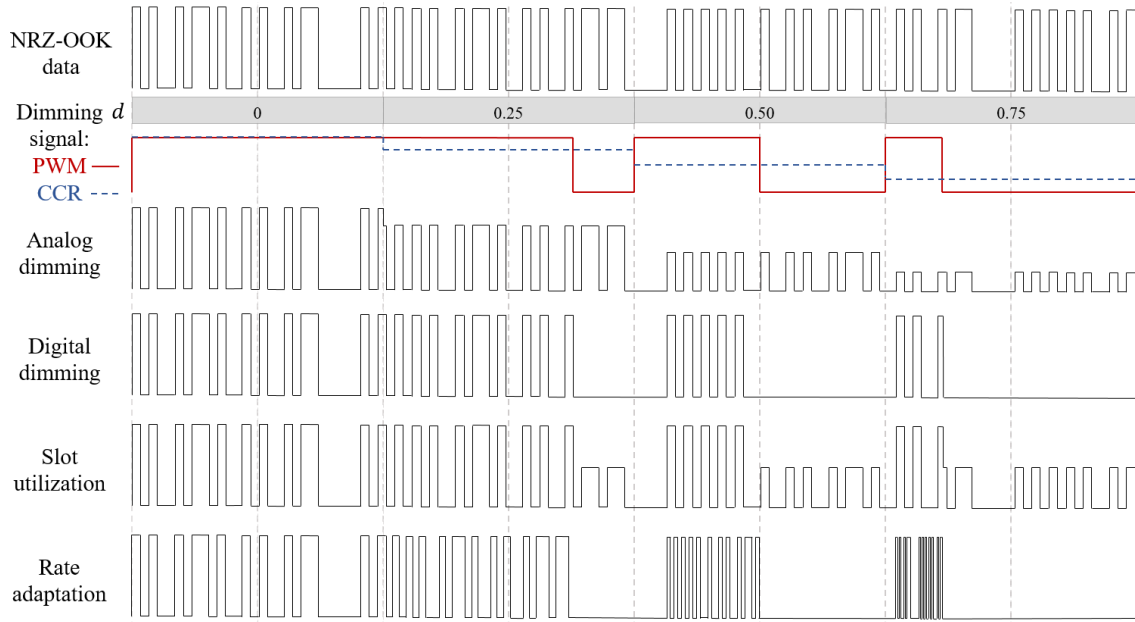


Figure 2.10: NRZ-OOK data stream resulting from implementation of adaptive schemes for different dimming targets

of the practical implementation of software defined VLC (SDVLC) [156], there are more scopes for practical implementation of such adaptive schemes, which are discussed in this section.

Slot Utilization (SU)

Slot utilization (SU) scheme involves the transmission of data bits regardless the state of the PWM dimming signal. Even when the dimming signal is ‘OFF’, data bits are superimposed on it, which ensures the number of transmitted bits are constant, maintaining a fixed data rate [23]. This scheme is highly beneficial for the communication aspects of the VLC system, since seamless transmission is maintained throughout the entire dimming range of the system. It does not involve varying the instantaneous data rate of the VLC system, which makes it practical and cost effective. This scheme can be defined by

$$y(t) = \begin{cases} x_1(t) + x_2(t) + \dots x_n(t) & d = 1 \\ x_1(t) + A.x_2(t) + x_3(t) + \dots A.x_n(t) & 0 \leq d < 1 \end{cases} \quad (2.20)$$

where, n is each sample of the transmitted signal until dimming signal changes its state. From Figure 2.10, it can be seen that when the dimming signal is low, bits are transmitted with a lower amplitude. Thus, this scheme achieves data transmission at the cost of lower dimming precision.

Jang *et al.* simulated the combination of 1 Mb/s NRZ-OOK data with PWM dimming signal [37], which was practically implemented by Cho *et al.* at a data rate of 10 kbps [38]. Although the communication aspects of this technique had been previously investigated, the extent to which this technique can be implemented based on photometric performance had not yet been studied, which raises the following research question:

- How does transmission of bits when the duty cycle is low in slot utilization affect the overall illuminance and does it hamper the dimming precision?

Rate Adaptation (RA)

Rate adaptation scheme on the other hand maintains link stability under digital dimming by adjusting the the instantaneous data rate of the VLC link based on the dimming target. It can be observed from Figure 2.10 that as the dimming target increases, more bits are packed into the transmitted waveform during the duration the PWM signal remains high. This instantaneous data rate can be calculated by rearranging equation 2.19 as

$$R_{ad} = \frac{R}{1-d} \quad 0 \leq d \leq 1 \quad (2.21)$$

Based on a recent analysis conducted by Wang *et al.*, for a 50 Mb/s NRZ-OOK VLC system, the required data rate for RA scheme reaches values of upto 500 Mb/s, which is not feasible for practical implementation [39]. The RA technique is also susceptible to noise due to reduced distances between symbols which is not analyzed thoroughly in the simulation profile since the channel is assumed to

operate at a high SNR regime [136]. Thus experimental investigation which takes into account the challenges in implementing this technique in a practical scenario and gives a detailed insight in how effective this technique is in comparison to the aforementioned dimming schemes needs to be carried out. The possibilities of incorporation of multiple adaptive schemes for formulating a dimming algorithm that can capitalize on the unique strengths of each scheme needs to be explored as well, which raises the research question:

- Can different adaptive schemes be simultaneously utilized to subdue the stringent requirement on either of them enabling dimming with better performance in terms of communication?

2.7 Wavelength Division Multiplexing (WDM)

When multi-source VLC is considered either by implementing RGB LEDs or LDs, each channel can be modulated independently provided white color balancing is maintained [157]. At the receiver, optical filters with transmittance within each source's wavelength range are used to extract data from the corresponding channels allowing increase in aggregate data rate due to multiple parallel data streams. This technique of utilizing different wavelengths for multiplexing is generally referred to as WDM [158]. The fundamental operation of WDM systems using red, green and blue channel is depicted in Figure 2.11.

Using WDM techniques on RGB LEDs yield higher data rates than pc-LEDs [56]. A similar trend is noticeable when considering RGB LDs compared to blue LDs with phosphor. Since the emission profile of LDs is much narrower than LEDs (typically RGB LEDs occupies most of the visible spectrum), it allows for efficient utilization of the visible spectrum, where hundreds of LDs can transmit data in parallel [44]. Thus using LDs for WDM-based VLC systems can provide data rates above 100 Gb/s, which cannot be matched by LEDs [44]. However, the

biasing of individual channel needs to be regulated for achieving chromaticity coordinates within the acceptable limits set by illumination standards [159]. Most of the work regarding WDM-based VLC till date only focused on the communication aspects and overlooked the quality of illumination [160]. Thus, an investigation regarding the limits of WDM-based VLC by simultaneous consideration of illumination and communication needs to be carried out.

2.8 Receivers for VLC

In VLC, constructive and destructive interference patterns occurs on a micron scale and averaged by the receiver, which is thousand times greater in size. Therefore, VLC exhibits no Doppler shift [56]. As a result, sophisticated receiver tracking algorithm are not needed, which allows a photodiode (PD) to be simply used as the receiver [67]. There are generally two types of photo detectors used in VLC systems: PIN⁶ PD and avalanche PD (APD), the latter having a higher gain. The downside of using an APD is the excess shot noise generated by the higher photocurrent [161]. PIN PDs have been the predominant PD used in VLC due to high

⁶A wide intrinsic ('i') semiconductor region is sandwiched between 'p' type and 'n' type semiconductor regions, hence P-I-N

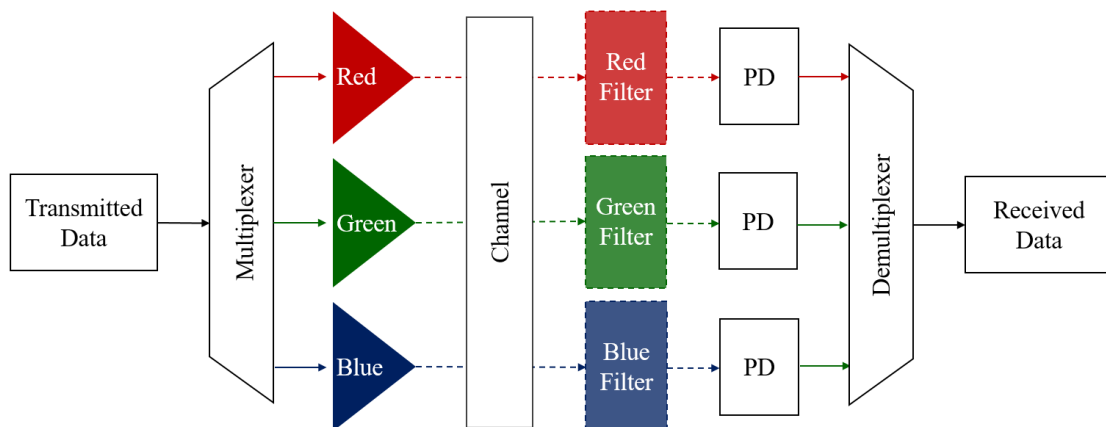


Figure 2.11: Fundamental WDM VLC system using red, green and blue sources

temperature tolerance, lower cost and are ideal in scenarios where the receiver gets flooded with relatively high intensity light.

Typical silicon PIN PDs used in VLC have responsivity curves peaking at 800 nm, with higher sensitivity to red light than green or blue [157]. WDM VLC systems utilizing RGB LEDs had shown variations in data rates and performance for different channels. The red channel generally has a higher frequency response and data rate than the blue and green channels [158, 162].

An optical receiver's front end usually consists of a pre-amplifier, which amplifies the weak current induced in the PD. The amplifiers used in VLC can be classified mainly into three categories: low impedance amplifier, high impedance amplifier and trans-impedance amplifier (TIA). The choice and design of the front end is usually a trade-off between speed and sensitivity [163]. If a high impedance amplifier is used, the thermal noise is significantly reduced; thereby improving receiver sensitivity. However the main disadvantage of high impedance front end is the low bandwidth. Thermal noise prevails in the receiver connected to a low impedance front end making this class of amplifiers to be impractical for use in VLC systems. TIA on the other hand provides an equal balance of high sensitivity along with large bandwidth. As a reason, this class of amplifier had become increasingly popular and had been used in various VLC systems [164, 128, 165].

2.9 Performance Enhancement in VLC

Despite having inherent advantages compared to traditional communication systems, VLC still faces numerous challenges, which need to be addressed. Limited bandwidth and slow modulation response of LEDs are the key challenges which limit the achievable data rate in LED-based VLC.

Commercial high brightness pc-LEDs have very low modulation bandwidth [166]. In case of pc-LEDs, the blue LED chip have a 3 dB bandwidth of around

20 MHz and the phosphor coating used to convert the blue light to white further lowers the bandwidth to ~ 2 MHz [167, 78]. If the entire white spectrum is used at detection, the modulation bandwidth is limited to ~ 2.5 MHz [124]. At higher frequencies, due to its low time constant, the yellow phosphor will not respond to the modulated signal in the LED drive current, hence generating a steady light, which could saturate the receiver and increase shot noise. Blue filtering enhances the 3 dB bandwidth of the LED to ~ 20 MHz by reflecting off the slow phosphor component of the light.

Early methods of increasing the frequency response of LEDs include current shaping, or in other words pulse shaping. This method was initially used in optical fiber communication, which reduces the rise and fall time of rc-LEDs. In its simplest case, a resistor in parallel with a capacitor is placed in series with the LED. When switching on, excess current flowing through the capacitor helps the LED reach its steady state faster. When switching off, the capacitor helps sweep out the carriers by reverse biasing the diode [87, 168]. Current shaping can be viewed as a basic form of transmitter equalization, enhancing the response time of the LED, thereby increasing the 3 dB bandwidth.

Equalization at the transmitter and receiver can also help in increasing the overall bandwidth. Simple pre-equalization at the transmitter to increase the usable bandwidth of a single LED has been demonstrated in [124]. Demonstrations on post-equalization at the receiver using a simple first order equalizer after PD signal amplification, has yielded a bandwidth of 50 MHz and data rate of 100 Mb/s [126, 169]. Adaptive decision feedback equalization (DFE) technique using least mean squares (LMS) algorithm showed improvements in data rates [116]. Frequency-domain channel equalization methods can also help in superior performance for OFDM-based VLC [170].

Optical beamforming is a technology of focusing LED light on a desired target. A Spatial Light Modulator (SLM) [171] is used to focus the LED light. SLM can

modulate optical phase or amplitude on each pixel, it can also modulate light spatially in amplitude and phase. In [17], a location detecting algorithm is discussed to detect the exact position of the receiver. Packets are exchanged between transmitter and receiver and direction code is used when packets are exchanged to find out the exact location. SNR of the VLC system was reported to be improved by 13.4 dB.

For more complex multi-carrier systems utilizing OFDM, sub-carrier equalization [172], signal clipping [173], symmetrical clipping [174], pre-distortion and post-distortion can be employed to counteract with the effect of non-linearities [175, 176]. These techniques had been mainly employed for LED based systems since the modulation bandwidth is limited. For LD-based systems, there are other challenges, which need to be addressed as discussed in Section 2.10.3.

2.10 Illumination Control for VLC Systems

When simultaneous data transmission along with control of illumination are considered, there are constraints regarding link stability alongside photometric response, which are needed to be considered. As mentioned in Section 2.4, the three main sources considered in this work are pc-LEDs, RGB LEDs and LDs. The normalized SPDs along with respective coordinates in the CIE 1931 diagram for these sources are depicted in Figure 2.12. CIE 1931 is chosen over the more uniform CIE 1964 color space for ease of comparison with the works presented in [28, 44]. Both pc-LEDs and RGB LEDs can generate light at a desirable CCT range unlike LDs, which generally tend to generate light with much higher CCT when operated at their ideal biasing currents. This section would summarize the key challenges associated with controlling the illumination while transmitting data for these sources.

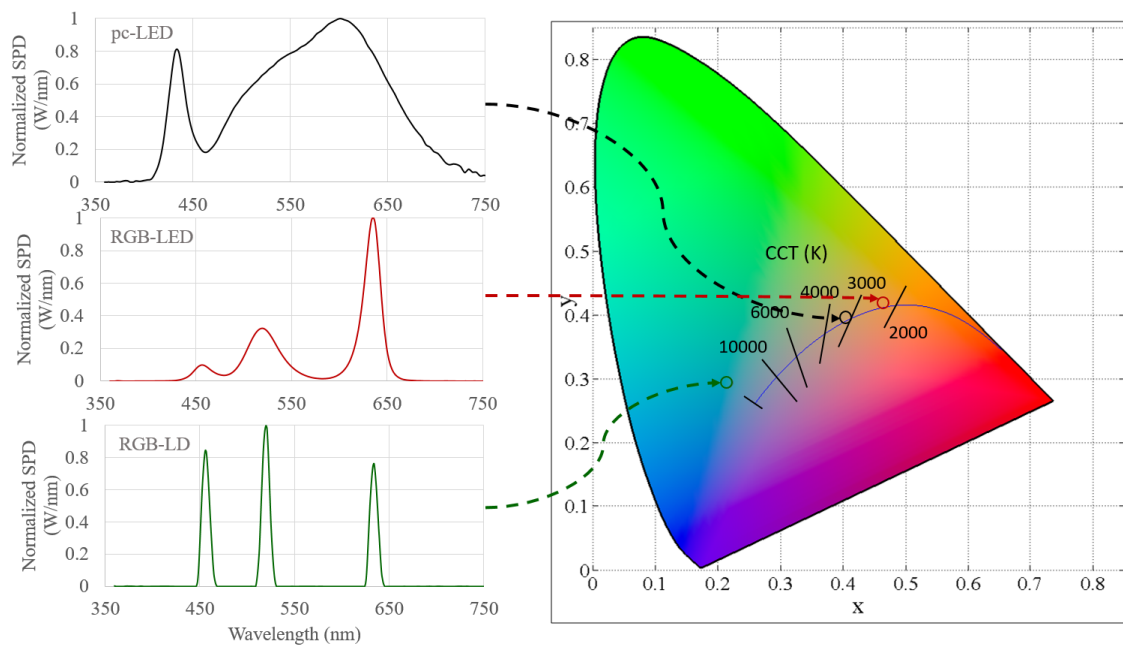


Figure 2.12: Normalized SPDs and respective locations on CIE 1931 diagram for pc-LED, RGB LED and RGB LD

2.10.1 Illumination Control in pc-LED Systems

For pc-LED based VLC systems, the number of photometric parameters that can be controlled are limited. The amount of phosphor determines the CCT of the white light, which cannot be tuned based on user requirements. The CRI of the light being generated is also fixed with warmer sources generally having higher CRI (80 - 90) than cooler sources (70-80) [177]. This CRI is much higher than the white light generated from RGB LED and LD sources. However, the remote phosphor technique in most of the commercial pc-LEDs is inefficient in producing light output in the higher wavelength region, LED lighting specially gives a low value for $R9$ (the CRI for red color). Red enhanced pc-LEDs had been proposed to increase the overall CRI by increasing the value of $R9$ [178]. As shown in Figure 2.13, red objects reflect light with better saturation due to red enhancement, which helps in rendering all the colors in the CRI test sample (depicted in Figure 2.5). This light with high CRI can be used for color matching and color inspection related applications. This raises another research question:

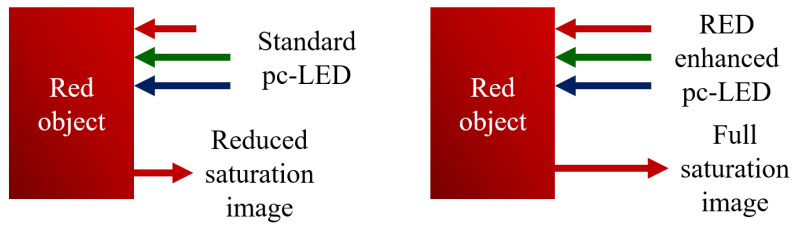


Figure 2.13: Concept of increase in saturation of red objects under red enhanced lighting

Table 2.6: Summary of work done for dimming in NRZ-OOK based VLC systems

Group	Data Rate	CCR	PWM	SU	RA	Experimental Analysis	Photometric Parameters
Jang <i>et al.</i> [37]	1 Mb/s	✗	✗	✓	✗	✗	✗
Cho <i>et al.</i> [38]	1 kb/s	✗	✗	✓	✗	✓	✗
Wang <i>et al.</i> [39]	50 Mb/s	✗	✗	✗	✓	✗	✗

- Is it possible to employ red enhancement to obtain a high value for CRI for LD and pc-LED based lighting system?

Therefore, in case of pc-LED based VLC systems, the only controllable aspect of the illumination is the illuminance, which can be regulated by implementing the dimming schemes and adaptive techniques discussed in Section 2.6. The work done previously regarding concurrent dimming and data transmission for NRZ-OOK based VLC system is summarized in Table 2.6. As discussed earlier, most of the dimming and adaptive schemes solely focused on the communication aspects, important photometric parameters such as dimming precision and chromaticity shifts had been left unexplored. This links back to the research questions 1, 2, 3 and 4. Thus, the investigation of all of the aforementioned schemes considering parameters associated with photometry and communication under a single experimental framework is an area requiring attention.

2.10.2 Illumination Control in RGB-LED Systems

In contrast to pc-LEDs, RGB LEDs opens up scopes for full control of chromaticity, by controlling the biasing current for each individual LED chip, the color

temperature can be tuned to cater to different applications (Table 2.1). Although the effect of CCT on communication aspects of VLC had been analyzed theoretically in certain works [42, 40], there has been no work on using adaptive dimming schemes predominantly used for concurrent dimming and communication in white LED-based VLC systems for CCT regulation. Only CCR and PWM scheme had been previously used for controlling the biasing currents in RGB-LED-based VLC systems. Since blue biasing needs to be limited for generating warmer light, using CCR scheme can increase the BER while PWM can decrease the achievable bit rate. In such a scenario, the adaptive schemes discussed in Section 2.6.2 can help in controlling the intensity of the blue channel while maintaining the data rate at an acceptable BER. This raises the following research question:

- Can adaptive dimming schemes be implemented for regulating the CCT of RGB LED-based VLC systems for maintaining the data rate and the BER of the system at acceptable limits?

2.10.3 Illumination Control in LD-based Systems

Based on a study by Neumann *et al.*, it was observed that diffused laser light does not compromise the user experience compared with conventional light luminaires, which pioneered the work towards LD-VLC [66]. Most of the LD-based VLC systems till date had mainly focused on achieving gigabit class communication and although the communication prospects are promising, there are several challenges regarding the illumination aspects that need to be addressed [57].

Acceptable CCT and CRI

Table 2.7 summarizes the recently demonstrated LD-based VLC systems where some photometric parameters were considered. It can be observed that only one

Table 2.7: Comparison of CCTs and CRIs achieved for LD-based VLC systems

Source	CCT (K)	CRI	Ref.
Blue LD with phosphor	7092	✗	[46]
Blue LD with phosphorous diffuser	5217	✗	[96]
Red LD (blue and green for illumination)	5835	✗	[48]
RGB	8000	✗	[44]
RGB	8382	54.4	[47]

work achieved a CCT of ~ 5800 K, which is within the intended application specific range of CCT (Table 2.1). It only used the red channel for transmission of data while the blue and green channel were left unmodulated in order to keep the chromaticity coordinates in the bottom center of the CIE 1931 color space (Figure 2.3), which denotes to the cool white region. In terms of communication capacity, this means, that there are two unused channels (green and blue), which if utilized would have given much higher aggregate data rates. The other RGB based works used three channels but with much ‘cooler’ white light. Using phosphor based blue LD can generate light with CCTs based on the amount of phosphor coating [96], but the promising aspects of utilizing higher number of parallel channels due to the narrow emission profile is undermined, which is one of the key benefits of using LDs for VLC.

For regulation of CCT, CCR is the scheme predominantly used for controlling the biasing current in each channel. But when stringent dimming is required for the blue channel at warmer color temperatures, CCR might become susceptible to noise and other schemes like PWM, SU and RA might outperform the CCR scheme. This raises another research question:

- Can adaptive dimming schemes be implemented for regulating the blue and green channels to generate light within the usable CCT range and safety standards for RGB LD-based VLC systems?

As discussed in Section 2.3.1, color quality evaluation by CRI is important to

justify the VLC system is competent with standards accepted in lighting industry [97, 159]. However, as seen from Table 2.7, CRI had not been considered in most of the VLC systems except for a very recent work by Wu *et al.* [47]. However, the reported CRI of ~ 55 is still very low compared to commercial lighting infrastructures exhibiting values above 90. The main challenge for LD-based lighting systems is the narrow emission profile, which increases the spectrum discontinuity of the light being generated. Sunlight exhibits a CRI of 100 due to the fact that its broad spectrum is evenly distributed within a wide range of wavelengths. One way to increase the overall CRI of LD-based systems would be the addition of a pc-LED to reduce the spectral discontinuity. LEDs are much more cost effective compared to LDs in the current context, thus addition of LED to an already expensive LD-based system would not significantly increase the overall system cost. The concept of combining LDs with LEDs is quite unique, the only work on such a hybrid system utilized a red LD with a pc-LED to achieve a CRI of 83 for a data rate of 400 Mb/s [55]. However, the impact of utilizing multiple LDs for a hybrid LED-LD-based VLC system to achieve gigabit class communication is an area that can be explored. This is in line with the research question 6 raised in Section 2.10.1.

Presence of Speckle Patterns

Another important aspect to be considered is the presence of speckle patterns due to high coherence of lasers. Laser speckles in an illuminated area can be visually disturbing, which might induce health complications [57]. Speckle contrast of a laser pumped phosphor based system was reduced to 1.7% at 5000 lm by proper engineering design, which is similar to that of a blue LED [179]. Other solutions involve the use of glass diffusers, hadamard matrices, vibrating reflectors and speckle reduction actuators but their usage comes at the cost of system efficiency. Speckle reduction below the visible level ($\leq 10\%$) has been reported by Lemop-

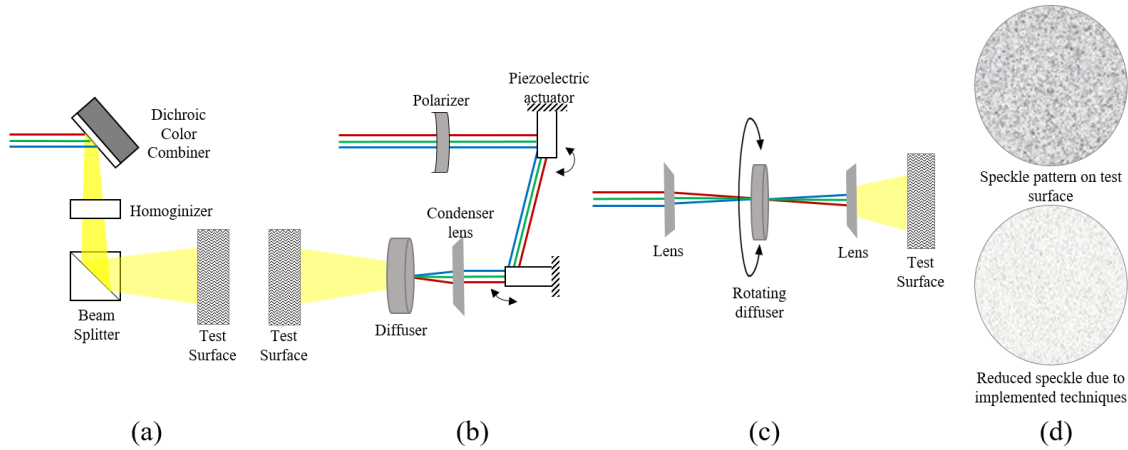


Figure 2.14: Illustration of three different techniques generally implemented to reduce speckle contrast for laser based lighting sources

tix. The techniques traditionally applied for reducing speckle pattern is further depicted in Figure 2.14. The first technique (Figure 2.14(a)) uses homogenizer and beam splitter to blend in the intensity across the entire illuminated area [51]. The second method (Figure 2.14(b)) shows how the beam is steered by two piezoelectric actuators, which causes angular diversity of laser beam to suppress speckle [52]. Rotating diffusers can be used to reduce speckle by angular dispersion of the incident beam as demonstrated in Figure 2.14(c) [53]. Vibrating actuators and beam shapers uses a similar approach as the third method in reducing speckles [180].

The quantification of speckle is a vital consideration when it is required to be reduced. However, this is a complex problem and till date there is no standardized method of calculating speckle. One way of measuring amount of speckle is by means of speckle contrast ratio (C) given as:

$$C = \frac{\langle I^2 \rangle - \langle I \rangle^2}{I} \tag{2.22}$$

where, the numerator is the standard deviation of intensity fluctuation and the denominator is the mean intensity speckle patterns [181, 182]. The denominator is often divided into objective and subjective speckle, the former is referred to when

there is no imaging involved and the latter is used when an imaging system is involved. This value ranges from 0 to 1, with images with low amount of speckle exhibiting a value close to 0.

The factors that determine the speckle reduction technique that can be applied are LD output power, beam size and the power consumption of the actuator itself [179]. LDs integrated with these sophisticated technologies might be entitled to be compliant with the IEC 62471 standard and can even be categorized as a lamp [183]. This links to the following research question:

- Can easily incorporable vibrating diffuser mitigate speckles in the white light generated from a LD-based VLC system?

Table 2.8: Laser safety classes based on transmitted power [184]

Class	Transmission power (mW)
Class 1	0-0.2
Class 2	0.2-1
Class 3A	1-5
Class 3B	5-500

Safety Concern

The major issue which might hamper the rapid growth of LD-VLC technology is safety concerns involving the use of LDs. In terms of wavelength, the IEC 60825 rulings permit longer wavelength devices to output much more power than shorter ones [185]. The safety standards for point source emitters based on transmission power were classified into four classes as shown in Table 2.8. Indoor systems are recommended to be Class 1 eye safe under all conditions [57]. LEDs being large area devices can utilize much higher launch powers (250 - 750 mW) depending on the wavelength of the source. In contrast, the power is limited to only 0.2 mW for LDs to be Class 1 eye safe. Lasers operating in Class 3B can be rendered as Class 1 eye safe by passing the beams through diffusers allowing

higher launch power (~ 100 mW). While such diffusers can achieve efficiencies of about 70 %, computer aided holograms offer a means to generate custom tailored radiation patterns with efficiencies approaching 100 % [57]. The maximum achievable data rate of a system at an acceptable BER is dependent on the SNR, energy per bit and bandwidth. Although the power constraint due to eye safety yields lower SNR for LDs compared to LEDs, the drawback can be overcome by the higher bandwidth of these sources.

2.10.4 Psychophysical Evaluation of LD Lighting

Although CRI is widely used to evaluate the quality of illumination in lighting industries, studies had shown that these parameters have no correlation to people's color preference [186, 187]. Human preference of any light sources can be characterized by conducting a psychophysical assessment where the relationship between physical stimuli and the respective sensations and perceptions are investigated quantitatively.

At the developing stages of solid state lighting industry, LEDs were extensively evaluated in comparison with traditional lighting systems by various psychophysical assessments where groups of people judged the quality of LED illumination [188]. As the LED industry matured and gained reputation to be a competent light source, other complex factors like visual perception, intelligent outdoor lighting, attention guidance and color control interfaces had been investigated on the basis of human perception [189, 190, 191, 192]. However, for LD-based lighting systems, there had been only one assessment where LDs were compared with incandescent and LED light sources in terms of overall preference [66]. In that work, it was reported that the overall preference of saturation was the driving factor, which played an important role in overall preference. Other factors such as contrast, visual comfort, naturalness of colors, pleasantness and brightness are needed to be considered for obtaining a more thorough compar-

ison. Since LDs are mainly being considered for high speed VLC, the comparison needs to be conducted in comparison with LEDs and other traditional light sources can be ignored. This raises another research question:

- How is the human perception of LD-based lighting in comparison to LED-based lighting in terms of overall preference, contrast, saturation, visual comfort, naturalness of colors and pleasantness?

Human subjective assessment are generally acquired using a 'Likert Scale' [193]. It is a psychometric response scale, which is used to obtain a participant's preferences or degree of agreement for a particular statement. Likert scales in general are non-comparative and unidimensional in nature. It is the most widely used approach to scaling responses in survey research.

Statistical data can generally be classified into three categories: numerical (discrete and continuous), categorical (data representing a characteristic such as gender, marital status etc.) and ordinal (a mix between numerical and categorical data where the variables have natural and ordered categories). Individual responses to a likert scale should be treated as ordinal data. The statistical significance of ordinal data is generally calculated using non-parametric tests. A null hypothesis is derived concerning the probability distribution of the response of a particular population and based on hypothesis tests, a p-value is calculated, which helps in identifying whether the responses are statistically significant. There are different types of non-parametric hypothesis test, but in this work the two tests mainly considered are the Mann-Whitney-Wilcoxon (MWW) rank sum test and the Chi-square (χ^2) test [194]. The MWW test was also used by Neumann *et al.* for statistical analysis of human preference for LD-based lighting [66]. Lower p-values (< 0.05) indicate the test is statistically significant whereas higher p-values (> 0.05) indicate the test is statistically insignificant based on the null hypothesis defined at the beginning of the test.

2.11 Conclusion

In this chapter, the literature associated with the basic fundamental understanding of the working principles of VLC in terms of parameters associated with communication and illumination were concisely presented. The growing trend towards replacement of traditional lighting infrastructures with energy efficient LEDs opened up the scopes for utilizing them for concurrent data transmission and illumination. However, considering the stringent requirements and growing number of wireless communication devices, communication is required at gigabit class range, which can be effectively delivered utilizing LDs due to their superior modulation capabilities.

When simultaneous communication and illumination are considered, a competent VLC system must have the capabilities of achieving full control over various parameters associated with lighting quality while maintaining the original data rate. This can be effectively provided utilizing various dimming techniques. Although, in literature, these schemes had been analyzed by simulation, considering the communication aspects, a detailed experimental analysis of how each scheme works in terms of the photometric parameters is an area requiring attention.

Dimming schemes can be classified into pulse regulated schemes and analog dimming. Although, pulse regulated schemes and CCR had been investigated in terms of driver efficiency and non-linearities, it is important to compare their performance based on the photometric parameters such as CCT, CRI and illuminance distribution, which raises the following issues:

1. How does FM perform compared to PWM when photometric parameters such as CRI, CCT and linearity of illuminance are being considered?
2. How much chromaticity shift is induced when CCR and PWM are implemented in a VLC system?

Although dimming schemes achieve control over illumination, the link stability considering the SNR and data rate of the system is hampered by these schemes. Adaptive dimming schemes can resolve this issue by making sure the data transmission remains uninterrupted. However, the schemes were proposed mainly to enhance the transmission rate and their effect on the overall illuminance was overlooked, which links to other two important issues:

3. How does transmission of bits when the duty cycle is low in slot utilization affect the overall illuminance and does it hamper the dimming precision?
4. Can different adaptive schemes be simultaneously utilized to subdue the stringent requirement on either of them enabling dimming with better performance in terms of communication?

For multi chip LED-based VLC systems, the effect of CCT on the link capacity had been investigated previously but the implementation of adaptive dimming schemes for regulating the CCT in the warm, neutral and cool-white region had not been explored. This raises another issue:

5. Can adaptive dimming schemes be implemented for regulating the CCT of RGB LED-based VLC systems for maintaining the data rate and the BER of the system at acceptable limits?

Although, the prospects of RGB LD-based VLC systems are promising in terms of communication aspects. Most of the work in literature had only considered CCT with values going beyond the practical range of 2700 K - 6500 K. Besides that, laser based lighting raises several questions in terms of presence of speckle pattern and eye and skin safety. Various mechanisms considering the diffuser optics can be employed to render the laser eye safe and reduce speckles. All these work regarding LD-VLC raises other key issues:

6. Can adaptive dimming schemes be implemented for regulating the blue and green channels to generate light within the usable CCT range and safety standards for RGB LD-based VLC systems?
7. Can easily incorporable vibrating diffuser mitigate speckles in the white light generated from a LD-based VLC system?
8. How is the human perception of LD-based lighting in comparison to LED-based lighting in terms of overall preference, contrast, saturation, visual comfort, naturalness of colors and pleasantness?

Color rendering capabilities of LD-based systems had been overlooked until very recently, where a CRI of ~ 55 was demonstrated. LDs suffer from low CRI due to spectral discontinuity, which occurs due to the narrow emission profile of these sources. Although, pc-LEDs have higher CRI than RGB LEDs or LDs, the CRI is still quite low when compared to incandescent sources due to the inability of replicating colors in the higher wavelength region. Although, red enhanced LEDs had been proposed, this concept can be implemented by a red LD, where the LD is used for red enhancement and gigabit class communication and the LED is used for illumination and spectrum continuity. This raises another important issue:

9. Is it possible to employ red enhancement to obtain a high value for CRI for LD and pc-LED based lighting system?

In the next chapters, dimming and adaptive schemes are implemented on pc-LED, RGB LED, RGB LD-based VLC systems to regulate the illuminance and CCT. Speckle mitigation is investigated by vibrating diffusers and the developed LD-based system is investigated based on psychophysical assessment of 40 individuals. Prospects of CRI enhancement by the combination of LDs with pc-LED to form a hybrid system is also explored.

DIMMABLE PC-LED-VLC SYSTEM WITH CONCURRENT DATA TRANSMISSION

3.1 Introduction

In the previous chapter, the different types of sources and their corresponding unique features that can be used in VLC were discussed. Among different types of LEDs, which are commercially available, pc-LEDs are the most widely used and installed due to their lower cost and ease of control. However, for these sources the lighting parameters that can be controlled are limited. The color temperature of light being produced is fixed depending on the amount of phosphor and the only variable photometric aspect is the luminous intensity, which can be controlled by dimming schemes like FM, CCR, SU and RA. It is also important that these sources operate at a constant CCT and do not induce any chromaticity shifts, which human occupants might notice. Thus, a dimming scheme being implemented must achieve control over the illuminance while minimizing chromaticity shifts. As discussed earlier, these issues raised the following research questions:

- How does FM perform compared to PWM when photometric parameters

such as CRI, CCT and linearity of illuminance are being considered?

- How much chromaticity shift is induced when CCR and PWM are implemented in a VLC system?
- How does transmission of bits when the duty cycle is low in slot utilization affect the overall illuminance and does it hamper the dimming precision?
- Can different adaptive schemes be simultaneously utilized to subdue the stringent requirement on either of them enabling dimming with better performance in terms of communication?

In this chapter, a NRZ-OOK based VLC system was developed, which could operate at a maximum speed of 20 Mb/s. This was achieved by employing a blue filter at the receiver, which helped in increasing the overall bandwidth from ~ 3 MHz to ~ 20 MHz. Based on a systematic approach of simultaneous evaluation of photometric and communicative parameters, different dimming schemes were investigated, which helped in justifying the superiority of digital dimming that answered the first two research questions. An analytical model was developed to validate all the experimental results in theory. Both experimental and analytical results followed similar trends with some minor differences. It was demonstrated that although adaptive schemes help in seamless digital dimming, there are certain restrictions in terms of bandwidth limitations and dimming precision, which none of the works in the literature reported since those investigations were simulation based and did not consider photometric parameters [37, 38, 39]. Based on the limitations of each adaptive scheme, a dimming algorithm was formulated, which utilizes multiple dimming techniques simultaneously depending on the dimming target and achieves seamless dimming while maintaining the data rate at an acceptable BER that answered the other two research questions.

The rest of the chapter is organized as follows. Initially the experimental setup and the reasons for different components being added into the VLC link are dis-

cussed in Section 3.2. Section 3.3 presents the LVI characterization of the LED that was utilized. The analytical model developed for theoretical evaluation and the methodology of this work are presented in Section 3.4 and 3.5 respectively. The comparison of digital dimming with frequency modulation (FM) and analog dimming are presented in Section 3.6 and 3.7 respectively. The methodology and evaluation of adaptive techniques are presented in Section 3.8 and 3.9. Based on the initial investigations, the proposed dimming scheme and the overall comparison of this scheme with digital dimming is presented in Section 3.10. Finally, a summary of the contributions and key outcomes is presented in Section 3.11.

3.2 Experimental Setup of LED-based VLC

The complete VLC system used in this work is depicted in Figure 3.1. The line of sight (LOS) VLC link uses a neutral white pc-LED (OSRAM LCW CP7P) as its source [195]. The LED was attached to a heat sink to ensure the effect of variation of junction temperature is minimized during the experiments. Pc-LEDs generally have 3-dB modulation bandwidth of ~ 3 MHz [124, 126]. By blue filtering, this can be extended to ~ 20 MHz [196]. The analytical and experimental characterization of frequency response of the LEDs are presented in Section 6.3.1. A low pass optical filter¹ (Thorlabs FES500) was used to remove the slow phosphor component and increase the system bandwidth to ~ 20 MHz. The transmittance of the filter as a function of wavelength is presented in Figure 3.2. Thus a baseband transmission rate of 10 Mb/s was chosen (1 MHz signal frequency represented a data rate of 1 Mb/s) for having a stable BER performance.

The modulated waveforms were generated using Tektronix arbitrary waveform generator (AWG) 5014c. The device is capable of generating any modulation scheme without any specialized hardware. It has 4 channels, each of which

¹A filter that passes signals with a frequency lower than a certain cut-off frequency and attenuates signals with frequencies higher than the cut-off frequency

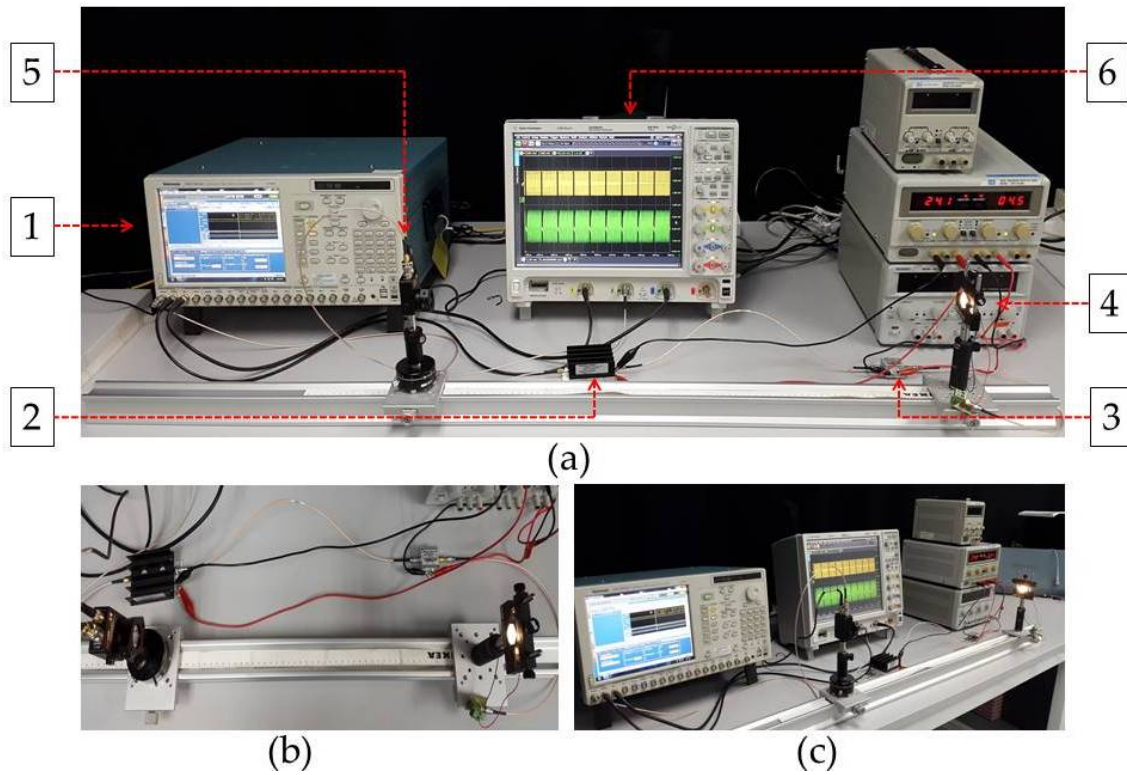


Figure 3.1: VLC system utilizing pc-LED as its transmitter and a Si PD as the receiver (a) front view, (b) top view, (c) side view

Table 3.1: System description

No.	Component	Device
1	Waveform Generator	Tektronix AWG 5014c
2	Amplifier	Mini Circuits ZHL-6A-S+
3	Bias Tee	Mini Circuits ZFBT-4R2GW-FT
4	Transmitter	Single Chip Oslon LED NUWH
5	Receiver	Thorlabs PDA-10A (Si-PD)
6	Oscilloscope	Agilent DSO 9054H

can sample at up to 1.2 GS/s, 480 MHz analog bandwidth and 14 bit vertical resolution. MATLAB[®] was used to create the required waveforms, which were uploaded to the AWG. This helped in facilitating signal processing and demodulation since it was easier to keep track of the bit patterns.

The generated waveforms from the AWG was amplified by means of a broad-band power amplifier Mini Circuits ZHL-6A+ (when necessary), to increase the strength of the transmitted signal, which will generate a discrete signal at the re-

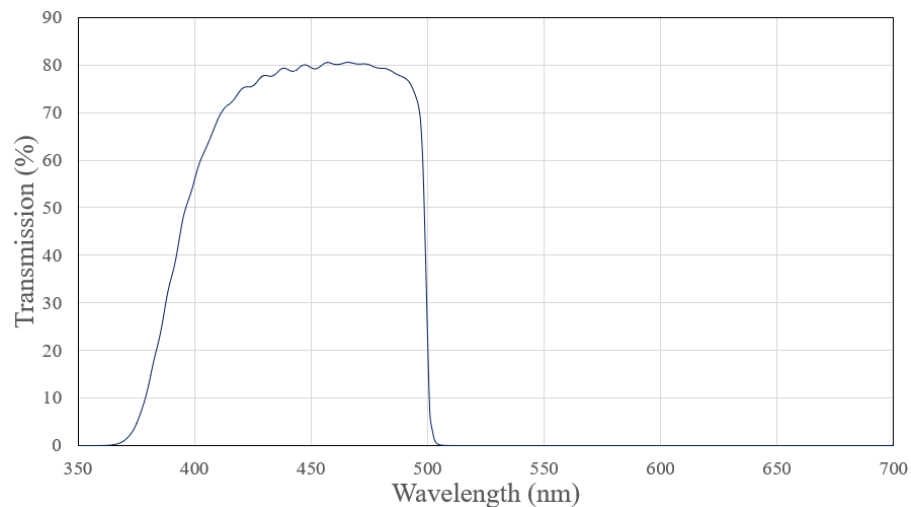


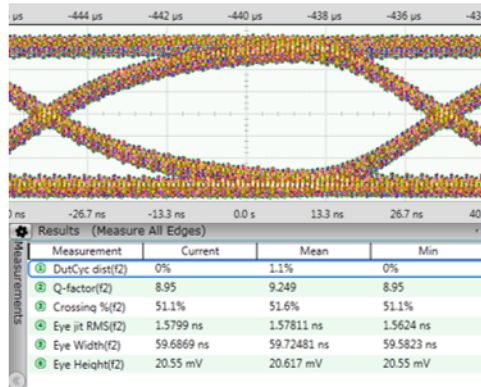
Figure 3.2: Transmittance of filter as a function of wavelength

ceiver. The amplifier was used in the receiver as well depending on the received signal power.

A wideband coaxial bias tee (Mini Circuits ZFBT-4R2GW-FT) was used to combine the high frequency modulated waveforms with the DC component from the power supply for biasing the LED at the operating region. It could operate at a maximum current of 500 mA and the cut off frequency range was 100 kHz to 4200 MHz.

A silicon PIN photodiode (Thorlabs PDA-10A) was used as the receiver where an oscilloscope (Agilent DSO 9054H) was used to capture the received waveform. A 20 MHz electrical low pass filter (Minicircuits BLP-21.4+) was used to filter out the high frequency noise components at the receiver. Further signal processing was done using customized digital filtering and smoothing functions in the oscilloscope. A high speed serial data analysis software (N5384A) was used in the oscilloscope to obtain the instantaneous eye diagram, which was used to compute the Q-factor, eye width, jitter and crossing [197].

The complimentary error function allows a simple way to calculate the BER from the Q factor as given by [198]



Q factor (instantaneous)	9.249
BER (instantaneous)	1.133×10^{-20}
BER (calculated)	2.536×10^{-19}
Difference	2.4227×10^{-19}

Figure 3.3: Instantaneous eye diagram obtained using the serial data analysis software and the corresponding BER values computed from the Q factor and by off-line demodulation.

$$BER = \frac{1}{2} \operatorname{erfc}\left(\frac{Q}{\sqrt{2}}\right) \quad (3.1)$$

The BER was also calculated at different instances by capturing the entire received waveform and demodulating it off-line using MATLAB[®]. One such eye diagram captured during the analysis along with the values of instantaneous BER and calculated BER is presented in Figure 3.3. The off-line calculated BER did not differ much from the instantaneous BER obtained using equation 3.1, thus the computational time of analysis was significantly reduced by monitoring the instantaneous eye diagram.

However, for investigating the communication performance of different dimming schemes, since a single pc-LED was being utilized, the ideal biasing voltage of 3.5 V could be supplied by the AWG provided the link distance was reduced to 0.25 m. Hence the inclusion of bias-T, which added complications in combining the dimming signal with the DC bias was avoided. The waveforms that were generated can be replicated by using customised driver circuit with fast switching electronics [23]. The experimental setup of the communication link is presented in Figure 3.4.

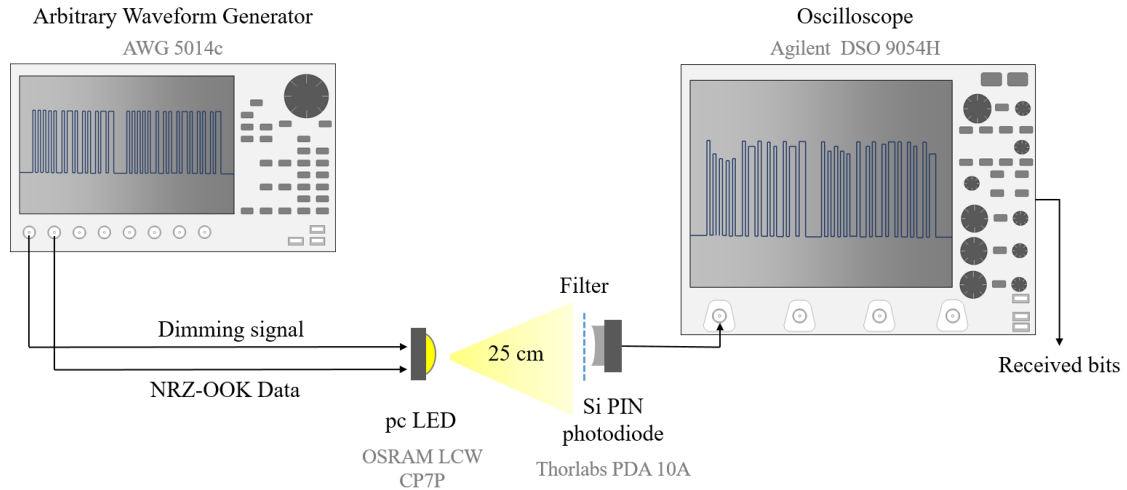


Figure 3.4: Experimental setup of the pc-LED based VLC system

3.3 Characterization of pc-LED

The photometric and radiometric evaluation of the dimming schemes was conducted using an integrating sphere with a diameter of 500 mm and the measurements were made using a dedicated CAS-120 array spectrometer as shown in Figure 3.5. The setup was also used to characterize the LVI response of the LED used for this work. Since light is confined and diffused within the boundaries of the sphere, it allows more precise interpretation of quality of illumination of the VLC system [33]. In some cases, measurements were made using the CL-500A spectrophotometer [199], which was placed in front of the light source at a similar distance without the integrating sphere.

The LVI response of the pc-LED that was used is presented in Figure 3.6. The non-linear characteristics of LED is clearly visible. LED non-linearity needs to be taken into account when modulating as amplitude distortion occurs at TOV and at the saturation current in the high peaks due to the $I-V$ characteristics of LEDs [56]. As discussed in Section 2.5, it has a higher impact on OFDM and causes increase in BER and inter-carrier interference (ICI). Thus selection of optimum point of operation is critical for superior link performance in VLC [200].

The normalized SPD of the pc-LED along with the responsivity of the photo-

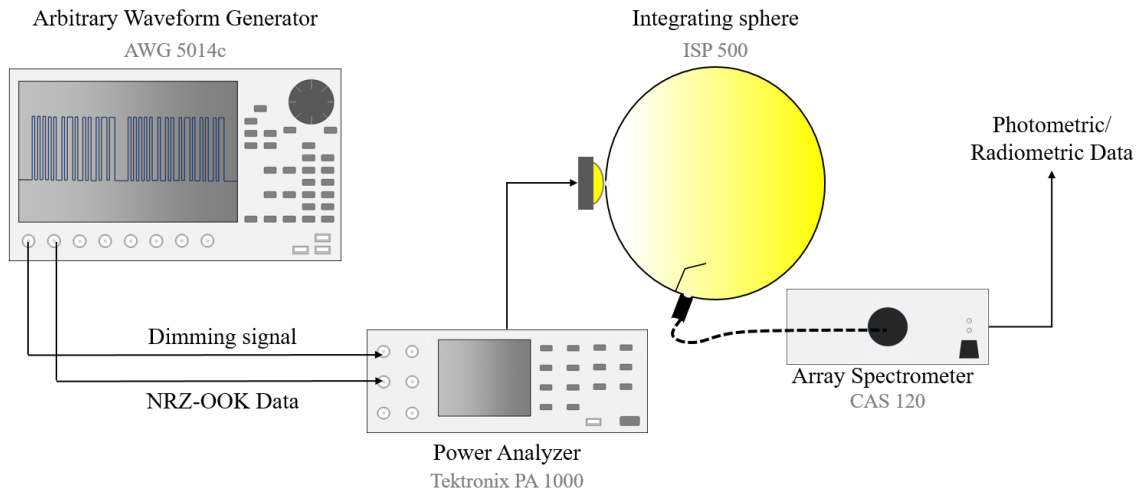


Figure 3.5: Experimental setup for investigation of the photometric and radiometric response of dimming schemes.

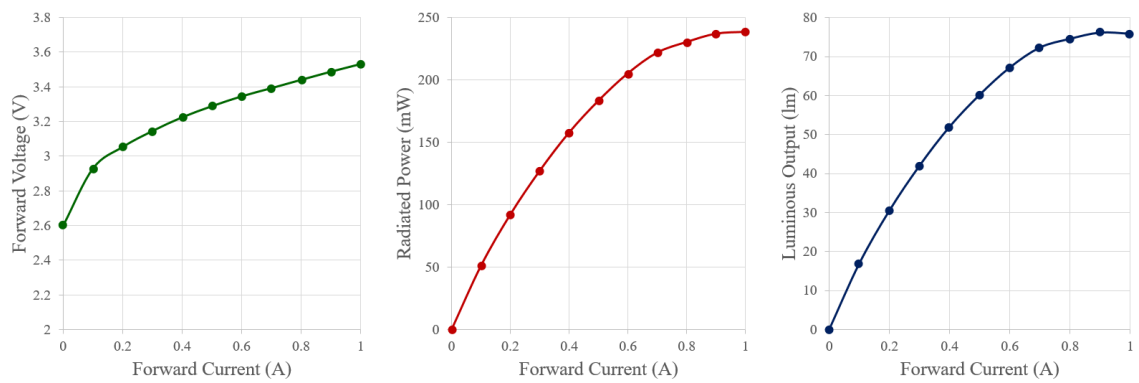


Figure 3.6: LVI characteristics of pc-LED

diode used for the VLC link is presented in Figure 3.7. Since pc-LEDs contains a blue emitting die combined with yellow emitting phosphor, there is a narrow blue peak (~ 435 nm) and a wider peak in the yellow region (~ 510 nm to 660 nm) [33].

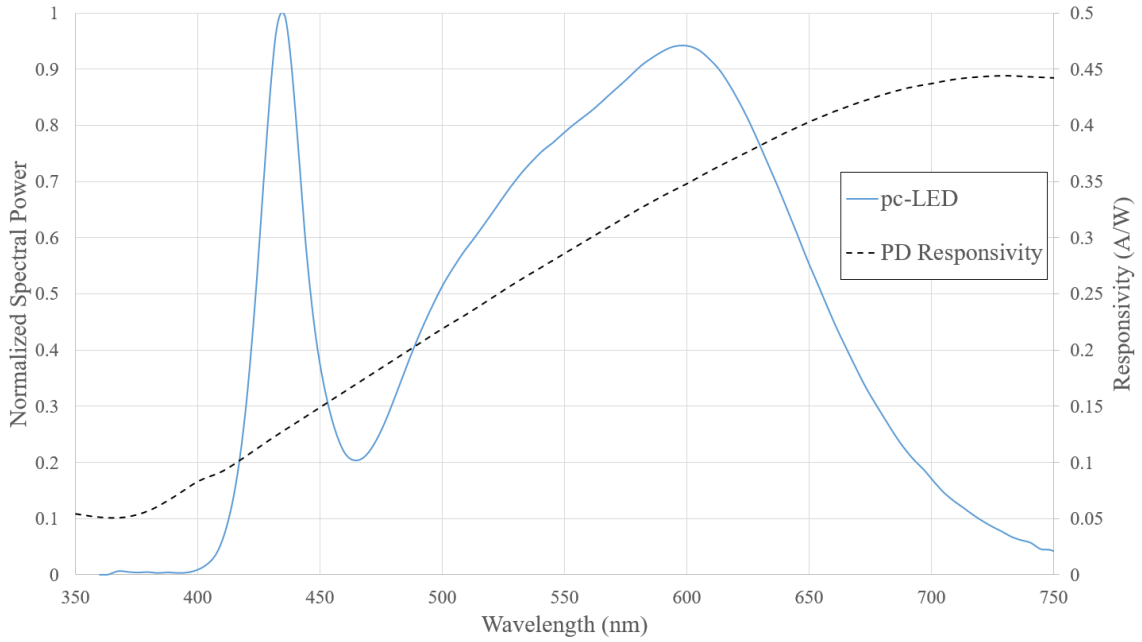


Figure 3.7: Normalized spectral power distribution of pc-LED and photodiode responsivity for different wavelengths in the visible range

3.4 Analytical Model of pc-LED-based VLC

The analytical model for the VLC system was developed in MATLAB[®]. The luminous intensity² of the light source is a key parameter, which has an impact on the spatial signal and light distribution. Referring back to eq. 2.1 associated with the luminous flux (L), the luminous intensity (l) is given by [22]

$$l = \frac{dL}{d\Omega} \quad (3.2)$$

Generally, LED's radiation is emitted in Lambertian pattern[22, 122, 201, 77], thus its luminous intensity for an angle ϕ is given as [22]

$$l(\phi) = l(0)\cos^m(\phi) \quad (3.3)$$

where $l(0)$ is the center luminous intensity and m is the order of the Lambertian

²Luminous intensity is a measure of wavelength-weighted power normalized to the human eye response emitted by a light source. It is measured in candela (cd)

Table 3.2: System parameters for analytical model of LED-based VLC system

	Parameters	Value
Transmitter	Wavelength (nm)	451
	Semi angle at half power ($^{\circ}$)	40
Channel	Distance (m)	0.25
	Background noise current (A)	202×10^{-6}
Receiver	Filter transmittance	0.925
	Area of PD (m^2)	8×10^{-6}
	Responsivity (A/W)	0.149

emission, given by the semi angle at half power of illuminance of the LED ($\Phi_{1/2}$) as [202]

$$m = \frac{\ln 2}{\ln(\cos(\Phi_{1/2}))} \quad (3.4)$$

The horizontal illuminance E_{hor} is given by [22]

$$E_{hor} = \frac{l(0)\cos^m(\phi)}{d^2\cos(\psi)} \quad (3.5)$$

where d is the distance between the LED and the detector, ϕ and ψ are the angle of irradiance and incidence respectively.

The received optical power at the receiver, P_r can be calculated by [203]

$$P_r = H(0)P_t \quad (3.6)$$

where P_t is the transmitted optical power and $H(0)$ is channel DC gain, which was defined initially in Section 2.3.2 by eq. 2.11. For optical link, the DC channel gain is given by [77, 203]

$$H(0) = \left\{ \begin{array}{l} \frac{(m+1)A_{det}}{2\pi d^2} \cos^m(\Phi) \cdot T_s(\psi) \cdot g(\psi) \cdot \cos(\psi), \quad 0 \leq \psi \leq \psi_{con} \\ 0, \quad \psi > \psi_{con} \end{array} \right\} \quad (3.7)$$

where A_{det} is the physical area of the PD, $T_s(\psi)$ is the optical filter gain, $g(\psi)$ and ψ_{con} are the concentrator gain and FOV, respectively. Using refractive index n ,

$g(\psi)$ is defined by:

$$g(\psi) \begin{cases} \frac{n^2}{\sin^2 \psi_{con}}, & 0 \leq \psi \leq \psi_{con} \\ 0, & \psi_{con} \leq 0 \end{cases} \quad (3.8)$$

The electrical SNR is related to the received optical power by [22]

$$SNR = \frac{R^2 P_r^2}{\sigma_n^2} \quad (3.9)$$

Some of the parameters like responsivity are related to the optical SNR given by equation 2.10. The parameter σ_n is the noise variance consisting of both shot and thermal noise. For NRZ-OOK modulation scheme, the BER is directly related to the SNR by [22]

$$BER = Q(\sqrt{SNR}) \quad (3.10)$$

where $Q()$ is Marcum's Q -function. The parameters used for the analytical model of the pc-LED-VLC system are summarized in Table 3.2.

3.5 Methodology

The methodology implemented in this work is summarized in Figure 3.8. The LVI characterization done using the integrating sphere is used for developing the analytical model in MATLAB[®]. The comparison of pulse regulated, analog, digital and adaptive schemes (discussed in the coming sections) are conducted experimentally considering parameters associated with communication and illumination. Theoretical validation of each scheme is also done at each step. All the results are compared under a single framework, which resulted in identifying their inadequacies considering certain practical aspects. This eventually led to the proposal of a novel dimming algorithm, which utilizes multiple adaptive schemes simultaneously.

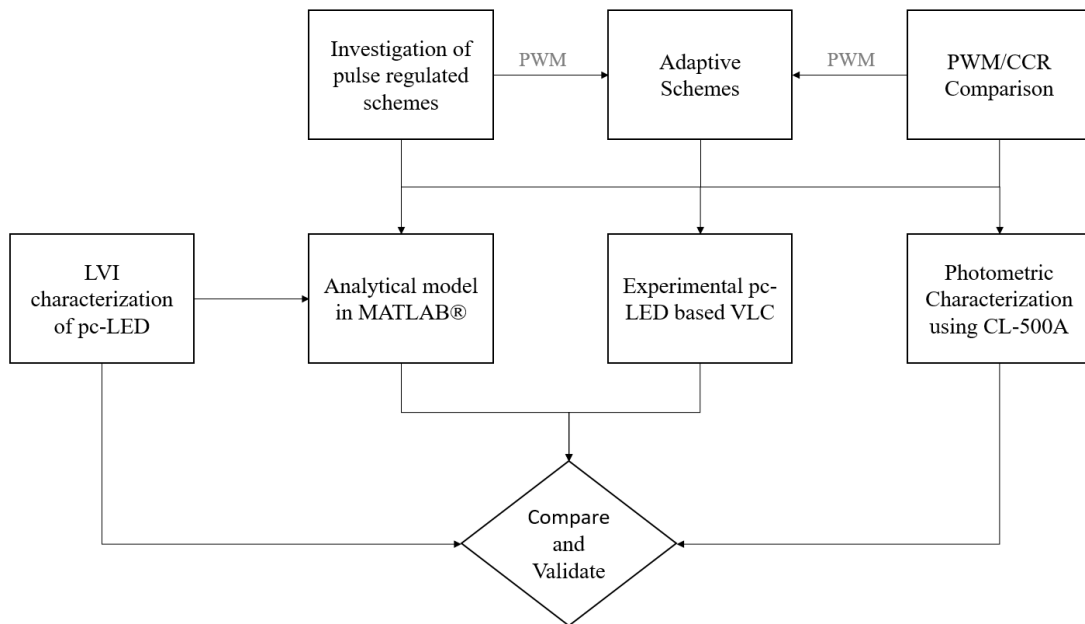


Figure 3.8: Methodology used for comparison and analysis of dimming schemes for pc-LED based VLC system

3.6 Investigation of Pulse Regulated Dimming Schemes

Referring back to Section 2.6.1, pulse regulated schemes can be classified into FM and PWM. FM consists of CPFM and CZFM. In contrast to PWM, FM was mainly proposed in [34] for driver circuit efficiency without accounting for the impact on photometric properties, which is characterized in this work. It was necessary to investigate the performance of LEDs under pulse regulated schemes before they could be used in VLC. This is because the FM schemes involve variation of frequency, which would have made the process of waveform incorporation more complex. The investigated waveforms are shown in Figure 3.9.

Figure 3.10 shows the overall experimental setup for the exclusive testing of different pulse regulated schemes. The DC power supply is used to power up the driver circuit with a driving voltage of 5V. A power MOSFET (IRF 630) was utilized for switching the pc-LED based on the signals generated by the micro-controller (Arduino Duemilanove). The photometric response of the LEDs is measured using the CL-500A spectrophotometer and the data is analyzed using

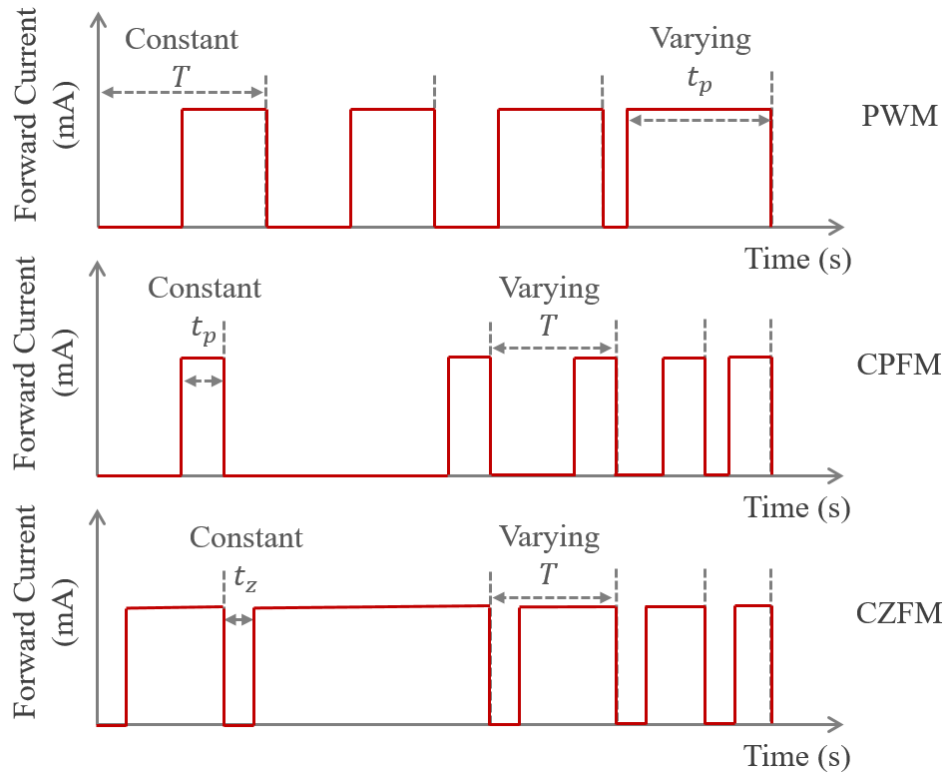


Figure 3.9: Investigated pulse regulated waveforms

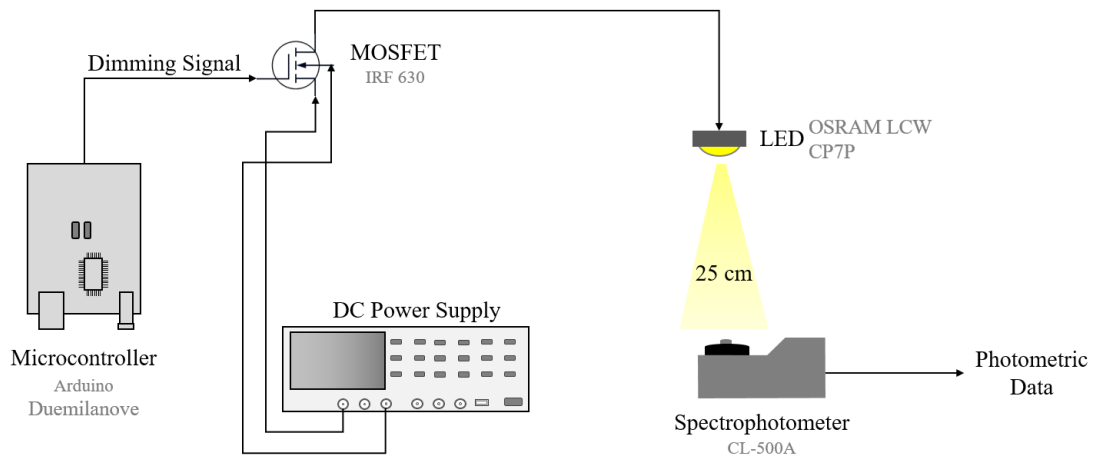


Figure 3.10: Experimental setup for the analysis of pulse regulated dimming schemes

the CL-S10w data management software.

The photometric parameters that were analyzed are the illuminance, CCT and CRI, which are summarized in Figure 3.11. A second order polynomial fit was used for curve fitting and from the results, the difference in the photometric per-

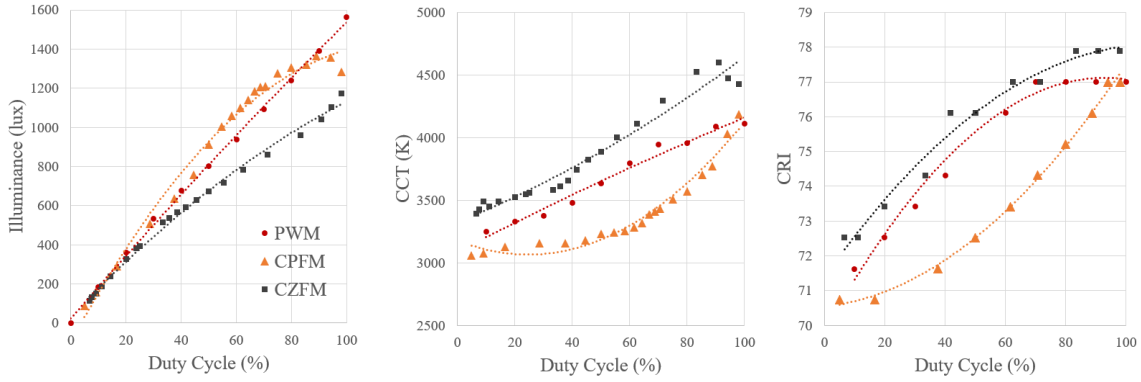


Figure 3.11: Distribution of illuminance, CCT and CRI for investigated pulse regulated dimming schemes

formance of these schemes can be observed. The illuminance, which was previously defined in Section 2.3.1 is seen to increase with the duty cycle for all of the pulse regulated schemes. This is because the illuminance of a LED is a linear function of the time, which is given by

$$E = \frac{t_{avg,ON}}{T} E_{max} = D E_{max} \quad (3.11)$$

where, E is the mean illuminance, $t_{avg,ON}$ is the average ‘ON’ time of the modulating pulse, T is the total time period of the pulse, E_{max} is the maximum illuminance of the LED at rated forward current and D is the average duty cycle of the modulating signal [204].

The three schemes have similar illuminance at lower duty cycle, but in the mid-range, CPFM has the highest illuminance and CZFM has the lowest. Referring back to Section 2.6, in CPFM scheme, t_{ON} is kept constant and t_{OFF} is linearly increasing at a constant rate, to increase the brightness of the LED, t_{ON} is incremented at a much greater rate, which accounts for a greater total ‘ON’ time of the pulse at the same average duty cycle compared to PWM and CZFM. This phenomenon is just the opposite in case of CZFM, since t_{OFF} is varied to vary the intensity of the LED. For decreasing the brightness, t_{OFF} is increased at a much greater rate. This causes the total ‘OFF’ duration of the pulses to be much greater

for the same average duty cycle causing the illuminance to be lower. When the duty cycle reaches a very high value ($D > 95\%$), CPFM takes a sharp fall. This is because t_{ON} becomes very high causing the frequency of the modulating signal ($f = \frac{1}{t_{ON}+t_{OFF}}$) to rapidly decrease below the minimum flicker frequency, causing flicker and thereby decreasing the mean illuminance. However, the illuminance for the general PWM scheme keeps linearly increasing causing PWM to have the highest illuminance when duty cycle is maximum ($D = 100\%$).

The LED used in this work had a rated CCT of ~ 3500 K. The CCTs for both of CPFM and CZFM increases with duty cycle. However, PWM provides the least variation in CCT. This phenomenon would be discussed in Section 3.7. The CRI of the light increases quite linearly by a value of 6. Although this change in CRI can be negligible, there is a similar trend for all the schemes compared to the previous plots. It was observed that $R9$ value (represents red color) was relatively low, which is a common problem with pc-LEDs. Since they emit blue light but use the phosphor coating to make it white, the color coordinates are generally towards the blue spectrum. Since the overall CRI (R_a) is determined only with mediumly saturated colors, the color rendering of saturated colors ($R9$ to $R12$), particularly $R9$, can be very poor even though R_a is fairly good, which falls in line with the discussion in Section 2.10.1. Saturated colors should somehow be considered. Thus, in some cases R_a is not a trustable index for color rendering performance of white LEDs [205]. This low value of $R9$ can be solved by adding red sources to the pc-LED based lighting system, which would be discussed in Chapter 6. It was observed that CZFM and PWM have CRI values much higher than CPFM scheme. Differences of CRI values of less than 5 points is not significant (e.g lamps with CRI of 82 and 85 should be considered equivalent) [206]. As a result, this small variation of CRI was not considered as an important performance parameter for the choice of dimming schemes in this project and it was assumed that the small variations of CRI occurred due to changing color temper-

ature and junction temperature.

The overall observations made from this investigation are:

- PWM scheme can be used for the entire range of dimming targets unlike CPFM and CZFM, which causes flicker at certain extremes of the duty cycle
- PWM scheme causes the lowest variation in CCT compared to CPFM and CZFM schemes
- CRI variation for all three pulse regulation schemes demonstrate similar trend
- PWM is the preferable pulse regulation mode that should be used to dim LEDs

3.7 Investigation of PWM and CCR Dimming for Illumination and VLC

Having justified the versatility of PWM scheme compared to other pulse regulated schemes, it was necessary to characterize its effect on the photometric and communicative performance of a VLC system in contrast to the CCR scheme. The proper incorporation of high speed data with dimming control requires development of sophisticated driver circuitry with CMOS electronics [207]. However, in this investigation the expected output from the driver was manually emulated using the AWG and the development of such high speed switching circuits was left as a future direction (Section 7.3.1). NRZ-OOK modulation is used to encode the data that needs to be transmitted since it reduces system complexity and cost compared to other spectrally efficient schemes. With high speed systems already demonstrated by using NRZ-OOK schemes [145, 128, 129, 149, 125], the main objective was to analyse and enhance the performance of this scheme under dif-

ferent dimming techniques. The waveform for a NRZ-OOK data stream under CCR and PWM dimming is depicted in Figure 3.12.

In case of CCR, the transmitted bits were scaled down to different amplitudes depending on the dimming target (d), which is defined by eq. 2.18. This can be modelled by the following equation:

$$y(t) = d.x(t) = A.x(t) \quad 0 \leq d \leq 1 \quad (3.12)$$

where $y(t)$ is the overall data stream that is transmitted, A is the amplitude scaling factor, which determines the signal amplitude of the transmitted bits and $x(t)$ is the original NRZ-OOK data stream. For CCR, $A = d$. Although the scheme is quite simple to implement, the key challenge expected from the perspective of link stability is data transmission when dimming target is very high, which would make it difficult for the receiver to distinguish the received bits from the shot noise due to low SNR.

PWM dimming on the other hand allows data transmission only when the duty cycle is high with a constant amplitude. Thus shot noise will have a con-

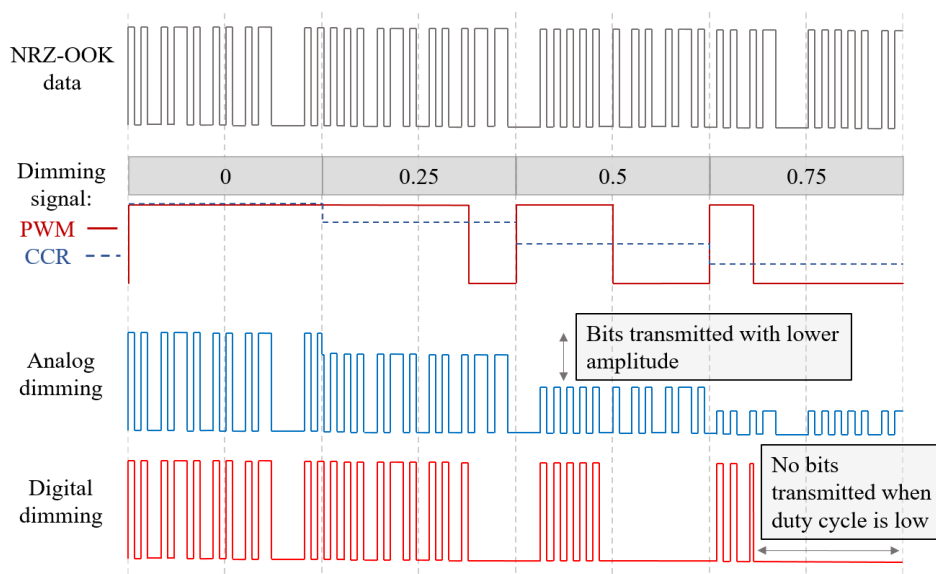


Figure 3.12: NRZ-OOK data stream after implementation of analog and digital dimming for different dimming targets

stant effect and if the SNR at the receiver is high enough, the transmission will occur with a low BER. However, the instantaneous data rate (R_{ad}) of the system would drop based on equation 2.19. This scheme can be defined by the following equation:

$$y(t) = \begin{cases} x_1(t) + x_2(t) + \dots x_n(t) & d = 1 \\ x_1(t) + 0.x_2(t) + x_3(t) + \dots 0.x_n(t) & 0 \leq d < 1 \end{cases} \quad (3.13)$$

where, n is each sample of the transmitted signal until dimming signal changes its state and $x_n(t)$ is the divided segment of the original data stream.

Figure 3.13 presents the distribution of illuminance and MacAdam ellipses at a SDCM of 3500 K for the VLC link under PWM and CCR dimming. It can be observed that the distribution of illuminance is much more linear for PWM. This is because the LED is operated at an average constant biasing current, which falls within the ideal operating region of the LED. In case of CCR, there is non-linearity for lower amplitudes. This non-linearity might induce changes in the dominant wavelength of photons emitted causing chromaticity shifts. **These results were presented as a contribution in [33].**

From the MacAdam ellipses, it can be observed that for both techniques, the points for maximum and minimum dimming levels lie within 2 steps of each other. This implies that human observers would notice some changes in color of the emitted light from the VLC system. The x and y coordinates for the chromaticity diagrams changes linearly based on the dimming target with the change being higher for CCR dimming. This changes are believed to be induced due to band filling and quantum-confined stark (QCSE) dominated effects [152]. The non-linearity in illuminance as observed in Figure 3.13 for the CCR scheme is believed to be causing the higher shift in chromaticity coordinates.

Referring back to the LVI characterization of the pc-LED discussed in Section 3.3, the amount of change in CCT induced by CCR in contrast to PWM was quan-

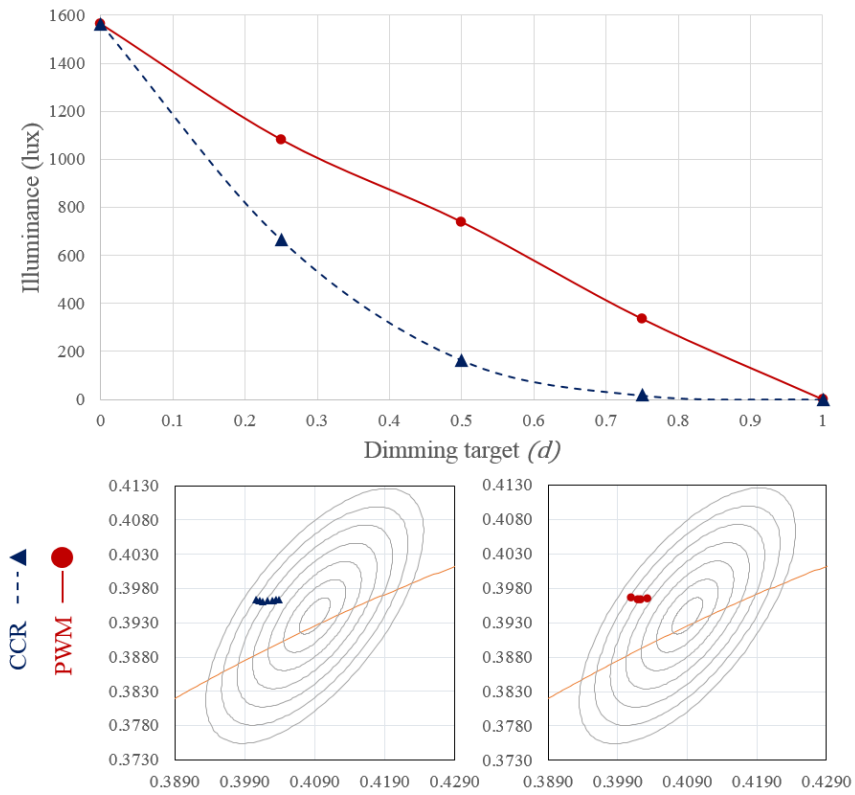


Figure 3.13: Variation of luminous flux with dimming targets for analog (blue) and digital (red) dimming. The MacAdam ellipse at a SDCM of 3500 K for these two schemes are provided.

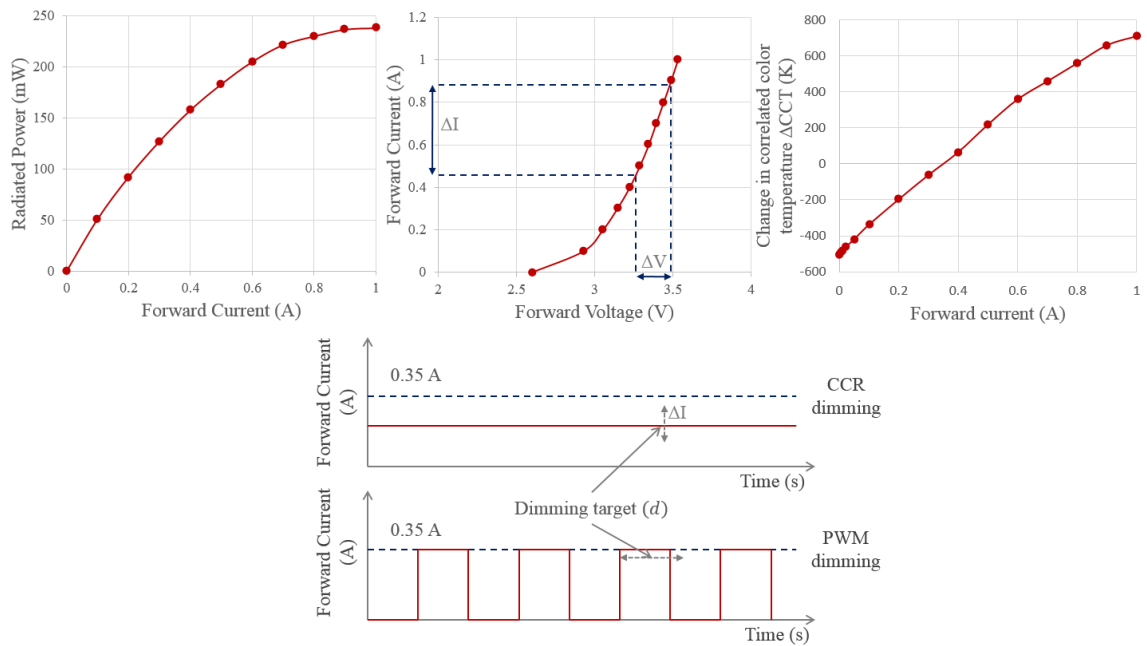


Figure 3.14: Relative variation of CCT due to PWM and CCR dimming techniques

tified, which is summarized in Figure 3.14. The ideal biasing point of operation was chosen to be 0.35 A as per the data sheet of the pc-LED [195]. PWM dimming was achieved by maintaining the amplitude of the forward current at the ideal biasing point of the LED. CCR dimming changed the forward current around the biasing point. It can be seen that a slight change in forward voltage (ΔV) causes a large change in forward current (ΔI). Based on the plot of change in CCT (ΔCCT), it is clearly evident that ΔI can cause a change of ~ 700 K when dimming target is varied to the minimum from the biasing point. **This characterization was presented as a contribution in [23] where the values were changed to relative values to portray a generalized concept.**

All these results indicate that PWM dimming outperforms CCR dimming in standard lighting systems when dimming precision, linearity in luminance, chromaticity shifts, CCT variation are preferred over ease of implementation and system cost. But PWM dimming raises an eminent challenge in achievable data rate, which directed the direction of this research towards development and investigation of adaptive schemes under digital dimming.

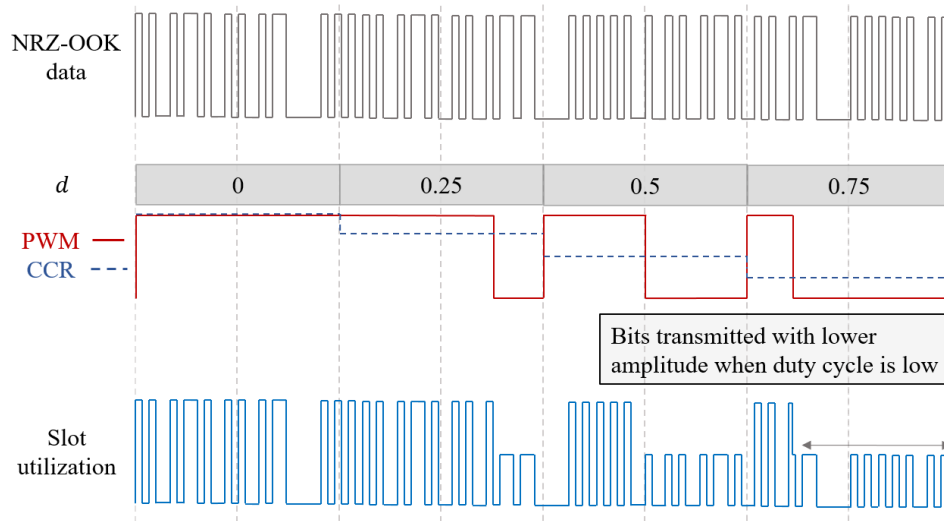


Figure 3.15: NRZ-OOK data stream after implementation of slot utilization scheme for different dimming targets

3.8 Slot Utilization (SU) Scheme

As discussed in Section 2.6.2, in order to counter the deterioration of data rate due to digital dimming, a new technique was developed where data bits were transmitted regardless the state of the PWM dimming signal but with a lower amplitude (whenever dimming signal is low). It was first simulated by Jang *et al.* for a 1 Mb/s NRZ-OOK system where the photometric characterization of the increase in illuminance was left unexplored and was practically demonstrated by Cho *et al.* at a data rate of 10 kb/s [37, 38].

Referring back to eq. 2.20, the value of A can be varied to achieve dimming based on the dimming target. The optimum value for A is a trade-off between dimming precision and the BER. The waveform for SU scheme implemented into NRZ-OOK data stream for different dimming targets (d) is presented in Figure 3.15. It can be considered as a hybrid scheme of PWM and CCR since amplitude scaling is also done at some parts of the waveform. The bits being transmitted when the dimming signal is low will have an impact on the overall luminous flux of the LED. But at first, it was necessary to identify the minimum value of A required for error free communication. This is because at lower values of A , the

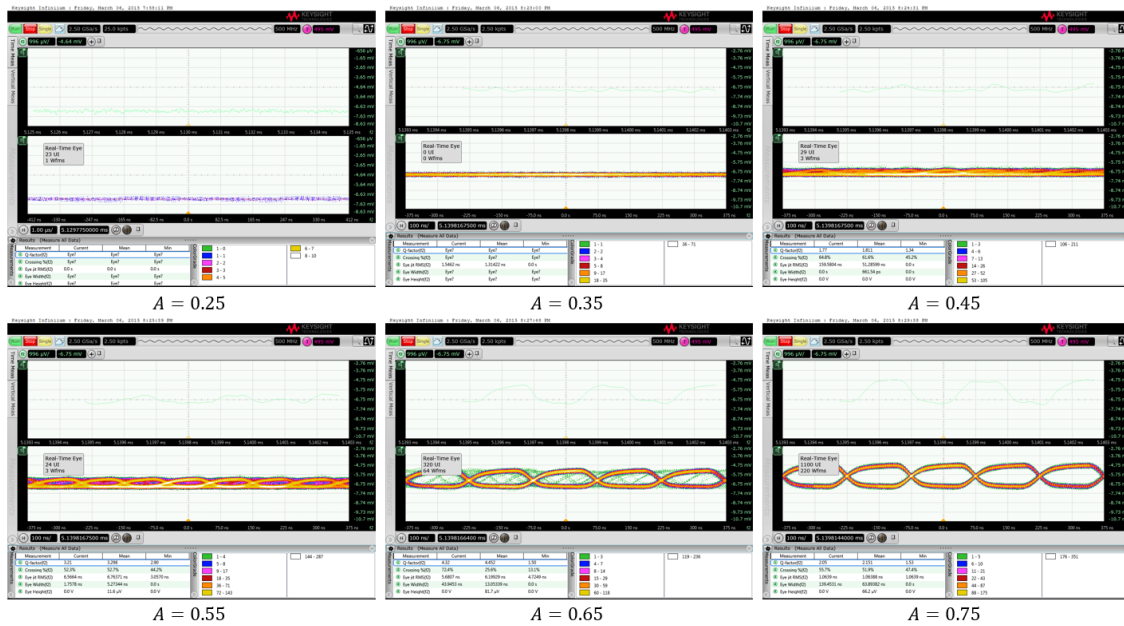


Figure 3.16: Eye diagrams of the received waveforms for different value of amplitude scaling factor during the off duration of the dimming signal

SNR at the receiver will be lower thereby causing higher number of bit errors.

The first series of eye diagrams obtained from different values of A by the experimental evaluation discussed in Section 3.2 is presented in Figure 3.16. The eye diagrams helped in gaining an estimation of minimum value of amplitude scaling factor (A) required for a stable link for all states of the PWM dimming signal. The link stability was further quantified by offline BER calculation for different values of A . Based on the setup depicted in Figure 3.4, the captured waveforms were demodulated using MATLAB[®].

Figure 3.17 shows the effect of A on BER, which was computed both experimentally and theoretically. The analytical results were gathered by measuring the radiometric power P_t emitted by the LED for different values of A using the LVI response of the investigated LED (Figure 3.6) and the model developed in Section 3.4. The BER remains very high at lower values of A due to interference from shot noise for which the receiver cannot distinguish the received bits with low amplitude (during the off state of the dimming signal) from the background noise. The SNR is also very low since the transmitted power (P_t) at lower values

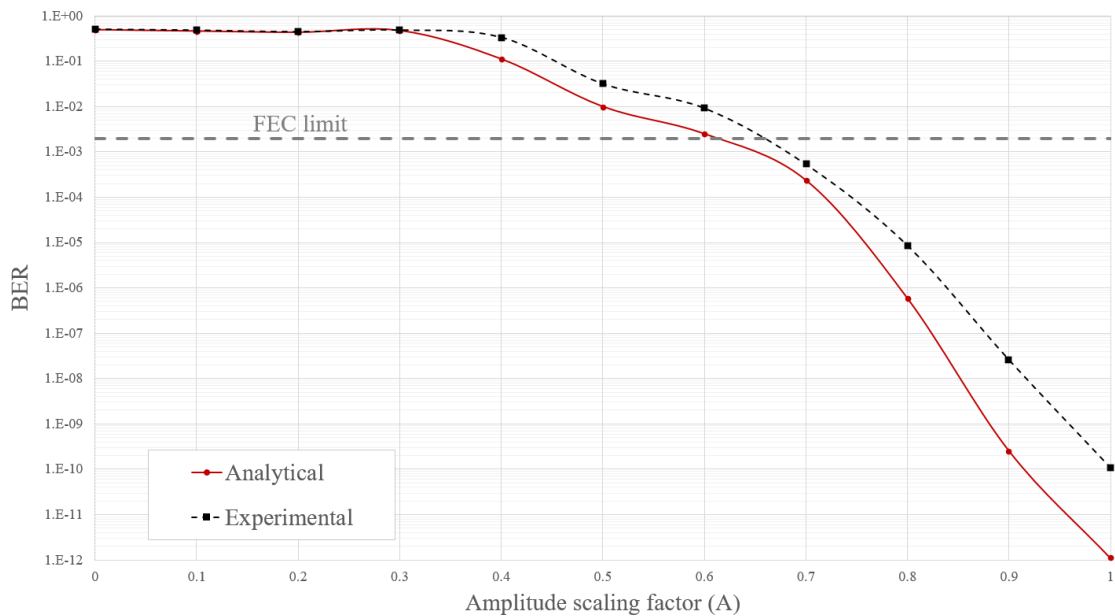


Figure 3.17: BER distribution of slot utilization scheme for increasing values of amplitude scaling factor (A).

of A is small, which increases the BER based on eq. 3.10. However, for larger values of A , the ones and zeroes have larger peaks, which allows the receiver to identify them as received bits from the threshold set by the noise. BER reaches an acceptable value of $\sim 1.2 \times 10^{-3}$ (below FEC limit of 2×10^{-3}) when the amplitude of the off-state is 2.6 V. This indicates that A is 0.65 since the overall amplitude of the signal was 4 V. The link performance remains consistent above that amplitude with very low BER indicating a stable operation since the system is operated well within its 3-dB modulation bandwidth.

The distribution of illuminance for different values of A for different duty cycles of PWM dimming signal is presented in Figure 3.18. The measurements were made using the setup depicted in Figure 3.5. The curves converge to a single point at ~ 1500 lux, which is the maximum illuminance provided by the single LED chip. This is because when the amplitude scaling factor is maximum, the amplitude of transmitted bits for on and off duration of PWM signal is equal, which means that the transmitted data stream would be analogous to a waveform where D is 100%. For higher duty cycles, the difference between minimum

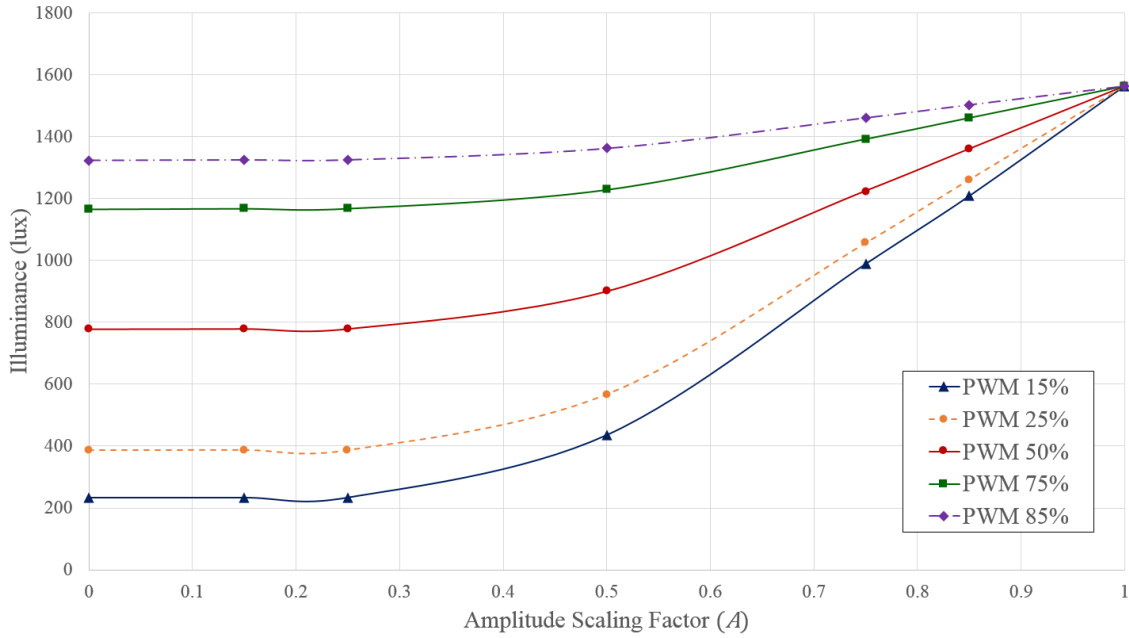


Figure 3.18: Illuminance distribution of slot utilization scheme for increasing values of amplitude scaling factor (A).

and maximum illuminance is low, which implies that the effect of A is negligible. This means when the duty cycle is high (dimming target is low), higher values of A can be utilized, which will provide error free communication and would not significantly affect the dimming precision.

In case of lower duty cycles, the difference between maximum and minimum illuminance for increasing off-state amplitude is much higher. This shows that A has a profound effect on the dimming precision when the dimming target is high. Lower duty cycle indicates high dimming level is required by the system, whereas maintaining communication by transmitting bits during the off duration of the PWM signal would increase the overall illuminance.

The percentage shift in dimming precision can be termed as dimming shift, which is measured as the percentage difference between illuminance due to SU E_{SU} compared to expected brightness level due to PWM dimming (E_{PWM}). The dimming shift is expressed as

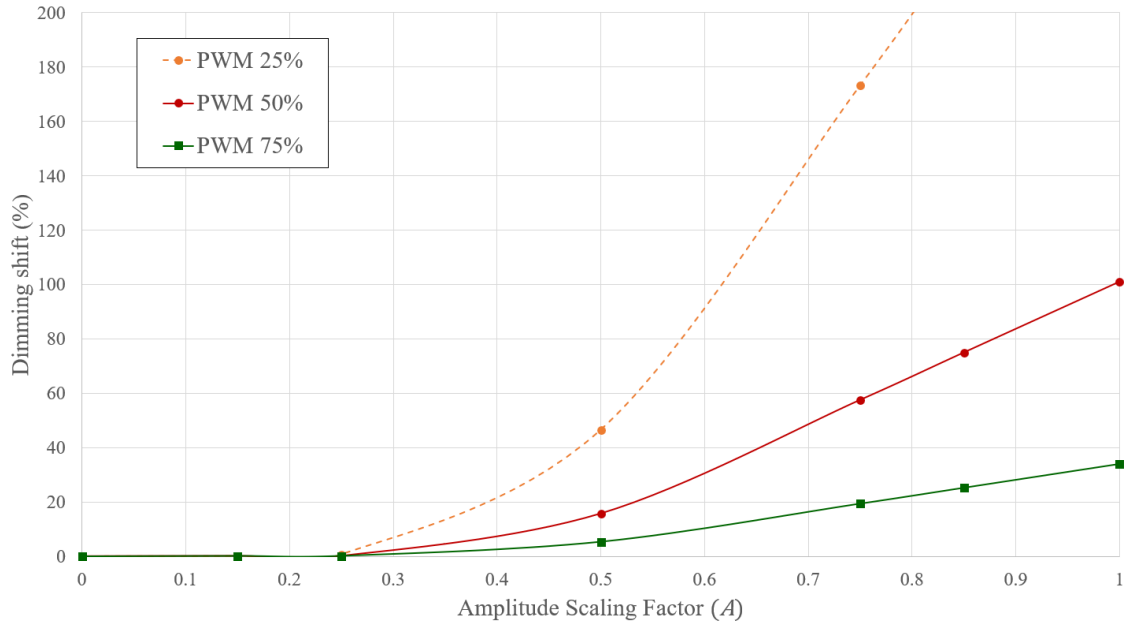


Figure 3.19: Dimming precision obtained for increasing values of amplitude scaling factor (A)

$$\text{dimming shift (\%)} = \frac{E_{SU} - E_{PWM}}{E_{PWM}} * 100 \% \quad (3.14)$$

Figure 3.19 is showing the distribution of dimming shift with the variation in amplitude scaling factor. It can be observed that the dimming shift is higher for lower duty cycles. This is because in case of a dimmed system, the average intensity is much lower, thus an offset in the off state of the PWM signal significantly increases the overall illuminance. The cut-off A for carrying SU at an acceptable BER was identified to be 0.65 (Figure 3.17), but from Figure 3.19 it can be seen that at such and amplitude there is a dimming shift of 40% (~ 18.6 lux increase in illuminance) for PWM signal with $D = 50\%$. This off-state amplitude has a lower shift of 15% for PWM signal with $D = 75\%$. However, it gives a much higher shift of around 125% (~ 29 lux increase in illuminance) for PWM signal with $D = 25\%$.

Based on the photometric results, it is clear that SU technique causes considerable increase in illuminance, which would hamper the dimming precision of a

VLC system. This problem could not be identified previously because most of the work done on this technique was simulation based and did not take photometric parameters into account. Solutions to this problem would be either reducing system noise, so that lower values of A could be utilized or combining this technique with other adaptive schemes such as rate adaptation.

3.9 Rate Adaptation (RA) Scheme

Rate adaptation (RA) scheme involves the regulation of instantaneous data rate of a system based on dimming targets under PWM dimming to ensure that the number of transmitted bits remain constant. The operating principle of rate adaptation scheme for a NRZ-OOK based VLC system is depicted in Figure 3.20. As the dimming target increases, more bits are needed to be packed into the ‘ON’ duration of the PWM dimming signal. As defined in Section 2.6.2, the required data rate is related to the instantaneous data rate based on eq. 2.21.

The required instantaneous data rate (R_{ad}) for different dimming targets (d) is shown in Figure 3.21. The adaptive data rate increases exponentially with in-

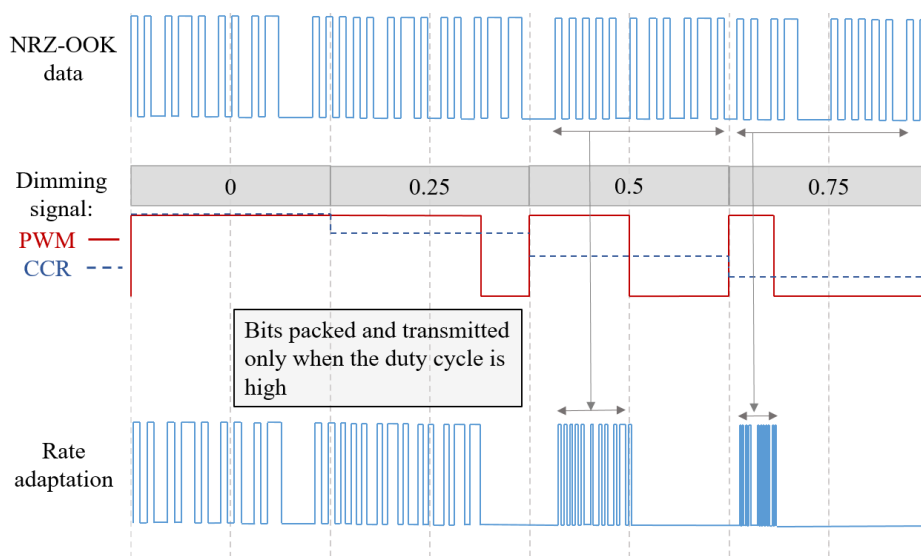


Figure 3.20: NRZ-OOK data stream after implementation of rate adaptation scheme for different dimming targets

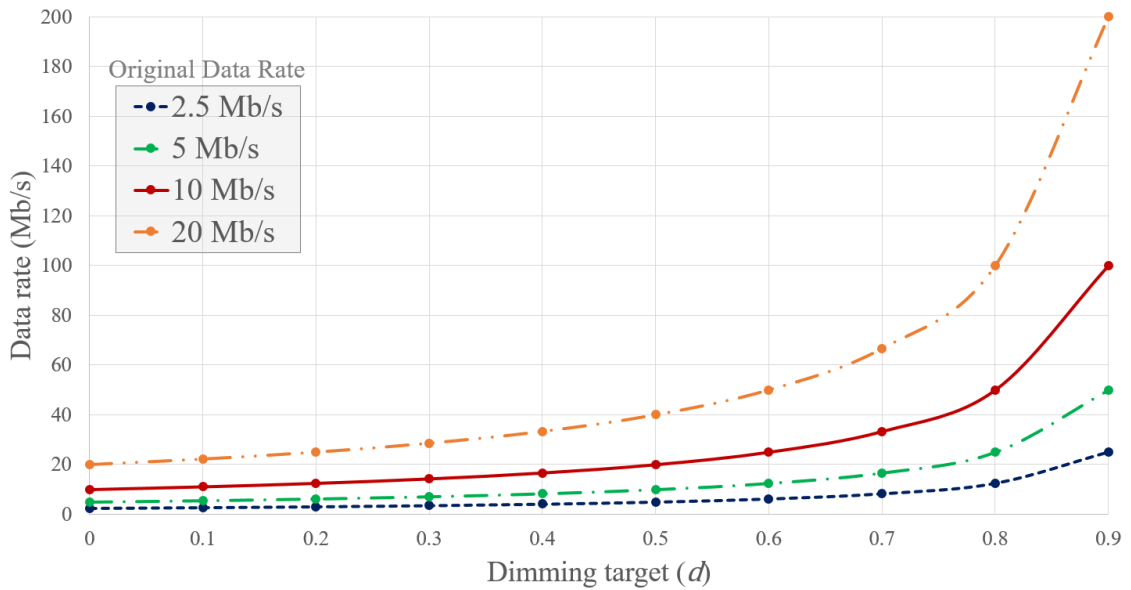


Figure 3.21: Required instantaneous data rate for different dimming targets

creasing dimming target in order to maintain the system transmission rate. When no dimming is required ($d = 0$), the adaptive rate is equal to the original bit rate of the system. For higher dimming targets, the data rate reaches values of upto 100 Mb/s, which is practically unattainable because of the limited modulation bandwidth of the LED.

The achievable data rate utilizing a single pc-LED chip at a link distance of 0.25 m for the experimental setup in Figure 3.1 was found to be ~ 2 Mb/s. Thus it was necessary to enhance the 3 dB modulation bandwidth of our VLC system. A blue filter was used in front of the receiver, which helped in reflecting off the slow component of the yellow phosphor and helped in enhancing the modulation bandwidth to ~ 20 MHz. A bandpass filter was used to eliminate undesired signal spikes detected by the receiver and a digital filtering technique was also utilized during the demodulation, which helped in increasing the maximum achievable bit rate.

An experimental BER analysis was done to validate the maximum achievable bit rate. As the data rate increases, the BER increases quite linearly due to bandwidth limitation, which causes the rectangular pulses to have a transient

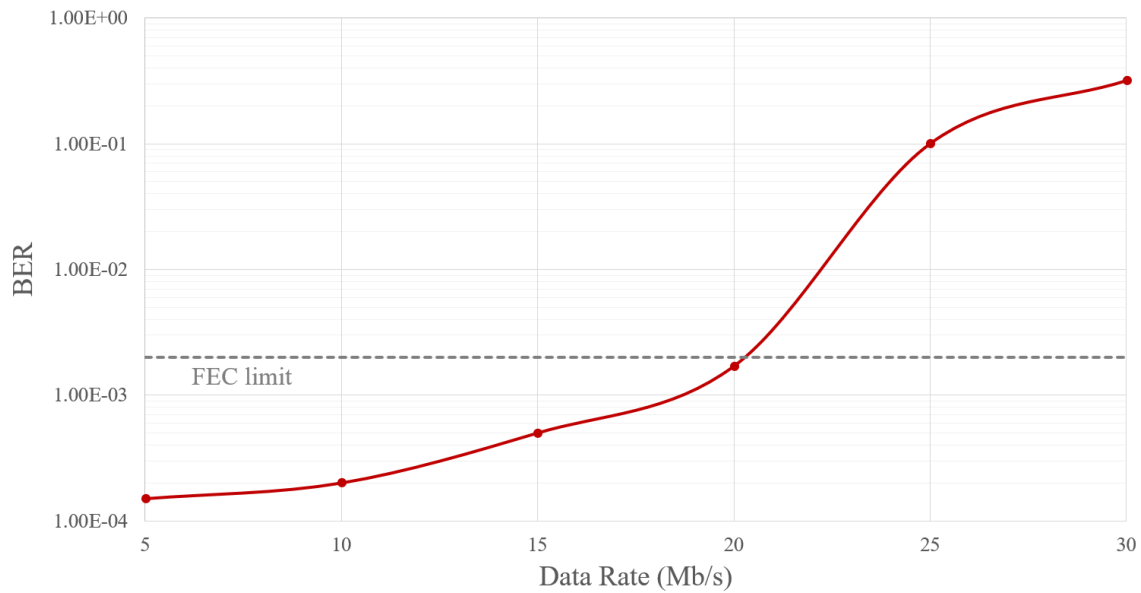


Figure 3.22: BER distribution for adaptive data rate

response, which cannot be properly demodulated even after the application of sophisticated digital filtering. The BER distribution for increasing data rate is presented in Figure 3.22. The BER remains below FEC limit for adaptive rates below 20 Mb/s. Thus, 20 Mb/s was identified as the cut-off adaptive rate for the RA scheme. Above 20 Mb/s, the BER rises to much higher values and the communication link can be assumed to be failing.

The cut off data rate of 20 Mb/s corresponds to a dimming target of 0 for 20 Mb/s system, 0.5 for 10 Mb/s system, 0.75 for 5 Mb/s system and 0.875 for 2.5 Mb/s system. Thus RA scheme becomes a trade off between original data rate requirement and ability to operate over a range of dimming target. For bandwidth enhanced VLC systems demonstrated in [145, 128, 129, 149, 125], RA scheme can fully capitalize on the entire range of dimming target with a high baseband transmission rate.

However, for this work, if the main priority is the ability to work over an entire range of dimming target, the RA scheme can be applied to a system operating originally at 2.5 Mb/s. However, such a low original transmission rate undermines the main objective of this work, which is high speed dimmable VLC.

Thus it was decided to keep the original rate at 10 Mb/s and explore the possibilities of combining this scheme with SU scheme to form an adaptive slot utilized dimming scheme. In this way, an original transmission rate of 10 Mb/s is maintained, which is around 1000 times higher than the previously demonstrated work by Cho *et al.* in [38] where the technique was implemented for a 10 kb/s system.

3.10 Proposed Dimming Algorithm

Although these adaptive schemes achieve uninterrupted data transmission for different ranges of dimming target, there are drawbacks when their performance is being considered for a practical scenario keeping both the photometric and communicative parameters under attention. The limited modulation bandwidth of LEDs restricts the extent to which RA can be implemented. On the other hand, transmission of bits when the duty cycle is low hampers dimming precision when SU is being applied. Based on both experimental and analytical investigations, we proposed an algorithm, which utilizes both schemes to fully minimize the deterioration in dimming precision and maximize the link stability for the entire range of the dimming constraint.

The choice of adaptive technique based on the dimming target requires a trade-off between dimming precision and BER. The main goal of this work was to maintain the communication data rate at 10 Mb/s throughout the entire range of the dimming target. Thus a selective combined dimming scheme is proposed, which would utilize either of the adaptive techniques taking the dimming target as the user input. The scheme can be defined by

$$y(t) = \begin{cases} x(t) & d \leq 0.5, R_{ad} = \frac{R}{1-d} \\ x_1(t) + A.x_2(t) + x_3(t) + \dots A.x_n(t) & 0.5 < d < 1, R_{ad} = R \end{cases} \quad (3.15)$$

Figure 3.23 shows the working principles of the proposed scheme. The vari-

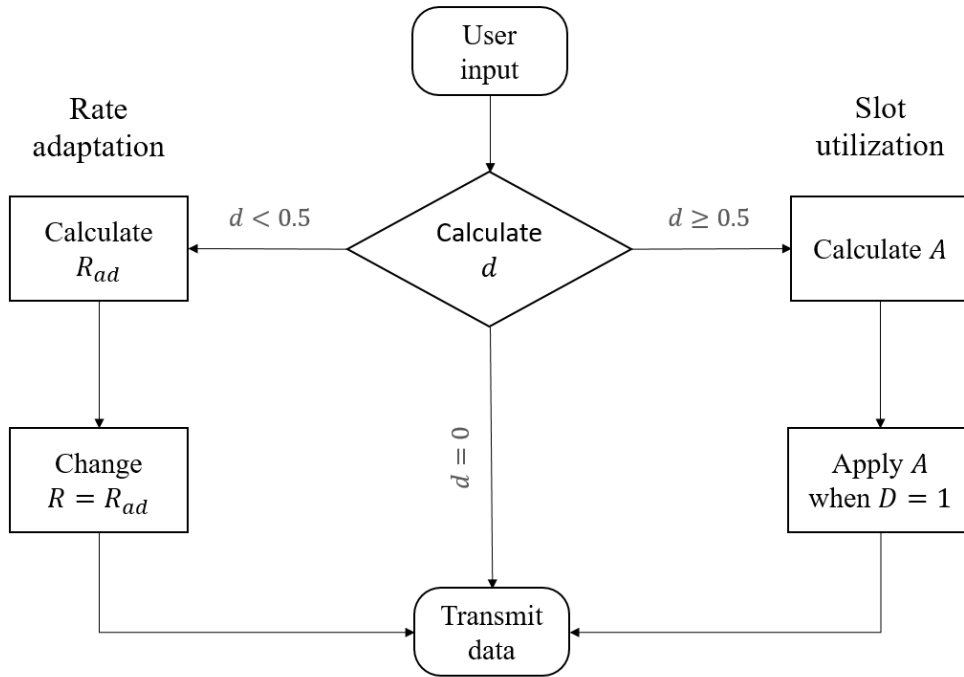


Figure 3.23: Flowchart of the proposed scheme

able parameters for this scheme are the amplitude of transmitted bits (A) and the data rate (R_{ad}), which are determined by the dimming target (d) taken as user input. When $d \leq 0.5$, RA is utilized, which transmits $x(t)$ at a rate R_{ad} , which is determined by d based on eq. 2.21. For higher dimming targets ($d > 0.5$), SU is employed by applying amplitude scaling into samples of the original waveform that is divided based on the state of the PWM dimming signal.

The adaptive slot utilized scheme was proposed based on analytical and experimental validations of parameters associated with photometry, radiometry, communication and energy efficiency under a single framework. One of the fundamental motivations behind dimming is to achieve power savings when general household and commercial usage is being considered. Thus it was necessary to record the average power consumption of all of the investigated schemes. A power analyzer (Tektronix PA 1000 [208]) was used to record the average power consumed by the LED when these schemes were applied based on the setup in Figure 3.5.

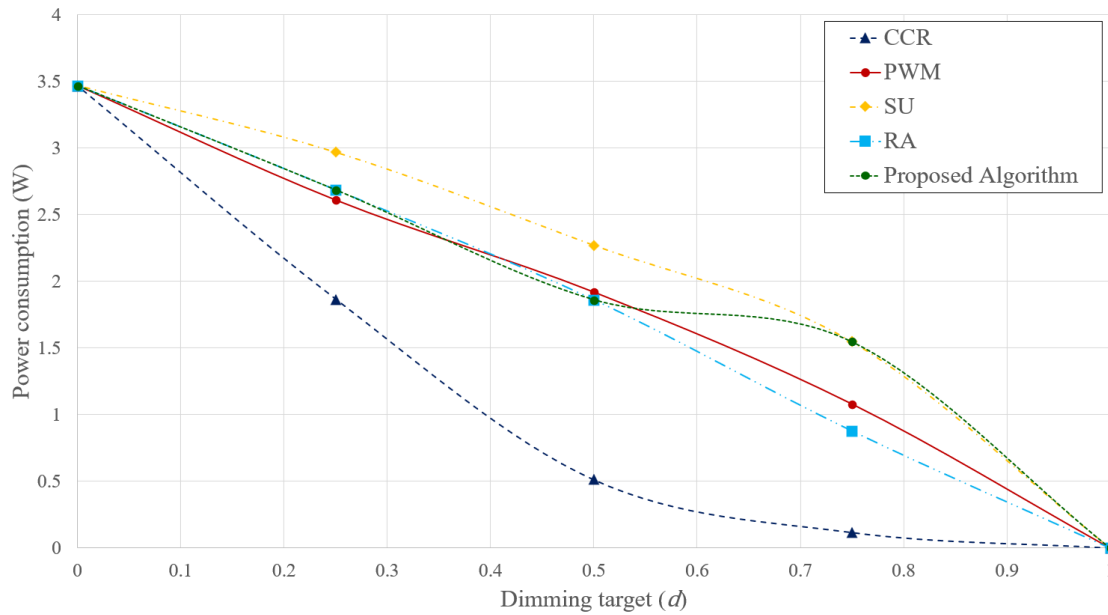


Figure 3.24: Power consumed by the investigated schemes for different levels of dimming target (d)

The power consumption for different dimming targets is presented in Figure 3.24. All the graphs converge to a maximum and minimum point of 70 mW and 0 mW respectively. This is consistent since all the waveforms for different schemes become identical when the dimming target is $d = 0$ and 1. It can be seen that CCR scheme achieves the highest savings in power consumption. Since CCR scheme directly changes the amplitude of the transmitted bits, it directly regulates the forward current, which in turn regulates the power consumption. The power consumption of PWM and RA decreases quite linearly with the dimming target. Thus it is hard to prefer either of them when power savings is being considered as the fundamental system criteria. Since SU involves transmission of bits regardless the state of dimming signal, it consumes the highest power amongst all these schemes for the entire range of the dimming target.

The overall comparison of the proposed algorithm and digital dimming scheme in terms of luminous flux, power consumption and system transmission rate is presented in Figure 3.25. It can be seen that it achieves high dimming precision for $d \leq 0.5$, for higher dimming targets there is added illuminance due to trans-

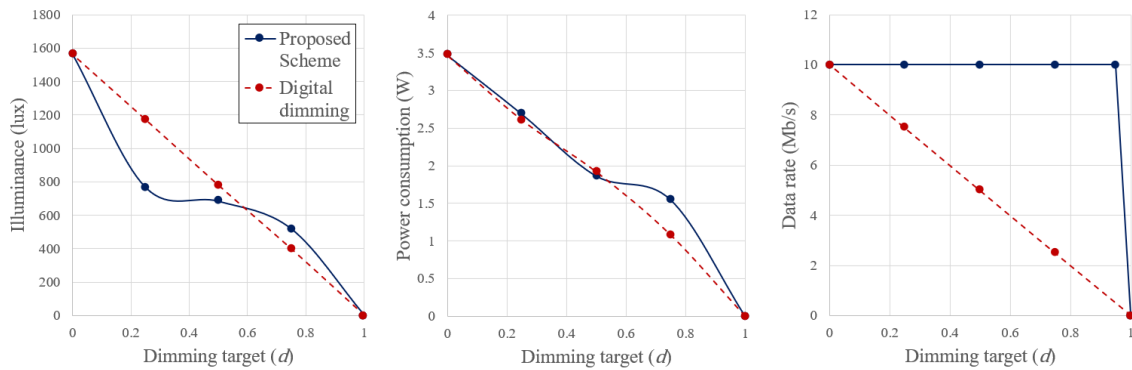


Figure 3.25: Overall comparison of the proposed scheme and standard digital dimming scheme for different values of dimming target in terms of illuminance (left), power consumption (middle) and achievable data rate (right)

mission of superimposed bits. In terms of power consumption, the proposed scheme has slightly higher consumption for higher dimming targets. This drop in energy savings can still be accepted since it allows superior communication performance by maintaining the system transmission rate at 10 Mb/s for the entire range of the dimming target, which was the overall objective for this work.

3.11 Conclusion

This chapter laid the foundation upon which work was done in the entire thesis for different types of transmitters. It was decided to explore the possibilities of implementation of VLC into existing lighting infrastructures. Since phosphor based LEDs are the predominant choice as sources for current lighting infrastructures, in this chapter, the VLC system was developed utilizing a pc-LED. The overall objective was to demonstrate a system, which is capable for providing Li-Fi access points for indoor wireless communication, hence the speed of transmission was targeted to be in the range of 5-20 Mb/s. NRZ-OOK modulation scheme was used for encoding data due to their versatility and higher power efficiency [153]. Four separate dimming schemes were designed for the link and investigated experimentally and analytically on the basis of photometric response and link stability. The linearity in CCT and illuminance distribution indicated PWM is superior in comparison to FM. An experimental characterization of pc-LED helped in explaining the chromaticity shifts induced by CCR dimming, which was added as a contribution in [23]. The superior capabilities of PWM dimming compared to CCR scheme when data transmission and chromaticity shifts are considered was also justified on the basis of experimental investigation, which was added as a contribution in [33]. Adaptive techniques like SU and RA were implemented into the VLC system to account for the data rate deterioration caused by PWM dimming. By photometric analysis, it was observed that SU causes significant increase in dimming shift, which could not be identified in literature since none of the works considered photometric aspects and the results of this work were presented as a contribution in [58] and answered research question 3. The bandwidth limitation challenges associated with RA scheme were also identified since this work considered a practical system. Based on the analysis of all of the aforementioned schemes, a dimming algorithm was proposed, which utilizes either

Table 3.3: Overall Comparison of Dimming Schemes for CCT Regulation

Scheme	BER			Data Rate (Mb/s)
	Dimming target (d)			
	0.25	0.5	0.75	
CCR	0.45027	0.031907	0.000533	10
PWM	1.08×10^{-10}	3.52×10^{-7}	2.36×10^{-5}	2.5, 5, 7.5
SU	8.65×10^{-6}	7.55×10^{-4}	0.00053	10
RA	1.75×10^{-4}	0.0017	0.5	10
Proposed	2.64×10^{-4}	4.92×10^{-4}	0.00071	10

RA or SU depending on the dimming target and is capable of maintaining the target data rate of 10 Mb/s with a BER below the FEC limit for the entire range of the dimming target. The overall comparison of the investigated and proposed schemes is summarized in Table 3.3.

The major observations made from this chapter are summarized as follows:

- PWM is the preferred pulse regulated scheme due to lower variation in CCT and linear illuminance distribution
- PWM is preferable over CCR due to linear dimming and lower chromaticity shifts
- The loss in achievable data rate for PWM can be effectively avoided by implementing SU and RA adaptive techniques
- SU causes a dimming shift of $\sim 15\%$ - $\sim 125\%$ depending on dimming target
- The adaptive data rate can reach values of 100 Mb/s for an original transmission rate of 10 Mb/s for RA scheme, which is very challenging for bandwidth limited pc-LEDs
- Combination of multiple adaptive schemes can provide data transmission at a target rate of 10 Mb/s at an acceptable BER with higher dimming precision for the entire range of the dimming target



Figure 3.26: Concept of VLC system integrated with an intelligent lighting framework

These observations answer the research questions 1,2,3 and 4, which are summarized in Section 2.11. In this chapter, we identified the necessity of utilizing proper dimming techniques to maintain standard illumination and practically demonstrated the scopes of implementing adaptive schemes to avoid deterioration in data rate due to different states of dimming signals. The proposed algorithm was able to maintain the system transmission rate of 10 Mb/s for the entire range of the dimming target and provided higher dimming precision compared to the exclusive implementation of SU scheme. This scheme can also be implemented into other NRZ-OOK based systems operating at higher data rates where bandwidth enhancement techniques had already been implemented [128, 145, 146, 147]. The concept of the proposed scheme being utilized in a practical scenario is depicted in Figure 3.26. The scheme can be integrated with a smart lighting architecture where end users would be able to control the color, warmth and the intensity of the emitted light alongside getting uninterrupted communication service from the transmitters [209]. The ambient light would also determine the intensity thus allowing scopes for energy savings during daytime. Based on the data received along with the user input, the controller would deter-

mine an appropriate dimming target and apply adaptive schemes based on the dimming requirement, which would then be used to simultaneously dim as well as transmit data using the LEDs.

Staying within context of this work, the goal was shifted towards increasing the achievable data rate by utilizing RGB sources for WDM based VLC, which is discussed in the next chapter. The observations made from this chapter can be used for controlling various aspects of white light generated from RGB sources including the color temperature, which might be a promising field to work on since no previous works attempted to employ adaptive schemes for CCT regulation.

RGB-LED-BASED VLC SYSTEM WITH ENHANCED ILLUMINATION

4.1 Introduction

The use of multi-chip sources as VLC transmitters allows each channel to be modulated independently, which accounts for higher aggregate data rate [157]. Unlike pc-LEDs, where the slow relaxation time of phosphor limits the speed of transmission, RGB-LEDs have higher modulation bandwidth and open scopes of WDM [80, 210, 211]. In WDM VLC systems, multiple data streams are individually carried by three unique wavelengths, which are separated by respective filters at the receiver [210].

Besides higher data rates, RGB LEDs provide possibilities of tuning individual colors, which helps in controlling the color temperature of the white light being generated. As discussed in Section 2.3.1, color temperature alters the emotional effect of a space and has a profound impact on the appearance of illuminated objects. Thus controllability of CCT is a promising feature ideal for next generation intelligent lighting solutions where VLC system can provide high speed wireless communication and high quality controllable illumination. Although the effect of CCT on communication aspects of VLC had been analyzed theoretically in certain works [42, 40], there has been no work on using adaptive dimming schemes

predominantly used for concurrent dimming and communication for CCT regulation, which raised the fourth research question:

- Can adaptive dimming schemes be implemented for regulating the CCT of RGB LED-based VLC systems for maintaining the data rate and the BER of the system at acceptable limits?

In the previous chapter, adaptive schemes were utilized for seamless dimming and data transmission for phosphor based white LEDs. In this chapter, these schemes are applied for a RGB LED-based VLC system to achieve seamless control of CCT while maintaining the communication at an acceptable BER. The impact of different color temperatures on the transmission capacity was characterized on the basis of the system performance with and without adaptive schemes. This helped in answering the research question that was raised for this particular aspect of WDM-based VLC system.

The rest of the chapter is organized as follows. Section 4.2 and 4.3 summarizes the experimental setup and measurements made to obtain the LVI response of the RGB LED being used. Section 4.4 describes the simulation framework that was used. The analytical model used to validate the experimental results and obtain the target biasing conditions for different CCTs is presented in Section 4.5. The methodology used in this work is explained in Section 4.6. The effect of CCT regulation on channel performance is presented in Section 4.7. The formulation and the resulting channel performance from the implementation of adaptive schemes are discussed in Section 4.8 and 4.9. Finally, a summary and the key outcomes from this chapter are presented in Section 4.10.

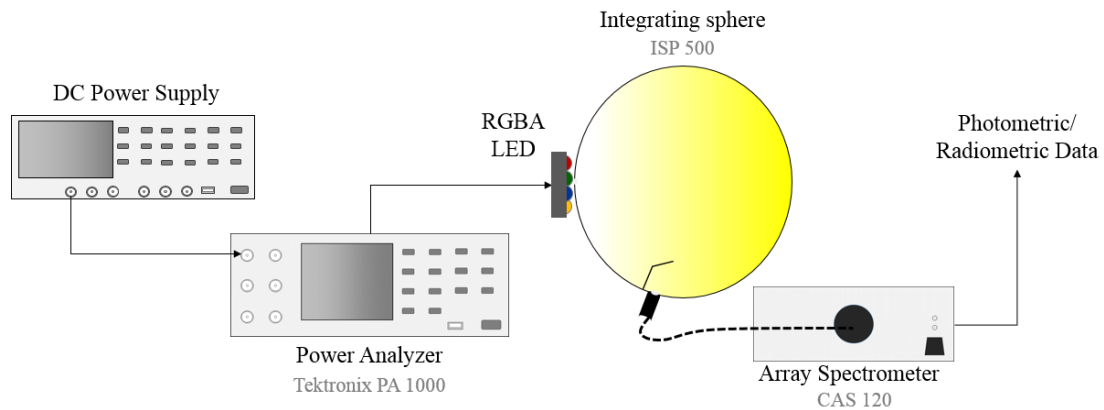


Figure 4.1: Experimental setup for characterization of the luminous response of the RGBA LED

4.2 Characterization of RGBA LED

In order to incorporate WDM based VLC, multiple LEDs operating at different wavelengths are needed to be combined. Thus, it was decided to work with a small multi-chip star LED, which would facilitate the incorporation of the source into different experimental configurations. The multi-chip LED used for the WDM-VLC is a 10 W Red, Green, Blue and Amber (RGBA) LED manufactured by LED Engin [212]. It has an ultra small footprint of $7\text{ mm} \times 7\text{ mm} \times 4.1\text{ mm}$ and is capable of producing any white color temperature with varying range of CRI values.

The initial experiment to obtain the LVI characteristics of the RGB LED was done based on the setup shown in Figure 4.1. The LED was powered up using a DC power supply and the power consumption along with the forward current and forward voltage across it was measured using a power analyzer. It was connected to a heat sink to mitigate the effect of junction temperature variation [213]. The integrating sphere was used to calculate all the radiometric and photometric data.

The radiometric power, luminous flux, scotopic flux, Tristimulus values, CIE 1931, CIE 1960 and CIE 1976 coordinates, dominant wavelength and various other parameters were measured for each LED chip as forward current was increased

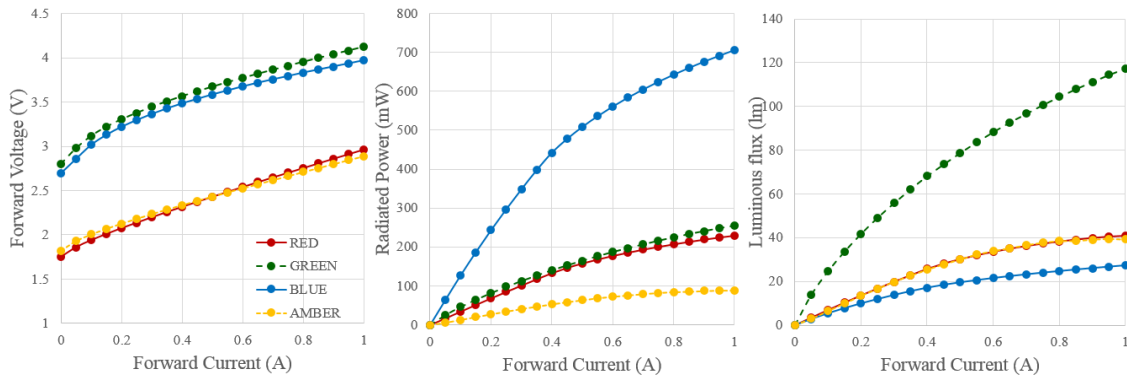


Figure 4.2: LVI response of the RGB LED

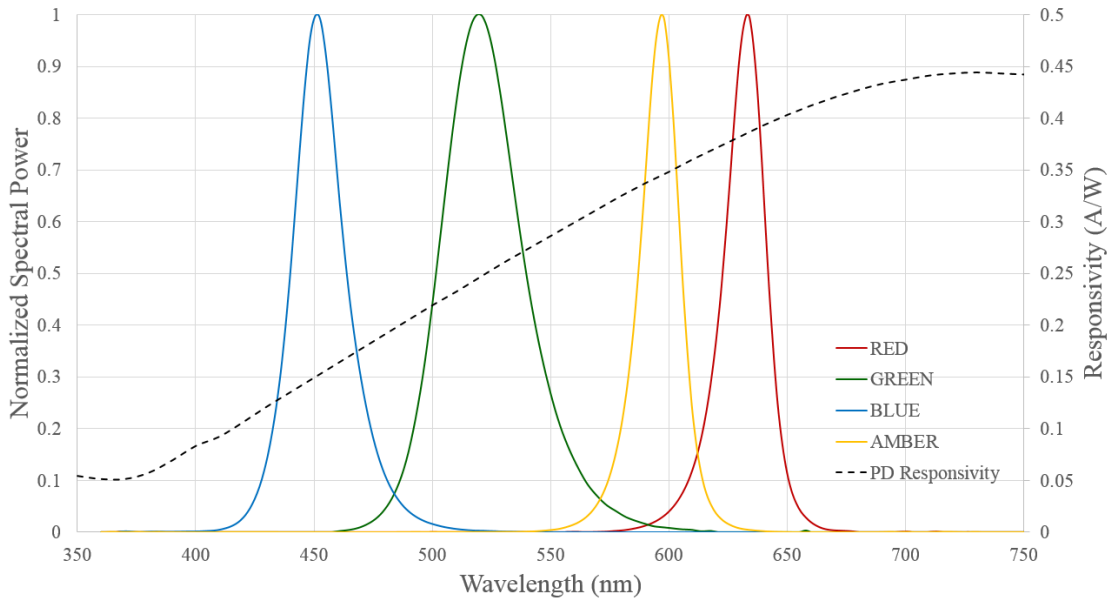


Figure 4.3: Normalized spectral power distribution of the LED and photodiode responsivity for different wavelengths in the visible range.

in steps of 50 mA. The LVI characteristics of the investigated LED is presented in Figure 4.2. It was observed that the voltage across green and blue LEDs were much higher than for red and amber sources. The luminous flux was much higher for the green LED since human eye is the most sensitive in that region (under photopic conditions) (Figure 2.2(b)), which corresponds to a much higher luminous flux based on equation 2.1. This phenomenon is different under low illumination levels when the human eye sensitivity shifts towards the blue, generally referred to as the Purkinje effect.

The blue chip had much higher radiated power and the amber chip had the least radiated power. Since the blue chip needs to compensate for the emission from three different chips in higher wavelength region, it needed to have higher radiated power. The radiated power for all the chips had an initial linear region of operation. Referring back to Figure 2.7, the point of operation for the VLC system was chosen based on three main conditions:

1. The biasing current must be in the linear operating region
2. The current must be within maximum rated conditions of the LED
3. The current must correspond to a target chromaticity coordinate planned on being achieved from overall mixing

The spectrum of each LED chip was also measured using the CL-500A spectrophotometer. The SPD was highest for blue chip and lowest for green. The normalized SPD along with the responsivity of the PD used in this work are presented in Figure 4.3.

4.3 Experimental Setup of WDM-LED-VLC

The experimental setup for the WDM based VLC link is depicted in Figure 4.4. The data stream generated by the AWG is combined with the DC offset using bias-Ts. An engineered diffuser (Thorlabs ED1C20) is used to mix the light produced from each chip. The wireless link distance is fixed at 0.5 m and optical filters centered at wavelengths of each individual LED die were utilized to separate the respective channels out. Since a single photodiode was used for the analysis, it was ensured that all the other channels were operating while the measurements were made for each channel. The amber LED was not used in this work since the main objective was the generation of light with different CCTs using a RGB system. CCT tunability can be achieved from RGB sources alone and amber LEDs

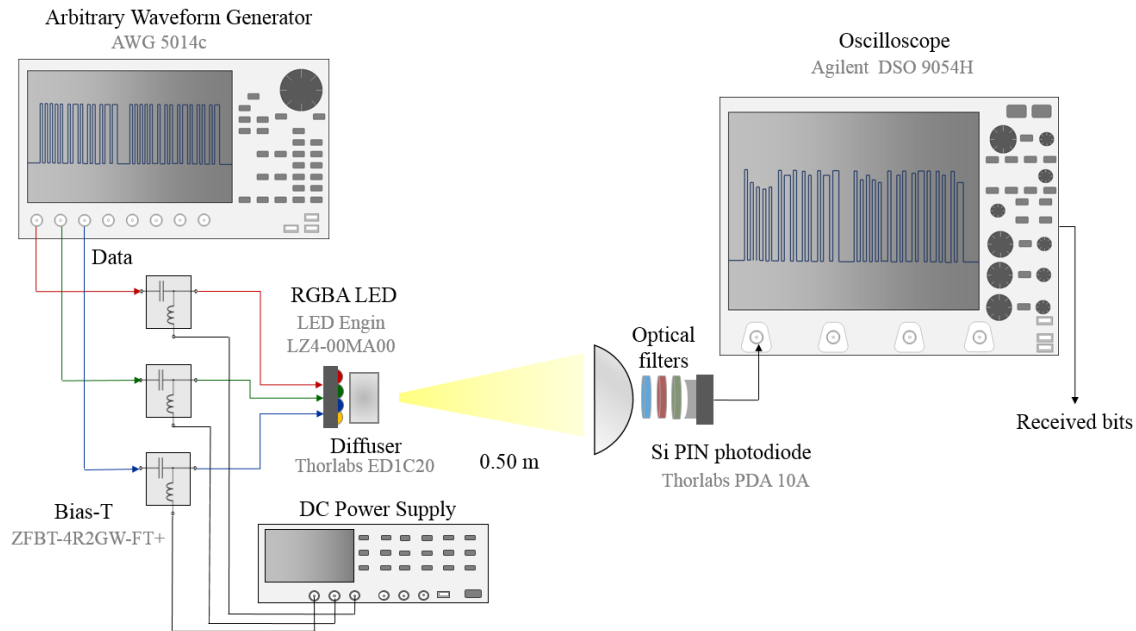


Figure 4.4: Experimental Setup of WDM VLC System utilizing a single RGBA LED as its transmitter

are generally incorporated into the system to increase the overall value of CRI as reported in [40]. A focusing lens (Thorlabs LMR75) was utilized to focus the light onto the photodiode and the rest of the process of demodulation is analogous to the system described in Section 3.2.

4.4 Simulation of WDM-LED-VLC

The RGB-WDM VLC system was simulated using the OptiSystem[®] software. A pseudo-random bit sequence (PRBS) generator was used to generate more than 1×10^6 bits, which was then encoded by a NRZ pulse generator. In OptiSystem[®], the modulation response of the LED is determined by the carrier dynamics and thus is limited by the carrier lifetime (T_n) and parasitic capacitance, which in turn is determined by the RC constant (T_{RC}). The LED 3-dB modulation bandwidth of the LED source can be expressed as [214]

$$f_{3dB} = \frac{\sqrt{3}}{2\pi(T_n + T_{RC})} \quad (4.1)$$

Table 4.1: System parameters for simulation of RGB WDM LED-VLC link

	Parameters	Value
Transmitter	Wavelength (nm)	451, 520, 633
	Beam divergence (mrad)	872
	Transmitter aperture diameter (mm)	7
	Electron lifetime, T_n (ns)	8.1
	RC constant, T_{RC} (ns)	8.1
	Slope efficiency (W/A)	0.705, 0.255, 0.229
Channel	Distance (m)	0.5
	Attenuation (dB/km)	0.19
Receiver	Modulation bandwidth (MHz)	150
	Receiver aperture diameter (mm)	75
	Responsivity (A/W)	0.149, 0.246, 0.393

Thus both T_n and T_{RC} were chosen to be 8.1 ns, which yielded a 3 dB modulation bandwidth of ~ 17 MHz that is equivalent to the values reported in literature [158]. The FSO channel is kept equivalent to the experimental setup with a distance of 0.5 m. The attenuation is fixed to a value of 0.19 dB/km based on the international attenuation coefficient range in the visible waveband for clear air [22]. The optical attenuator was adjusted to obtain different values of received power, which were required for different biasing conditions and CCTs. The photodiode was modelled based on the one used in the experiment (Thorlabs PDA 10AEC [215]) and a text file was used to input the different values of responsivities at different wavelengths as shown in Figure 4.3. The BER analyzer was used to calculate the values of BER, Q factor and SNR. The parameters of different components used in the simulation framework are summarized in Table 4.1.

4.5 Analytical Model of WDM-LED-VLC

The analytical model of the RGB WDM-VLC system was developed in MATLAB[®] for two main purposes:

1. Determine the biasing condition under illumination constraints for generating white light at different CCTs
2. Calculate the theoretical BER based on identified biasing conditions

4.5.1 Biasing Condition for Target Illumination Constraint

The sum of individual flux generated by each die in a multi-color LED determines the total luminous flux generated by the source. The chromaticity of the source is thus determined by the relative intensities of each source. The target chromaticity $[x_d, y_d]$ can be used to determine the mixing ratio \mathbf{d} using [216]

$$\begin{pmatrix} \frac{x_r}{y_r} & \frac{x_g}{y_g} & \frac{x_b}{y_b} \\ 1 & 1 & 1 \\ \frac{1 - x_r - y_r}{y_r} & \frac{1 - x_g - y_g}{y_g} & \frac{1 - x_b - y_b}{y_b} \end{pmatrix} \mathbf{d} = \begin{pmatrix} \frac{x_d}{y_d} \\ 1 \\ \frac{1 - x_d - y_d}{y_d} \end{pmatrix} \quad (4.2)$$

where $[x_r, y_r]$, $[x_g, y_g]$, $[x_b, y_b]$ are the chromaticity coordinates of the red, green and blue LED dies respectively. By theory, the sum of the elements in \mathbf{d} should be equal to 1. The total luminous flux generated by the LED denoted by L (equation 2.1) is equal to the sum of individual luminous fluxes across different chips in the RGB cluster (provided their SPDs do not overlap)

$$L = \bar{\eta} \cdot \mathbf{I} \quad (4.3)$$

where $\bar{\eta}$ is the optical gain (lumen output per ampere of current) and can be calculated by:

$$\bar{\eta} = [\eta_r, \eta_g, \eta_b] \quad (4.4)$$

From eq. 4.3, $\mathbf{I} = [I_r, I_g, I_b]'$ is the vector representing the forward bias currents. The mixing ratio (\mathbf{d}) determines the relative luminous flux for each LED and thus

the forward currents for a single channel i can be expressed by

$$\eta_i I_i = L d_i \quad (4.5)$$

These equations (eq. 4.2 - 4.5) were used to identify the biasing currents required for different target chromaticity coordinates. Since the optical gain of the LED could deteriorate with age and LED junction temperature [216, 217], an actual system needs to be recalibrated after prolonged usage of the luminaire as the transmitter.

4.5.2 Analytical Model of Link Performance of RGB LED-based VLC

The analytical model is similar to the model developed in Section 3.4. The LVI characterization in Section 4.2 was used to obtain values of transmitted power (P_t) at different biasing conditions, which was then used to calculate the respective BER and SNR using the biasing currents identified in Section 4.5.1. Compared to the calculations made for a pc-LED based systems, the parameters which would change in this analysis are the wavelengths of emission and the responsivities at the receiver (since different colors of light will have different responsivities). Since narrowband filters are used at the receiver, the impact of interference or channel crosstalk are assumed to be negligible. The parameters used for the analytical model of the WDM-VLC system are summarized in Table 4.2.

Table 4.2: System parameters for analytical model of RGB WDM LED-VLC link

	Parameters	Value
Transmitter	Wavelength (nm)	451, 520, 633
	Chromaticity coordinates	[0.1522, 0.0295], [0.1608, 0.7054], [0.6971, 0.3008]
	Optical gain, η_r, η_g, η_b (lm/A)	40, 140, 115
	Semi angle at half power ($^\circ$)	47
Channel	Distance (m)	0.5
	Total illuminance, E (lux)	500
	Background noise current (A)	202×10^{-6}
Receiver	Filter transmittance	0.925, 0.965, 0.985
	Area of PD (m^2)	8×10^{-6}
	Responsivity (A/W)	0.149, 0.246, 0.393

4.6 Methodology

The process applied in investigation and validation of the experimental, simulation and analytical based results is depicted in Figure 4.5. Initially the LVI characterization done using the integrating sphere (Section 4.2) is used to develop the analytical model described in Section 4.5. This led to the identification of biasing conditions (I_r, I_g, I_b) for achieving target chromaticity coordinates (x_d, y_d). The LVI response of the LED (Figure 4.2) was again used to identify the transmitted power (P_t), which was then used for both the experimental link and simulation based analysis described in Section 4.3 and 4.4 respectively. The BER obtained experimentally and by simulation was then compared to the theoretical BER calculated using eq. 3.10. The chromaticity coordinates were also calculated practically using both the integrating sphere and CL-500A spectrophotometer (x_c, y_c) alongside other photometric parameters and compared to the target coordinates.

The RGBA LED used in this research can be mixed to provide a wide range of CCTs that replicate artificial and natural light sources (e.g. daylight, skylight, halogen, incandescent etc.). The main focus was towards generating white light, which can be tuned to meet specific preferences and mood as mentioned in Section 2.3.1 while abiding to limits set by lighting standards. Three main CCTs were chosen for the analysis: 2700 K (warm white), 3500 K (neutral white) and 6500 K

(cool white). The link performance was analyzed experimentally, theoretically and experimentally for each color temperature.

4.7 Effect of CCT Regulation on Channel Performance

Initially the biasing conditions obtained from the analytical modelling described in Section 4.5 was used to measure the parameters associated with the illumination and communication of the link. The SPDs for the three target CCTs are presented in Figure 4.6. The peak power for the green source does not vary much since they are operated at similar biasing currents. The red LED has a higher peak for warmer light and the blue LED's power is required to be substantially reduced to achieve the same hue. Some minor changes in biasing condition needed to be made in order to achieve these CCTs while keeping the D_{uv} within the acceptable limits ($D_{uv} < \pm 0.006$) [159].

The simulation framework described in Section 4.4 was modified to have the same transmitted power as the biasing conditions. The BER distribution of each

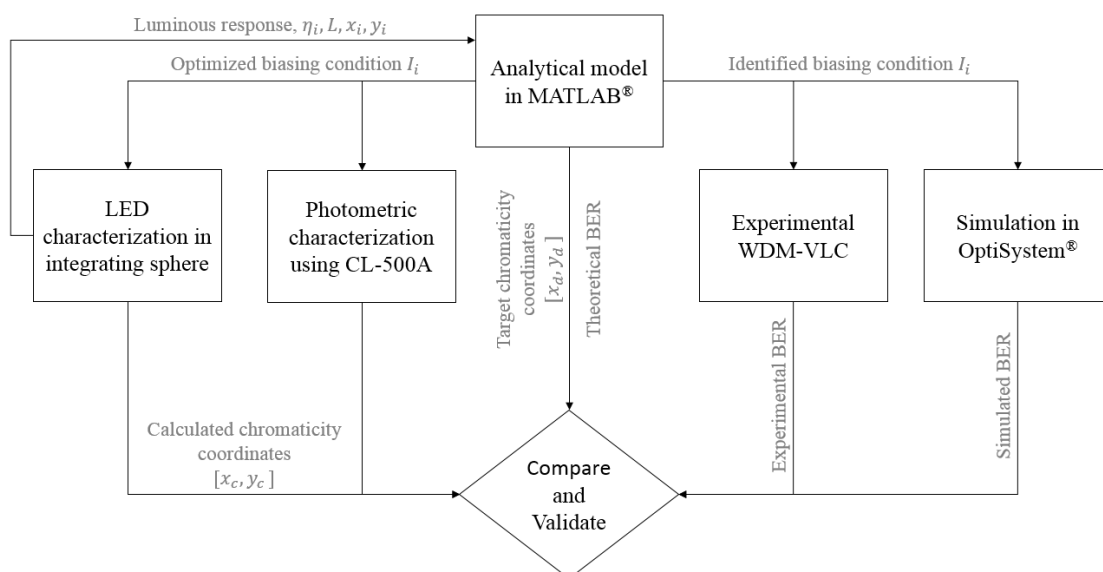


Figure 4.5: Flow chart associated with optimization of biasing conditions and validation of experimental and simulation based results

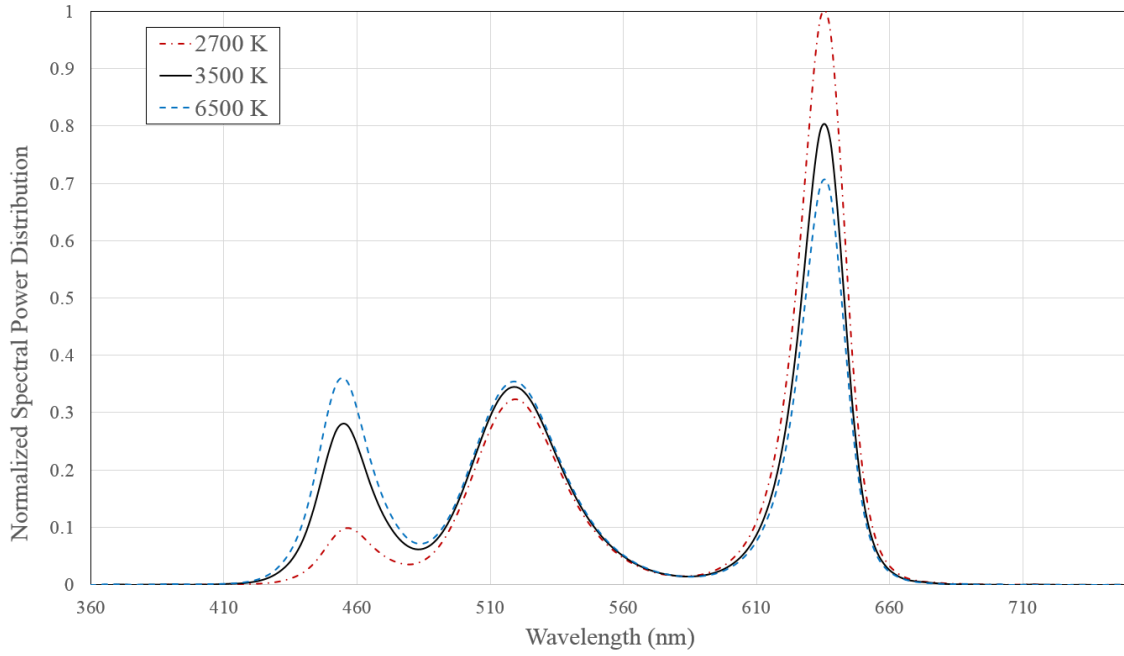


Figure 4.6: Spectral power distribution for CCTs of 2700K, 3500 K and 6500 K for RGB LED-based VLC.

Table 4.3: Biasing conditions required for target CCTs for RGB LED-based VLC

	Warm white	Neutral white	Cool white
Parameters	2700 K	3500 K	6500 K
x_d, y_d	[0.463, 0.42]	[0.409, 0.393]	[0.313, 0.337]
I_r, I_g, I_b (A)	0.70, 0.81, 0.045	0.61, 0.88, 0.067	0.48, 0.95, 0.18
P_{tr}, P_{tg}, P_{tb} (mW)	193, 225, 64	178, 240, 126	158, 248, 243

channel for different CCTs as a function of data rate is presented in Figure 4.7. CCR was implemented for CCT regulation. Since the modulation bandwidth of each LED was modelled to be ~ 17 MHz, the BER increases above the FEC limit at around 17 Mb/s for all channels. However, due to the individual biasing conditions, the received power varies for each LED at the PD, which determines the SNR, thus the BER performance is different for each channel. Based on the limited modulation bandwidth of the LEDs along with the channel response, it was decided to select a baseband operation data rate of 15 Mb/s for each channel, which would yield an aggregate data rate of 45 Mb/s. Thus, it is important that each channel has a BER within the FEC limit at 15 Mb/s.

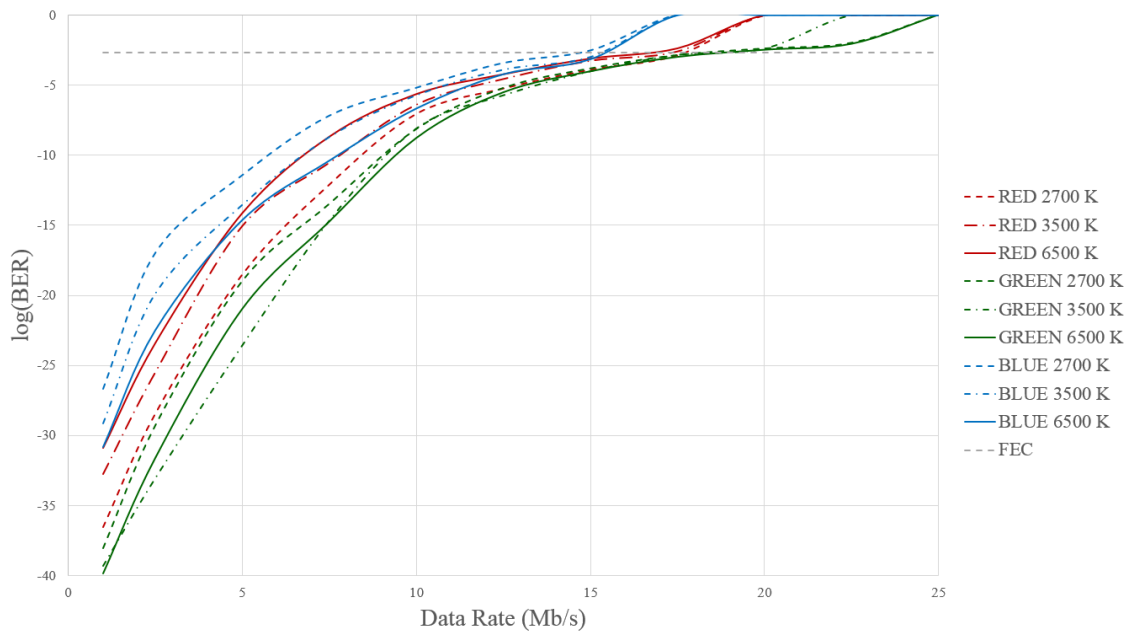


Figure 4.7: BER distribution as function of data rate for separate channels at each color temperatures.

The green channel outperforms all the channel since it has the highest amount of radiated power as seen from Table 4.3. The red channel has a moderate BER distribution, which is well within the FEC limit for all CCTs. And since the blue biasing condition needs to be limited, it has much higher BER compared to other channels. The eye diagrams and the simulated BER for blue channel for the three CCTs are presented in Figure 4.8. It is evident that the performance of the blue channel at 2700 K is not sufficient for reliable data transmission. The BER is 0.00288, which is greater than the FEC limit (0.002).

Table 4.4 summarizes the BER values obtained by simulation, experiment and analytical modelling. All of the analysis follows a similar distribution although there is considerable difference between the analytical results compared to the simulation and experimental results. This difference occurs due to bandwidth limitation considered for both the analyses. However, since the distribution follows a logical pattern when compared to the analytical model and experimental model, the simulation model is considered to be viable and is the basis on which the optimizing of the biasing technique was done in the following sections.

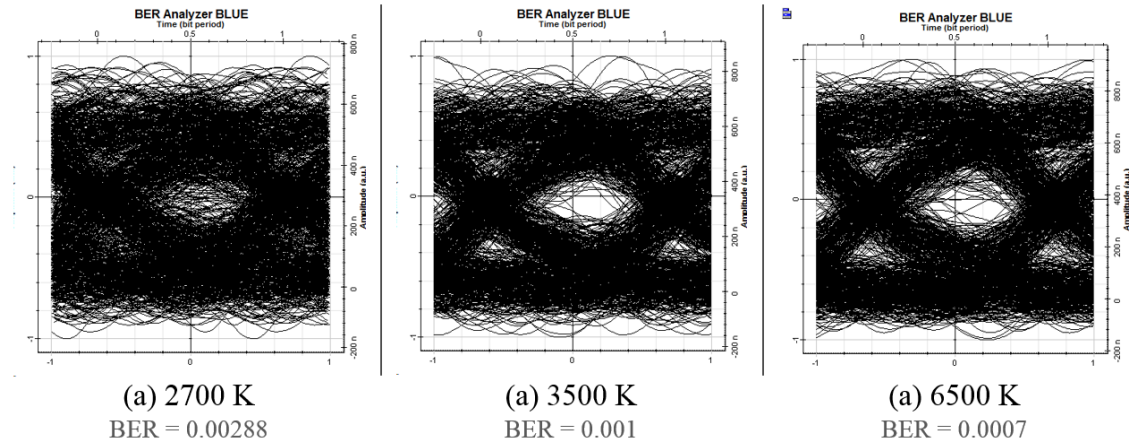


Figure 4.8: Eye diagram of the blue channel for CCT of a) 2700 K, b) 3500 K and c) 6500 K.

Table 4.4: Analytical, simulation based and experimental BER values for different CCTs

		2700 K	3500 K	6500 K
Analytical	R	5.62×10^{-43}	1.85×10^{-36}	2.49×10^{-29}
	G	1.60×10^{-36}	1.26×10^{-41}	4.5×10^{-44}
	B	2.6×10^{-3}	1.60×10^{-8}	1.65×10^{-26}
Experimental	R	3.73×10^{-36}	1.68×10^{-35}	5.92×10^{-25}
	G	5.54×10^{-34}	1.89×10^{-34}	1.72×10^{-37}
	B	4.66×10^{-3}	2.98×10^{-8}	4.59×10^{-24}
Simulation	R	1.32×10^{-4}	5.29×10^{-4}	7.94×10^{-4}
	G	1.4×10^{-4}	9.97×10^{-5}	9.18×10^{-5}
	B	2.88×10^{-3}	1×10^{-3}	7.25×10^{-4}

4.8 Dimming Schemes for CCT Regulation

As seen from the previous section, CCR dimming at lower CCTs causes increase in BER and hampers the communication capacity of the blue channel. As a result, the dimming schemes that were previously investigated for the VLC system (Section 3.7 to 3.9) are implemented to evaluate their effect on system capacity and performance alongside the changes in illumination constraints. A summary of the different dimming schemes developed to control the CCT of the light emitted is depicted in Figure 4.9.

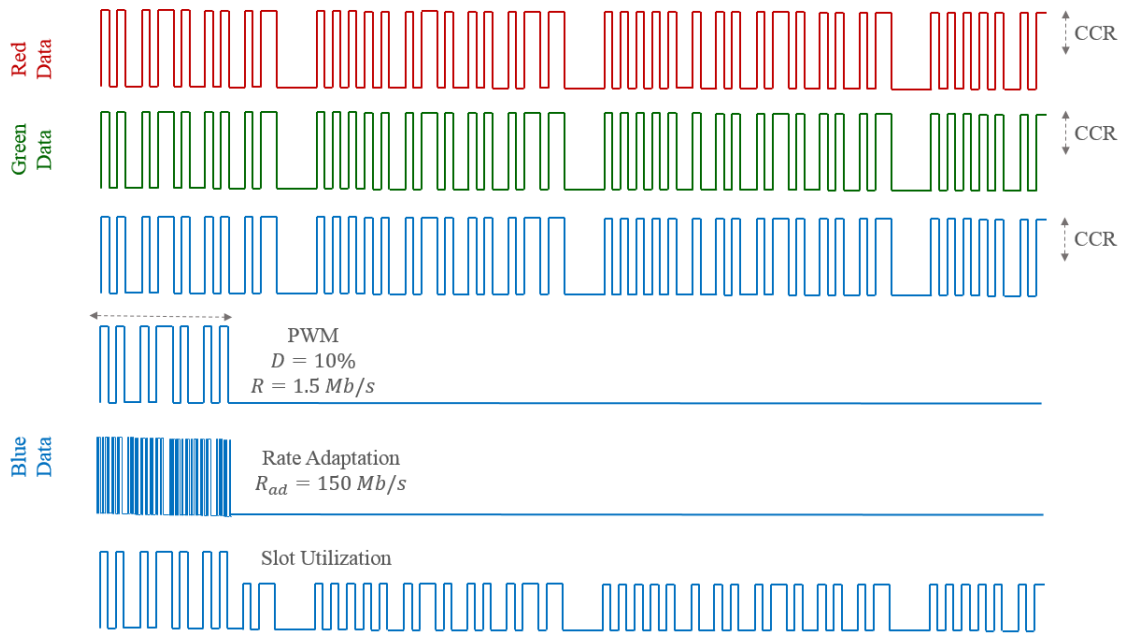


Figure 4.9: Dimming schemes utilized to control the CCT of emitted light for the WDM-VLC system.

4.8.1 Analog Dimming for CCT Control

The effect of CCR dimming on the system has already been summarized where the forward current was adjusted (amplitude of transmitted bits was altered) to achieve dimming. When considering the communication parameters, it does not affect the instantaneous data rate, but determines the SNR at the receiver. According to the analytical model in Section 4.5, the biasing conditions of red and green channel does not change much to attain the targeted CCTs, CCR dimming can be used for these channels to achieve the desirable biasing conditions. However, as seen from Section 4.7, CCR dimming works for the blue channel for CCTs of 6500 K and 3500 K, but does not work for warmer temperatures.

4.8.2 Digital Dimming for CCT Control

The biasing condition for achieving a CCT of 2700 K requires the blue LED to operate at a radiated flux of ~ 64 mW. This means that the LED needs to operate at ~ 10 % of its maximum ratings (705 mW), which means the dimming target

$d = 0.9$. Thus, referring back to eq. 2.19, the maximum achievable data rate for $d = 0.9$ is only 1.5 Mb/s as shown in Figure 4.9. Considering the CCR control of red and green channels, which gives a data rate of 30 Mb/s, the aggregate data rate of the WDM-LED-VLC system is thus 31.5 Mb/s.

4.8.3 Slot Utilization for CCT Control

SU scheme is implemented on top of the digital dimming scheme, based on the analytical model the minimum transmitted power (P_t) required for BER to be above the FEC limit was calculated to be around 65 mW. This was chosen to be the value of (A) referring back to eq. 2.20. Based on eq. 3.14, it is evident the dimming precision would be hampered when this scheme is applied. But a proper experimental characterization needs to be done to quantify, how far the calculated coordinates (x_c, y_c) will fall from the target coordinates (x_d, y_d).

4.8.4 Rate Adaptation for CCT Control

Considering a baseband transmission rate of 15 Mb/s for each channel, referring back to eq. 2.19, for a dimming target of 0.9, the adaptive data rate (R_{ad}) needs to be equal to 150 Mb/s. As mentioned earlier, the 3 dB modulation bandwidth of RGB LEDs is ~ 17 MHz and by utilizing filtering techniques, experimentally that was stretched to ~ 20 MHz allowing the maximum possible attainable data rate for each channel to be roughly 20 Mb/s. Thus utilizing rate adaptation scheme for this WDM-VLC system is not feasible.

4.9 Comparison of Investigated Dimming Schemes for CCT Control

For the blue channel, it was decided to implement PWM and SU for achieving the desired CCT since CCR dimming gives high BER and RA is beyond the system transmission capacity. The calculated chromaticity coordinates (x_c, y_c) along with their position in the CIE 1931 diagram is presented in Figure 4.10. The rest of the parameters are summarized in Table 4.5. The CRI value for SU and PWM was 48 and 45 respectively. Since the difference is less than 5 points, it can be assumed to be similar [28].

For PWM, the chromaticity coordinates fall in between the second and third step, which implies that the change in color temperature will be barely visible to human observers [103, 41]. In contrast, SU has much better position and falls within the first step of the MacAdam ellipse implying that the change in color temperature would not be visible. This happens for SU due to the presence of bits in the blue channel during the ‘OFF’ duration of the PWM dimming signal, which means that the emitted light will be slightly cooler, which makes the chromaticity shift towards the left in the CIE 1931 diagram. The D_{uv} value of +0.0027 for SU is lower than PWM. Based on American National Standards Institute (ANSI) standards, for a nominal CCT of 2700 K, the maximum allowable change in D_{uv} is ± 0.006 , which means both schemes provide quite accurate control of CCT [159].

Table 4.5: Photometric results of digital dimming and slot utilization for achieving CCT of 2700 K

Scheme	Illuminance (lux)	x	y	CCT	u'	v'	D_{uv}	CRI
Slot Utilization	1621.1	0.4628	0.4186	2722	0.2608	0.5308	+0.0027	48
Digital Dimming	1319.2	0.4671	0.4234	2699	0.2614	0.5332	+0.0041	45

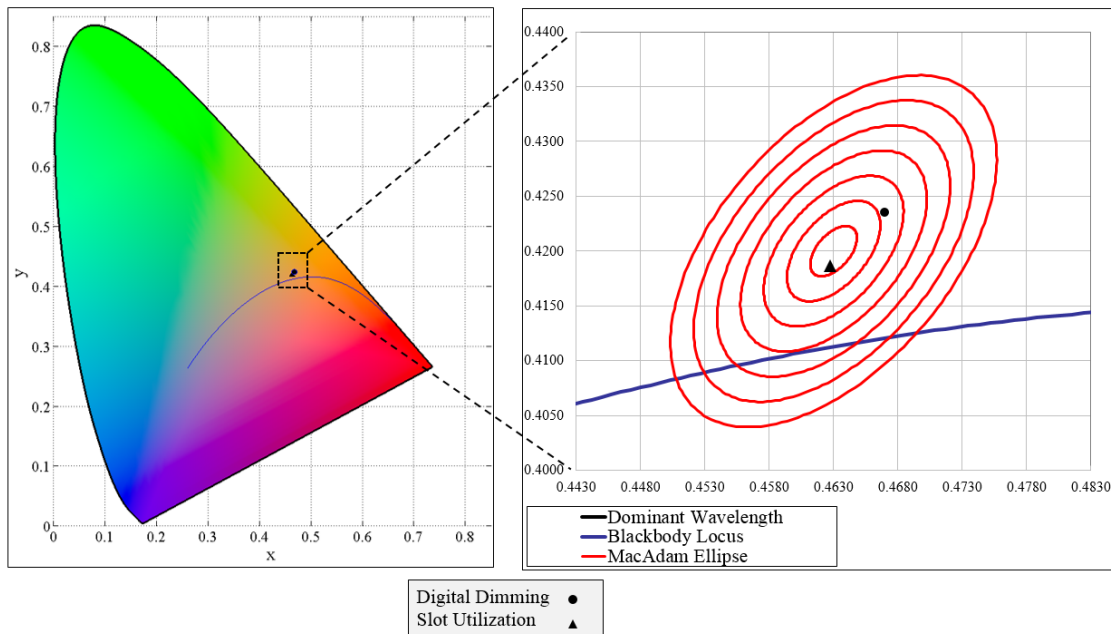


Figure 4.10: The x,y coordinates for digital dimming and slot utilization in the CIE 1931 diagram and their position in the MacAdam ellipse at SDCM of 2700 K.

The comparison of the schemes in terms of communication parameters is tabulated in Table 4.6. These values were obtained experimentally. CCR and RA schemes were considered for comparison purposes. CCR has a BER lower than the FEC limit since the SNR at receiver is very low. PWM provides the lowest BER since the data bits were transmitted at rated biasing conditions but the actual data rate of the system was the lowest. Amongst the adaptive schemes, RA has a BER of 1 (maximum possible BER) since transmission rate is 150 Mb/s, which is way beyond the modulation bandwidth of the transmitter. SU on the other hand has a marginal BER within the FEC limit and maintains the channel transmission rate of 15 Mb/s.

4.10 Conclusion

In this chapter, the VLC system developed previously utilizing phosphor based white LEDs was modified to accommodate a RGB multi chip LED to augment the system transmission capacity by means of WDM. At best case scenarios, com-

Table 4.6: Overall Comparison of Dimming Schemes for CCT Regulation

CCT (K)	Scheme	E (lux)	Data Rate (Mb/s)	Maximum BER	
				Analytical	Experimental
6500	CCR	1630	45	1.65×10^{-26}	7.94×10^{-4}
	PWM	1720	29	5.62×10^{-43}	2.67×10^{-14}
	SU	2154	45	1.65×10^{-22}	3.42×10^{-4}
3500	CCR	1583	45	1.4×10^{-8}	1×10^{-3}
	PWM	1612	28	5.62×10^{-43}	2.82×10^{-14}
	SU	1824	45	2.85×10^{-5}	2.21×10^{-4}
2700	CCR	1297	45	2.6×10^{-3}	2.88×10^{-3}
	PWM	1319	26	5.62×10^{-43}	2.82×10^{-14}
	SU	1621	45	2.1×10^{-4}	1.45×10^{-3}

pared to the previously demonstrated speed of 10 Mb/s achieved by pc-LED, the overall data rate was increased to 45 Mb/s with the RGB LED utilizing NRZ-OOK modulation. However, instead of just producing white light at different intensity levels, which is believed to hold a similar BER distribution as pc-LED-based systems, another controllable parameter, the color temperature was included into the investigation. Dimming functionality of pc-LED and RGB-LED is believed to be similar, for the multi-chip source instead of a single LED, three LEDs needed to be controlled simultaneously. But CCT controllability, which might cater to various applications and moods besides dimming was given priority since color tunability is an additional useful feature that can be achieved by RGB LEDs unlike pc-LEDs. The major observations that were made from this work with multi-chip WDM LED-based VLC are:

- Control of color temperature has a profound impact on individual channel transmission capacity
- The blue channel needs to be regulated the most for achieving warmer color temperatures, which accounts for loss of SNR at warmer CCTs
- For neutral white (CCT of 3500 K) and warm white light (CCT of 2700 K), the BER at the receiver for the blue channel is beyond FEC limit under CCR regulation

- PWM regulation can control the CCT for all channels but at a loss of achievable data rate
- SU has a point in the center of the MacAdam ellipse since it shifts the point in the left of the CIE 1931 due to additional superimposed blue data bits being transferred
- RA can achieve CCT regulation but at required data rates beyond the system bandwidth

Thus, the observations helped in answering the research question 5 discussed in Section 2.11. The adamant perspective of utilizing adaptive schemes for solely controlling luminous intensity was questioned in this work by implementing them for the regulation of CCT. Although the principles behind the control of luminous intensity was similar to the findings in the previous chapter, the variation of relative intensity of each wavelength, which thereby generates white light with different color temperatures helped in sustaining the original transmission rate of 45 Mb/s by implementing SU scheme. Compared to PWM scheme, which achieved a BER of 5.62×10^{-43} but at an overall data rate of 26 Mb/s for warm white light, the SU scheme sustained the target data rate of 45 Mb/s but at a received BER of 2.1×10^{-4} . This chapter helped in identifying the challenges associated with CCT regulation for RGB LED based systems, the observations made and the ideas developed would be implemented for a RGB LD-based system in the next chapter, which is foreseen to provide gigabit class communication.

RGB-LD-BASED VLC SYSTEM WITH ENHANCED ILLUMINATION

5.1 Introduction

In this chapter, the analytical model developed for identifying the optimum biasing conditions for generating light of different color temperatures in the previous chapter is modified to incorporate LDs into the system. Looking back to the work done in this thesis, from an overall perspective it was observed that utilizing multi chip LEDs compared to phosphor based white LEDs gives an overall increase in transmission capacity. However, apart from the use of complex modulation schemes and equalization techniques, the achievable data rate is still quite low and does not provide gigabit class communication, which can be provided by LDs. However there are several issues regarding the use of LDs for illumination:

- Can adaptive dimming schemes be implemented for regulating the blue and green channels to generate light within the usable CCT range and safety standards for RGB LD-based VLC systems?
- Can easily incorporable vibrating diffuser mitigate speckles in the white light generated from a LD-based VLC system?
- How is the human perception of LD-based lighting in comparison to LED-

based lighting in terms of overall preference, contrast, saturation, visual comfort, naturalness of colors and pleasantness?

The same approach of implementing adaptive techniques to capitalize on the stringent biasing requirements on the blue and green channels to achieve warmer color temperature was achieved. The main objective of this work was to generate light for a RGB system in a realistic CCT range of 6500 K to 2700 K unlike most of the previous works, where the CCT was above 7000 K [44, 47]. Although Janjua *et al.* achieved a CCT of ~ 5800 K, the blue channel and green channels were not used for communication, which undermines one of the fundamental advantages of WDM based systems [48]. Different link configurations were also investigated to incorporate higher number of sources to fully capitalize on the narrow emission profiles of LDs. Based on the investigation, the optimum biasing and dimming levels for white light at different CCTs were identified. These identified settings were implemented for objective testing of speckle pattern by using a multispectral imaging system. A spring mounted module for diffuser was designed to mitigate speckle pattern. Subjective testing involving human perception evaluation was also conducted using a light box and compared with LED-based illumination system operating at the same CCT. Thus, the work done in this chapter helped in answering all the research questions that were associated with LD-VLC.

The rest of this chapter is organized as follows. The LVI characteristics of the LD and the link setup are described in Section 5.2 and 5.3 respectively. The simulation framework used for instantaneous link evaluation is presented in Section 5.4. The analytical model used for theoretical validation and identification of optimum biasing condition is presented in Section 5.5. The methodology used for comparison and validation of results is laid out in Section 5.6. The experimental results involving unregulated biasing, CCT regulated biasing, adaptive dimming based biasing and a proposed link configuration are presented in Section 5.7, 5.8,

5.9 and 5.10 respectively. Simulation results demonstrating gigabit class communication is presented in Section 5.11. The characterization and evaluation of light quality based on subjective and objective testing is presented in Section 5.12. Finally, the key outcomes and contribution arising from this chapter are summarized in Section 5.13.

5.2 Characterization of LDs

The LDs utilized in this work were commercially available off the shelf InGaN based LDs. They are mainly suggested for applications involving stage lighting, automotive lighting, medical applications etc. The LDs that were utilized for this work are listed in Table 5.1. The experimental setup for characterizing the LVI response of LDs is presented in Figure 5.1. Since LDs release heat as they operate and are highly sensitive to fluctuations in temperature, a thermoelectric cooler (TEC) controller (LDT-5412B) was used to regulate the operational temperature of the LDs (generally to 25°C). This also helped in prolonged usage without damaging the LDs since they are expensive compared to off the shelf LEDs. The TEC controller was connected to a compatible mount (LDM-4405), which is designed specifically for TO-Can LDs. The rest of the arrangement is similar to the setup described in Section 4.2.

The LDs were specifically chosen based on the works presented in [44], [47], [218], [96], [48]. Most of the work regarding LD based VLC reports a high CCT when RGB based WDM-VLC is considered, remote phosphor techniques had demonstrated lower CCTs (~ 5000 K) [46, 96]. This work focused on achieving tunable CCTs in the range of 2700 K to 6500 K utilizing RGB LDs, thus it was decided to work with a high power red LD (HL63163DG) initially to open the possibilities of having warmer white light being generated. The LVI response of the other LDs that were not eventually utilized due to impractical CCTs are not

Table 5.1: Ratings of the LDs used for the WDM-LD-VLC

Model	Operating Wavelength (nm)	Operating Current (mA)	Output Power (mW)	Package
HL63163DG	633	170	100	TO18
HL6320G	635	70	10	TO38
HL6388MG	637	340	250	TO56
HL6501MG	658	70	35	TO18
HL6545MG	660	170	130	TO56
HL6738MG	690	100	40	TO38
PL520	520	150	50	TO38
L520P120	520	120	340	TO38
DJ532-40	532	330	40	TO95
PL450B	450	165	120	TO38

included in the results.

The LVI response for the three LDs utilized in the RGB LD-VLC system initially for a case temperature of 25°C is presented in Figure 5.2. As expected, the non linearity is much more prominent than the response for RGB LEDs (Figure 4.2). As a result, a suitable linear region of operation was chosen for the WDM-VLC system to avoid amplitude distortion. This investigation helped in identifying optimum maximum and minimum biasing point for the transmitters. The normalized SPD of the LDs are presented in Figure 5.3. The emission profile is

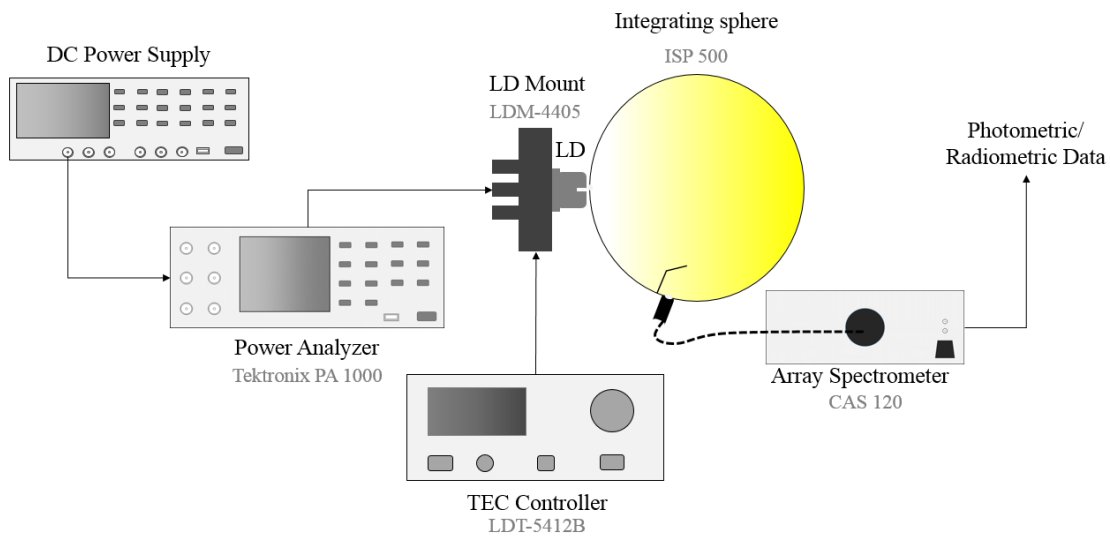


Figure 5.1: Experimental setup for characterizing LVI response of LDs.

much narrower in comparison to the RGB LEDs (Figure 4.3).

5.3 Experimental Setup of WDM-LD-VLC

The experimental setup for the WDM based VLC utilizing LDs is presented in Figure 5.4. The DC offset is added to the NRZ-OOK data stream by the same bias-Ts used previously. NRZ-OOK modulation is used for ease of comparison to the LED based VLC systems developed initially as well as the simplicity and resilience of the scheme in generating non-linearities in lasers [219]. The output of each LD is collimated by a pair of aspheric lenses (Thorlabs A110TM-A followed by Thorlabs ACL4532). The output from the green LD is combined with the blue LD using a bandpass filter (Brightline 447/60). The output from the red LD is combined to the two beams using a red bandpass filter (Brightline 650/150).

At the receiver end, the generated white light is collected by a by an aspheric lens (Thorlabs ACL4532) and focused onto the same Si-PIN photodetector used previously in Section 3.2 and 4.3. Since the electrical filters available were mainly acquired for LED-VLC systems, the cut off frequency was much lower than required. Thus only digital filter along with smoothing functions were used in the oscilloscope to acquire the received waveform. The eye diagram was used to calculate the BER, which was then compared to the offline BER calculated in

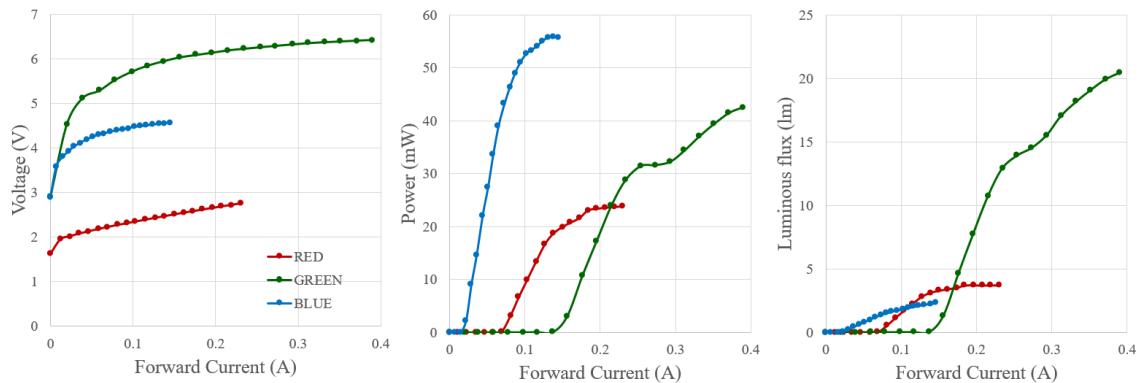


Figure 5.2: LVI characteristics of (a) HL6501MG (b) PL520 (c) PL450B LDs.

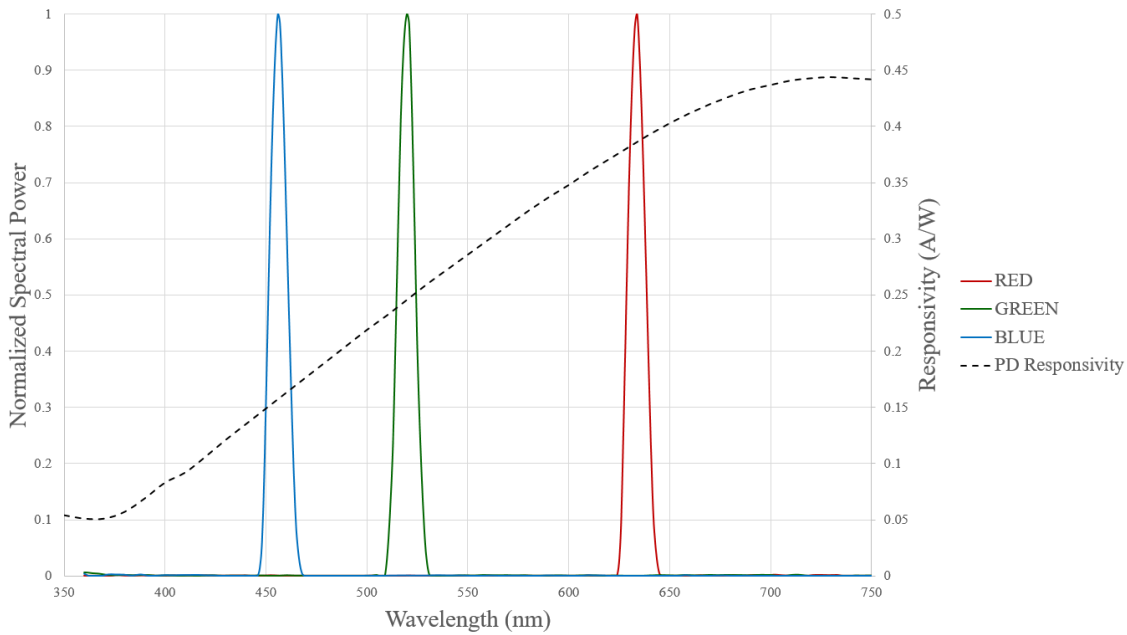


Figure 5.3: Normalized spectral power distribution of the LDs and photodiode responsivity for different wavelengths in the visible range.

MATLAB[®].

5.4 Simulation of WDM-LD-VLC

The RGB-WDM LD-VLC system was simulated in OptiSystem[®] and the configuration was similar to the setup presented in Section 4.4. Directly modulated laser sources were used as transmitters. Parameters such as slope efficiency, threshold current, maximum current, emission wavelength were adjusted to replicate the LDs used practically. Since the LDs used were identical to the work by Tsonev *et al.*, the frequency response of the front end elements were considered to be 230 MHz, 780 MHz and 1 GHz for red, green and blue LDs respectively [44].

The standard FSO channel had a link distance of 2.15 m, which is the standard ceiling to desk distance used in most of the VLC system models [22]. The rest of the parameters for the channel are kept similar to the one described in Section 4.4. However, since lenses were used in the experimental setup depicted in Figure 5.4, the receiver aperture diameter was set to be 45 mm based on the specifications of

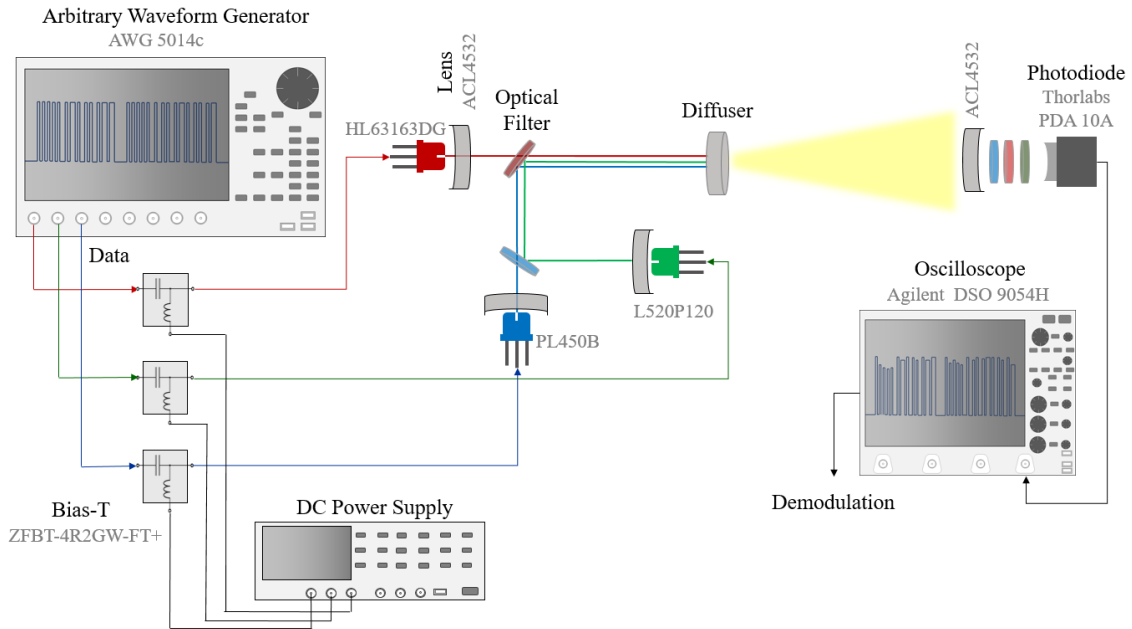


Figure 5.4: Experimental setup of WDM VLC utilizing LDs to generate white light while providing communication.

the actual lens used (ACL4532).

The received power was varied using an optical attenuator to match with the received power at different CCTs due to the different biasing conditions of the LDs (Table 5.5). The main objective of using the simulation framework for LD-based VLC was to demonstrate the ability of LDs to achieve gigabit class communication speed, which was unachievable due to the 3-dB bandwidth of the photodiode (150 MHz), AWG (500 MHz) and oscilloscope (500 MHz) in the practical experiments. This is because most of the equipment for the practical link were acquired keeping LEDs into consideration and these components had bandwidth at least an order of magnitude higher than the LEDs, but not the LDs. Thus, it was decided to utilize a faster photodiode (Newfocus 1601 FS [220]) with a 3 dB bandwidth of 1 GHz in simulation, which had been used in many high speed VLC systems demonstrated in literature [44, 46, 138, 221]. The inherent limitation faced in the practical experiments can be overcome by simulation to demonstrate the true potentials of LD-based communication. The rest of the parameters used in

Table 5.2: System parameters for simulation of RGB WDM LD-VLC link

Parameters		Value
Transmitter	Wavelength (nm)	460, 520, 633
	Beam divergence (mrad)	262, 401, 314
	Transmitter aperture diameter (mm)	9.24
	Threshold current (mA)	30, 140, 70
	3 dB bandwidth (MHz)	1000, 780, 230
	Slope efficiency (W/A)	0.72, 0.44, 0.53
Channel	Distance (m)	2.15
	Attenuation (dB/km)	0.19
Receiver	Modulation bandwidth (GHz)	1
	Receiver aperture diameter (mm)	45
	Responsivity (A/W)	0.21, 0.33, 0.46

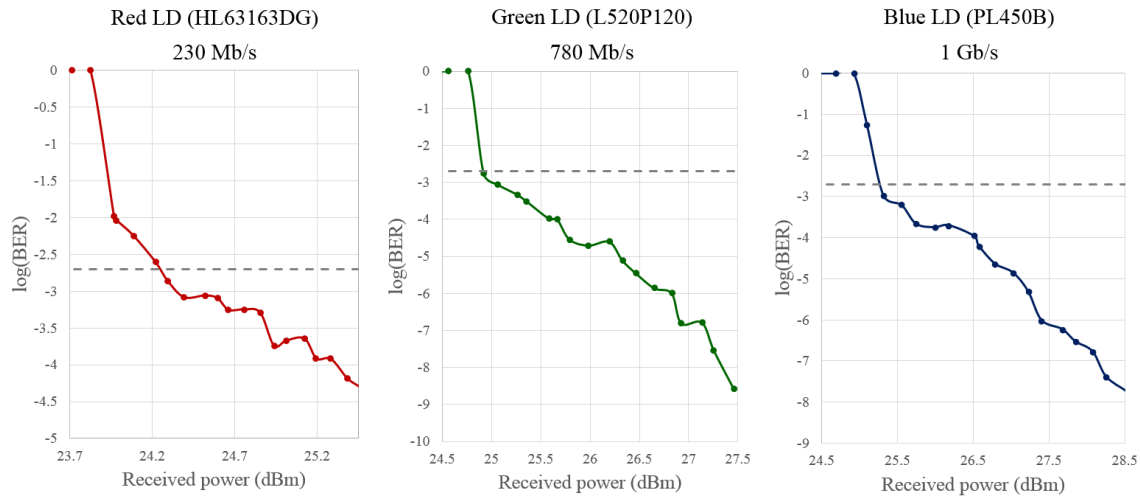


Figure 5.5: Simulation of BER distribution against received power for each channel at their maximum achievable data rate

the simulation framework are summarized in Table 5.2. Based on the simulation parameters and the 3 dB bandwidth of each LDs, the results of the simulation are summarized in Figure 5.5. Although the data rate can be slightly increased, since NRZ-OOK modulation scheme was utilized, it was decided to stick to the baseband transmission rate and thus the 3 dB bandwidth was chosen as the maximum data rate of operation. Although higher order modulation schemes can achieve higher data rates, in this work, the main objective was analyzing the performance of each channel considering baseband transmission rate. Hence, at ideal biasing conditions, the total aggregate data rate is 2.01 Gb/s.

5.5 Analytical Model of WDM-LD-VLC

The analytical calculation was done in MATLAB[®], in a similar manner to Section 4.5. Initially the required biasing current (I_r, I_g, I_b) to provide target chromaticity coordinates $[x_d, y_d]$ was determined using eq. 4.2. The rest of the details are summarized in Section 4.5.1. The LVI response of LEDs and LDs are considerably different from each other, as a result the same mixing ratio could not be used. Besides that, the RGBA LED utilized had identical dies, whereas the LDs utilized for the RGB LD-based VLC system were quite different in terms of operating power and beam divergence, since they were produced by different manufacturers. As a result, the same principle was applied as described in Section 4.5.1, but many more variables were added to obtain accurate interpretation of required biasing condition for different target CCTs.

For analytical calculation of BER and SNR for the LD-based VLC system, the same channel approximations were made as discussed in Section 4.5.2. However there were several parameters, which needed to be changed. The semi angle at half power ($\Phi_{1/2}$) is different for each LD, based on eq. 3.4, this implies that the order of Lambertian emission would also be different. Due to the lower values of $\Phi_{1/2}$, the link performance improved significantly, which helped in increasing the overall link distance from 0.5 m to 1 m. Since the same optical filters were used

Table 5.3: System Parameters for Analytical Model of RGB LD-based VLC

	Parameters	Value
Transmitter	Wavelength (nm)	450, 520, 633
	Chromaticity coordinates	[0.156, 0.019], [0.062, 0.813], [0.709, 0.290]
	Optical gain, η_r, η_g, η_b (lm/A)	8.54, 26.59, 16.38
	Semi angle at half power($^\circ$)	10, 12, 10
Channel	Distance (m)	1
	Total illuminance, E (lux)	500
	Background noise current (A)	202×10^{-6}
Receiver	Filter transmittance	0.925, 0.965, 0.985
	Area of PD (m^2)	8×10^{-6}
	Responsivity (A/W)	0.149, 0.246, 0.382

at the receiver, the transmittance values for the filters were the same. However, the responsivity of the PD was different for the red LD since the peak wavelength is different compared to the red LED used previously. The parameters used for analytical modelling of the LD-based VLC system are summarized in Table 5.3.

5.6 Methodology

The methodology implemented in this work for CCT regulation is similar to the RGB LED based system discussed in Section 4.6. However, the LVI characteristic of LDs is quite unique, which changes the analytical model and hence the biasing conditions. Objective and subjective testing done are also included in comparison and validation of the quality of light being generated at different color temperatures. The flow chart showing the methodology undertaken for this work is presented in Figure 5.6.

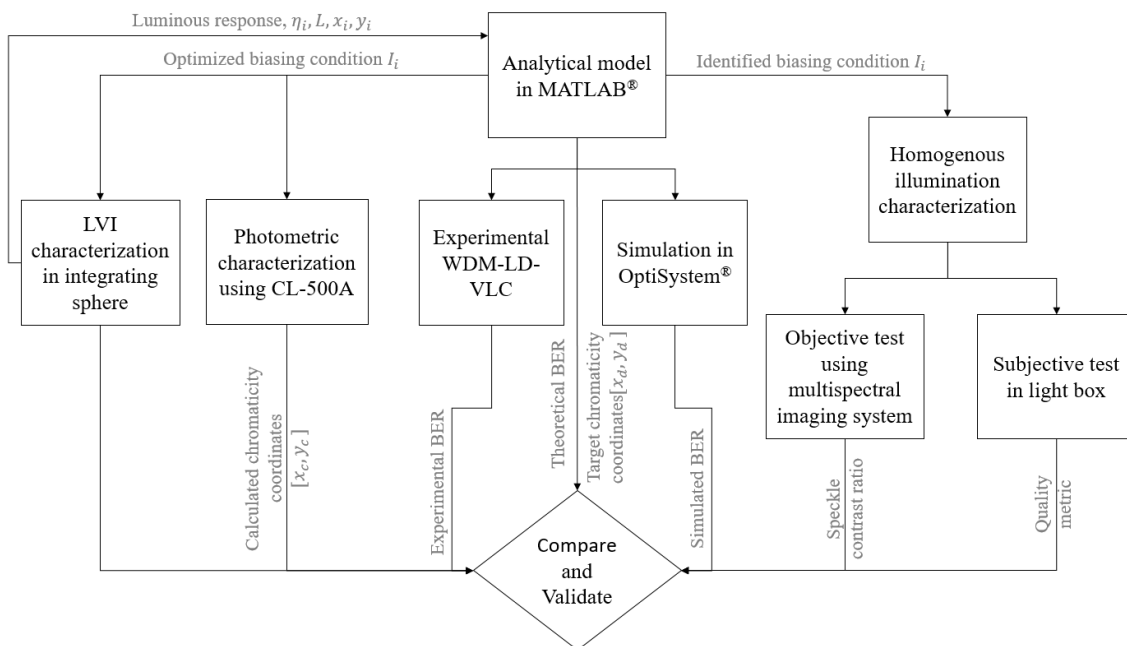


Figure 5.6: Methodology used for CCT regulation and generation of high quality lighting for a LD-based VLC system

5.7 Individual R, G, and B LD-based VLC System

Based on the experimental setup depicted in Figure 5.4, the link distance was set to 2.15 m (standard link distance for ceiling to desk). The operational temperature of the LD was regulated to be 25°C. The biasing condition was kept to the maximum operating current for each LD with the objective of maximizing the communication capacity of the link.

Having the highest optical output power, the green LD outperformed both the red and the blue laser diodes. Although, the red and the blue LDs have similar optical output power at similar operating current, the red source outperformed the blue source since the PD has a higher responsivity at its operating wavelength as seen from Figure 5.3. The maximum achievable speeds and their corresponding BER for each link is summarized in Table 5.4. It must be noted that the bandwidth of the PD used for this work is 150 MHz and the bandwidths of the sources used as reported in [44] is much higher. Thus, the link is limited by the performance of the receiver, which causes performance degradation as reported in [130] for LD based VLC communication. If a PD with a larger bandwidth is utilized, the system is foreseen to operate in the gigabit class range. However, it was decided to continue experimental work with this PD since all the characterization had been done in the previous chapters for this particular receiver (Thorlabs PDA 10A [215]) and it also helps in comparison of LD-VLC with LED-VLC. The simulation based modelling was changed to a PD with higher speed to demonstrate the maximum achievable speed by these LDs.

The normalized SPD and the corresponding coordinate in the CIE 1931 diagram is depicted in Figure 5.8. The CCT of the illumination was measured to be ~ 22000 K, which is really high and does not fall along the MacAdam ellipse. Besides that, the D_{uv} is measured to be +0.0450, which means the light is not viable for use in practical lighting scenarios. The light generated had a relatively high

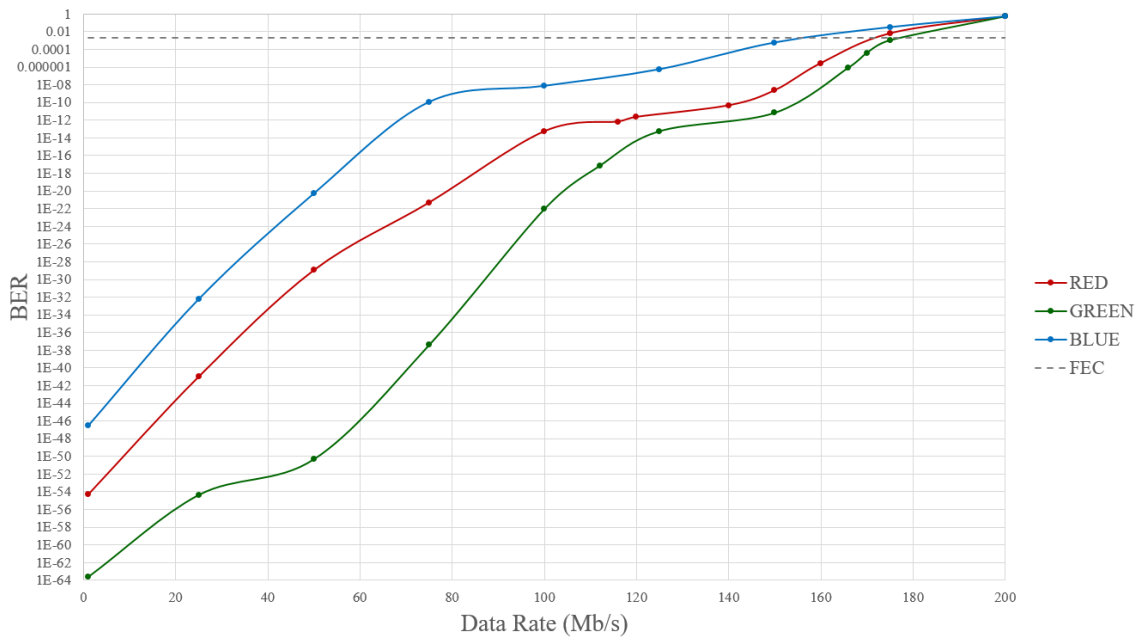


Figure 5.7: BER distribution as a function of data rate for red, green and blue laser diodes for a link distance of 2.15m for link operating at maximum biasing conditions.

Table 5.4: Result from experimental LD-based VLC System

Channel	Data Rate (Mb/s)	Peak Wavelength (nm)	PD Responsivity (A/W)	Biasing Current (A)	Radiated Power (mW)	BER
Red	160	633	0.412	0.2	25.11	2.73×10^{-6}
Green	170	520	0.246	0.3	35.32	4.02×10^{-5}
Blue	150	450	0.149	0.12	27.87	5.73×10^{-4}

CRI of 52 with the lowest CRI for the red band.

These results suggest that although high speed communication can be achieved using LDs as sources for VLC, the photometric parameters are compromised when they are operated at their optimal biasing currents, as a result, the biasing conditions must be carefully reduced for some of the channels in order to get lower CCT and homogeneous illumination. The initial phase of this work would focus on utilizing three sources to achieve warm white, neutral white and cool white lighting. Afterwards, due to the narrow emission profile, which opens up the scope of utilizing multiple sources in parallel as suggested in [44], more red

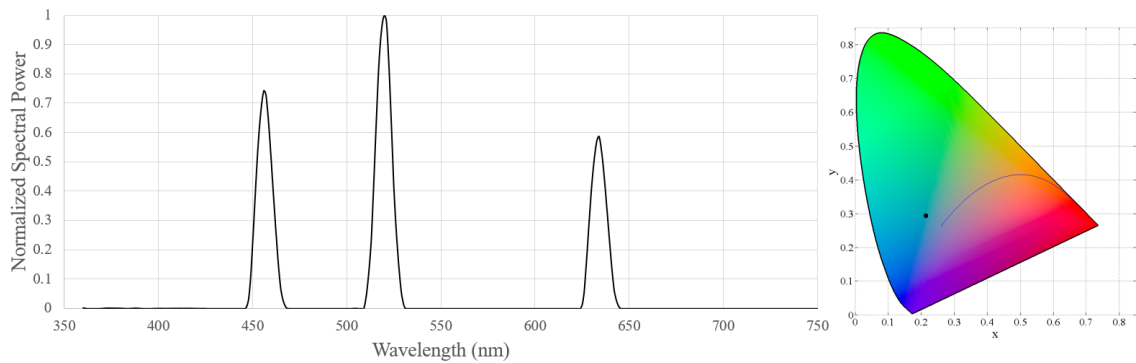


Figure 5.8: Normalized SPD and the corresponding CIE 1931 diagram for the RGB LD-based VLC System.

sources would be added to the system in order to get better quality of illumination.

5.8 CCT Tunable RGB-based VLC System

Based on the characterization done in Section 5.2 and the analytical model developed in Section 5.5, the biasing currents required for achieving different CCTs were identified, which are summarized in Table 5.5. The main focus of this work was to achieve cool white, neutral white and warm white illumination and quantify the impact of CCT tuning on the communication aspects of LD-VLC.

Table 5.5: Biasing conditions required for target CCTs for RGB LD-based VLC

	Warm white	Neutral white	Cool white
Parameters	2700 K	3500 K	6500 K
x_d, y_d	[0.463, 0.42]	[0.409, 0.393]	[0.313, 0.337]
I_r, I_g, I_b (A)	0.25, 0.21, 0.022	0.22, 0.23, 0.036	0.18, 0.25, 0.058
P_{tr}, P_{tg}, P_{tb} (mW)	26.2, 24.1, 2.23	23.8, 28.96, 14.6	22.7, 31.5, 33.5

The SPDs for the target CCTs are presented in Figure 5.9. As noted from Section 4.7, the blue biasing condition needs to be compromised in order to achieve warmer light. But compared to Figure 4.6, the peaks are much narrower and the overall illuminance had to be drastically decreased in order to mix these three

Table 5.6: Photometric results for targeted CCTs of RGB LD-based VLC system

CCT	Warm white	Neutral white	Cool white
Parameters	2700 K	3500 K	6500 K
x_c, y_c	[0.453, 0.402]	[0.407, 0.398]	[0.312, 0.328]
D_{uv}	-0.0024	0.003	0.0026
u', v'	[0.262, 0.523]	[0.234, 0.515]	[0.198, 0.466]
E (lux)	602	606	641

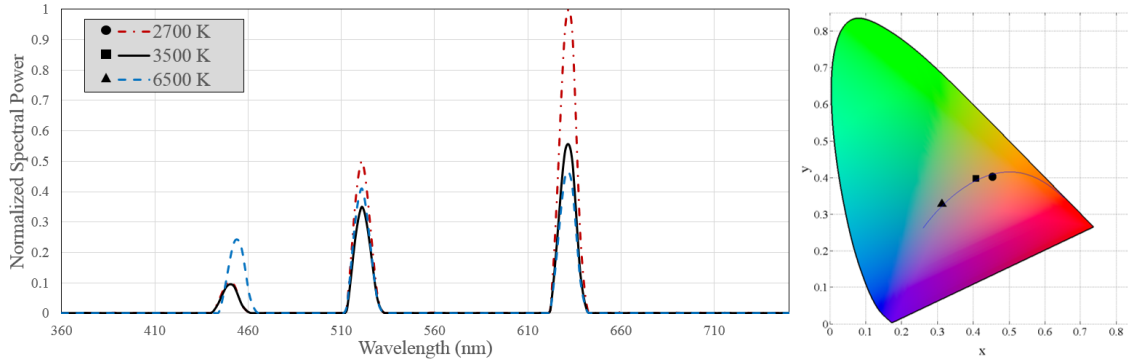


Figure 5.9: Normalized spectral power distribution for CCTs of 2700 K, 3500 K and 6500 K for RGB LD-based VLC system.

LDs effectively in order to generate white light. The results from the photometric analysis are tabulated in Table 5.6. The value of D_{uv} fell within the intended range (± 0.006) and the illuminance for the three scenarios were above 500 lux. The blue channel’s power had to be compromised in order to achieve warmer light, thus it was necessary to evaluate the performance of the link for these biasing conditions.

Initially CCR scheme was implemented to regulate the CCTs for all the channels. BER for the red and the green channels are well below the FEC limit for all the CCTs. The blue channel being operated in much lower biasing current had a BER of 2.74×10^{-4} for a CCT of 6500 K, which is acceptable, however the BER for the blue channel is well below the FEC limit for CCTs of 3500 K and 2700 K. Since the radiated power for these CCTs is low, the optical SNR at the receiver for the link distance is much lower. This can be countered by the following scenarios:

1. Utilizing the blue channel only for illumination purposes with total loss of

transmission capacity

2. Implementing adaptive dimming schemes onto the blue channel with partial loss in transmission capacity
3. Reducing link distance to account for the deterioration in SNR at the receiver
4. Introducing more sources in other wavelengths so that the blue channel can be operated at higher biasing current whilst the additional sources would yield higher aggregate data rate

Scenario 1 is not being considered because the blue LD has the highest 3-dB modulation bandwidth of 1 GHz, not utilizing the blue channel would make it more difficult to achieve gigabit class communication, which is one of the key objectives in this work. Although, scenario 4 seems to have promising outcomes, each of these were investigated so that this overall analysis took into account all sorts of scenarios like limited resources in terms of sources (expense of LDs), limitation in transmitted power due to concerns about skin and eye safety etc. The investigation of each scenario is summarized in the following sections.

5.9 Adaptive Dimming Control for CCT Regulation of RGB-based LD VLC

The dimming schemes that were applied to regulate the CCT of RGB LED-based systems as discussed in Section 4.8 can be applied on LD-based systems as well. These schemes were investigated only for CCT of 3500 K and 2700 K for the blue channel, since CCR scheme was sufficient for CCT of 6500 K for the blue channel and all color temperatures of red and green channels. An overall baseband transmission rate of 150 Mb/s was chosen for the blue channel. For PWM dimming,

Table 5.7: Communication performance of adaptive dimming schemes for CCT regulation of blue channel

CCT	3500 K		2700 K	
Schemes	BER	Data Rate (Mb/s)	BER	Data Rate (Mb/s)
CCR	5.41×10^{-1}	150	1	150
PWM	4.79×10^{-4}	37.5	3.36×10^{-4}	22.5
Slot Utilization	1.22×10^{-1}	150	9.78×10^{-1}	150
Rate Adaptation	1	600	1	1000

the required duty cycle (D) was 15% and 25% for 2700 K and 3500 K respectively. This causes loss of transmission capacity and decreases the achievable data rate based on eq. 2.18 and 2.19. For SU scheme, the required amplitude scaling factor (A) is insufficient for achieving a stable BER, since the transmitted power is much lower when compared to LED-based systems. RA requires adaptive data rate above 600 Mb/s, which is well beyond the modulation capabilities of the PD, AWG and oscilloscope used in this work. The results are summarized in Table 5.7. Based on the results, PWM dimming scheme was chosen for CCT regulation for achieving a BER below the FEC limit. Thus the aggregate data rate for the RGB LD-based VLC system is 367.5 Mb/s for achieving a CCT of 3500 K and 352.5 Mb/s for 2700 K.

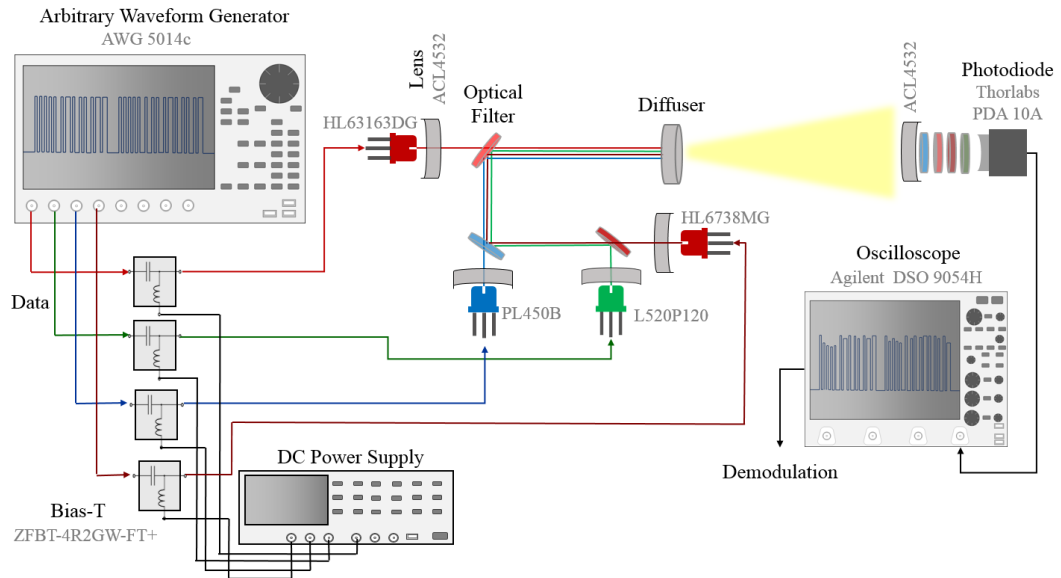


Figure 5.10: Experimental setup of RRGB LD-based VLC utilizing 2 red LDs along with green and blue LD to generate white light while providing communication.

5.10 RRGB LD-based VLC System

An additional red LD was introduced into the LD-based VLC system for improving optical power at higher wavelengths, which allowed in increasing the transmitted power of the blue LD for achieving practical CCTs. Besides that, the Si-PIN photodiodes have higher responsivity in the red region, hence, the addition of red sources can improve link performance. A dark red LD (HL6738MG) was chosen as the fourth LD for the link. Its properties can be found in Table 5.1. The LVI characteristics of the LD was analyzed in a way similar to Section 5.2. Although the output power is considerably low, this particular LD was chosen since the lasing wavelength is considerably spaced out from the red LD (HL63163DG), which helped in efficient separation of each WDM channel at the receiver by utilizing an additional optical filter (BrightLine[®] 642/10 nm). The experimental setup for this RRGB link is depicted in Figure 5.10. The 4 channels of the AWG was utilized simultaneously to generate NRZ-OOK data at different data rates, which was then combined with DC power using 4 bias-Ts and used to drive the LDs.

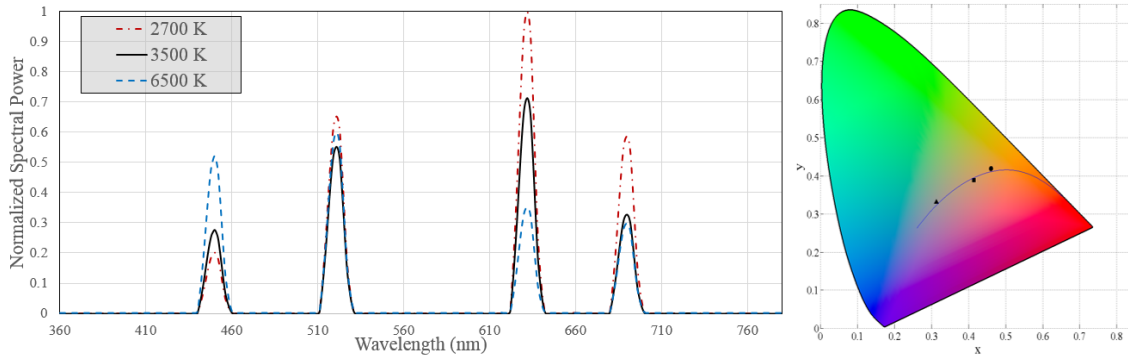


Figure 5.11: Normalized spectral power distribution for CCTs of 2700 K, 3500 K and 6500 K for RRGB LD-based VLC system.

Table 5.8: Photometric results for targeted CCTs of RRGB LD-based VLC system

CCT	Warm white	Neutral white	Cool white
Parameters	2700 K	3500 K	6500 K
x_c, y_c	[0.460, 0.419]	[0.414, 0.313]	[0.313, 0.332]
D_{uv}	0.0018	-0.0037	0.0058
u', v'	[0.259, 0.530]	[0.242, 0.512]	[0.197, 0.470]
E (lux)	743	749	793

The four beams were combined together using optical filters and passed through a combination of ground glass and engineered diffusers. The rest of the setup is similar to the previously described setup in Section 5.3.

Since there were two different red sources, the signal current was divided between the two LDs in a way that ensured the low power dark red channel had enough SNR for a stable link performance. The high power light red channel biasing was mainly altered, since it had the best performance for all the CCTs. The normalized SPDs for this RRGB system along with the resulting coordinates in the CIE 1931 diagram for achieving all three target CCTs are shown in Figure 5.11. The photometric results are also summarized in Table 5.8. The overall illuminance was increased compared to the RGB system due to the additional LD. However, from the SPD, the increase in the blue region is quite visible. The CIE 1931 coordinates fall near the MacAdam ellipse with D_{uv} values within the range of acceptable standards indicating the white illumination at different color tem-

Table 5.9: BER and maximum achievable data rate for each channel of RRGB LD-based VLC for different CCTs

Channel	Warm white 2700 K	Neutral white 3500 K	Cool white 6500 K	Data Rate (Mb/s)
Red 1	4.81×10^{-6}	3.14×10^{-4}	1.24×10^{-3}	160
Red 2	2.16×10^{-4}	1.18×10^{-3}	1.67×10^{-3}	150
Blue	1.98×10^{-3}	8.75×10^{-4}	6.49×10^{-5}	150
Green	2.49×10^{-7}	5.15×10^{-4}	1.78×10^{-5}	170

peratures is acceptable [159].

Based on the setup depicted in Figure 5.10, the communication parameters were investigated using similar techniques discussed in Section 4.3. The results are summarized in Table 5.9. Although the maximum achievable data rate depends on the bandwidth of the PD (the main limiting factor for this link), it varies for each link since digital filtering and smoothing functions were utilized for each channel and the effectiveness of these functions is governed by the optical SNR, which in turn is determined by the biasing condition. It can be seen that the blue channel can function much more efficiently with the BER below the FEC limit for all CCTs. Thus, CCR scheme can regulate the CCTs at an acceptable BER and data rate is not compromised.

The aggregate data rate for the four channels is ~ 630 Mb/s. This work had demonstrated the potential of utilizing multiple LDs to achieve high aggregate data rate making full use of the narrow emission profile of the LDs as proposed by Tsonev *et al.* [44]. A higher power blue LD could have been used to add more red and green channels but due to the limitation of optical filters and channels in AWG, this could not be executed. This is not possible for LED based systems due to their comparatively wider emission profiles.

Table 5.10: Simulation results of LD-VLC at different CCTs

Link type	CCT (K)	Red channel (Gb/s)	Green channel (Gb/s)	Blue channel (Gb/s)	Aggregate data rate (Gb/s)
RGB	22000	0.23	0.78	1	2.01
RGB (with regulation)	6500	0.23	0.78	1	2.01
	3500	0.23	0.78	0.25	1.26
	2700	0.23	0.78	0.15	1.16
RRGB	6500-2700	0.46	0.78	1	2.24

5.11 Simulation Results at Proposed Approaches

Based on the simulation framework presented in Section 5.4, and the findings from the previous sections, the maximum baseband transmission rate of the system for each channel could be calculated for the approaches proposed to regulate the CCT. These results are summarized in Table 5.10.

The required dimming targets were assumed to be equal to the values discussed in Section 5.9. Therefore for CCT regulation by PWM dimming, the duty cycle (D) for 3500 K and 2700 K is 25% and 15% respectively. Therefore, blue LD with a superior bandwidth of 1 GHz, which can provide a baseband transmission rate of 1 Gb/s needs to operate at 0.25 Gb/s and 0.15 Gb/s respectively. The rest of the channels can be regulated by CCR, which won't affect the data rates. In case of the proposed RRGB link configuration, there will be two red channels giving an aggregate rate of 460 Mb/s. And since PWM dimming is not required, the data rates of the individual channel are not affected. Thus the RRGB link can provide the highest aggregate data rate of 2.24 Gb/s.

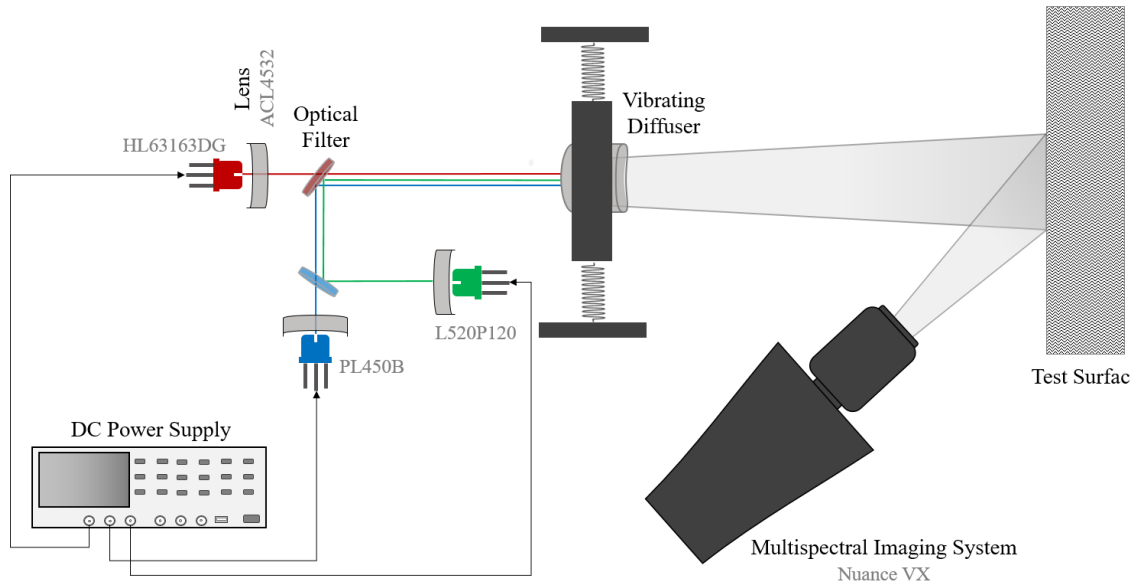


Figure 5.12: Experimental setup for measurement of speckle patterns

5.12 Homogeneous Illumination from LD based Lighting System

5.12.1 Speckle Mitigation

As mentioned in Section 2.10.3, presence of speckle pattern is one of the key concerns of LD-based VLC systems. In this work, a multispectral imaging system (MIS) was used to analyze the speckle patterns generated by LDs when illuminating a white test surface. The experimental setup is depicted in Figure 5.12. The speckle reduction was achieved by means of a vibrating actuator, which was developed based on the concepts presented in [180].

The vibrating actuator was developed in a 3D-printer, which had a mounting for the diffusers investigated in the Section 5.12.2. A standard DC motor made the actuator vibrate on springs attached to the mount. This reduced the speckle from the laser beam passing through the vibrating diffuser. Images were taken using the MIS and a dedicated Nuance[®] software was used to analyze the speckle patterns. Multiple points were randomly chosen for calculation of the standard

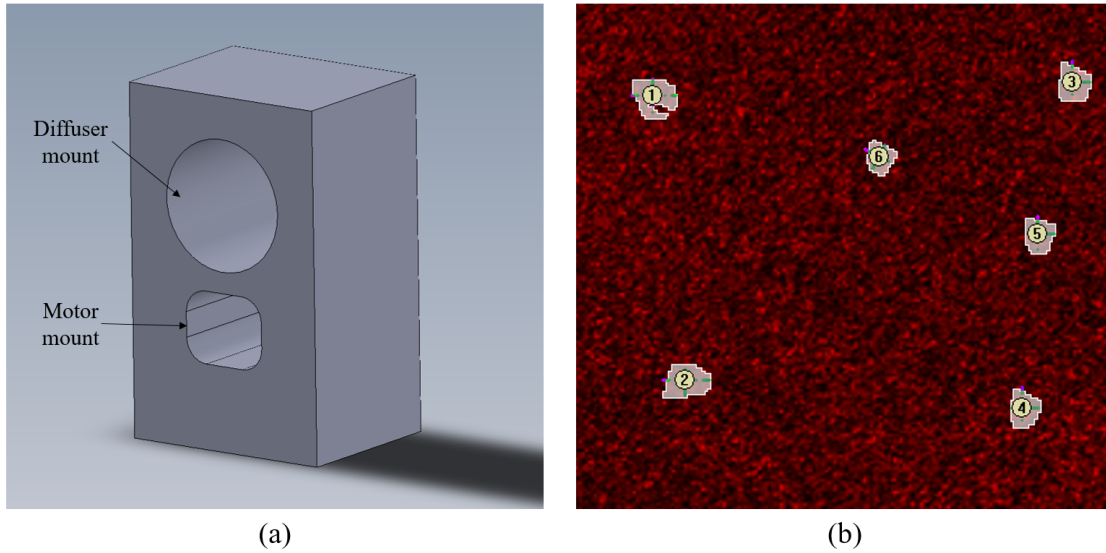


Figure 5.13: (a) 3D autocad drawing of vibrating mount for diffuser (b) Speckle pattern obtained from MIS and random points selected to calculate intensity fluctuations

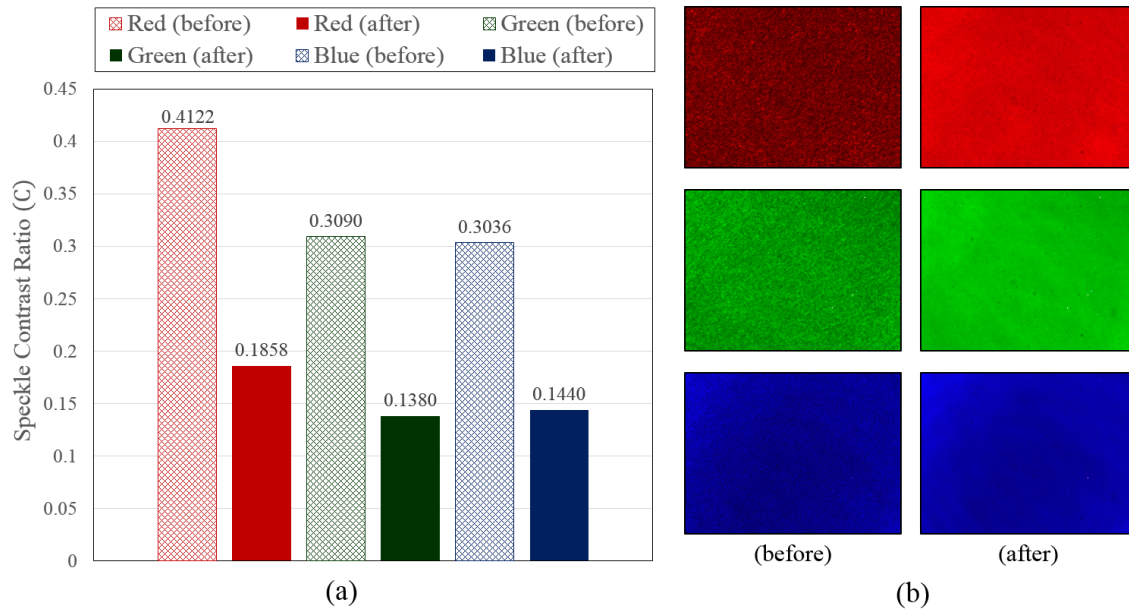


Figure 5.14: (a) Speckle contrast ratio for different LDs (b) Speckle patterns for different LDs

deviation and average speckle intensity, which was then used to calculate the speckle contrast ratio using equation 2.22. The 3D model for the designed mount along with a typical speckle pattern used for calculation are depicted in Figure 5.13.

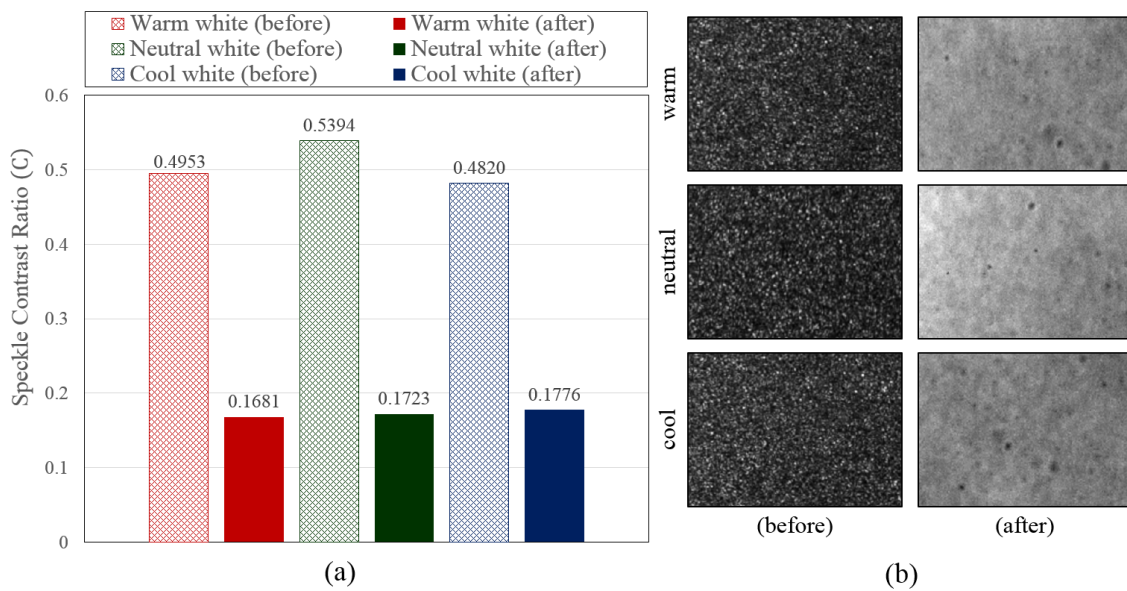


Figure 5.15: (a) Speckle contrast ratio for warm, neutral and cool-white light generated from RGB LDs (b) Speckle patterns for different CCTs of light generated

At first, speckle mitigation of individual red, green and blue LD was conducted to identify the sources with highest speckle contrast ratio. Figure 5.14 shows the distribution of speckle contrast ratio (C) and the speckle patterns obtained for red, green and blue LDs. C is the highest for the red LD, blue and green LDs have lower values of C . A significant decrease in the value of C is observed due to the use of the designed mount. The analysis of C being an objective parameter is not the only measurement that can validate the effectiveness of the designed mount. Subjective speckle needs to be analyzed since human perception is categorized based on this parameter. Hence, images of the illuminated surface were analyzed as presented in Figure 5.14(b), where it is quite clear that speckle is significantly reduced.

Following the initial analysis, the effect of the vibrating diffuser on white light generated from LDs was characterized. Based on the biasing conditions identified in Table 5.5, white light with three different color temperatures (warm, neutral and cool white) was generated and the speckle patterns were analyzed. The speckle contrast ratio distribution is presented in Figure 5.15. Comparing the

results with Figure 5.14, the value of C is slightly higher for the white light compared to the individual red, green and blue LDs. This is because there are three sources, which create an accumulated speckle pattern. However, the difference in C is not significant between different CCTs. As seen in Table 5.5, although the individual red, green and blue LDs are operated at different biasing currents, the generation of white light at CCTs of 2700 K, 3500 K and 6500 K requires mainly the regulation of blue and red channel with one of them being increased and vice versa for the other. Since, speckle is accumulated from each source, this means that the total speckle would tend to remain similar.

5.12.2 Diffuser Characterization

The spatial coherence of lasers can be mitigated by passing it through a transmissive diffuser, which generally contains a thin plate of translucent material and makes the light safer to eye and reduces speckle [122]. For a RGB LD-based system, the diffuser mixes the three beams and generate white light. Hence, characterizing different types of diffusers in terms of the generated white light and their impact on communication is an important aspect to consider.

For analyzing the effect of diffusers on the generated white light, the experimental setup is identical to Figure 5.12. Two types of diffusers were compared, which were used in [44, 66, 222], ground glass diffusers, which have Gaussian intensity distributions and engineered diffusers, which have non-Gaussian distribution. The diffusers were held by mounts and the vibrating module that was designed was not used. This helped in identifying the best possible diffuser, which was then installed on the designed module for optimum speckle mitigation and psychophysical assessment. The speckle contrast ratio was measured in a similar manner using the MIS for different types of diffusers. The ground glass diffusers that were tested in this work had polished surfaces for greater uniformity in comparison to sand blasted diffusers. They had various grits providing different ranges of scattering, from fine to coarse. Finer grit allows higher transmission, while a coarser grit creates a wider diffusion pattern at the expense of transmission. On the other hand, different divergence angled engineered diffusers were investigated in this work. An objective analysis was conducted, where the speckle contrast ratio (C) was calculated. The different values of speckle contrast ratio obtained for different types of diffusers are summarized in Figure 5.16.

In the figure, 'GD' stands for ground glass diffusers and 'ED' stands for engineered diffusers. Compared to GDs, EDs generate light with lower speckle. This is because the speckle pattern due to the transmission through different lenses might not follow a Gaussian distribution, which means Gaussian scattering of

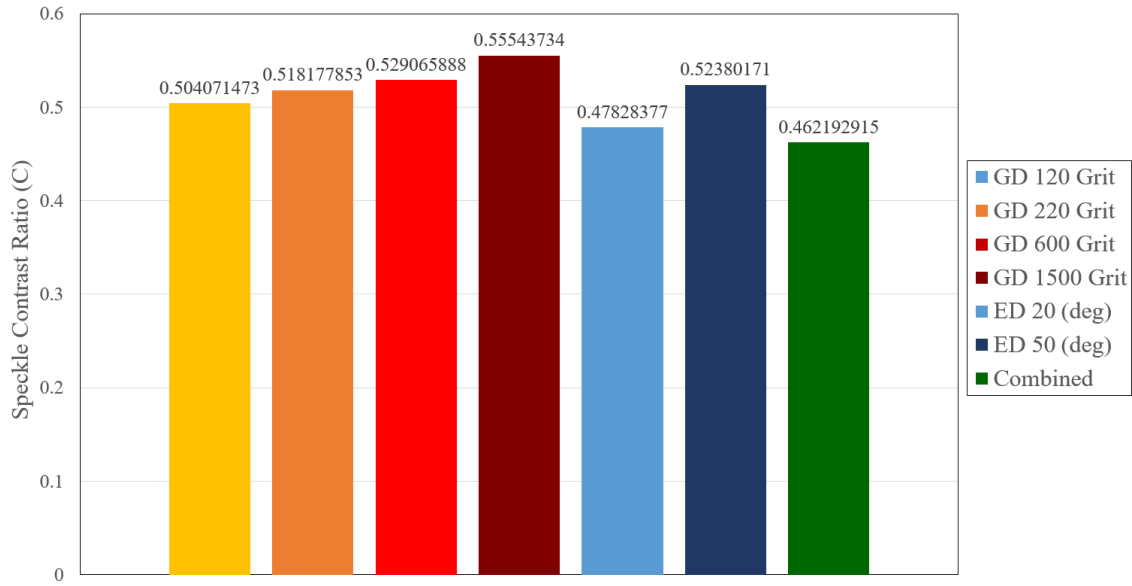


Figure 5.16: Speckle contrast ratios of different types of diffusers

light might have destructive interference compared to divergent scattering [223]. It can be observed that coarser grit in GDs are better for the LD-based system. This comes at the cost of loss in transmission power, which might impact the SNR of the link. In case of the EDs, higher divergence angle yields lower value of C . The best result was obtained when a coarse GD was combined with an ED. However, the intensity of the light was reduced much more strongly. Considering the effect of diffusers on communication, it was observed that the amount of grit or divergent did not affect the link performance significantly. It was only when a combination of diffusers were used, the SNR became too low at the receiver causing the BER to rise above the FEC limit.

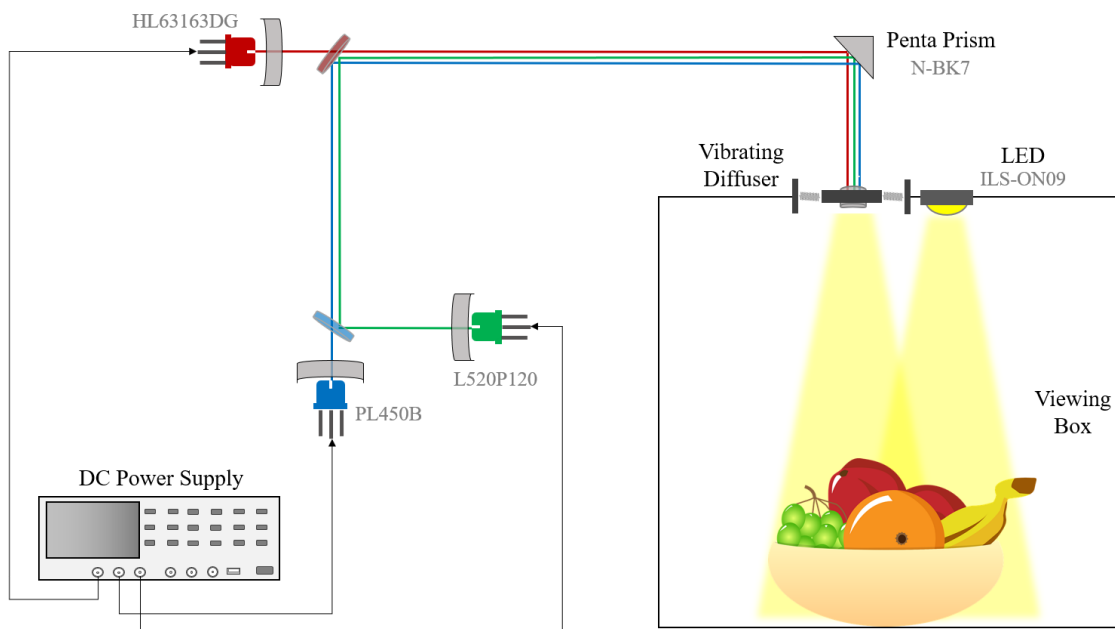


Figure 5.17: Experimental setup for psychophysical evaluation of human preference of LD-based and LED-based lighting

5.12.3 Human Perception Investigation

The design and development of the vibrating diffuser module alongside the use of engineered diffuser helped in effective mitigation of speckle pattern, which was quantified by the MIS. White light was generated by the LD-based VLC system at an acceptable CCT range (2700 K - 6500 K) by the implementation of adaptive dimming techniques at an acceptable BER. However, it was necessary to evaluate the human perception towards the proposed LD-based VLC system by implementing the derived techniques to validate that this system can be used for concurrent illumination and communication in a practical scenario. The methods for human perception investigation by means of psychophysical evaluation and the corresponding statistical analysis of the obtained data had already been discussed in Section 2.10.4. It was decided to only compare the human preference between LED and LD-based lighting. Since LDs are considered as potential replacement of LEDs, correlation between other traditional sources are not necessary.

The test consisted of 42 volunteers (32 males and 10 females). The number of volunteers for the specific age ranges were: 6 (20-22 years), 19 (23-25 years), 10 (26-28 years), 4 (29-31 years), 3 (32-40 years). To ensure all the participants had normal color vision, Ishihara test was conducted, where the participants were asked to identify 16 separate numbers hidden in Ishihara test plates [224]. Data from the 2 test subjects who appeared to be color deficient were not used.

The experimental setup for the psychophysical evaluation is presented in Figure 5.17. The vibrating diffuser module was installed on top of the viewing box along with a phosphor based LED array (ILS ILH-ON09-NUWH). The MIS was used to capture multiple images at different locations of the viewing box to ensure that the speckle contrast ratio is at an acceptable range. Fruits of different colors were placed inside the box, which the participants could refer to for the assessment. The illuminance for both the sources was set to ~ 200 lux, which is sufficient for the small viewing box and is considered to have an identical impact for a practical room scenario where illuminance level of 500 lux is required. Due to limitation of resources, it was decided to evaluate human perception for a single CCT. Hence the neutral-white CCT was chosen (~ 4000 K), which is in the middle of warm-white and cool-white range. The biasing conditions identified in Table 5.5 were slightly altered to achieve a CCT of 4000 K.

The participants in this test were asked to complete a questionnaire, which had individual questions regarding various aspects of lighting such as brightness, naturalness, pleasantness, visual comfort, naturalness of color, saturation, contrast and overall preference. The questionnaire along with the certificate of human ethics approval are attached in Section A.1 and A.2 in the Appendix. Although most of the observers were unaware about color science, the questionnaire was designed to be self-explanatory. However, parameters like saturation and contrast were explained to the participants on their requests.

The light was switched between the LED and LD for each question so that

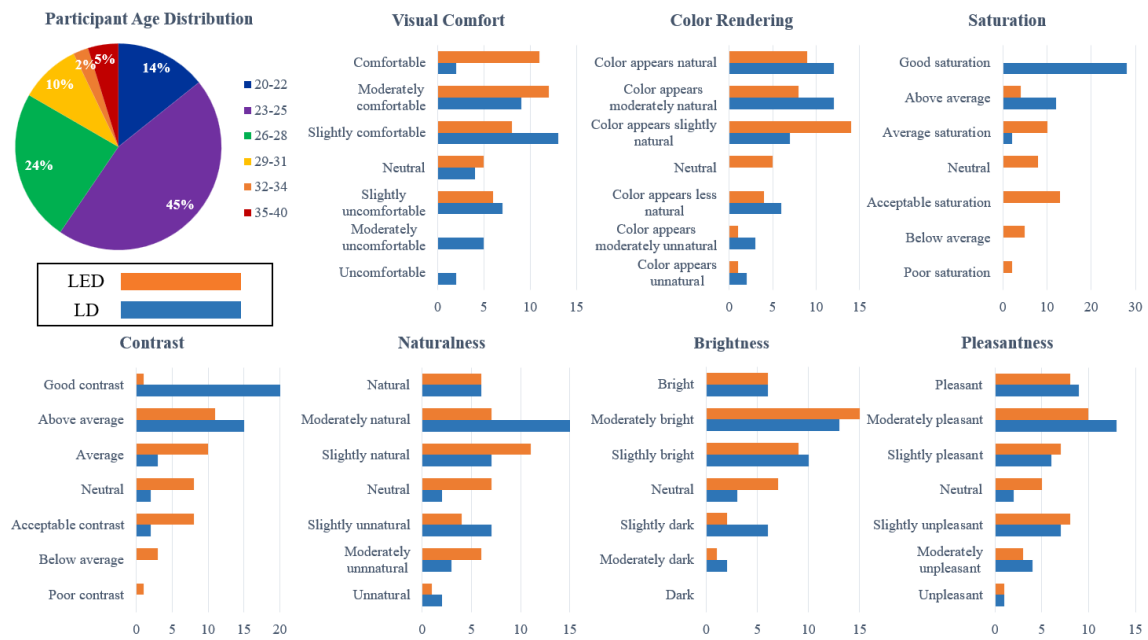


Figure 5.18: Bar charts of preferences for visual comfort, color rendering, saturation, contrast, naturalness, brightness and pleasantness

the participants could compare them before making each assessment, which was obtained on a Likert scale of preference. A 7-point Likert scale was used for the questionnaire (-3: strongly disagree, -2: moderately disagree, -1: slightly disagree, 0: neutral, +1: slightly agree, +2: moderately agree, +3: strongly agree), which was scaled up by 4 for data analysis resulting in a scale from 1 to 7. The raw data obtained is presented in Section A.3 in the Appendix. The bar charts of preferences of the volunteers for different aspects of lighting along with their age distribution are summarized in Figure 5.18.

Since Likert data is ordinal in nature, the central tendency is defined by median and the mode. As discussed in Section 2.10.4, non-parametric hypothesis test was conducted to calculate the statistical significance of each question. Since most of the questions had two individual scales for LED and LD, the Mann-Whitney-Wilcoxon (MWW) rank sum test was conducted. For the final question of overall preference, which had a single scale of preference, the Chi-square (χ^2) test was conducted. The p-values obtained from the MWW and χ^2 tests were used to characterize the probability that the data are consistent with the null hypothesis.

Table 5.11: Summary of statistical data for psychophysical evaluation of LD and LED-based lighting

Parameter	Type	Mean	Median	Mode	Std. Dev	Range	Sum	Z-score	p-value
Visual	LD	4.48	5	5	1.52	6	179	-2.6	0.00093
Comfort	LED	5.38	6	6	1.39	4	215		
Color	LD	5.38	6	7	1.64	5	215	1.35	0.17702
Rendering	LED	5.05	5	5	1.45	6	202		
Saturation	LD	6.65	7	7	0.58	2	266	7.33	< 0.00001
	LED	3.73	3.5	3	1.38	5	149		
Pleasantness	LD	5.08	6	6	1.76	6	203	0.96	0.33706
	LED	4.73	5	6	1.71	6	189		
Contrast	LD	6.25	6.5	7	0.98	4	250	5.55	< 0.00001
	LED	4.40	5	6	1.45	6	176		
Naturalness	LD	5.03	6	6	1.62	6	201	1.42	0.1556
	LED	4.53	5	5	1.71	6	181		
Brightness	LD	5.10	5	6	1.45	5	204	-0.53	0.59612
	LED	5.33	6	6	1.23	5	213		
Overall preference		2.93	2	2	1.59	5	117	N/A	0.000504

The null hypothesis in this evaluation was that preference distribution for LD-based lighting is the same as LED-based lighting. The summary of the responses along with the calculated p-values are presented in Table 5.11.

Based on the results from the statistical analysis, it can be observed that for visual comfort, saturation, contrast and overall preference, the preference for one source over another is statistically significant. In order to determine which source is being preferred to, the Z-score can be observed. A negative Z-score indicates more preference for LED whereas a positive Z-score indicates higher preference towards LD. Thus, LED is being preferred for visual comfort and LD is being preferred for saturation and contrast. From post-assessment discussion, it was observed that the participants could be widely categorized into two groups: those who prefer more or those who prefer less saturation in colors. Since objects illuminated by a laser source appear more saturated, there was higher preference towards this source, which is in line with the observation in [66]. The bar chart associated with the overall preference towards LED or LD is presented in Figure 5.19. It can be observed that 78 % participants had slight, moderate or strong

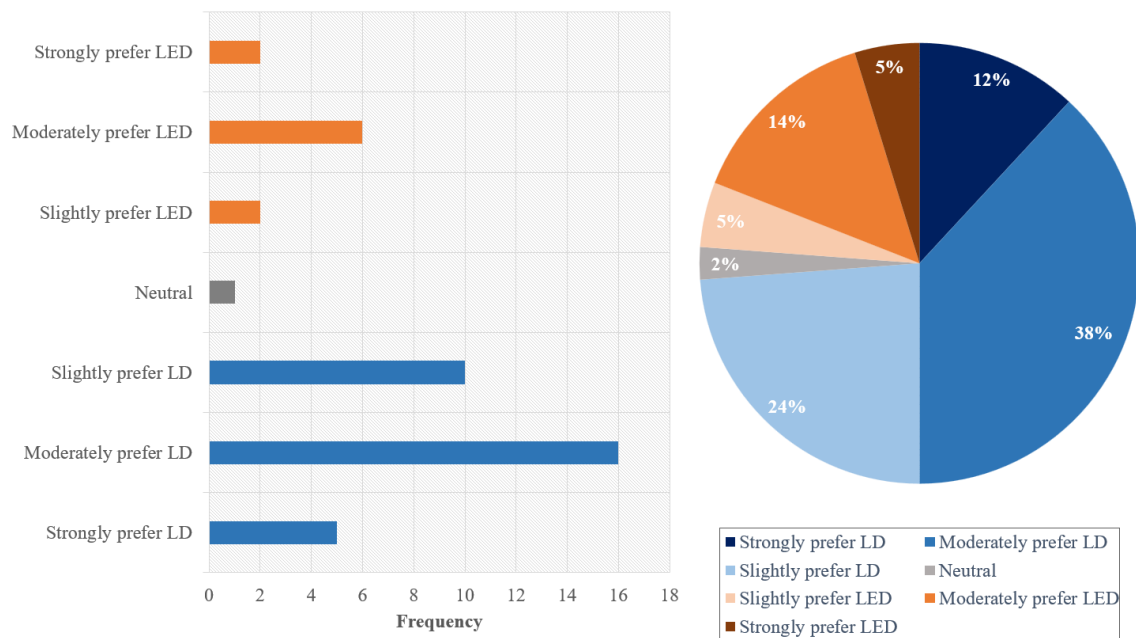


Figure 5.19: Overall preference of participants for LED/LD

preference for LD-based lighting. Since this particular question had a single Likert scale, the χ^2 test was performed to calculate the p-value. The p-value was 0.000504 (< 0.05) hence the preference towards LD is statistically significant.

5.13 Conclusion

In this chapter, in order to develop a VLC system that operates at gigabit class range, LDs were incorporated into the system, utilizing the WDM based framework developed in the previous chapter. Although the communication aspects of this source is promising, their practical adaptability is still a major concern due to their sensitivity to temperature and inability to provide high quality illumination. This work tried in bridging the gap between LDs and practical illumination by attempting to generate light at an acceptable CCT range, which can cater to different popular applications. There were a number of challenges regarding the illumination quality and the stringent biasing conditions hampering link stability, which were successfully addressed. The major observations made in this work are:

- LVI response of LDs is much more non-linear compared to LEDs, which might induce challenges specially considering complex modulation schemes like OFDM
- Thermal dependence of LDs is much higher compared to LEDs hence a heat sink is not solely capable of ensuring a linear output, thus TEC controllers always need to be utilized for LDs
- For a RGB system, operating the LDs at their optimum biasing condition yields much cooler white light (~ 22000 K), which is impractical for use in indoor environments
- Under CCT regulation, the blue channel gives BER above the FEC limit when CCR is used for dimming, this observation is similar to the RGB LED based system
- PWM is the only scheme, which can achieve an acceptable BER, unlike LED-based systems where SU achieved an acceptable BER. Therefore, there is a

decrease in aggregate data rate

- RRGB systems allows finer control of CCT compared to RGB systems with CCR scheme being capable of CCT regulation without any loss in transmission capacity
- Simulation results yield a data rate of 2.24 Gb/s for the proposed RRGB system utilizing simple NRZ-OOK modulation
- Vibrating diffuser helps in destroying the coherence of the laser based white light and reduces speckle contrast ratio by 68 %
- Engineered diffuser with coarser grit are better suited for mixing LD based light
- LD-based lighting is preferred over LED-based lighting when illumination aspects like contrast and saturation are considered
- Overall preference of human observers is towards LDs since generally their inclination is strongly biased towards saturation

These observations answer research questions 6, 7 and 8 discussed in Section 2.11. The concept of integration of adaptive schemes into LD-based system was explored in this work to generate high quality white light. It was noticed that CCT regulation decreases the overall capacity from 2.01 Gb/s to 1.26 Gb/s and 1.16 Gb/s for 3500 K and 2700 K respectively. However, the proposed RRGB system can achieve the entire range of CCTs by utilizing CCR scheme only, which does not compromise with the transmission capacity and provides a higher aggregate data rate of 2.24 Gb/s. Figure 5.20 presents the concept of such a scenario in a practical application, where CCT can be controlled to cater to different spaces requiring different moods. The three areas that are mainly considered in the presented office space are meeting room, lounge and workplace. Workplace generally requires high level of alertness, which can be exerted by cool white light. For

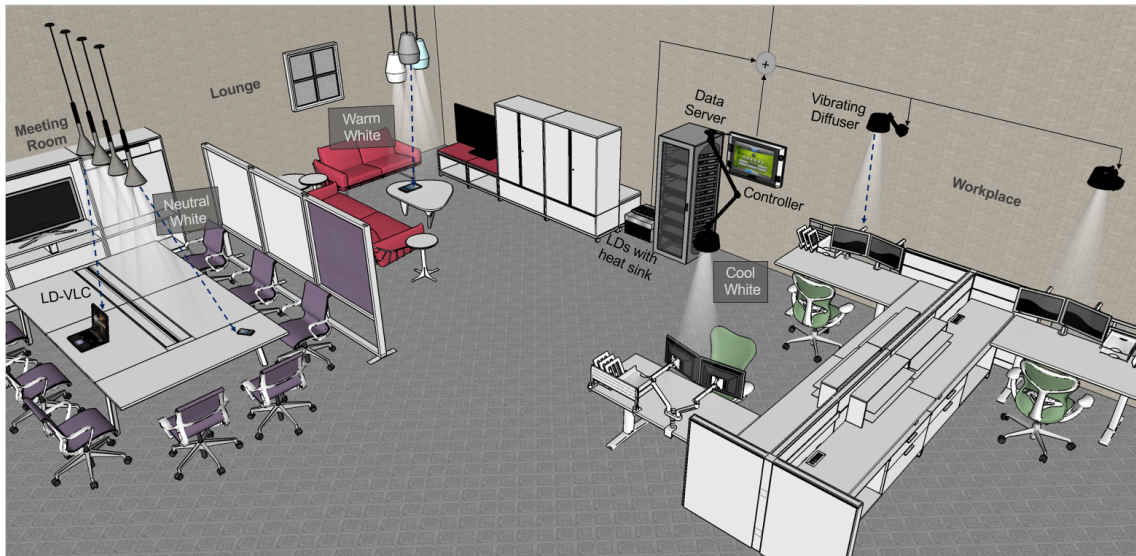


Figure 5.20: Concept of practical implementation of CCT regulation of LD-VLC for an office space

meeting rooms, neutral white light that provides friendly and inviting mood is required. For lounge spaces where normally employees go for relaxing, warm white light is ideal for exerting a cozy environment. Thermal management is one of the key issues, which increases the complexity of the system. However lasers can be guided through fibers, which allows for large scale cost effective cooling at hidden locations [57].

In order to ensure homogeneous illumination from the proposed system, objective and subjective tests were conducted. The presence of speckle pattern was identified from the initial investigations and by means of a engineered diffuser with a vibrating module, the speckle contrast ratio was decreased by 68 %. Psychophysical evaluation of 40 participants indicated a 74 % overall preference towards the proposed LD-based VLC system. However, the measured CRI of 35 was still quite low compared to LED-based lighting. Thus, it was decided to explore the possibilities of LED-LD-based hybrid systems, capable of providing gigabit class communication with superior color rendering capabilities, which is discussed in the next chapter.

HYBRID LED-LD-BASED VLC SYSTEM WITH SUPERIOR COLOR RENDERING

6.1 Introduction

In this chapter, the main objective was to explore the possibilities of consolidation of different sources in order to overcome the inadequacies observed in the previous systems and propose a hybrid system, which has superior performance in terms of achievable data rate and quality of illumination. Despite achieving white light at an acceptable color temperature, the main drawback of the proposed LD-based system in Chapter 5 was the low value of CRI of 35. The highest CRI of ~ 54 for LD-based VLC demonstrated in [47] was achieved at a CCT of 8382 K. It was observed that generating light with higher CCT can increase the CRI but the maximum achievable CRI of 52 was still low in comparison to industrial lighting standards. On the other hand, although pc-LEDs exhibit the highest CRI amongst the transmitters considered for VLC, it is quite low compared to traditional incandescent sources due to its inefficiency in producing light output in the higher wavelength region. This can be resolved by red enhanced LEDs, which creates higher saturation for colors of higher wavelength. This raised the

research question:

- Is it possible to employ red enhancement to obtain a high value for CRI for LD and pc-LED based lighting system?

The prospect of implementing red enhancement by LDs and spectrum continuity by LEDs, which can give CRI values higher than either of the sources used separately is quite unique. The only work on such a hybrid system utilized a red LD with a pc-LED to achieve a CRI of 83 for a data rate of 400 Mb/s [55]. Amongst LED sources, pc-LEDs are the preferable option over RGB LEDs since their intensity distribution is widely spread across the entire visible range. Thus, it was decided to explore different link configurations utilizing a single pc-LED and multiple LDs. Initially a quantitative comparison of LEDs and LDs was conducted experimentally regarding thermal management and bandwidth. This analysis helped in clearly assessing the limitations of each sources, on the basis of that the hybrid system was proposed. The hybrid system was investigated considering mainly the CRI. When the optimum setting in terms of CRI was obtained, the experimental and simulation based setups were used for evaluation of link performance. This helped in demonstrating a practically functional hybrid VLC system, which answered the research question discussed earlier.

The rest of this chapter is organized as follows. The methodology involving characterizations done previously and new measurements is described in Section 6.2. This is followed by the quantitative evaluation of LEDs and LDs done in Section 6.3. The performance of the hybrid system considering the photometric parameters for different link configurations is presented in Section 6.4. Based on the results, the experimental and simulation based communication performance for the hybrid system is evaluated in Section 6.5. Finally, the summary and key outcomes of this work is presented in Section 6.6.

6.2 Methodology

In this work, the LVI characterizations done for pc-LEDs and LDs presented in Section 3.3 and 5.2 was used as a reference. The analytical models developed in Section 3.4 and 5.5 were used to evaluate the theoretical BER. However, the identification of optimum biasing levels for the LDs could not be carried out theoretically using the equations in Section 4.5, because the pc-LED had an impact on the location of the chromaticity coordinates on the CIE 1931 diagram. The thermal and bandwidth characterization helped in identifying the key differences of each source, which gave an overview of the limitations of the work done in the previous chapters. For each link configuration, the optimum CRI was obtained by altering the biasing condition and the communication parameters were analyzed at the identified biasing levels both experimentally and by simulation. All of these results obtained by simulation, experiments and theory were compared and validated.

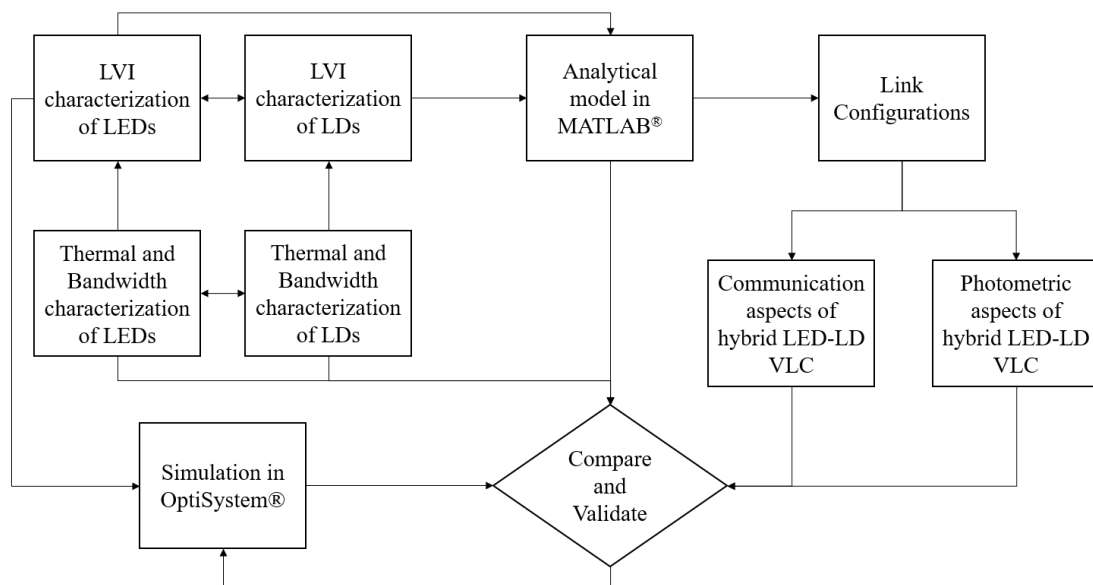


Figure 6.1: Methodology implemented for development and evaluation of LED-LD hybrid VLC system

6.3 Quantitative Comparison of LEDs and LDs

This section investigates the performance of the LEDs and LDs used for all the systems proposed in this thesis in terms of bandwidth and thermal management. Parameters associated with thermal management helps in comprehension of the feasibility of these sources for practical adaptation. Bandwidth is one of the fundamental properties, which determines the achievable speed of transmission, hence comparison of this property helped in justifying the use of hybrid systems.

6.3.1 Bandwidth Characterization

VLC system bandwidths are generally limited by the frequency response of the LEDs since PDs generally have 3-dB bandwidths of an order of magnitude higher than the LED. Although, some work had demonstrated system operation beyond the 3-dB bandwidth of the LEDs [162, 174, 225, 226, 140] to achieve higher data rates, in this work, the focus was towards utilizing optical sources with higher modulation bandwidths (LDs) and investigate their effect on a bandwidth limited link.

Due to the lack of an optical spectrum analyzer, the 3dB bandwidth of the link was measured using an oscilloscope. Despite being time domain instruments, high-end oscilloscopes can digitize waveforms and process the time domain signals into the frequency domain. The experimental setup for this investigation was similar to the systems depicted in Figure 5.4 and 4.4 with the link distance changed to a minimum in order to disregard the channel effects. A step function was used as an excitation signal from the AWG assuming the AWG has a flat response. The received response to the step input is then differentiated, which produced an impulse function. An FFT function is then applied onto the impulse function to obtain the output signal spectrum. The signal spectrum obtained for a pc-LED is shown in Figure 6.2. From the figure, the 3dB drop in the response

can be calculated to be approximately 18.8 MHz, which is almost equal to the 20 MHz bandwidths (after blue filtering) reported in [124, 196].

The overall frequency response of a VLC channel can be modelled as [227]

$$H(f) = (H_{LOS}(f) + H_{NLOS}(f))H_T(f) \tag{6.1}$$

where $H_{LOS}(f)$ and $H_{NLOS}(f)$ are the line of sight (LOS) and non-line of sight (NLOS) wireless channel responses and $H_T(f)$ is the frequency response of the optical source. The frequency response of LEDs and LDs can be assumed to have a similar distribution with the LD exhibiting much higher 3-dB bandwidth. The modulation response of an LED/LD can be modelled as a Gaussian low pass filter by [228]

$$|H_T(f)|^2 = e^{-\left(\frac{f}{f_o}\right)^2} \tag{6.2}$$

The frequency response of this modelling and the experimental frequency re-

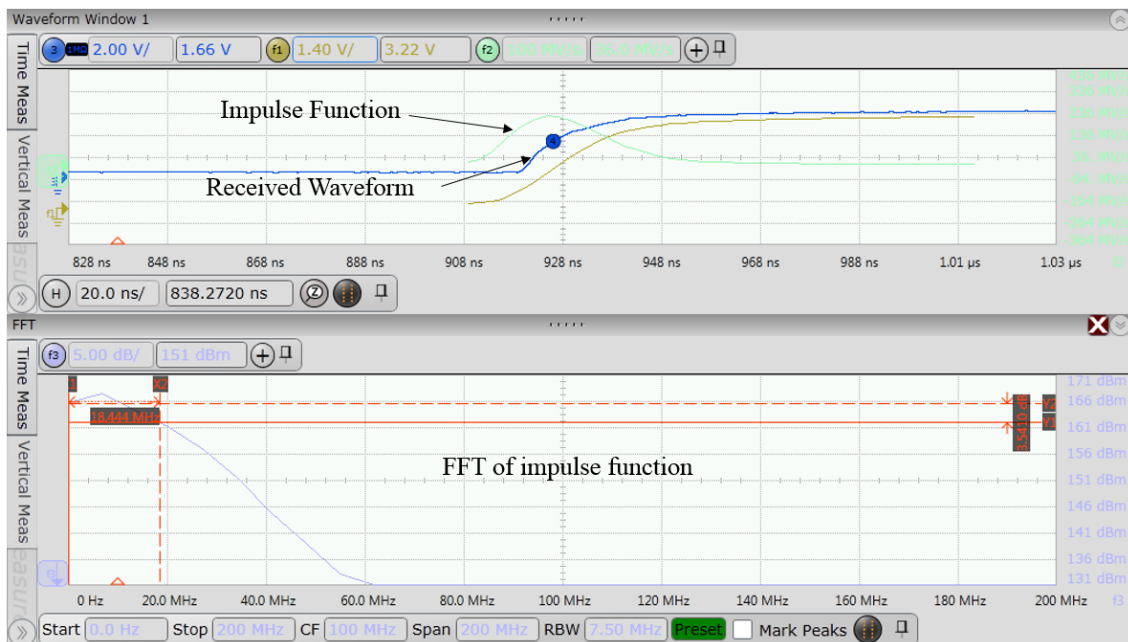


Figure 6.2: Step response, derivative impulse function and FFT of the derivative (frequency response of the investigated system)

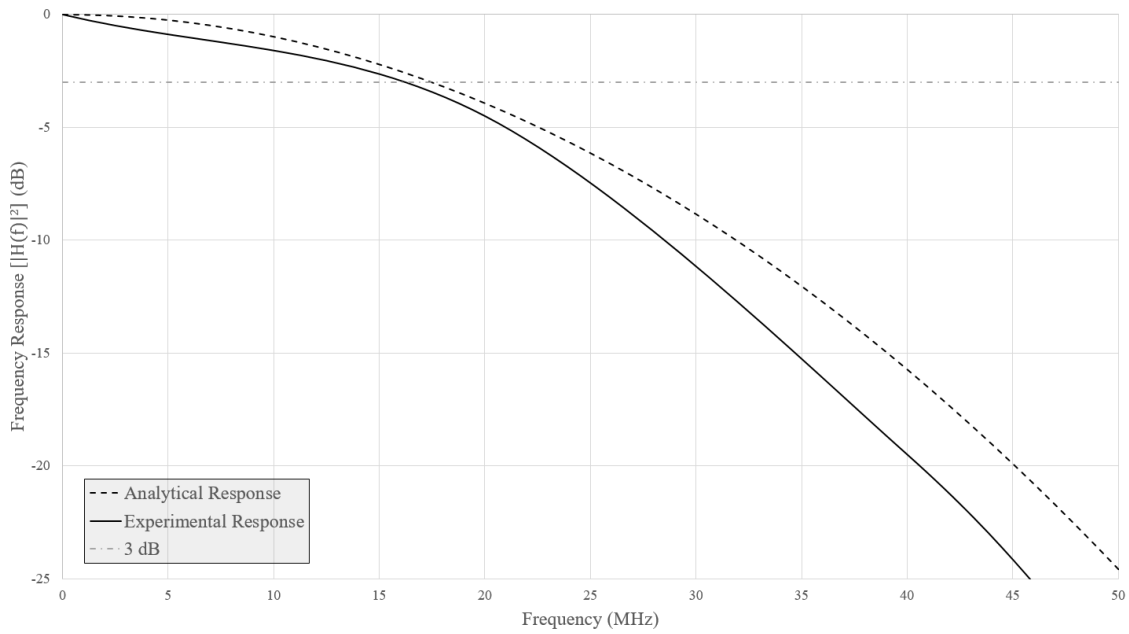


Figure 6.3: Analytical and experimental frequency response of the pc-LED after blue filtering

sponse for the investigated pc-LED are shown in Figure 6.3. The responses follow a similar pattern and do not vary significantly. Thus, this model can be used to model the frequency response of the LDs for comparison purposes, since their modulation bandwidth as reported in literature is much higher than the bandwidth of the PD, AWG and oscilloscope used for this work. The frequency response of all types of sources used for this work are summarized in Figure 6.4.

From the diagram, the blue LD has the highest bandwidth compared to all the optical sources that were utilized. GaN based blue LD exhibit high 3-dB modulation bandwidth (900 MHz - 1 GHz) [44]. The green and red LD has modulation bandwidths of ~ 780 MHz and ~ 230 MHz respectively [218, 44]. The pc-LED has a bandwidth of ~ 3 MHz and the RGB LED has a bandwidth of ~ 18 MHz [124, 158]. This model helps in visualizing the overall superiority of LDs compared to off-the-shelf LEDs as transmitters for VLC.

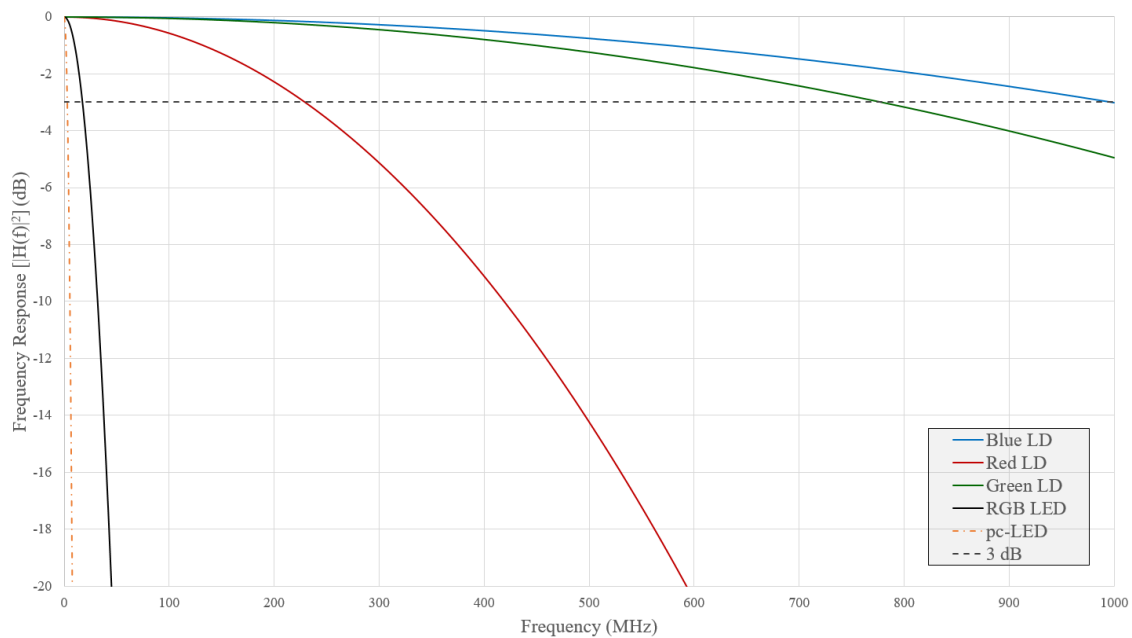


Figure 6.4: Frequency responses of blue LD (PL450B), red LD (HL63163DG), green LD (L520P120), pc-LED (Osram LCW) and RGB-LED (LED Engin RGBA)

6.3.2 Thermal Performance Characterization

A comparison of the thermal performance of LEDs and LDs used in this work under an identical experimental framework helped in determining the scopes of exclusive and/or mutual implementation of both for future SSL technologies. A visual IR thermometer (Fluke[®] VT04) was used to measure the ambient temperature of a 3.5 W single chip pc-LED (Seoul Z-LED) and a 120 mW green LD (L520P120). IR images of the sources were also captured for analyzing their heat distribution. The sources were mounted on an insulating material to minimize the effect of contact with a conducting mount. The distance from the source was fixed at 15 cm to avoid parallax error. Temperature was measured in every 10 seconds and was discontinued once it reached a stable value. Based on initial tests, it was decided that an overall period of 430 seconds was sufficient to demonstrate their difference in thermal behaviour. The sources were switched off and the decrease in temperature was also measured. The results are depicted in Figure 6.5.

As seen from the figure, the LD generates much higher amount of heat at a

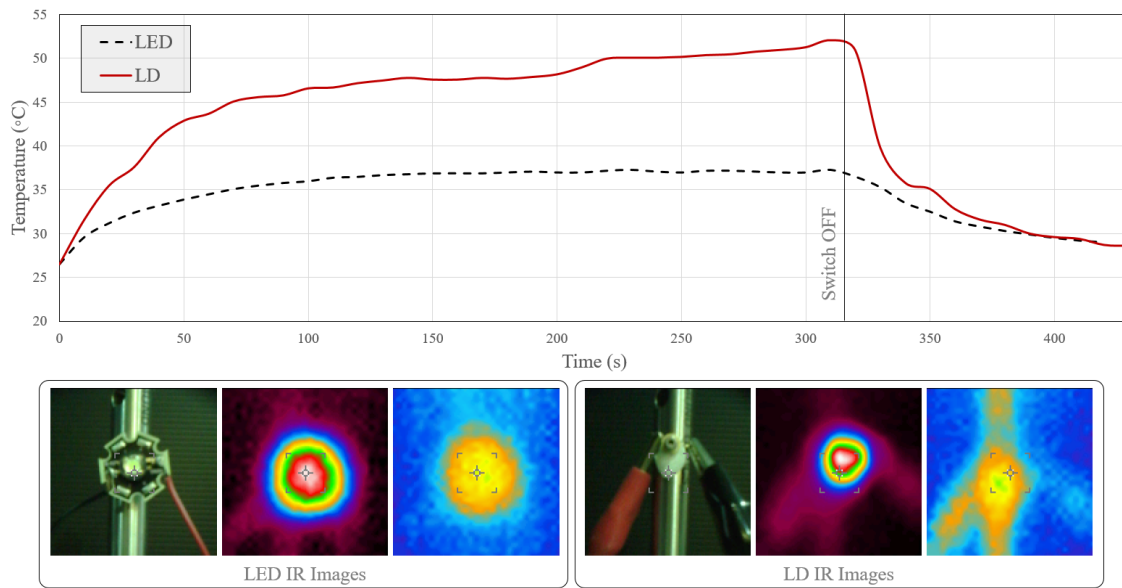


Figure 6.5: Thermal performance of pc-LED and green LD over a span 430 seconds

much greater rate compared to the LED. The temperature for the LD rises to ($\sim 50^{\circ}\text{C}$) and kept increasing by 0.3°C every 10 seconds. Since the maximum operating case temperature for the LD is rated at 60°C and the ambient temperature reaching such high values implies case temperature is more higher, it was decided to switch off the LD to prevent damaging the component. In case of the LED, the ambient temperature rises to a stable value of $\sim 30^{\circ}\text{C}$ and increases at a very slow rate of 0.1°C every 1 minute.

On switching off the sources, the rate of drop of temperature is equally higher for the LD compared to the LED. The IR images show the positioning of the sources before they were switched on and the heat distribution at maximum temperature and after being switched off. Due to the high amount of heat being generated from the LD, the surrounding mounts also gets heated as seen from the IR image, despite minimal contact with the source.

The TEC controller can regulate the case temperature and experiments were also conducted to characterize the effect of operating temperature on LVI characteristics for the LDs, based on the experimental setup depicted in Figure 5.1. This

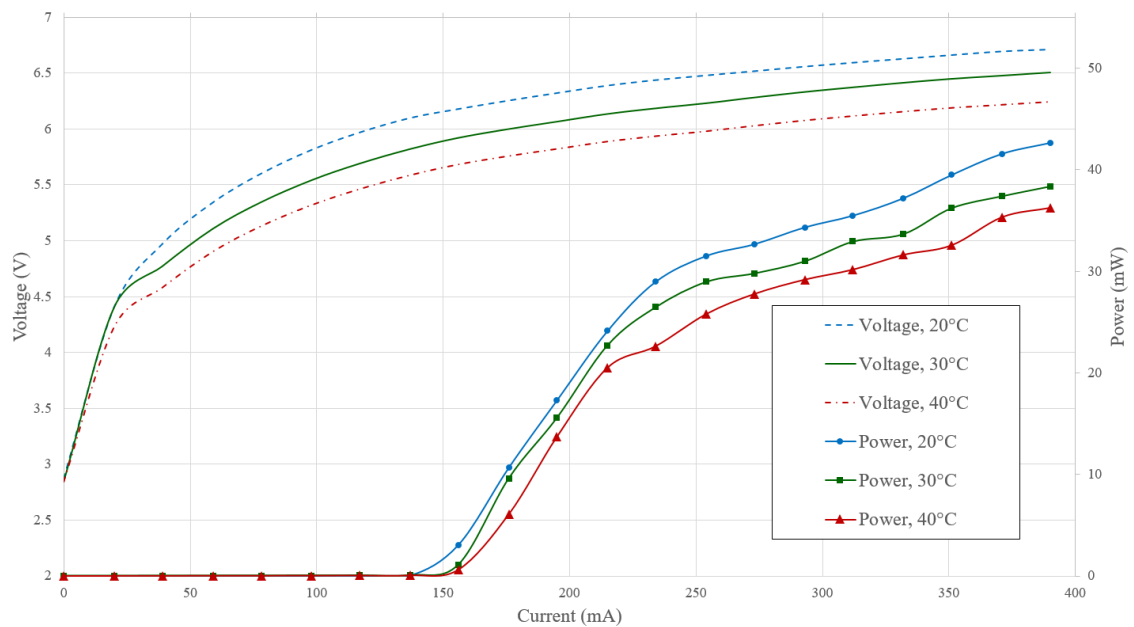


Figure 6.6: LVI responses of LD for different case temperatures

was particularly done for the LDs since the emission profile had a much stronger relation to the case temperature in comparison to LEDs. The LVI response for case temperatures of 20, 30 and 40°C are presented in Figure 6.6. The responses vary significantly for different case temperatures. The radiated power drops significantly with increasing temperature. As temperature increases, the thermal population increases at higher lasing levels, which reduces the slope efficiency thereby reducing the radiated power [229].

For WDM systems employing color mixing of multiple LDs, the radiated power needs to be highly accurate to ensure proper blending of different colors for high quality white light. Based on these experiments, it is quite clear that thermal management is a key issue concerning LDs in contrast to LEDs, which must be addressed if practical implementation is considered for various lighting and VLC based applications. At the current context, this can be resolved by guiding laser beams from hidden locations as shown in Figure 5.20. However, this problem might be solved by the rapidly evolving LD-chip manufacturing industry in the near future. Thus, the hybrid system that is investigated in the next sections do

not consider the miniaturization of the transmitters, it rather focuses on the performance associated with communication and illumination.

6.4 Photometric Aspects of Hybrid LED-LD based VLC System

The experimental setup for the hybrid VLC system is depicted in Figure 6.7. The setup is shown for a single red LD (HL63163DG). However, a combination of other laser sources were also used to change the color temperature and regulate the D_{uv} value within an acceptable range. The other sources that were utilized had already been previously used for LD-based systems and their properties are summarized in Table 5.1. A high power neutral white LED array (OSLON 150 9+ powerstar whites [230]) was used to allow the LDs to be biased at linear operating region, which helped in enhancing communication capacity. A neutral white LED was chosen to allow the regulation of CCT by introducing red and green sources. The photometric measurements were made using the CL-500A spectrophotometer. In order to ensure that the mixing was done uniformly, engineered diffusers were used. One of the key parameters that was analyzed for this work was the CRI. Since CRI was reported low for the LD-based systems developed in Chapter 5, the main objective was to increase the value of CRI by introducing an LED, which would be mainly used for illumination while the LDs are used for communication.

Three unique cases were investigated in this work:

1. Addition of a single red LD to increase overall CRI
2. Addition of two red LDs to increase CRI alongside getting warmer illumination

3. Combination of one green LD and two red LDs to have high CRI illumination and enable gigabit class communication

6.4.1 Case 1: Single Red LD-LED Hybrid System

Based on the experimental setup in Figure 6.7, the biasing current of the LD was gradually increased and the CRI was monitored. The initial CRI from the LED alone was measured to be 75. It was noticed that once the threshold current for the LD was reached, the CRI increased with the biasing current to a maximum value of 87 and then dropped drastically. The neutral white LED previously had a overall CRI (R_a) of 77. This low CRI is a common phenomena for pc-LEDs since the remote phosphor technique is inefficient in producing light output in the higher wavelength region thus giving lower values of R_9 , which inevitably reduces the value of R_a . The addition of the red LD helped in increasing the value of R_9 , which helped in an overall increase in R_a . This helps in full saturation of red objects as explained in Section 2.10.1.

The normalized SPD of the proposed hybrid system (Case 1) along with the position of the coordinates in the CIE 1931 diagram are summarized in Figure 6.8.

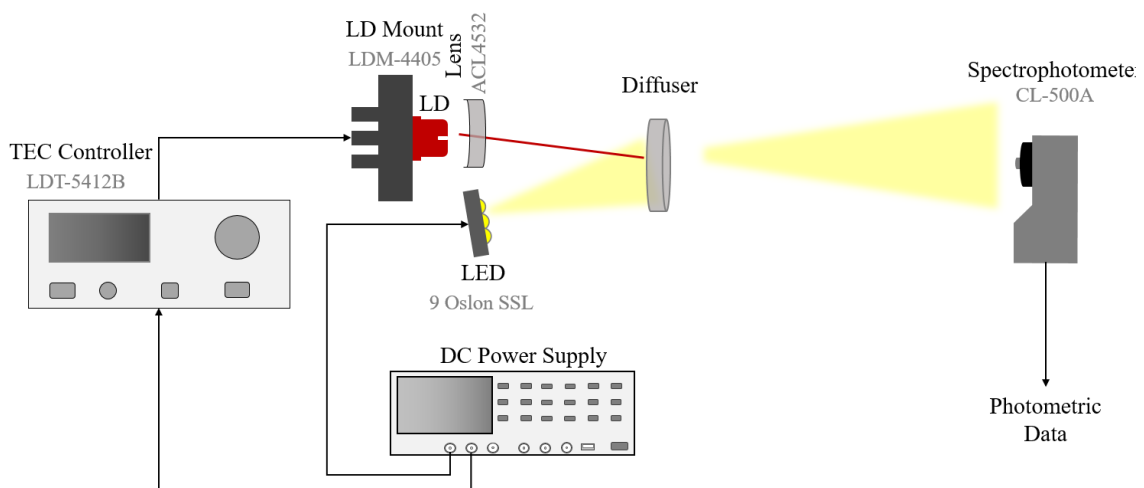


Figure 6.7: Experimental setup for measurement of illumination quality of hybrid LED-LD-based VLC utilizing a red LD and a neutral white LED array

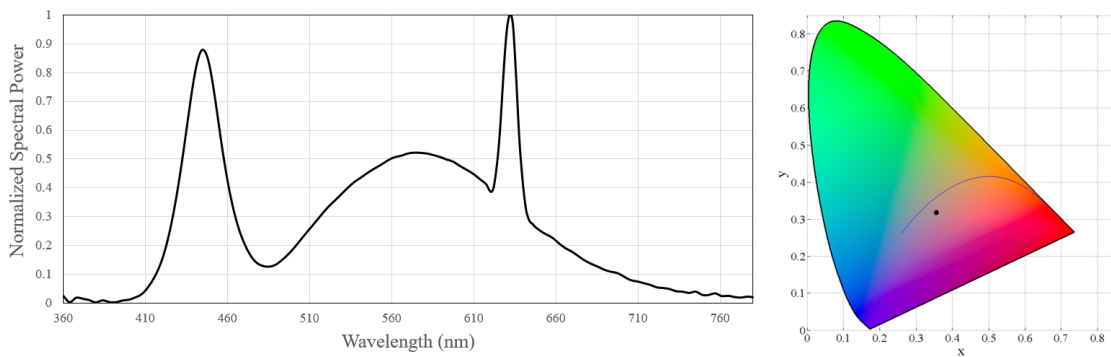


Figure 6.8: Normalized spectral power distribution of Case 1 along with the coordinates in the CIE 1931 diagram

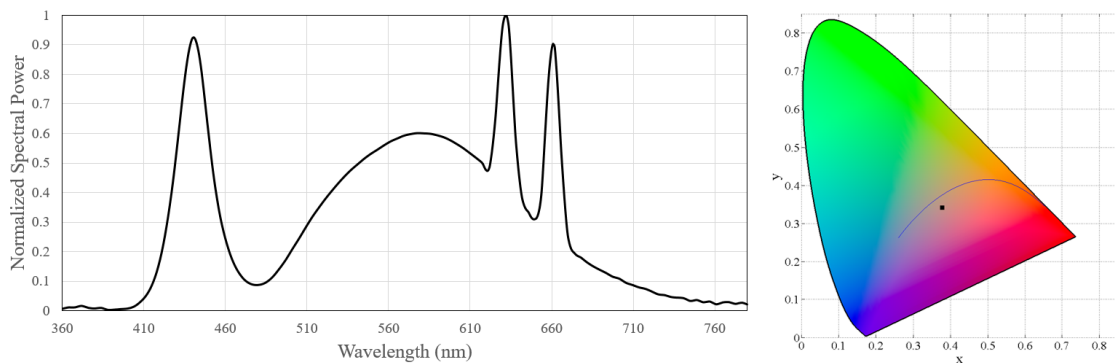


Figure 6.9: Normalized spectral power distribution of Case 2 along with the CIE 1931 diagram

The peak for the SPD occurs at 633 nm (lasing wavelength of the LD) and the rest of the distribution is similar to the SPD of a pc-LED. The CCT is ~ 4400 K with a D_{uv} of -0.022 , which implies it does not meet with the industry standards [98, 159]. The overall objective was to increase R_a and although the coordinates do not fall in line with the Blackbody locus, instead of reducing the biasing current for the red LD, which would undermine the communication capacity, it was decided to add a green LD to shift the coordinates towards the locus in order to bring the D_{uv} value within an acceptable range (Section 6.4.3). The communication aspects of this and the other hybrid systems are covered in Section 6.5.

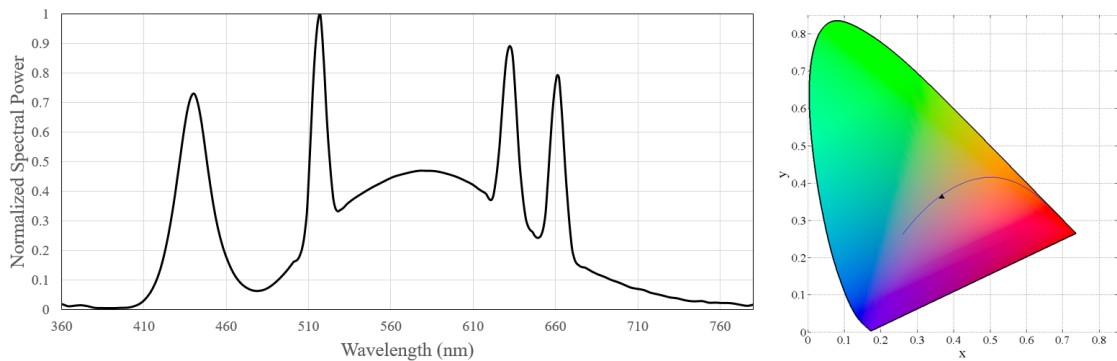


Figure 6.10: Normalized spectral power distribution of Case 3 along with the CIE 1931 diagram

6.4.2 Case 2: Multiple Red LDs-LED Hybrid System

The main motivation behind adding another red LD (HL6545MG) into the hybrid system was to counter for the higher rated radiated power output from the green LD (L520P120) as it can be seen from Table 5.1. Since the receiver limits the system bandwidth, having more sources allows for higher utilization of parallel channels giving rise to higher aggregate data rate. Besides, the Si PD has greater responsivity towards red region, which will improve link performance.

The normalized SPD along with the CIE 1931 diagram for Case 2 is presented in Figure 6.9. The SPD has a peak at 633 nm, although the darker red channel could be biased to have higher output, it was decided to maintain the biasing condition of the previous LD, which had been predominantly used in most of the LD-based experiments conducted previously that would facilitate in analytical modelling of the system. It can be seen that the point shifted towards the red region compared to the previous single LD setup. A warmer light was obtained with a CCT of ~ 3800 K with a D_{uv} of -0.017. This means that by further increasing the biasing current for the red LDs, much warmer illumination can be generated, which can fall closely within the Blackbody locus. However, in this work, the focus was operating near the neutral white region, which is the original color temperature of the LED. Thus, the unacceptable D_{uv} was regulated by adding a green LD into the hybrid system containing two red LDs, which is discussed in

the next section.

6.4.3 Case 3: Multiple LDs-LED Hybrid System

The investigations in Section 6.4.1 and 6.4.2 led to the development of this system (Case 3). Since 3 LDs were being utilized for this analysis, alignment of the sources with 3 sets of lenses and TEC mount was a challenge. The LED was placed directly in front of the diffuser, and the LDs were arranged at different heights so that they were perpendicular to the target plane. The lenses that were used for collimation (ACL4532) were used to focus the lasers onto the center of the diffuser so that the lights from the three LDs mixed uniformly with the LED. The normalized SPD for this three LD-LED-based hybrid system is shown in Figure 6.10.

The CCT of the system is ~ 4300 K, which is in the neutral white zone and is not much different from the original CCT of the LED alone (4000 K). Although, further tuning of the biasing currents of the LDs could have given a CCT nearer the original CCT, it was decided to maintain the current biasing condition, which is essential for stability of the link, which is discussed in Section 6.5. The D_{uv} was -0.002 is within the acceptable range (± 0.006). An overall CRI of 89 was recorded, which is much higher than the LED illumination alone.

6.4.4 Overall Comparison

The photometric results of different configurations of hybrid system are summarized in Table 6.1. Figure 6.11 presents the CRI of individual color samples along with the overall CRI for pc-LED and the three cases that were investigated. The normalized SPDs for the cases are also presented. The CRI is seen to improve tremendously for hybrid systems compared to LED standalone system. This happens due to increase of CRI for red color ($R9$). The D_{uv} for Case 3 falls

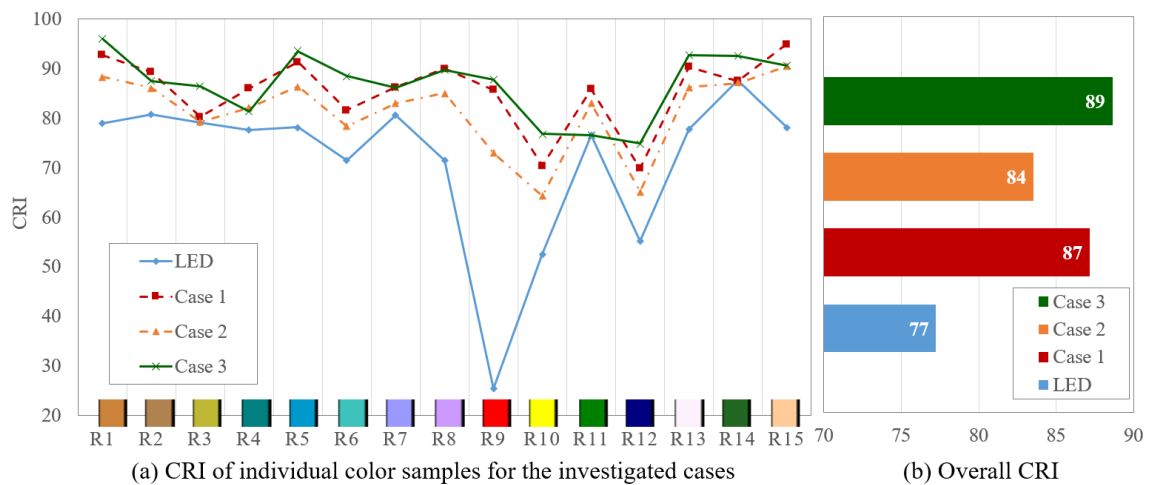


Figure 6.11: a) CRI of individual colors for the three cases (b) Overall CRI of the investigated cases

Table 6.1: Comparison of photometric parameters for different investigated cases of hybrid LED-LD-based VLC system

Parameter	Standalone		Hybrid	
	LED	Case 1	Case 2	Case 3
E (lux)	500	587	628	713
x_c, y_c	0.355, 0.335	0.0244, 0.318	0.377, 0.342	0.367, 0.363
CCT (K)	4569	4411	3790	4287
D_{uv}	-0.002	-0.022	-0.017	-0.002
u', v'	0.224, 0.477	0.232, 0.469	0.238, 0.485	0.222, 0.494
CRI (R_a)	77	87	84	89
$R9$	25	86	73	88

within the acceptable range, although there is a slight decrease in CCT. The overall illuminance (E) is the highest for Case 3 since three optical sources are being simultaneously utilized besides the LED. This means that the link distance for this hybrid system can be increased although the effect on other channels need to be experimentally characterized.

6.5 Communication Aspects of Hybrid LED-LD-based VLC System

6.5.1 Experimental Analysis

The experimental setup for the hybrid VLC system consisting of a single red LD along with a neutral white LED array is presented in Figure 6.12. The LED is used only for illumination purposes. This is because LEDs can provide a maximum data rate of ~ 20 Mb/s. Thus, the increase in data rate is not significant compared to the baseband operation of the red LD at 150 Mb/s. A narrowband red optical filter (BrightLine[®] 642/10 nm) was used at the receiver to filter out the red component of the diffused light. This helped in reducing shot noise and provided an acceptable BER at a distance of 1 m. Since there was a single PD that could be utilized, for each of the investigated cases (Section 6.4.1 - 6.4.3), a single channel was modulated while the other optical sources were kept on. The oscilloscope was used to obtain the eye diagram, which was then used to calculate the BER using eq. 3.1.

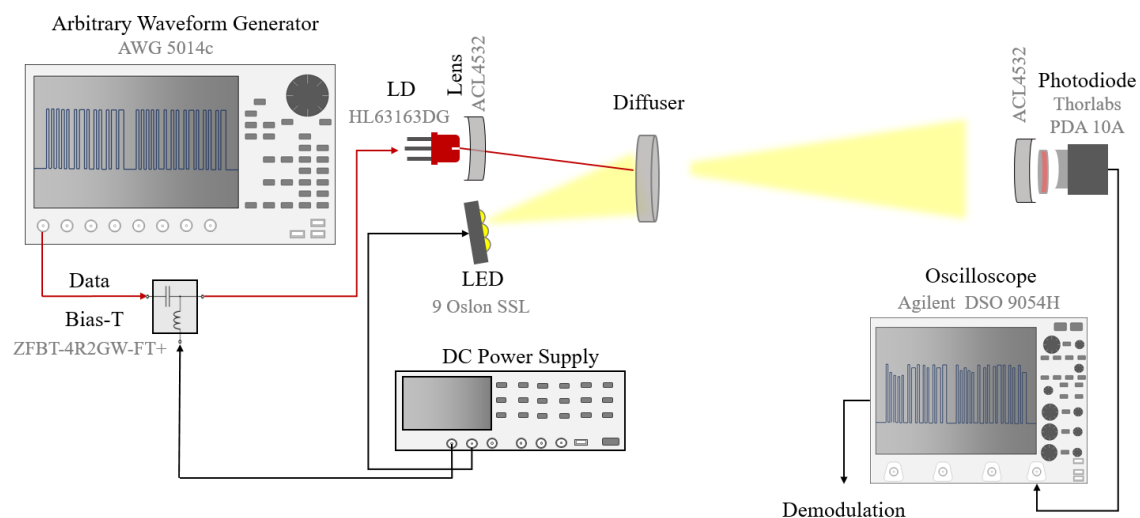


Figure 6.12: Experimental setup of hybrid LED-LD-based VLC utilizing a red LD, which is directly modulated along with a neutral white LED array used for communication exclusively

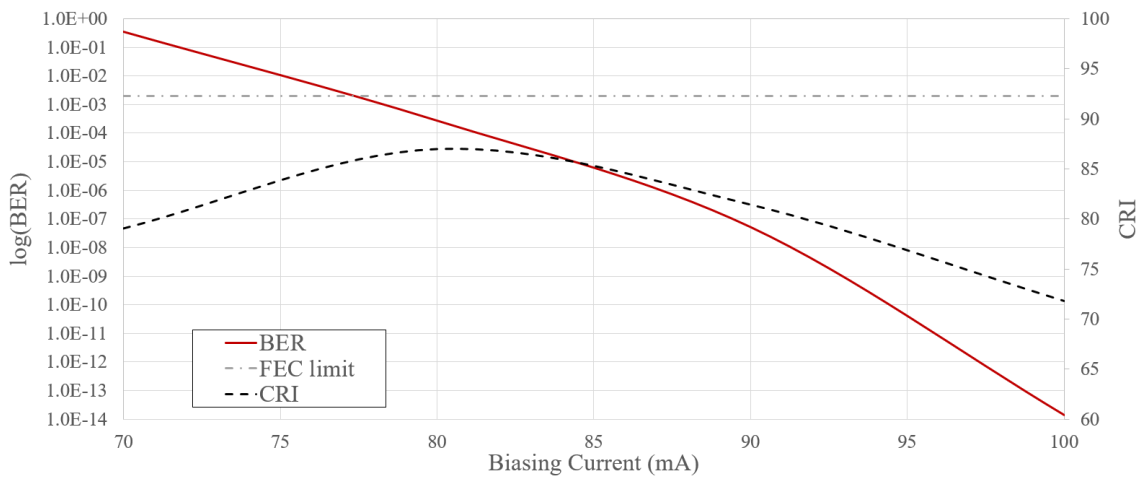


Figure 6.13: BER and CRI distribution for case 1

It was necessary to characterize the link to obtain the ideal biasing condition, which will provide high CRI alongside a BER within the FEC limits. Thus the analytical model developed in Section 5.5 was used to compute the BER for different values of investigated biasing currents by referring back to the LVI characterization done in Section 5.2. Since the same optical filter was being used for the hybrid system, the filter coefficients practically eliminates the shot noise from the LED lighting in an identical manner, which allowed us to utilize the same analytical model.

For Case 1, the BER and the CRI distribution as a function of forward current through the LD is presented in Figure 6.13. The threshold current for the LD was ~ 70 mA, hence the BER remains very high for lower biasing currents. It drops below the FEC limit at ~ 77 mA and keeps decreasing. It can be seen that the CRI peaks at around 78 mA based on the results presented in Section 6.4.1. Thus the optimum biasing current for the link is 78 mA, where the BER is within the FEC limit and the CRI is much higher than the standalone LED system.

For Case 2, both the sources have similar current and voltage ratings except for the lasing wavelength, which led to an ideal BER distribution for the darker red source (HL6545MG) as presented in Figure 6.13. Thus in order to ensure both the LDs were operating in their linear region, the forward current for the LED was

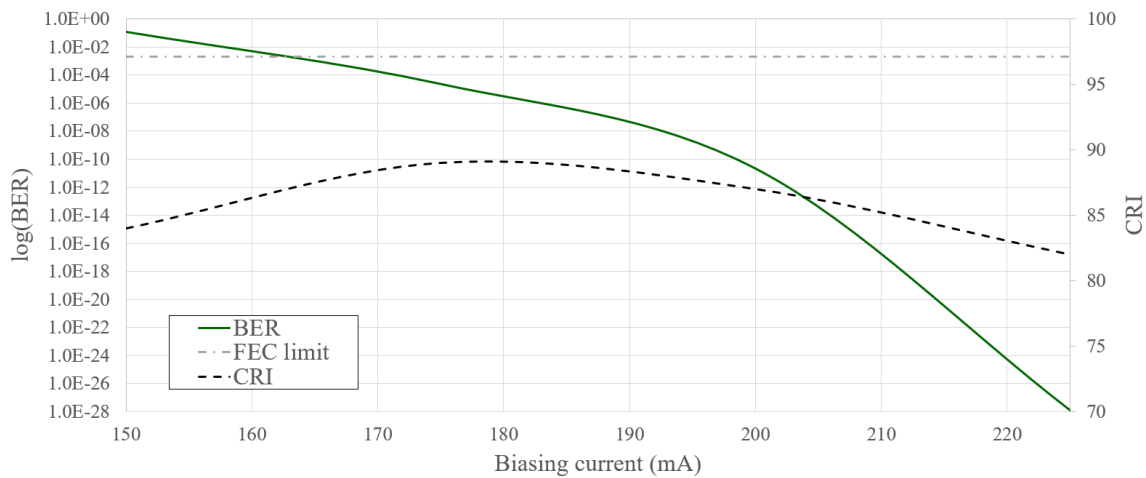


Figure 6.14: BER and CRI distribution for case 3

increased from 0.5 A to 0.65 A, which compensated the addition of a red source. The simultaneous modulation of the two red sources gave higher BER since there was shot noise present from both sources operating at close proximity in terms of wavelength. Although narrowband optical filters can solve this problem, there is still significant interference leading to higher BER. But the advantage in terms of gain in communication capacity due to two red channels operating in parallel and the higher responsivity of the Si-PIN photodiode towards red sources was noteworthy.

For Case 3 consisting of three LDs along with the pc-LED, the green LD had to be operated well above the threshold current, since it had to compensate for the downward shift of the chromaticity coordinates due to the operation of two red sources. The BER and CRI distribution for this scenario is presented in Figure 6.14. The BER has a lower distribution compared to the red channel, this is because the green LD has higher radiated power (Figure 5.2) for the given biasing condition. The CRI is much higher than the standalone system for the entire chosen biasing range, which means that the main objective of increasing CRI was fulfilled. The biasing condition for the green channel is thus 200 mA.

Based on the identified biasing conditions and the experimental setup depicted in Figure 6.12, an investigation was conducted to identify the maximum

Table 6.2: Comparison of parameters concerning communication for different scenarios of hybrid LED-LD-based VLC system

Parameter	Standalone		Hybrid	
	LED	Case 1	Case 2	Case 3
I_{bias} (mA)	500	78	80, 78	80, 78, 200
P_t (mW)	10,500	4.31	4.35, 4.28	4.35, 4.28, 17.297
BER (analytical)	N/A	2.7×10^{-4}	2.7×10^{-4}	2.7×10^{-4} , 2.13×10^{-11}
BER (experimental)	N/A	4.9×10^{-3}	3.8×10^{-4}	7.9×10^{-4} , 4.2×10^{-3} , 6.3×10^{-4}
Data Rate (Mb/s) (experimental)	18 Mb/s	160	320	490

possible data rate practically achievable. These results are summarized in Table 6.2. The LED standalone system is mentioned as a reference. The analytical BER for one and two LD based hybrid system is equal. The narrow filter integral for both is approximately same, hence, the same theoretical equations were used for calculating their BER for simplicity. The experimental BER being derived from Q-factor of the eye diagram tends to be higher in some cases than the theoretical values, since it depends on the quality of the eye diagram, which remained similar for most of the scenarios. Based on the results presented in Section 5.7, the red and green LDs were modulated at maximum transmission rates and the maximum speed achieved from the red channel was 160 Mb/s whereas the green channel could operate at 170 Mb/s. Thus, the aggregate data rate for the three source hybrid system was 490 Mb/s. This data rate is much higher than the 20 Mb/s speed of the standalone LED system, which proves the effectiveness of incorporating LDs as optical transmitters for hybrid systems. The hybrid system outperforms LD-based and LED-based VLC system when communication and illumination are mutually considered. But since the achievable data rate is limited by the photodiode, it was decided to simulate the system for obtaining the maximum achievable data rate.

6.5.2 Simulation Results

The simulation framework in this work is based on the work done in Section 4.4 and Section 5.4. Since the LED was left unmodulated and narrow band filters were utilized at the receiver, the interference from the other channels were negligible. The main reason behind using the simulation framework was to investigate the performance of the proposed system when a faster photodiode is being used. Since, the LDs were being operated almost at their optimum biasing current, the maximum achievable data rates were similar to Section 5.4. The results are summarized in Table 6.3. Based on the simulation results, using case 1 provides a data rate of 240 Mb/s, case 2 provides a data rate of 480 Mb/s and case 3 provides an aggregate data rate of 1.26 Gb/s.

Table 6.3: Simulation of different configurations of hybrid LED-LD-based VLC system

Parameter	Standalone		Hybrid	
	LED	Case 1	Case 2	Case 3
I_{bias} (mA)	500	78	80, 78	80, 78, 200
P_t (mW)	10,500	30	35, 32	35, 32, 75
BER (simulation)	N/A	2.5×10^{-5}	$1.8 \times 10^{-5}, 3.6 \times 10^{-3}$	$1.8 \times 10^{-5}, 3.6 \times 10^{-3}, 7.2 \times 10^{-7}$
Data Rate (Mb/s) (simulation)	N/A	240	480	1260

Based on the analytical, experimental and simulation based results of parameters associated with communication and illumination, it is clearly evident that hybrid LED-LD systems can offer gigabit class communication alongside high quality illumination. The balance between the two main functionalities of VLC, which was lacking in the systems developed in the previous chapters can be restored by this hybrid approach. However, there are certain challenges associated with the miniaturization of the sources and beam alignment, which need to be resolved for practical adaptation.

6.6 Conclusion

In this chapter, the observations made from all the previous chapters were combined to capitalize on the limitations of each sources in order to develop a hybrid system. This approach had been overlooked in most of the work, but considering practical adaptability, combining laser diodes into a LED luminaire to enable Li-Fi access points operating beyond gigabit class range is much more feasible than acquiring a LD based system. The only challenge for such a hybrid system is design of the luminaire where the thermal management is taken care of. The major observations that were made in this work are:

- Gaussian low pass filter modelling allows for accurate interpretation of frequency response of high speed sources, which could not be measured experimentally
- Blue LDs have the highest 3 dB bandwidth compared to all the other sources that were used in this thesis
- Thermal management is a key issue concerning LDs unlike LEDs
- Addition of a red LD to a pc-LED significantly increases the value of R_a , which works on the principle of red enhanced LED lights
- Although addition of red LD decreases the color temperature, this can be countered by adding multiple LDs into the system
- The highest recorded CRI of 89 was obtained from a setup having 3 LDs and 1 pc-LED
- An experimental data rate of 490 Mb/s was achieved by the hybrid system in comparison to the standalone LED system achieving a data rate of 10 Mb/s

- In simulation, the maximum achievable data rate of the proposed hybrid system was 1.26 Gb/s

The observations helped in answering the issues raised in research question 9 in Section 2.11. The proposed hybrid system gave a balanced performance of superior illumination quality alongside high speed communication. The demonstrated CRI of 89 is much higher when LDs and LEDs are considered separately, which demonstrated CRIs of 35 and 77 respectively. The maximum achievable data rate of the proposed system is 1.26 Gb/s, which is much higher when standalone LED systems operating at 20 Mb/s are considered. In comparison to the RRGB system proposed earlier, where a data rate of 2.24 Gb/s was achieved, this system does not significantly hamper the transmission capacity in contrast to the increase in CRI observed. The data rate can be even further increased by utilizing spectrally efficient OFDM modulation schemes. This concept of consolidation of sources of different characteristics has several challenges. The main challenge will be the miniaturization of multiple sources to account for thermal management and fit into a luminaire, which can be plugged in into lighting infrastructures. This chapter helped in quantifying the key differences between all the sources used in this thesis, which helped in identifying their limitations for practical adaptation considering different scenarios. The next chapter summarizes the key contributions that were made at each chapter and the future work that can be undertaken building upon the progress made in this work.

CONCLUSION

7.1 Looking Back

In the last two decades, the unprecedented growth of wireless communication systems along with their increasing demands on wireless data traffic is restraining the availability of the limited and expensive radio RF spectrum, which is driving the needs for complementary wireless transmission techniques. This gave rise to VLC, an emerging technology in the field of wireless communication, which concurrently provides communication alongside illumination and can be incorporated into existing lighting infrastructures as a complementary functionality. VLC utilizes a light source as its transmitter, where information is modulated into the intensity of the emitted light. The frequency of the modulating signal is kept high enough (typically above 300 Hz) so that occupants assume the source to be normally lit.

Because of the growing trend towards replacement of traditional lighting infrastructures with SSL, most of the VLC systems till date had considered LEDs as transmitters because of their superior switching capabilities compared to traditional incandescent and fluorescent sources. VLC systems utilizing LEDs generally use single chip or multi-chip approach, which assign pc-LEDs or RGB LEDs as sources respectively. However, for communication at much higher speeds (gigabit class range), the modulation bandwidth of these LEDs ranging around 20

MHz is still considered to be quite low. In such cases, LDs can be utilized, which have much higher direct modulation speeds, making them a better candidate for front-end transmitters, when communication is required at much higher speeds. In this thesis, these three sources were considered for VLC by simultaneous consideration of important parameters associated with illumination and communication.

7.2 Overview of Thesis

Chapter 2 presented a comprehensive review of literature associated with LED and LD based VLC systems. The factors associated with simultaneous illumination and communication were analyzed, which led to the consideration of dimming and adaptive schemes that can provide concurrent data transmission under intensity regulation. From the review, it was observed that for white LEDs, most of the work associated with dimming overlooked important photometric aspects such as linearity of illuminance, chromaticity shift and dimming precision, when pulse regulated schemes (FM and PWM), analog scheme (CCR) and adaptive schemes (SU and RA) are considered. These raised the following research questions:

1. How does FM perform compared to PWM when photometric parameters such as CRI, CCT and linearity of illuminance are being considered?
2. How much chromaticity shift is induced when CCR and PWM are implemented in a VLC system?
3. How does transmission of bits when the duty cycle is low in slot utilization affect the overall illuminance and does it hamper the dimming precision?
4. Can different adaptive schemes be simultaneously utilized to subdue the

stringent requirement on either of them enabling dimming with better performance in terms of communication?

Apart from providing higher data rates by WDM, in comparison to pc-LEDs, RGB LEDs can allow control of CCT besides illuminance, which can provide application specific solutions. It was observed that although the effect of color temperature on the channel capacity was theoretically analysed, adaptive schemes for channel biasing under different CCTs had not been considered. It was noted that a lot of VLC systems were moving towards LDs for higher data rates, however, most of the systems did not provide white lighting with practical CCT and CRI. The review identified key issues regarding speckle pattern, low CRI, lack of human perception investigation, hybrid link configurations, which raised several questions like:

5. Can adaptive dimming schemes be implemented for regulating the CCT of RGB LED-based VLC systems for maintaining the data rate and the BER of the system at acceptable limits?
6. Can adaptive dimming schemes be implemented for regulating the blue and green channels to generate light within the usable CCT range and safety standards for RGB LD-based VLC systems?
7. Can easily incorporable vibrating diffuser mitigate speckles in the white light generated from a LD-based VLC system?
8. How is the human perception of LD-based lighting in comparison to LED-based lighting in terms of overall preference, contrast, saturation, visual comfort, naturalness of colors and pleasantness?
9. Is it possible to employ red enhancement to obtain a high value for CRI for LD and pc-LED based lighting system?

Chapter 3 investigated the effect of general dimming schemes by considering all the parameters associated with photometry and communication. Initial investigations with pulse regulated schemes revealed that PWM can be used for the entire range of the dimming target unlike other FM schemes and achieves lower variation in CCT, which answered research question 1. The same experimental framework was then used to evaluate the performance of PWM and CCR; it was observed that CCR scheme caused higher chromaticity shifts and non-linear dimming, which justified the use of PWM. This helped in answering the issues raised in research question 2. However, data rate was compromised, when VLC data was incorporated with PWM dimming signal, thus SU and RA adaptive schemes were developed on the basis of simulated systems demonstrated in literature and was investigated on the basis of practical experiments, simulations and in theory. SU hampered the dimming precision and RA had limitations due to the limited modulation bandwidth of the LEDs. Thus, a dimming algorithm was proposed, which utilized either of the adaptive schemes depending on the dimming target and achieved a constant data rate of 10 Mb/s with a BER below the FEC limit for the entire range of dimming target. The proposed algorithm outperformed the exclusive implementation of either of the adaptive schemes, which answered research question 4.

Chapter 4 moved towards utilizing RGB LEDs for increasing the aggregate data rate of the system from 10 Mb/s to 45 Mb/s. However, instead of fixating on dimming, which can be achieved by simultaneous control of biasing current for each channel, the focus was moved towards the CCT regulation that can cater to unique applications. An analytical model was developed, which helped in identifying the optimum biasing current required for generating white light at different CCTs. It was observed that the biasing requirement for the blue channel in particular hampered the achievable data rate, due to low SNR at the receiver. Thus, adaptive schemes were evaluated for regulating the CCT to generate warm-

white, neutral-white and cool-white lighting. Given the biasing circumstances and bandwidth limitations, SU scheme outperformed all the other schemes and sustained the target data rate of 45 Mb/s in comparison to 31.5 Mb/s, which was achieved by PWM. Thus, compared to the traditionally used CCR, SU adaptive scheme achieves superior CCT regulation, which answered research question 5.

Chapter 5 adapted the concept of integration of adaptive dimming schemes for CCT regulation in LD-based VLC system. There were a number of challenges regarding thermal management and speckle pattern that were addressed moving from LEDs to LDs. A vibrating module was designed which helped in reducing speckle contrast ratio by 68 %, which answered research question 7. It was noticed that CCT regulation substantially reduced the achievable data rate from 2.01 Gb/s to 1.16 Gb/s. Thus, a RRGB based link configuration was proposed, which capitalized on the narrow emission profile of the LDs and achieved CCT regulation for the entire range with even a higher aggregate data rate of 2.24 Gb/s that answered research question 6. The LD-based VLC system was also validated based on the perception evaluation of 42 human observers, which helped in answering several queries raised in research question 8. Statistically significant preference of 78 % for LDs over LEDs was observed, which was a testament to the compilation of various system level modifications and schemes that were proposed in this work.

Chapter 6 made a correlation between all the sources that were used in the previous chapters and thus provided a quantitative evaluation of the features and lacking of each transmitter. A low pass filter modelling technique was used to emulate the frequency response of the LEDs and LDs, which closely matched with experimental measurements. Pc-LEDs were combined with LDs and evaluated in terms of CRI and achievable data rate at acceptable BER. The LDs helped in enhancing the colors of illuminated objects at higher wavelengths, which used a similar concept to the red enhanced LED-based lighting but in turn provided

gigabit class data rates that answered research question 9. The CRI was increased from 77 to 89 and the data rate was increased from 20 Mb/s to 1.2 Gb/s by the proposed hybrid system consisting of three LDs and a single pc-LED array.

The key outcomes from each chapter are summarized in Table 7.1. The '✓' indicates the parameters that were considered and the schemes that were investigated. Looking back, initially a dimmable VLC system utilizing a pc-LED was developed, which could maintain a data rate of 10 Mb/s at a CRI of 77 by utilizing adaptive schemes. These schemes were then applied into a WDM based RGB-LED-VLC system for CCT regulation at a range of 2700 K - 6500 K, while maintaining an increased data rate of 45 Mb/s and a moderate CRI of 48. CCT regulation and unique link configuration assessment of LDs helped in providing a data rate of 2.24 Gb/s but a low CRI of 35. By combining both the sources to form a hybrid system, a balanced data rate of 1.16 Gb/s, which was in the gigabit class range was reached, while achieving a much higher CRI of 89.

From an overall perspective, it can be concluded that the prospects of VLC

Table 7.1: Overall summary of key outcomes and investigated parameters

Parameters	pc-LED (Chapter 3)	RGB-LED (Chapter 4)	RGB-LD (Chapter 5)	Hybrid (Chapter 6)
Data Rate (Mb/s)	10 Mb/s	45 Mb/s	2.24 Gb/s	1.16 Gb/s
BER	✓	✓	✓	✓
Received Power (mW)	✓	✓	✓	✓
SNR	✓	✓	✓	✓
Channel Gain	✓	✓	✓	✓
Illuminance (lux)	Regulated	✓	✓	✓
CCT (K)	✓	Regulated	Regulated	✓
CRI	77	48	35	89
D_{uv}		✓	✓	✓
Speckle contrast ratio			✓	✓
PWM	✓	✓	✓	✓
CCR	✓	✓	✓	✓
SU	✓	✓	✓	✓
RA	✓			
Transmitter configuration	N/A		✓	✓

is promising and the limitations in transmission capacity imposed by LEDs can be effectively resolved by LDs. Pc-LEDs can provide communication for various applications enabling IoT services requiring low data rates for connectivity and localisation purposes. RGB-LEDs can provide higher data rates and controllability features, which can be used in smart homes for mood based lighting and Li-Fi access points. LDs can provide much higher speeds for demanding applications, which can justify its higher cost. The CRI of LD-based lighting can be expected to increase, when there are commercially available LDs operating in all the regions of the visible spectrum, until then, hybrid LED-LD systems can provide gigabit class communication alongside high quality illumination.

7.3 Future Work

This section outlines the future work that can be pursued from the findings in this thesis.

7.3.1 Development of High Speed Dimmable VLC Driver

In this work, the experimental setup used to implement the dimming schemes on the transmitter side had a AWG connected to a bias-T. However, for practical VLC systems, high speed driver circuitry needs to be developed, which is compact enough for fitting into system-on-chip lighting modules [231]. Low power CMOS technology was used to produce system-on-chip LED drivers, which allowed flicker free lighting with a wide dimming range for VLC system [207]. There are various constraints that require consideration before the high frequency VLC signal can be applied into the driver circuit. For feedback loop stability, the power supply switching frequency must be lower than the DC-DC converter resonant frequency. As a result, the resonant frequency of the DC-DC converter limits the bandwidth of the feedback loop, which in turn limits the transmission

rate of the VLC transmitters [23]. Thus integrating CMOS electronics to enable the implementation of the proposed dimming algorithm into on chip system is an promising area, which requires attention.

7.3.2 Implementation of Adaptive Schemes for RGBA LED-VLC System

In recent times, RGBA LEDs which consist of an additional amber channel are becoming increasingly popular for use in VLC due to their superior photometric performance and higher parallel channel capacity [40, 232, 233]. Although, the color temperature regulation in this work was achieved for a RGB LED mainly considering the popularity of RGB sources over RGBA sources, the consideration of RGBA systems can alleviate the stringent requirement on the blue channel thus leading to CCR scheme being sufficient for CCT regulation.

7.3.3 Incorporating other Modulation Schemes for the Dimming Algorithm

In this work, NRZ-OOK modulation scheme was mainly considered due to its versatility and power efficiency. However, as discussed in Section 2.5, there are plenty of other schemes, which can be used for VLC. Spectrally efficient schemes like OFDM can provide higher data rates and capitalize on the limited modulation bandwidth of LEDs [234]. Although different modifications to OFDM had been proposed to allow concurrent dimming such as reversing the polarity of transmitted symbols [235], there are inherent complications regarding low PWM line rate, which needs to be accounted for OFDM [36]. The combination of OFDM with PWM dimming signal had already been demonstrated in many works [28, 236, 237]. Thus, the dimming algorithm proposed in this work can be extended to consider OFDM modulation since it is built upon the basis of PWM dimming

to enable transmission at higher speeds.

7.3.4 Addition of Amber LD for Higher CRI

As discussed earlier, addition of amber sources for RGB systems generally tend to show an increase in CRI due to higher spectral continuity in the SPD. Although the pioneering work done by Neumann *et al.* in [66] utilized a yellow LD besides the RGB sources, the impact of yellow LD onto the CRI was not characterized. However, LDs operating in that region of wavelength is unavailable commercially, which was the main reason the RAGB LD system was not analyzed in this work. The low CRI of LD-based system, which led to the development of the hybrid system in this work can be increased by adding an amber LD into the system. This might lead to a LD-based system having superior color rendering capabilities, which may avoid the complications of designing a hybrid LED-LD VLC system.

7.3.5 Consideration of Color Blindness when Conducting Psychophysical Tests

Although, most of the people share a common color vision sensory experience, there are some for whom the perception of colors is different than the general trend. Color vision deficiency affects quite a considerable number of people. Although in this work, Ishihara test was conducted to ensure all the participants had normal color vision; given the noticeable number of color vision impaired people, the consideration of color blind population for all aspects of acceptable CCT ranges, psychophysical evaluation, photometric tests can lead to a more thorough analysis of this work.

7.3.6 Miniaturization of LD-based Transmitter System for Practical Adaptability

The LD-based transmitter front end used for experimental analysis had a lot of optical front end components (lens, diffuser, optical post and mounts) and TEC mounts, which needs to fit into a compact space when practical transmission systems are considered. Although, the main approach taken in this work was based on the concept presented in [57] where it was suggested the laser sources can be placed at hidden location where thermal management can be handled and lasers can be guided by fibers, this still falls short of the versatility and ease of deployment of LEDs. However, the LD manufacturing is a rapidly maturing industry, with chip development constantly evolving that is enabling reduction in cost and heat generation [46]. If LDs with superior heat dissipation capabilities are developed in the future, the LD-based systems investigated in this work can be minimized to fit into a compact space, which can lead to commercially competent lighting and communication device.

Bibliography

- [1] "The 50 best inventions," 2011. [Online]. Available: <http://content.time.com/time/magazine/article/0,9171,2099708,00.html>
- [2] "Wireless data from every light bulb," 2011. [Online]. Available: https://www.ted.com/talks/harald_haas_wireless_data_from_every_light_bulb
- [3] "Li-fi 100 times faster than wi-fi," 2015. [Online]. Available: <http://www.bbc.com/news/technology-34942685>
- [4] H. Haas, L. Yin, Y. Wang, and C. Chen, "What is lifi?" *Journal of Lightwave Technology*, vol. 34, no. 6, pp. 1533–1544, 2016.
- [5] A. G. Bell, W. G. Adams, Tyndall, and W. H. Preece, "Discussion on the photophone and the conversion of radiant energy into sound," *Journal of the Society of Telegraph Engineers*, vol. 9, no. 34, pp. 375–383, 1880.
- [6] D. Jackson, T. Buffaloe, and S. Leeb, "Fiat lux: a fluorescent lamp digital transceiver," *IEEE Transactions on Industry Applications*, vol. 34, no. 3, pp. 625–630, 1998.
- [7] K. Kulhavy, "Home:ronja," RONJA, 2012. [Online]. Available: <http://ronja.twibright.com/>
- [8] Y. Tanaka, S. Haruyama, and M. Nakagawa, "Wireless optical transmissions with white colored led for wireless home links," in *11th IEEE International Symposium on Personal, Indoor and Mobile Radio Communications (PIMRC 2000)*, vol. 2, London, UK, 2000, pp. 1325–1329.
- [9] VLCC, "Visible light communications consortium," 2007. [Online]. Available: <http://www.vlcc.net/modules/xpage1/>
- [10] *Short-Range Wireless Optical Communication Using Visible Light*, IEEE Standard for Local and Metropolitan Area Networks–Part 15.7 Std., 2011.
- [11] "Cisco visual networking index: Global mobile data traffic forecast update, 2016-2021," Cisco, Tech. Rep., 2017. [Online]. Available:

- <https://www.cisco.com/c/en/us/solutions/collateral/service-provider/visual-networking-index-vni/mobile-white-paper-c11-520862.pdf>
- [12] "Cisco visual networking index: Global mobile data traffic forecast update, 2013-2018," Cisco, Tech. Rep., 2014. [Online]. Available: <https://blog.acens.com/wp-content/images/cisco-global-mobile-data-2013%E2%80%932018-blog-acens.pdf>
- [13] J. Luo, L. Fan, and H. Li, "Indoor positioning systems based on visible light communication: State of the art," *IEEE Communications Surveys Tutorials*, vol. 19, no. 4, pp. 2871–2893, 2017.
- [14] H. Baldwin, "Wireless bandwidth: Are we running out of room?" 2012. [Online]. Available: <http://www.computerworld.com/s/article/9223670/Wireless-bandwidth-Are-we-running-out-of-room->
- [15] C. Jastrow, K. Munter, R. Piesiewicz, T. Kurner, M. Koch, and T. Kleine-Ostmann, "300 ghz transmission system," *Electronics Letters*, vol. 44, no. 3, pp. 213–214, 2008.
- [16] I. Hosako, N. Sekine, M. Patrashin, S. Saito, K. Fukunaga, Y. Kasai, P. Baron, T. Seta, J. Mendrok, and S. Ochiai, "At the dawn of a new era in terahertz technology," *Proceedings of the IEEE*, vol. 95, no. 8, pp. 1611–1623, 2007.
- [17] S. M. Kim and S. M. Kim, "Performance improvement of visible light communications using optical beamforming," in *Fifth International Conference on Ubiquitous and Future Networks (ICUFN)*, Da Nang, Vietnam, 2013, pp. 362–365.
- [18] H. Ma, L. Lampe, and S. Hranilovic, "Hybrid visible light and power line communication for indoor multiuser downlink," *IEEE/OSA Journal of Optical Communications and Networking*, vol. 9, no. 8, pp. 635–647, 2017.
- [19] J. Penning, S. Schober, K. Stober, and M. Yamada, "Adoption of light-emitting diodes in common lighting applications," U.S. Department of Energy, Tech. Rep., 2017. [Online]. Available: https://energy.gov/sites/prod/files/2017/08/f35/led-adoption-jul2017_0.pdf
- [20] T. Baumgartner, F. Wunderlich, A. Jaunich, T. Sato, and G. Bundy, "Lighting the way: Perspectives on the global lighting market," McKinsey & Company, Tech. Rep., 2012. [Online]. Available: <http://www.ledsmagazine.com/articles/2011/08/mckinsey-releases-lighting-market-report.html>
- [21] "Diode laser lighting could compete with led, research suggests," 2011. [Online]. Available: http://www.huffingtonpost.com/2011/11/12/diode-laser-lights_n.1088545.html
- [22] Z. Ghassemlooy, W. Popoola, and S. Rajbhandari, *Optical Wireless Communications: System and Channel Modelling with MATLAB*, 1st ed. Boca Raton, FL, USA: CRC Press, Inc., 2012.

- [23] F. Zafar, D. Karunatilaka, and R. Parthiban, "Dimming schemes for visible light communication: the state of research," *IEEE Wireless Communications*, vol. 22, no. 2, pp. 29–35, 2015.
- [24] S. Wu, H. Wang, and C. H. Youn, "Visible light communications for 5g wireless networking systems: from fixed to mobile communications," *IEEE Network*, vol. 28, no. 6, pp. 41–45, 2014.
- [25] M. Khalighi and M. Uysal, "Survey on free space optical communication: A communication theory perspective," *IEEE Communications Surveys Tutorials*, vol. PP, no. 99, pp. 1–1, 2014.
- [26] A. Sevincer, A. Bhattarai, M. Bilgi, M. Yuksel, and N. Pala, "Lightnets: smart lighting and mobile optical wireless networks - a survey," *IEEE Communications Surveys Tutorials*, vol. 15, no. 4, pp. 1620–1641, 2013.
- [27] O. R. Popoola, F. B. Ogunkoya, W. O. Popoola, R. Ramirez-Iniguez, and S. Sinanovic, "Indoor localization based on multiple leds position estimation," in *IEEE 17th International Workshop on Signal Processing Advances in Wireless Communications (SPAWC)*, July 2016, pp. 1–6.
- [28] J. Gancarz, H. Elgala, and T. Little, "Impact of lighting requirements on vlc systems," *IEEE Communications Magazine*, vol. 51, no. 12, pp. 34–41, 2013.
- [29] D. Karunatilaka, "Wavelength division multiplexed visible light communication performance under illumination constraints," Ph.D. dissertation, 2016.
- [30] T. D. C. Little and H. Elgala, "Adaptation of ofdm under visible light communications and illumination constraints," in *48th Asilomar Conference on Signals, Systems and Computers*, 2014, pp. 1739–1744.
- [31] S. Rajagopal, R. D. Roberts, and L. Sang-Kyu, "Ieee 802.15.7 visible light communication: modulation schemes and dimming support," *IEEE Communications Magazine*, vol. 50, no. 3, pp. 72–82, 2012.
- [32] Y. Yang, Z. Zeng, J. Cheng, and C. Guo, "Spatial dimming scheme for optical ofdm based visible light communication," *Opt. Express*, vol. 24, no. 26, pp. 30 254–30 263, 2016.
- [33] F. Zafar, V. Kalavally, M. Bakaul, and R. Parthiban, "Experimental investigation of analog and digital dimming techniques on photometric performance of an indoor visible light communication (vlc) system," in *Fourteenth International Conference on Solid State Lighting and LED-based Illumination Systems*, vol. Proc. SPIE 9571, San Diego, California, USA, 2015, pp. 95 710D–95 710D–8.
- [34] I. Galkin, I. Milashevski, and O. Teteryonok, "Comparative study of steady-state performance of led drivers at different modulation techniques," in *7th International Conference-Workshop Compatibility and Power Electronics (CPE)*, June 2011, pp. 382–387.

- [35] M. Dyble, N. Narendran, A. Bierman, and T. Klein, "Impact of dimming white leds: chromaticity shifts due to different dimming methods," in *Proc. of SPIE 5941, 5th International Conference on Solid State Lighting*, Bellingham, Washington, USA, 2005, pp. 291–299.
- [36] G. Ntogari, T. Kamalakis, J. Walewski, and T. Sphicopoulos, "Combining illumination dimming based on pulse-width modulation with visible-light communications based on discrete multitone," *IEEE/OSA Journal of Optical Communications and Networking*, vol. 3, no. 1, pp. 56–65, 2011.
- [37] H.-J. Jang, J.-H. Choi, E. B. Cho, and C. G. Lee, "Simulation of a vlc system with 1 mb/s nrzook data with dimming signal," in *International Conference on Advanced Infocom Technology (ICAIT)*, Wuhan, China, 2011, pp. 1–3.
- [38] E. Cho, J.-H. Choi, C. Park, M. Kang, S. Shin, Z. Ghassemlooy, and C. G. Lee, "Nrz-ook signaling with led dimming for visible light communication link," in *16th European Conference on Networks and Optical Communications (NOC)*, 2011, pp. 32–35.
- [39] Z. Wang, W.-D. Zhong, C. Yu, J. Chen, C. P. S. Francois, and W. Chen, "Performance of dimming control scheme in visible light communication system," *Optics Express*, vol. 20, no. 17, pp. 18 861–18 868, 2012.
- [40] D. Karunatilaka, V. Kalavally, and R. Parthiban, "Improving lighting quality and capacity of ofdm-based wdm-vlc systems," *IEEE Photonics Technology Letters*, vol. 28, no. 20, pp. 2149–2152, 2016.
- [41] *Optibin Technology Overview*, Philips Color Kinetics, 2010. [Online]. Available: <http://www.colorkinetics.com/ls/guides-brochures/PCK-Technology-Overview-Optibin.pdf>
- [42] C. Tang, M. Jiang, H. Shen, and C. Zhao, "Analysis and optimization of pldpc coded rgb-led-based vlc systems," *IEEE Photonics Journal*, vol. 7, no. 6, pp. 1–13, 2015.
- [43] C. Lee, C. Zhang, M. Cantore, R. Farrell, S. H. Oh, T. Margalith, J. S. Speck, S. Nakamura, J. E. Bowers, and S. P. DenBaars, "2.6 ghz high-speed visible light communication of 450 nm gan laser diode by direct modulation," in *2015 IEEE Summer Topicals Meeting Series (SUM)*, 2015, pp. 112–113.
- [44] D. Tsonev, S. Videv, and H. Haas, "Towards a 100 gb/s visible light wireless access network," *Opt. Express*, vol. 23, no. 2, pp. 1627–1637, 2015.
- [45] S. Watson, M. Tan, S. P. Najda, P. Perlin, M. Leszczynski, G. Targowski, S. Grzanka, and A. E. Kelly, "Visible light communications using a directly modulated 422 nm gan laser diode," *Opt. Lett.*, vol. 38, no. 19, pp. 3792–3794, 2013.

- [46] H. Chun, S. Rajbhandari, D. Tsonev, G. Faulkner, H. Haas, and D. O'Brien, "Visible light communication using laser diode based remote phosphor technique," in *IEEE International Conference on Communication Workshop (ICCW)*, June 2015, pp. 1392–1397.
- [47] T.-C. Wu, Y.-C. Chi, H.-Y. Wang, C.-T. Tsai, Y.-F. Huang, and G.-R. Lin, "Tricolor r/g/b laser diode based eye-safe white lighting communication beyond 8 gbit/s," *Scientific Reports*, vol. 7, no. 11, 2017.
- [48] B. Janjua, H. M. Oubei, J. R. D. Retamal, T. K. Ng, C.-T. Tsai, H.-Y. Wang, Y.-C. Chi, H.-C. Kuo, G.-R. Lin, J.-H. He, and B. S. Ooi, "Going beyond 4 gbps data rate by employing rgb laser diodes for visible light communication," *Opt. Express*, vol. 23, no. 14, pp. 18746–18753, Jul 2015.
- [49] K. A. Stetson, "A review of speckle photography and interferometry," *Optical Engineering*, vol. 14, pp. 14 – 14 – 8, 1975.
- [50] W. Thomas and C. Middlebrook, "Non-moving hadamard matrix diffusers for speckle reduction in laser pico-projectors," *Journal of Modern Optics*, vol. 61, no. sup1, pp. S74–S80, Aug. 2014.
- [51] F. P. Shevlin, "Speckle reduction in laser-illuminated picoprojectors," in *Proc. SPIE*, vol. 8252, 2012, pp. 82520J06–82520J14.
- [52] G. Ouyang, M. Akram, K. Wang, Z. Tong, and X. Chen, "Laser speckle reduction based on angular diversity induced by piezoelectric benders," *Journal of the European Optical Society - Rapid publications*, vol. 8, no. 0, 2013.
- [53] C.-Y. Chen, W.-C. Su, C.-H. Lin, M.-D. Ke, Q.-L. Deng, and K.-Y. Chiu, "Reduction of speckles and distortion in projection system by using a rotating diffuser," *Optical Review*, vol. 19, no. 6, pp. 440–443, 2012.
- [54] R. Stevenson, "Better chips for better led bulbs," March 2012. [Online]. Available: <http://spectrum.ieee.org/semiconductors/optoelectronics/better-chips-for-better-led-bulbs>
- [55] T. Borogovac and T. Little, "Laser visible light communications," in *IEEE Photonics Society Summer Topical Meeting Series*, 2012, pp. 117–118.
- [56] D. Karunatilaka, F. Zafar, V. Kalavally, and R. Parthiban, "Led based indoor visible light communications: State of the art," *IEEE Communications Surveys Tutorials*, vol. 17, no. 3, pp. 1649–1678, 2015.
- [57] F. Zafar, M. Bakaul, and R. Parthiban, "Laser-diode-based visible light communication: Toward gigabit class communication," *IEEE Communications Magazine*, vol. 55, no. 2, pp. 144–151, 2017.
- [58] F. Zafar, V. Kalavally, and R. Parthiban, "Effect of slot utilization dimming scheme on the photometric performance of a high speed visible light communication (vlc) system," in *15th International Symposium on the Science and Technology of Lighting*, 2016.

- [59] D. Karunatilaka, F. Zafar, V. Kalavally, and R. Parthiban, "A viable model for snr determination in ofdm based visible light communication systems," in *IEEE Summer Topicals Meeting Series (SUM)*, July 2015, pp. 53–54.
- [60] R. Wood, "Wireless network traffic worldwide: forecasts and analysis 2013-2018," Analysys Mason Limited, Tech. Rep., 2013.
- [61] H. Parikh, J. Chokshi, N. Gala, and T. Biradar, "Wirelessly transmitting a grayscale image using visible light," in *International Conference on Advances in Technology and Engineering (ICATE)*, Mumbai, India, 2013, pp. 1–6.
- [62] M. Kavehrad, "Sustainable energy-efficient wireless applications using light," *IEEE Communications Magazine*, vol. 48, no. 12, pp. 66–73, 2010.
- [63] J. Kim and E. Schubert, "Transcending the replacement paradigm of solid-state lighting," *Optics Express*, vol. 16, no. 26, pp. 21 835–21 842, 2008.
- [64] N. Bardsley, S. Bland, L. Pattison, M. Pattison, K. Stober, F. Welsh, and M. Yamada, "Solid-state lighting research and development: multi-year program plan," U.S. Department of Energy, Tech. Rep., 2014. [Online]. Available: <http://www1.eere.energy.gov/buildings/ssl/techroadmaps.html>
- [65] H. Ma, L. Lampe, and S. Hranilovic, "Integration of indoor visible light and power line communication systems," in *17th IEEE International Symposium on Power Line Communications and its Applications (ISPLC)*, Johannesburg, South Africa, 2013, pp. 291–296.
- [66] A. Neumann, J. J. Wierer, W. Davis, Y. Ohno, S. R. J. Brueck, and J. Tsao, "Four-color laser white illuminant demonstrating high color-rendering quality," *Opt. Express*, vol. 19, no. S4, pp. A982–A990, Jul 2011.
- [67] A. Jovicic, J. Li, and T. Richardson, "Visible light communication: opportunities, challenges and the path to market," *IEEE Communications Magazine*, vol. 51, no. 12, pp. 26–32, 2013.
- [68] D. O'brien, "Visible light communications: Challenges and potential," in *IEEE Photonics Conference (IPC)*, Arlington, Virginia, USA, 2011, pp. 365–366.
- [69] P. Ryan, "Application of the public-trust doctrine and principles of natural resource management to electromagnetic spectrum," *Michigan Telecommunications and Technology Law Review*, vol. 10, no. 2, p. 285, 2004.
- [70] M. Oh, "A flicker mitigation modulation scheme for visible light communications," in *15th International Conference on Advanced Communication Technology (ICACT)*, PyeongChang, Korea, 2013, pp. 933–936.

- [71] B. Love, D. Love, and J. Krogmeier, "Like deck chairs on the titanic: Why spectrum reallocation wont avert the coming data crunch but technology might keep the wireless industry afloat," *Washington University Law Review*, vol. 89, p. 705, 2012.
- [72] C. Gabriel, "Wireless broadband alliance industry report 2013: Global trends in public wi-fi," Marvedis Rethink - Wireless Broadband Alliance, Tech. Rep., 2013. [Online]. Available: <http://www.wballiance.com/wba/wp-content/uploads/downloads/2013/11/WBA-Industry-Report-2013.pdf>
- [73] A. M. Căilean and M. Dimian, "Current challenges for visible light communications usage in vehicle applications: A survey," *IEEE Communications Surveys Tutorials*, vol. 19, no. 4, pp. 2681–2703, 2017.
- [74] D. Borah, A. Boucouvalas, C. Davis, S. Hranilovic, and K. Yiannopoulos, "A review of communication-oriented optical wireless systems," *EURASIP Journal on Wireless Communications and Networking*, vol. 2012, no. 1, pp. 91–119, 2012.
- [75] G. Dede, T. Kamalakis, and D. Varoutas, "Evaluation of optical wireless technologies in home networking: An analytical hierarchy process approach," *IEEE/OSA Journal of Optical Communications and Networking*, vol. 3, no. 11, pp. 850–859, 2011.
- [76] S. Zhao, J. Xu, and O. Trescases, "A dimmable led driver for visible light communication (vlc) based on llc resonant dc-dc converter operating in burst mode," in *28th Annual IEEE Applied Power Electronics Conference and Exposition (APEC)*, Long Beach, California, USA, 2013, pp. 2144–2150.
- [77] T. Komine and M. Nakagawa, "Fundamental analysis for visible-light communication system using led lights," *IEEE Transactions on Consumer Electronics*, vol. 50, no. 1, pp. 100–107, 2004.
- [78] M. Biagi, T. Borogovac, and T. Little, "Adaptive receiver for indoor visible light communications," *Journal of Lightwave Technology*, vol. 31, no. 23, pp. 3676–3686, 2013.
- [79] C. Chow, C. Yeh, Y. Liu, P. Huang, and Y. Liu, "Adaptive scheme for maintaining the performance of the in-home white-led visible light wireless communications using ofdm," *Optics Communications*, vol. 292, no. 1, pp. 49 – 52, 2013.
- [80] Y. Wang, Y. Wang, N. Chi, J. Yu, and H. Shang, "Demonstration of 575-mb/s downlink and 225-mb/s uplink bi-directional scm-wdm visible light communication using rgb led and phosphor-based led," *Optics Express*, vol. 21, no. 1, pp. 1203–1208, 2013.

- [81] F. Yang, Y. Sun, and J. Gao, "Adaptive laco-ofdm with variable layer for visible light communication," *IEEE Photonics Journal*, vol. 9, no. 6, pp. 1–8, 2017.
- [82] M. J. Eckelman, P. T. Anastas, and J. B. Zimmerman, "Spatial assessment of net mercury emissions from the use of fluorescent bulbs," *Environmental science & technology*, vol. 42, no. 22, pp. 8564–8570, 2008.
- [83] S. Bose-O'Reilly, K. M. McCarty, N. Steckling, and B. Lettmeier, "Mercury exposure and children's health," *Current problems in pediatric and adolescent health cares*, vol. 40, no. 8, pp. 186–215, 2010.
- [84] Y. Cai, W. Guan, Y. Wu, C. Xie, Y. Chen, and L. Fang, "Indoor high precision three-dimensional positioning system based on visible light communication using particle swarm optimization," *IEEE Photonics Journal*, vol. 9, no. 6, pp. 1–20, 2017.
- [85] "Infrared data association," 2012. [Online]. Available: <http://www.irda.org/>
- [86] J. Tuenge, "Ssl pricing and efficacy trend analysis for utility program planning," U.S. department of energy, Tech. Rep., 2013. [Online]. Available: http://apps1.eere.energy.gov/buildings/publications/pdfs/ssl/ssl_trend-analysis_2013.pdf
- [87] E. Schubert, *Light-Emitting Diodes*. Cambridge University Press, 2006.
- [88] F. R. Gfeller and U. Bapst, "Wireless in-house data communication via diffuse infrared radiation," *Proceedings of the IEEE*, vol. 67, no. 11, pp. 1474–1486, 1979.
- [89] W. A. H. Rushton, "Review lecture. pigments and signals in colour vision," *The Journal of Physiology*, vol. 220, no. 3, pp. 1P–31P, Feb. 1972.
- [90] J. Schanda, *Colorimetry: Understanding the CIE System*. John Wiley & Sons, Inc., 2007.
- [91] K. H. Loo, Y. M. Lai, S. C. Tan, and C. K. Tse, "On the color stability of phosphor-converted white leds under dc, pwm, and bilevel drive," *IEEE Transactions on Power Electronics*, vol. 27, no. 2, pp. 974–984, 2012.
- [92] D. L. MacAdam, "Specification of small chromaticity differences," *J. Opt. Soc. Am.*, vol. 33, no. 1, pp. 18–26, 1943.
- [93] S. Peyvandi, J. Hernández-Andrés, F. J. Olmo, J. L. Nieves, and J. Romero, "Colorimetric analysis of outdoor illumination across varieties of atmospheric conditions." *Journal of the Optical Society of America. A, Optics, image science, and vision*, vol. 33, pp. 1049–59, 2016.

- [94] *LED Lighting Selecting Guide*, Pure Michigan Energy Office. [Online]. Available: https://www.michigan.gov/documents/mdcd/Energy_Observer_-_Selecting_LED_Lighting_422716_7.pdf
- [95] G. Wyszecki and W. S. Stiles, *Color Science: Concepts and Methods, Quantitative Data and Formulae*, 2nd ed. New York: John Wiley & Sons, Inc., 1982.
- [96] Y.-C. Chi, D.-H. Hsieh, C.-Y. Lin, H.-Y. Chen, C.-Y. Huang, J.-H. He, B. Ooi, S. P. DenBaars, S. Nakamura, H.-C. Kuo, and G.-R. Lin, "Phosphorous diffuser diverged blue laser diode for indoor lighting and communication," *Scientific Reports*, vol. 5, pp. 18 690–18 699, 2015.
- [97] *Energy Star Criteria for Solid State Lighting Luminaires*, US Department of Energy Std., 2008.
- [98] *Standard for Electric Lamps: Specifications for the Chromaticity of Solid State Lighting Products. ANSI C78.377*, American National Standards Institute Std.
- [99] J. Romero, J. Hernández-Andrés, J. L. Nieves, and J. A. García, "Color coordinates of objects with daylight changes," *Color Research & Application*, vol. 28, no. 1, pp. 25–35, 2003.
- [100] M. R. Pointer and G. G. Attridge, "The number of discernible colours," *Color Research & Application*, vol. 23, no. 1, pp. 52–54, 1998.
- [101] S. Ratnasingam, S. Collins, and J. Hernández-Andrés, "Analysis of colour constancy algorithms using the knowledge of variation of correlated colour temperature of daylight with solar elevation," *EURASIP Journal on Image and Video Processing*, vol. 2013, no. 1, p. 14, 2013.
- [102] M. H. Crawford, "Leds for solid-state lighting: Performance challenges and recent advances," *IEEE Journal of Selected Topics in Quantum Electronics*, vol. 15, no. 4, pp. 1028–1040, 2009.
- [103] M. S. Rea and J. P. Freyssinier-Nova, "Color rendering: A tale of two metrics," *Color Research and Application*, vol. 33, no. 3, pp. 192–202, 2008.
- [104] A. Zukauskas, R. Vaicekauskas, F. Ivanauskas, H. Vaitkevicius, P. Vitta, and M. S. Shur, "Statistical approach to color quality of solid-state lamps," *IEEE Journal of Selected Topics in Quantum Electronics*, vol. 15, no. 6, pp. 1753–1762, 2009.
- [105] D. Steigerwald, J. Bhat, D. Collins, R. Fletcher, M. Holcomb, M. Ludowise, P. Martin, and S. Rudaz, "Illumination with solid state lighting technology," *IEEE Journal of Selected Topics in Quantum Electronics*, vol. 8, no. 2, pp. 310–320, 2002.

- [106] H.-C. Guo, Y.-F. Xu, X.-J. Li, L. Zhang, Y.-J. Wang, and N. Chi, "A high-speed phosphorescent led-based visible light communication system utilizing sqgnrc precoding technique," *Photonic Network Communications*, vol. 34, no. 3, pp. 461–467, 2017.
- [107] H. Le Minh, Z. Ghassemlooy, A. Burton, and P. A. Haigh, "Equalization for organic light emitting diodes in visible light communications," in *IEEE GLOBECOM Workshops (GC Wkshps)*, Houston, Texas, USA, 2011, pp. 828–832.
- [108] Z. Ghassemlooy, "Oled-based visible light communications," in *IEEE Photonics Society Summer Topical Meeting Series*, Seattle, Washington, USA, 2012, pp. 102–104.
- [109] P. A. Haigh, Z. Ghassemlooy, M. Hoa Le, S. Rajbhandari, F. Arca, S. F. Tedde, O. Hayden, and I. Papakonstantinou, "Exploiting equalization techniques for improving data rates in organic optoelectronic devices for visible light communications," *Journal of Lightwave Technology*, vol. 30, no. 19, pp. 3081–3088, 2012.
- [110] H. Chun, C.-J. Chiang, and D. C. O'Brien, "Visible light communication using oleds: Illumination and channel modeling," in *International Workshop on Optical Wireless Communications (IWOW)*, Pisa, Italy, 2012, pp. 1–3.
- [111] A. Kelly, J. McKendry, S. Zhang, D. Massoubre, B. Rae, R. Green, R. Henderson, and M. Dawson, "High-speed gan micro-led arrays for data communications," in *14th International Conference on Transparent Optical Networks (ICTON)*, Coventry, UK, 2012, pp. 1–5.
- [112] J. J. D. McKendry, R. P. Green, A. E. Kelly, G. Zheng, B. Guilhabert, D. Massoubre, E. Gu, and M. D. Dawson, "High speed visible light communications using individual pixels in a micro light emitting diode array," *IEEE Photonics Technology Letters*, vol. 22, no. 18, pp. 1346–1348, 2010.
- [113] J. J. D. McKendry, D. Massoubre, S. Zhang, B. R. Rae, R. P. Green, E. Gu, R. K. Henderson, A. E. Kelly, and M. D. Dawson, "Visible-light communications using a cmos-controlled micro-light-emitting-diode array," *Journal of Lightwave Technology*, vol. 30, no. 1, pp. 61–67, 2012.
- [114] S. Zhang, S. Watson, J. J. McKendry, D. Massoubre, A. Cogman, E. Gu, R. K. Henderson, A. E. Kelly, and M. D. Dawson, "1.5 gbit/s multi-channel visible light communications using cmos-controlled gan-based leds," *Journal of Lightwave Technology*, vol. 31, no. 8, pp. 1211–1216, 2013.
- [115] E. Schubert, Y.-H. Wang, A. Cho, L.-W. Tu, and G. Zydzik, "Resonant cavity light emitting diode," *Applied Physics Letters*, vol. 60, no. 8, pp. 921–923, 1992.

- [116] T. Komine, L. Jun Hwan, S. Haruyama, and M. Nakagawa, "Adaptive equalization system for visible light wireless communication utilizing multiple white led lighting equipment," *IEEE Transactions on Wireless Communications*, vol. 8, no. 6, pp. 2892–2900, 2009.
- [117] H. Oh, J. Joo, J. Lee, J. Baek, J. Seo, and J. Kwak, "Structural optimization of high-power algainp resonant cavity light-emitting diodes for visible light communications," *Japanese Journal of Applied Physics*, vol. 47, pp. 6214–6216, 2008.
- [118] S. Nakamura, M. Senoh, S. Nagahama, N. Iwasa, T. Yamada, T. Matsushita, Y. Sugimoto, and H. Kiyoku, "Optical gain and carrier lifetime of ingan multi-quantum well structure laser diodes," *Applied Physics Letters*, vol. 69, no. 11, pp. 1568–1570, 1996.
- [119] L. Y. Kuritzky and J. S. Speck, "Lighting for the 21st century with laser diodes based on non-basal plane orientations of gan," *MRS Communications*, vol. 5, pp. 463–473, 2015.
- [120] J. J. Wierer, J. Y. Tsao, and D. S. Sizov, "Comparison between blue lasers and light-emitting diodes for future solid-state lighting," *Laser & Photonics Reviews*, vol. 7, no. 6, pp. 963–993, 2013.
- [121] R. Kuller and T. Laike, "The impact of flicker from fluorescent lighting on well-being, performance and physiological arousal," *Ergonomics*, vol. 41, no. 4, pp. 433–447, 1998.
- [122] J. M. Kahn and J. R. Barry, "Wireless infrared communications," *Proceedings of the IEEE*, vol. 85, no. 2, pp. 265–298, 1997.
- [123] M. Zhang and Z. Zhang, "Fractionally spaced equalization in visible light communication," in *IEEE Wireless Communications and Networking Conference (WCNC)*, Shanghai, China, 2013, pp. 4282–4287.
- [124] M. Hoa Le, D. O'Brien, G. Faulkner, L. Zeng, L. Kyungwoo, J. Daekwang, and O. YunJe, "80 mbit/s visible light communications using pre-equalized white led," in *34th European Conference on Optical Communication (ECOC)*, Brussels, Belgium, 2008, pp. 1–2.
- [125] J. Vucic, C. Kottke, S. Nerreter, K. Habel, A. Buttner, K. D. Langer, and J. W. Walewski, "125 mbit/s over 5 m wireless distance by use of ooc-modulated phosphorescent white leds," in *35th European Conference on Optical Communication (ECOC)*, Vienna, Austria, 2009, pp. 1–2.
- [126] M. Hoa Le, D. O'Brien, G. Faulkner, Z. Lubin, L. Kyungwoo, J. Daekwang, O. YunJe, and W. Eun Tae, "100-mb/s nrz visible light communications using a postequalized white led," *IEEE Photonics Technology Letters*, vol. 21, no. 15, pp. 1063–1065, 2009.

- [127] Z. Lubin, M. Hoa Le, D. O'Brien, G. Faulkner, L. Kyungwoo, J. Daekwang, and O. YunJe, "Equalisation for high-speed visible light communications using white-leds," in *6th International Symposium on Communication Systems, Networks and Digital Signal Processing (CNSDSP)*, Graz, Austria, 2008, pp. 170–173.
- [128] H. Li, X. Chen, B. Huang, D. Tang, and H. Chen, "High bandwidth visible light communications based on a post-equalization circuit," *IEEE Photonics Technology Letters*, vol. 26, no. 2, pp. 119–122, 2014.
- [129] N. Fujimoto and H. Mochizuki, "614 mbit/s ooc-based transmission by the duobinary technique using a single commercially available visible led for high-speed visible light communications," in *European Conference and Exhibition on Optical Communication (ECEO)*. Amsterdam Netherlands: Optical Society of America, 2012.
- [130] C. Lee, C. Zhang, M. Cantore, R. M. Farrell, S. H. Oh, T. Margalith, J. S. Speck, S. Nakamura, J. E. Bowers, and S. P. DenBaars, "4 gbps direct modulation of 450 nm gan laser for high-speed visible light communication," *Opt. Express*, vol. 23, no. 12, pp. 16 232–16 237, 2015.
- [131] H.-J. Jang, J.-H. Choi, Z. Ghassemlooy, and C. G. Lee, "Pwm-based ppm format for dimming control in visible light communication system," in *8th International Symposium on Communication Systems, Networks Digital Signal Processing (CSNDSP)*, Poznan, Poland, 2012, pp. 1–5.
- [132] J. Rufo, C. Quintana, F. Delgado, J. Rabadan, and R. Perez-Jimenez, "Considerations on modulations and protocols suitable for visible light communications (vlc) channels: Low and medium baud rate indoor visible light communications links," in *IEEE Consumer Communications and Networking Conference (CCNC)*, Las Vegas, Nevada, USA, 2011, pp. 362–364.
- [133] S. He, G. Ren, Z. Zhong, and Y. Zhao, "M-ary variable period modulation for indoor visible light communication system," *IEEE Communications Letters*, vol. 17, no. 7, pp. 1325–1328, 2013.
- [134] H. Elgala, R. Mesleh, and H. Haas, "Indoor optical wireless communication: potential and state-of-the-art," *IEEE Communications Magazine*, vol. 49, no. 9, pp. 56–62, 2011.
- [135] S. Arnon, "The effect of clock jitter in visible light communication applications," *Journal of Lightwave Technology*, vol. 30, no. 21, pp. 3434–3439, 2012.
- [136] S. H. Lee, K.-I. Ahn, and J. K. Kwon, "Multilevel transmission in dimmable visible light communication systems," *Journal of Lightwave Technology*, vol. 31, no. 20, pp. 3267–3276, 2013.
- [137] H. Elgala, R. Mesleh, H. Haas, and B. Pricope, "Ofdm visible light wireless communication based on white leds," in *IEEE 65th Vehicular Technology Conference (VTC)*, Dublin, Ireland, 2007, pp. 2185–2189.

- [138] D. Tsonev, H. Chun, S. Rajbhandari, J. McKendry, S. Videv, E. Gu, M. Haji, S. Watson, A. Kelly, G. Faulkner, M. Dawson, H. Haas, and D. O'Brien, "A 3-gb/s single-led ofdm-based wireless vlc link using a gallium nitride μ led," *IEEE Photonics Technology Letters*, vol. 26, no. 7, pp. 637–640, 2014.
- [139] A. Azhar, T. Tran, and D. O'Brien, "A gigabit/s indoor wireless transmission using mimo-ofdm visible-light communications," *IEEE Photonics Technology Letters*, vol. 25, no. 2, pp. 171–174, 2013.
- [140] G. Cossu, A. M. Khalid, P. Choudhury, R. Corsini, and E. Ciaramella, "3.4 gbit/s visible optical wireless transmission based on rgb led," *Optics Express*, vol. 20, no. 26, pp. B501–B506, 2012.
- [141] S. Dimitrov, S. Sinanovic, and H. Haas, "Clipping noise in ofdm-based optical wireless communication systems," *IEEE Transactions on Communications*, vol. 60, no. 4, pp. 1072–1081, 2012.
- [142] L. Xiaodong and J. Cimini, L. J., "Effects of clipping and filtering on the performance of ofdm," *IEEE Communications Letters*, vol. 2, no. 5, pp. 131–133, 1998.
- [143] J. S. Sheu, B. J. Li, and J. K. Lain, "Led non-linearity mitigation techniques for optical ofdm-based visible light communications," *IET Optoelectronics*, vol. 11, no. 6, pp. 259–264, 2017.
- [144] S. Zhao and X. Ma, "A spectral-efficient transmission scheme for dimmable visible light communication systems," *Journal of Lightwave Technology*, vol. 35, no. 17, pp. 3801–3809, 2017.
- [145] N. Fujimoto and H. Mochizuki, "477 mbit/s visible light transmission based on ook-nrz modulation using a single commercially available visible led and a practical led driver with a pre-emphasis circuit," in *Optical Fiber Communication Conference and Exposition and the National Fiber Optic Engineers Conference (OFC/NFOEC)*, Anaheim, California, USA, 2013, pp. 1–3.
- [146] S. Rajbhandari, P. Haigh, Z. Ghassemlooy, and W. Popoola, "Wavelet-neural network vlc receiver in the presence of artificial light interference," *IEEE Photonics Technology Letters*, vol. 25, no. 15, pp. 1424–1427, 2013.
- [147] P. Binh, V. Trong, D. Hung, P. Renucci, A. Balocchi, and X. Marie, "Demonstration of 300 mbit/s free space optical link with commercial visible led," in *11th IEEE International New Circuits and Systems Conference (NEWCAS)*, Paris, France, 2013, pp. 1–3.
- [148] L. Fan, L. Ding, F. Liu, and Y. Wang, "Design of wireless optical access system using led based android mobile," in *International Conference on Wireless Communications Signal Processing (WCSP)*, Hangzhou, China, 2013, pp. 1–4.

- [149] J. Vucic, C. Kottke, S. Nerreter, K. Habel, A. Buttner, K. D. Langer, and J. W. Walewski, "230 mbit/s via a wireless visible-light link based on oof modulation of phosphorescent white leds," in *Optical Fiber Communication Conference and Exposition and the National Fiber Optic Engineers Conference (OFC/NFOEC)*, San Diego, California, USA, 2010, pp. 1–3.
- [150] M. Hoa Le, D. O'Brien, G. Faulkner, Z. Lubin, L. Kyungwoo, J. Daekwang, and O. YunJe, "High-speed visible light communications using multiple-resonant equalization," *IEEE Photonics Technology Letters*, vol. 20, no. 14, pp. 1243–1245, 2008.
- [151] S. Lou, C. Gong, N. Wu, and Z. Xu, "Joint dimming and communication design for visible light communication," *IEEE Communications Letters*, vol. 21, no. 5, pp. 1043–1046, 2017.
- [152] Y. Gu, N. Narendran, T. Dong, and H. Wu, "Spectral and luminous efficacy change of high-power leds under different dimming methods," in *Sixth International Conference on Solid State Lighting*, vol. 6337, San Diego, California, USA, 2006, pp. 63 370J–63 370J–7.
- [153] K. Lee and H. Park, "Modulations for visible light communications with dimming control," *IEEE Photonics Technology Letters*, vol. 23, no. 16, pp. 1136–1138, 2011.
- [154] H.-S. Kim, D.-R. Kim, S.-H. Yang, Y.-H. Son, and S.-K. Han, "Transmission performance variation by dimming control in carrier allocation based visible light communication," in *17th Opto-Electronics and Communications Conference (OECC)*, Busan, Korea, 2012, pp. 743–744.
- [155] L. Kwonhyung and P. Hyuncheol, "Modulations for visible light communications with dimming control," *IEEE Photonics Technology Letters*, vol. 23, no. 16, pp. 1136–1138, 2011.
- [156] M. Rahaim, T. Borogovac, T. Little, A. Mirvakili, and V. Joyner, "Demonstration of a software defined visible light communication system," *Mobicom 2011, Poster and Demonstration Competition*, Tech. Rep., 2011.
- [157] Y. Tanaka, T. Komine, S. Haruyama, and M. Nakagawa, "Indoor visible light data transmission system utilizing white led lights," *IEICE transactions on communications*, vol. 86, no. 8, pp. 2440–2454, 2003.
- [158] J. Vucic, C. Kottke, K. Habel, and K. D. Langer, "803 mbit/s visible light wdm link based on dmt modulation of a single rgb led luminary," in *Optical Fiber Communication Conference and Exposition and the National Fiber Optic Engineers Conference (OFC/NFOEC)*, Los Angeles, USA, 2011, pp. 1–3.
- [159] NEMA / ANSI ANSLG C78.377-2008: *Specifications for the Chromaticity of Solid State Lighting (SSL) Products*, American National Standards Institute, 2008. [Online]. Available: <https://www.nema.org/Standards/ComplimentaryDocuments/C78.377-2015-contents-and-scope.pdf>

- [160] S. Yao, X. Zhang, H. Qian, and X. Luo, "Joint dimming and data transmission optimization for multi-user visible light communication system," *IEEE Access*, vol. 5, pp. 5455–5462, 2017.
- [161] S. Hranilovic, *Wireless optical communication systems*. Springer, 2004.
- [162] C. Kottke, K. Habel, L. Grobe, J. Hilt, L. F. del Rosal, A. Paraskevopoulos, and K. Langer, "Single-channel wireless transmission at 806 mbit/s using a white-light led and a pin-based receiver," in *14th International Conference on Transparent Optical Networks (ICTON)*, Coventry, UK, 2012, pp. 1–4.
- [163] R. R. Iniguez, S. M. Idrus, and Z. Sun, *Optical Wireless Communications*. Auerbach Publications, 2008.
- [164] K. Pujapanda, "Lifi integrated to power-lines for smart illumination cum communication," in *International Conference on Communication Systems and Network Technologies (CSNT)*, Gwalior, India, 2013, pp. 875–878.
- [165] P. Haigh, Z. Ghassemlooy, S. Rajbhandari, and I. Papakonstantinou, "Visible light communications using organic light emitting diodes," *IEEE Communications Magazine*, vol. 51, no. 8, pp. 148–154, 2013.
- [166] W. Popoola, E. Poves, and H. Haas, "Error performance of generalised space shift keying for indoor visible light communications," *IEEE Transactions on Communications*, vol. 61, no. 5, pp. 1968–1976, 2013.
- [167] J. Grubor, S. Randel, K. D. Langer, and J. W. Walewski, "Broadband information broadcasting using led-based interior lighting," *Journal of Lightwave Technology*, vol. 26, no. 24, pp. 3883–3892, 2008.
- [168] E. Schubert, N. Hunt, R. Malik, M. Micovic, and D. Miller, "Temperature and modulation characteristics of resonant-cavity light-emitting diodes," *Journal of Lightwave Technology*, vol. 14, no. 7, pp. 1721–1729, 1996.
- [169] C. W. Chow, C. H. Yeh, Y. F. Liu, and Y. Liu, "Improved modulation speed of led visible light communication system integrated to main electricity network," *Electronics Letters*, vol. 47, no. 15, pp. 867–868, 2011.
- [170] B. Lin, X. Tang, Z. Ghassemlooy, S. Zhang, Y. Li, Y. Wu, and H. Li, "Efficient frequency-domain channel equalisation methods for ofdm visible light communications," *IET Communications*, vol. 11, no. 1, pp. 25–29, 2017.
- [171] J. Remenyi, P. Varhegyi, L. Domjan, P. Koppa, and E. Lorincz, "Amplitude, phase, and hybrid ternary modulation modes of a twisted-nematic liquid-crystal display at 400 nm," *Applied Optics*, vol. 42, no. 17, pp. 3428–3434, 2003.
- [172] J. Vucic, C. Kottke, S. Nerreter, K. Langer, and J. W. Walewski, "513 mbit/s visible light communications link based on dmt-modulation of a white led," *Journal of Lightwave Technology*, vol. 28, no. 24, pp. 3512–3518, 2010.

- [173] H. Elgala, R. Mesleh, and H. Haas, "A study of led nonlinearity effects on optical wireless transmission using ofdm," in *6th IEEE and IFIP International Conference on Wireless and Optical Communications Networks (WOCN)*, Cairo, Egypt, 2009, pp. 1–5.
- [174] A. M. Khalid, G. Cossu, R. Corsini, P. Choudhury, and E. Ciaramella, "1-gb/s transmission over a phosphorescent white led by using rate-adaptive discrete multitone modulation," *IEEE Photonics Journal*, vol. 4, no. 5, pp. 1465–1473, 2012.
- [175] H. Elgala, R. Mesleh, and H. Haas, "Predistortion in optical wireless transmission using ofdm," in *9th International Conference on Hybrid Intelligent Systems (HIS)*, Shenyang, LiaoNing, China, 2009, pp. 184–189.
- [176] D. Lee, K. Choi, K.-D. Kim, and Y. Park, "Visible light wireless communications based on predistorted ofdm," *Optics Communications*, vol. 285, no. 7, pp. 1767–1770, 2012.
- [177] "Building technologies program: Solid-state lighting technology fact sheet," U.S. Department of Energy, Tech. Rep., 2013.
- [178] T. Minh, N. Nhan, T. Vo, and N. Anh, "Enhancement of color rendering index for white light led lamps by red $\text{Y}_2\text{O}_3:\text{Eu}^{3+}$ phosphor," *Advances in Electrical and Electronic Engineering*, vol. 14, no. 3, 2016.
- [179] C. Basu, M. Meinhardt-Wollweber, and B. Roth, "Lighting with laser diodes," *Advanced Optical Technologies*, vol. 2, pp. 313–321, Aug. 2013.
- [180] P.-H. Yao, C.-H. Chen, and C.-H. Chen, "Low speckle laser illuminated projection system with a vibrating diffractive beam shaper," *Opt. Express*, vol. 20, no. 15, pp. 16 552–16 566, 2012.
- [181] Y. Zhao, "A pragmatic speckle measurement method," Visteon Electronics GmbH, Tech. Rep., 2016. [Online]. Available: https://www.visteon.com/products/documents/speckle_measurement.pdf
- [182] S. Roelandt, Y. Meuret, G. Craggs, G. Verschaffelt, P. Janssens, and H. Thienpont, "Standardized speckle measurement method matched to human speckle perception in laser projection systems," *Opt. Express*, vol. 20, no. 8, pp. 8770–8783, 2012.
- [183] *Photobiological safety of lamps and lamp systems. IEC 62471*, International Electrotechnical Commission Std.
- [184] D. J. T. Heatley, D. R. Wisely, I. Neild, and P. Cochrane, "Optical wireless: the story so far," *IEEE Communications Magazine*, vol. 36, no. 12, pp. 72–74, 79–82, 1998.
- [185] *Safety of laser products:IEC 60825*, International Electrotechnical Commission Std., 2001.

- [186] L. D. Nadarajah Narendran, "Color rendering properties of led light sources," in *Solid State Lighting II*, vol. 4776, 2002, pp. 4776 – 4776 – 7.
- [187] N. Pousset, G. Obein, and A. Razet, "Visual experiment on led lighting quality with color quality scale colored samples," in *Proceedings of CIE 2010: Lighting Quality and Energy Efficiency*, 2010, pp. 722–729.
- [188] R. L. Maria Thompson, Una-May O'Reilly, "Psychophysical evaluations of various color rendering from led-based architectural lighting," vol. 6669, 2007, pp. 6669 – 6669 – 12.
- [189] B. A. Kurniawan, Y. Nakashima, and M. Takamatsu, "Analysis of visual perception of light emitting diode brightness in dense fog with various droplet sizes," *Optical Review*, vol. 15, no. 3, pp. 166–172, 2008.
- [190] V. Viliūnas, H. Vaitkevičius, R. Stanikūnas, P. Vitta, R. Bliumas, A. Auškalnytė, A. Tuzikas, A. Petruelis, L. Dabašinskas, and A. Žukauskas, "Subjective evaluation of luminance distribution for intelligent outdoor lighting," *Lighting Research & Technology*, vol. 46, no. 4, pp. 421–433, 2014.
- [191] A. Ampenberger, S. Staggl, and W. Pohl, "Attention guidance, perceived brightness and energy demand in retail lighting," *Energy Procedia*, vol. 111, no. Supplement C, pp. 658 – 668, 2017, 8th International Conference on Sustainability in Energy and Buildings, SEB-16, 11-13 September 2016, Turin, Italy.
- [192] W. Hu and W. Davis, "Development and evaluation of colour control interfaces for led lighting," in *Light, Energy and the Environment*. Optical Society of America, 2016, p. SSTu2D.4.
- [193] R. Likert, "A technique for the measurement of attitudes," *Archives of Psychology*, vol. 22, no. 140, pp. 1–55, 1932.
- [194] W. J. Conover, *Practical Nonparametric Statistics*, 3rd ed., J. W. . Sons, Ed., 1971.
- [195] *Oslon1 PowerStar Whites*, Osram Opto Semiconductors. [Online]. Available: <http://docs-europe.electrocomponents.com/webdocs/0e9e/0900766b80e9ea5a.pdf>
- [196] J. Grubor, S. Randel, K. D. Langer, and J. W. Walewski, "Bandwidth-efficient indoor optical wireless communications with white light-emitting diodes," in *6th International Symposium on Communication Systems, Networks and Digital Signal Processing (CNSDSP)*, Graz, Austria, 2008, pp. 165–169.
- [197] *High-Speed Serial Data Analysis and Clock Recovery Software*, Keysight, 2016, n5384A. [Online]. Available: <http://literature.cdn.keysight.com/litweb/pdf/5989-0108EN.pdf?id=352001>

- [198] W. Freude, R. Schmogrow, B. Nebendahl, M. Winter, A. Josten, D. Hillerkuss, S. Koenig, J. Meyer, M. Dreschmann, M. Huebner, C. Koos, J. Becker, and J. Leuthold, "Quality metrics for optical signals: Eye diagram, Q-factor, OSNR, EVM and BER," in *14th International Conference on Transparent Optical Networks (ICTON)*, vol. 1, 2012, pp. 3–6.
- [199] *Illuminance Spectrophotometer CL-500A Brochure*, 2017. [Online]. Available: https://www.konicaminolta.com/instruments/download/catalog/light/pdf/cl500a_catalog_eng.pdf
- [200] I. Stefan, H. Elgala, R. Mesleh, D. O'Brien, and H. Haas, "Optical wireless ofdm system on fpga: Study of led nonlinearity effects," in *IEEE 73rd Vehicular Technology Conference (VTC)*, Budapest, Hungary, 2011, pp. 1–5.
- [201] S. Dimitrov and H. Haas, *Principles of LED Light Communications*. Cambridge University Press, 2015.
- [202] L. Wu, Z. Zhang, J. Dang, and H. Liu, "Adaptive modulation schemes for visible light communications," *Journal of Lightwave Technology*, vol. 33, no. 1, pp. 117–125, 2015.
- [203] J. Barry, *Wireless infrared communications*. Springer, 1994, vol. 280.
- [204] K. H. Loo, W. K. Lun, S. C. Tan, Y. M. Lai, and C. K. Tse, "On driving techniques for leds: Toward a generalized methodology," *IEEE Transactions on Power Electronics*, vol. 24, no. 12, pp. 2967–2976, 2009.
- [205] Z. Lei, G. Xia, L. Ting, G. Xiaoling, L. Q. Ming, and S. Guangdi, "Color rendering and luminous efficacy of trichromatic and tetrachromatic led-based white {LEDs}," *Microelectronics Journal*, vol. 38, no. 1, pp. 1 – 6, 2007.
- [206] K. Gordon, "Color rendering index and leds," U.S. Department of Energy, Washington, Tech. Rep., 2007.
- [207] A. Mirvakili and V. Koomson, "A flicker-free cmos led driver control circuit for visible light communication enabling concurrent data transmission and dimming control," *Analog Integrated Circuits and Signal Processing*, vol. 80, no. 2, pp. 283–292, 2014.
- [208] *PA1000 Single Phase AC Power Analyzer Datasheet*, Tektronix. [Online]. Available: <https://www.tek.com/datasheet/pa1000-single-phase-ac-power-analyzer-datasheet>
- [209] M. Figueiredo, L. N. Alves, and C. Ribeiro, "Lighting the wireless world: The promise and challenges of visible light communication," *IEEE Consumer Electronics Magazine*, vol. 6, no. 4, pp. 28–37, 2017.
- [210] F. Wu, C. Lin, C. Wei, C. Chen, Z. Chen, H. Huang, and S. Chi, "Performance comparison of ofdm signal and cap signal over high capacity rgb-led-based wdm visible light communication," *IEEE Photonics Journal*, vol. 5, no. 4, pp. 7901507–7901507, 2013.

- [211] N. Shrestha, M. Sohail, C. Viphavakit, P. Saengudomlert, and W. S. Mohammed, "Demonstration of visible light communications using rgb leds in an indoor environment," in *International Conference on Electrical Engineering/Electronics Computer Telecommunications and Information Technology (ECTI-CON)*, Chiang Mai, Thailand, 2010, pp. 1159–1163.
- [212] *High Luminous Efficacy RGBA LED Emitter*, LedEngin, 2011. [Online]. Available: <https://octopart.com/lz4-00ma00-ledengin-20501107>
- [213] S. Chhajed, Y. Xi, Y. Li, T. Gessmann, and E. Schubert, "Influence of junction temperature on chromaticity and color-rendering properties of trichromatic white-light sources based on light-emitting diodes," *Journal of Applied Physics*, vol. 97, no. 5, pp. 054 506–0–054 506–8, 2005.
- [214] *LED Modulation Response*, Optiwave, 2011. [Online]. Available: <https://optiwave.com/resources/applications-resources/optical-system-led-modulation-response/>
- [215] *PDA10A(-EC) Si Amplified Fixed Detector User Guide*, Thorlabs Inc., 2017. [Online]. Available: <https://www.thorlabs.com/drawings/d39f7d9fd375d161-BAFDD8DF-A917-BAF5-00F6D91DF7599D92/PDA10A-EC-Manual.pdf>
- [216] E. Monteiro and S. Hranilovic, "Design and implementation of color-shift keying for visible light communications," *Journal of Lightwave Technology*, vol. 32, no. 10, pp. 2053–2060, 2014.
- [217] N. Narendran and Y. Gu, "Life of led-based white light sources," *Journal of Display Technology*, vol. 1, no. 1, pp. 167–171, 2005.
- [218] Y.-C. Chi, D.-H. Hsieh, C.-T. Tsai, H.-Y. Chen, H.-C. Kuo, and G.-R. Lin, "450-nm gan laser diode enables high-speed visible light communication with 9-gbps qam-ofdm," *Opt. Express*, vol. 23, no. 10, pp. 13 051–13 059, May 2015.
- [219] T. Y. Elganimi, "Studying the ber performance, power- and bandwidth-efficiency for fso communication systems under various modulation schemes," in *IEEE Jordan Conference on Applied Electrical Engineering and Computing Technologies (AEECT)*, Dec 2013, pp. 1–6.
- [220] *Model 1601 and 1611 User's Manual: High-Speed Photoreceivers*, New Focus Inc. [Online]. Available: https://www.newport.com/medias/sys_master/images/images/h11/hd6/8796987883550/1601-1611-User-Manual-RevF.pdf
- [221] H. Chun, S. Rajbhandari, G. Faulkner, D. Tsonev, E. Xie, J. J. D. McKendry, E. Gu, M. D. Dawson, D. C. O'Brien, and H. Haas, "Led based wavelength division multiplexed 10 gb/s visible light communications," *Journal of Lightwave Technology*, vol. 34, no. 13, pp. 3047–3052, 2016.

- [222] A. Hussein and J. Elmirghani, "Mobile multi-gigabit visible light communication system in realistic indoor environment," *Journal of Lightwave Technology*, vol. 33, no. 15, pp. 3293–3307, Aug 2015.
- [223] B. M. Levine and J. C. Dainty, "Non-gaussian image plane speckle: Measurements from diffusers of known statistics," *Optics Communications*, vol. 45, pp. 252–257, 1983.
- [224] M. Kaufman, D. Lutz, and J. Norton, "Ishihara's tests for color blindness: A useful indicator of visual involvement in multiple sclerosis," *International Journal of MS Care*, vol. 2, no. 1, pp. 6–13, 2000.
- [225] G. Cossu, A. M. Khalid, P. Choudhury, R. Corsini, and E. Ciaramella, "2.1 gbit/s visible optical wireless transmission," in *European Conference and Exhibition on Optical Communication (ECOC)*, Amsterdam, Netherlands, 2012, pp. 4.16–4.18.
- [226] C. Kottke, J. Hilt, K. Habel, J. Vučić, and K.-D. Langer, "1.25 gbit/s visible light wdm link based on dmt modulation of a single rgb led luminary," in *38th European Conference and Exhibition on Optical Communication (ECOC)*, Amsterdam, Netherlands, 2012, pp. 1–3.
- [227] M. S. Uddin, J. S. Cha, J. Y. Kim, and Y. M. Jang, "Mitigation technique for receiver performance variation of multi-color channels in visible light communication," *Sensors*, vol. 11, no. 6, pp. 6131–6144, 2011.
- [228] I. E. Lee, M. L. Sim, and F. W. L. Kung, "Performance enhancement of outdoor visible-light communication system using selective combining receiver," *Optoelectronics, IET*, vol. 3, no. 1, pp. 30–39, 2009.
- [229] T. Kasamatsu, H. Sekita, and Y. Kuwano, "Temperature dependence and optimization of 970-nm diode-pumped yb:yag and yb:luag lasers," *Appl. Opt.*, vol. 38, no. 24, pp. 5149–5153, 1999.
- [230] *OSLON 150 9+ PowerStar Whites*, Osram Opto Semiconductors, 2017. [Online]. Available: <http://docs-asia.electrocomponents.com/webdocs/15b6/0900766b815b6c0d.pdf>
- [231] A. P. Putra, S. Fuada, Y. Aska, and T. Adiono, "System-on-chip architecture for high-speed data acquisition in visible light communication system," in *2016 International Symposium on Electronics and Smart Devices (ISESD)*, 2016, pp. 63–67.
- [232] G. Cossu, W. Ali, R. Corsini, and E. Ciaramella, "Gigabit-class optical wireless communication system at indoor distances (1.5 / 4 m)." *Optics express*, vol. 23, pp. 15700–5, Jun 2015.
- [233] Y. Wang, L. Tao, X. Huang, J. Shi, and N. Chi, "8-gb/s rgby led-based wdm vlc system employing high-order cap modulation and hybrid post equalizer," *IEEE Photonics Journal*, vol. 7, no. 6, pp. 1–7, 2015.

-
- [234] J. Armstrong, "Ofdm for optical communications," *Journal of Lightwave Technology*, vol. 27, no. 3, pp. 189–204, 2009.
- [235] H. Elgala and T. D. C. Little, "Reverse polarity optical-ofdm (rpo-ofdm): dimming compatible ofdm for gigabit vlc links," *Optics Express*, vol. 21, no. 20, pp. 24 288–24 299, 2013.
- [236] I. Stefan, H. Elgala, and H. Haas, "Study of dimming and led nonlinearity for aco-ofdm based vlc systems," in *IEEE Wireless Communications and Networking Conference (WCNC)*, Paris, France, 2012, pp. 990–994.
- [237] Z. Wang, C. Yu, W.-D. Zhong, J. Chen, and W. Chen, "Performance of variable m-qam ofdm visible light communication system with dimming control," in *17th Opto-Electronics and Communications Conference (OECC)*, Busan, South Korea, 2012, pp. 741–742.

PSYCHOPHYSICAL EVALUATION DATA

A.1 Questionnaire for Psychophysical Evaluation



Observer No.	
--------------	--

Gender	
Age	

**Psychophysical Evaluation of Laser Diode based White Light
Intelligent Lighting Laboratory
School of Engineering, Monash University Malaysia**

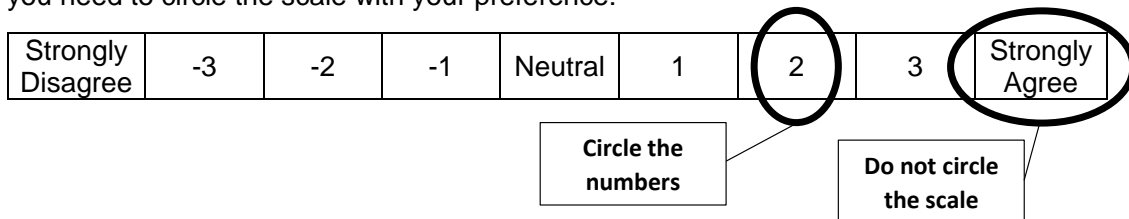
1. Color Vision Test

Please identify the numbers that appear in the charts presented in front of you which had been labelled alphabetically. **Fill up the table below with the numbers you see in each boxes corresponding to the alphabets in the chart.**

A	B	C	D
E	F	G	H
I	J	K	L
M	N	O	P



For all the tests below, a 7-point scale is being used. So based on your observations you need to circle the scale with your preference:



Pre-Illumination Alertness Level:

How are you feeling now?

1	2	3	4	5	6	7	8	9
Extremely alert	Very alert	Alert	Rather alert	Neither alert nor sleepy	Some signs of sleepiness	Sleepy	No effort to stay awake	Fighting Sleep

2. *Test of Illumination Contentment*

a. Brightness Test

Please rate the brightness of the overall scene inside the viewing box:

Illuminant A

Dark	-3	-2	-1	0	1	2	3	Bright
------	----	----	----	---	---	---	---	--------

Illuminant B

Dark	-3	-2	-1	0	1	2	3	Bright
------	----	----	----	---	---	---	---	--------



b. Naturalness

How do you rate the naturalness of the overall scene inside the viewing box?

Illuminant A

Unnatural	-3	-2	-1	0	1	2	3	Natural
-----------	----	----	----	---	---	---	---	---------

Illuminant B

Unnatural	-3	-2	-1	0	1	2	3	Natural
-----------	----	----	----	---	---	---	---	---------

c. Pleasantness

How do you feel towards the overall view inside the viewing box?

Illuminant A

Unpleasant	-3	-2	-1	0	1	2	3	Pleasant
------------	----	----	----	---	---	---	---	----------

Illuminant B

Unpleasant	-3	-2	-1	0	1	2	3	Pleasant
------------	----	----	----	---	---	---	---	----------

d. Visual Comfort

Please rate the overall view inside the viewing box in terms of visual comfort:

Illuminant A

Uncomfortable	-3	-2	-1	0	1	2	3	Comfortable
---------------	----	----	----	---	---	---	---	-------------

Illuminant B

Uncomfortable	-3	-2	-1	0	1	2	3	Comfortable
---------------	----	----	----	---	---	---	---	-------------



3. Test of Illumination Quality

a. Contrast

Rate the illuminated objects inside the viewing box in terms of contrast:

Illuminant A

Poor Contrast	-3	-2	-1	0	1	2	3	Good Contrast
---------------	----	----	----	---	---	---	---	---------------

Illuminant B

Poor Contrast	-3	-2	-1	0	1	2	3	Good Contrast
---------------	----	----	----	---	---	---	---	---------------

b. Color

Rate the illuminated objects inside the viewing box in terms of color:

Illuminant A

Color appears unnatural	-3	-2	-1	0	1	2	3	Color appears natural
-------------------------	----	----	----	---	---	---	---	-----------------------

Illuminant B

Color appears unnatural	-3	-2	-1	0	1	2	3	Color appears natural
-------------------------	----	----	----	---	---	---	---	-----------------------



c. Saturation

Rate the illuminated objects inside the viewing box in terms of saturation:

Illuminant A

Objects are under-saturated	-3	-2	-1	0	1	2	3	Good Saturation
-----------------------------	----	----	----	---	---	---	---	-----------------

Illuminant B

Objects are under-saturated	-3	-2	-1	0	1	2	3	Good Saturation
-----------------------------	----	----	----	---	---	---	---	-----------------

4. Overall Preference

Based on your overall observation which illuminant do you prefer?

Illuminant A	-3	-2	-1	0	1	2	3	Illuminant B
	Strongly prefer A	Moderately prefer A	Slightly prefer A	Neutral	Slightly prefer B	Moderately prefer B	Strongly prefer B	



5. *Test of Cognitive Performance*

Please **arrange the numbers** placed inside the box in ascending order:

Post-Illumination Alertness Level:

How are you feeling now?

1	2	3	4	5	6	7	8	9
Extremely alert	Very alert	Alert	Rather alert	Neither alert nor sleepy	Some signs of sleepiness	Sleepy	No effort to stay awake	Fighting Sleep

Thank you for your co-operation.

School of Engineering, Monash University Malaysia

A.2 Human Ethics Approval



Monash University Human Research Ethics Committee

Approval Certificate

This is to certify that the project below was considered by the Monash University Human Research Ethics Committee. The Committee was satisfied that the proposal meets the requirements of the *National Statement on Ethical Conduct in Human Research* and has granted approval.

Project Number: 11139
Project Title: Psycho-physical Evaluation of Laser Diode based white light
Chief Investigator: Dr v vineetha
Expiry Date: 09/10/2022

Terms of approval - failure to comply with the terms below is in breach of your approval and the *Australian Code for the Responsible Conduct of Research*.

1. The Chief Investigator is responsible for ensuring that permission letters are obtained, if relevant, before any data collection can occur at the specified organisation.
2. Approval is only valid whilst you hold a position at Monash University.
3. It is responsibility of the Chief Investigator to ensure that all investigators are aware of the terms of approval and to ensure the project is conducted as approved by MUHREC.
4. You should notify MUHREC immediately of any serious or unexpected adverse effects on participants or unforeseen events affecting the ethical acceptability of the project.
5. The Explanatory Statement must be on Monash letterhead and the Monash University complaints clause must include your project number.
6. Amendments to approved projects including changes to personnel must not commence without written approval from MUHREC.
7. Annual Report - continued approval of this project is dependent on the submission of an Annual Report.
8. Final Report - should be provided at the conclusion of the project. MUHREC should be notified if the project is discontinued before the expected completion date.
9. Monitoring - project may be subject to an audit or any other form of monitoring by MUHREC at any time.
10. Retention and storage of data - The Chief Investigator is responsible for the storage and retention of the original data pertaining to the project for a minimum period of five years.

Thank you for your assistance.

Professor Nip Thomson

Chair, MUHREC

CC: Mr Fahad Zafar

List of approved documents:

Document Type	File Name	Date	Version
Questionnaires / Surveys	Questionnaire for Participants	13/09/2017	1
Explanatory Statement	Explanatory Statement	03/10/2017	2

A.3 Data Obtained from Psychophysical Evaluation

Observer	Gender	Age	Pre- feeling	Brighthness		Naturalness		Pleasantness		Visual Comfort	
				A	B	A	B	A	B	A	B
1	M	27	3	1	2	2	1	2	-1	2	-1
2	M	24	3	0	1	1	2	2	1	2	2
3	F	23	3	3	2	2	3	2	2	2	3
4	F	23	2	2	0	0	1	2	-1	1	2
5	M	21	3	-1	1	-1	2	-1	2	-1	1
6	M	20	2	2	3	3	1	2	-1	1	3
7	M	34	6	3	-1	3	-2	2	-2	3	-1
8	M	24	2	1	2	2	1	3	-1	1	2
9	M	24	1	1	2	2	1	3	2	2	1
10	M	20	3	3	3	-1	0	1	-2	-1	1
11	M	23	6	-1	0	2	-1	-2	-1	2	1
12	M	22	2	-1	2	2	-2	1	-1	0	0
13	M	22	3	0	0	-2	2	-2	2	-2	2
14	M	24	6	-1	1	2	-2	3	0	-1	2
15	F	35	1	3	-2	3	-3	3	-3	0	0
16	M	25	5	3	0	3	0	3	0	2	0
17	M	27	3	1	2	1	2	-1	2	-2	2
18	M	29	4	-2	0	-1	0	1	0	-1	1
19	M	24	3	1	3	2	3	2	3	1	3
20	M	29	6	2	1	-1	0	-1	1	-1	3
21	M	21	7	2	1	1	0	2	0	1	0
22	M	26	4	2	3	1	2	2	3	2	2
23	F	23	5	2	3	-2	2	0	3	-2	3
24	M	31	5	1	2	-3	1	-2	2	-3	1
25	M	22	5	1	2	-1	2	-1	2	-1	1
26	M	20	3	2	2	-1	0	0	0	0	2
27	M	20	3	1	0	-1	-1	-1	1	-2	-1
28	M	20	7	0	0	1	-1	1	2	1	-1
29	M	21	5	2	1	2	1	3	3	2	3
30	M	22	3	2	1	1	3	3	2	1	3
31	F	20	3	2	3	2	3	2	3	1	3
32	M	23	6	3	2	2	3	2	3	2	3
33	M	24	4	2	3	2	3	1	3	1	3
34	M	23	5	1	2	2	1	2	1	1	2
35	M	24	5	1	2	0	1	-2	-2	-2	-1
36	F	21	3	1	2	-3	1	-1	1	1	2
37	F	22	5	-1	2	3	-2	-3	3	-3	3
38	F	22	6	2	-1	-2	0	3	-1	1	0
39	M	21	5	-2	2	1	-2	3	-1	3	-1
40	F	21	5	2	1	3	1	1	2	1	2
41	M	21	5	2	1	2	-1	2	1	0	2
42	F	24	6	-1	2	2	-2	-1	1	-1	1

Observer	Brighthness		Contrast		Color		Saturation		Overall Preference	Cognitive Time (s)	Post-Feeling
	A	B	A	B	A	B	A	B			
1	1	2	1	2	3	-1	3	-2	-2	21	2
2	0	1	3	-1	2	0	3	-2	-2	25	3
3	3	2	3	2	2	3	3	0	-1	28	3
4	2	0	2	1	2	1	2	-1	-1	40	4
5	-1	1	2	-1	1	2	3	1	-2	55	4
6	2	3	3	1	3	2	3	1	-2	23	3
7	3	-1	2	-2	3	-1	2	-1	-3	16	5
8	1	2	3	0	3	1	3	-2	-2	36	3
9	1	2	2	2	2	1	3	2	-2	25	2
10	3	3	3	0	-1	0	3	0	-1	39	3
11	-1	0	-1	1	1	2	3	1	-2	38	6
12	-1	2	3	-1	-1	1	2	-2	-1	19	2
13	0	0	2	-2	-1	-1	2	-1	2	17	3
14	-1	1	3	-1	3	0	3	-1	-2	25	6
15	3	-2	3	-2	1	3	3	0	-3	43	1
16	3	0	3	0	3	0	3	0	-3	16	4
17	1	2	0	1	1	2	3	-1	-1	23	3
18	-2	0	3	1	-2	0	3	0	-2	15	3
19	1	3	3	2	1	3	2	1	2	17	3
20	2	1	2	1	2	2	3	1	2	27	5
21	2	1	3	-1	3	1	3	-1	-1	20	4
22	2	3	2	3	2	3	3	2	2	49	4
23	2	3	-1	2	-3	3	2	0	3	46	3
24	1	2	2	0	-3	3	2	0	3	41	5
25	1	2	2	2	-1	2	2	1	2	36	3
26	2	2	3	1	3	1	3	-3	-2	30	2
27	1	0	2	1	-1	1	2	-1	1	31	4
28	0	0	2	-1	1	-1	2	-1	-1	21	7
29	2	1	3	2	2	3	3	2	-2	34	7
30	2	1	3	0	-1	2	3	-1	-2	18	2
31	2	3	3	2	2	3	3	2	1	18	3
32	3	2	3	2	3	2	3	1	-2	28	5
33	2	3	1	2	1	3	3	1	-1	37	4
34	1	2	2	0	3	1	2	0	-1	60	4
35	1	2	1	2	2	1	1	1	0	38	4
36	1	2	2	-1	2	1	3	-1	2	40	3
37	-1	2	3	-3	3	-3	3	-3	-2	33	3
38	2	-1	3	0	-2	1	1	-1	-3	60	7
39	-2	2	0	1	2	1	2	-1	-2	27	4
40	2	1	3	-1	3	1	3	-1	-3	15	3
41	2	1	2	1	2	-2	3	1	-2	18	3
42	-1	2	2	0	-2	1	3	-2	-1	15	4